Emerging Phenotypes of Type 2 Diabetes

Roosmarijn Lemmers

Emerging Phenotypes of Type 2 Diabetes

Roosmarijn Lemmers

Cover design: Anniek van Buuren
Production: ProefschriftMaken

ISBN: 978-94-6380-018-1

Publication of this thesis was financially supported by:
MMC Academie, Máxima Medisch Centrum Veldhoven
Erasmus Medisch Centrum, Rotterdam
Amphia Academie, Amphia Ziekenhuis Breda

Emerging Phenotypes of Type 2 Diabetes

Fenotypes in opmars van type 2 diabetes

Proefschrift

ter verkrijging van de graad van doctor aan de
Erasmus Universiteit Rotterdam
op gezag van de
rector magnificus

Prof.dr. R.C.M.E. Engels

en volgens besluit van het College voor Promoties.
De openbare verdediging zal plaatsvinden op

Woensdag 24 oktober 2018 om 11.30 uur

Roosmarijn Francisca Hilligje Lemmers
geboren te Zeist

Erasmus University Rotterdam

Promotiecommissie:

Promotor:	Prof.dr. E.J.G. Sijbrands
Overige leden:	Prof.dr. C. van Duijn
	Prof.dr. H.R.Haak
	Prof.dr. O.H. Franco
Copromotoren:	Dr. M. van Hoek
	Dr. A.G. Lieverse

Contents

CHAPTER 1

Introduction and aim of this thesis

Introduction

Type 2 diabetes and its complications

Type 2 diabetes is defined by hyperglycemia and caused by an imbalance between insulin resistance in peripheral tissues and the ability of the pancreatic β-cells to produce insulin [1]. An estimated 380 million people worldwide currently have type 2 diabetes [2,3]. Shockingly, at 45 years of age, the lifetime risk of developing type 2 diabetes was 31.3% in a Dutch study [4] and disease incidence is rising [2]. Type 2 diabetes pathophysiology comprises a spectrum of phenotypes with different metabolic and inflammatory disturbances and is currently incompletely understood. To improve prediction, prevention, and management of type 2 diabetes and its complications, more insight into pathophysiologic mechanisms is necessary [5].

The most important risk factors for type 2 diabetes are obesity, aging, lack of physical activity, a positive family history of type 2 diabetes, and African-American, Hispanic, or Asian ethnicity [2,6,7]. In type 2 diabetes, genetic susceptibility, epigenetic programming, and environmental factors (such as a high-fat high-caloric diet and lack of exercise) interact at multiple levels [1]. In healthy persons, glucose stimulates insulin secretion by the pancreatic β-cells, which then stimulates the uptake of glucose, amino acids, and fatty acids by peripheral tissues. When peripheral tissues become insulin-resistant, they need more insulin to take up nutrients, therefore the β-cells need to produce more insulin. Type 2 diabetes occurs when the β-cell cannot produce enough insulin to cope with the nutrient load and overcome the peripheral insulin resistance [1,8]. In addition to insulin resistance and β-cell dysfunction, increased glucagon levels, which is produced by the pancreatic α-cells and increases conversion of glycogen stored in the liver to glucose, add to hyperglycemia. Furthermore, a dysregulation of gut and brain hormone signals, such as GLP-1 and leptin, altered bile acid metabolism, changes in the gut microbiome, and neural control of glucose metabolism contribute to type 2 diabetes pathophysiology [8]. Type 2 diabetes is a heterogeneous disease in which the relative contribution of the mechanisms mentioned above differ from patient to patient.

The long-term disease burden of type 2 diabetes is largely caused by its vascular complications. Diabetes affects both large and small blood vessels and the complications are therefore referred to as macrovascular and microvascular. These complications include atherosclerosis, coronary artery disease, stroke, diabetic foot, retinopathy, nephropathy, and neuropathy. People with type 2 diabetes have twice the risk of cardiovascular disease as people without diabetes, independent from other risk factors [9]. Also, type 2 diabetes is a leading cause of blindness, renal disease, and lower limb amputation and a major cause of death, with 3.7 million deaths in 2012 attributable to hyperglycemia [2]. The complications of type 2 diabetes can to a large extent be explained by dyslipidemia, hyperglycemia, insulin resistance, and hemodynamic changes like hypertension. These disturbed sys-

temic processes cause cellular changes in receptive tissues such as the endothelium and neurons, leading to oxidative stress and endothelial dysfunction [10]. In addition, platelet hyper-reactivity, endothelial damage, and increased activity of coagulation factors cause a pro-thrombotic state. Together, these pro-inflammatory and pro-thrombotic changes contribute to vascular complications [10-12]. Although the exact mechanisms leading to the various complications differ, metabolic and pro-inflammatory disturbances play a role in the development of all. Current treatment options for reducing vascular complication risk focus on the classical risk factors: hyperglycemia, hypertension, and dyslipidemia. Unfortunately, intensive treatment of these factors only reduces macro- and microvascular complications by approximately 50% [13-15]. The unexplained, large residual risk is currently unaccounted for in prevention, prediction and treatment.

Metabolic and inflammatory disturbances in type 2 diabetes

Markers of inflammation are associated with risk of type 2 diabetes and its complications [16,17]. Strong links exist between the immune system, adipose tissue, and lipid and glucose metabolism [18]. Lipid metabolism is often already disturbed before the onset of type 2 diabetes, especially in obese individuals. Increased triglyceride and free fatty acid levels, decreased adiponectin levels, insulin resistance, and other yet unknown factors increase very-low-density lipoprotein (VLDL) production and high-density lipoprotein (HDL) catabolism. Eventually, this results in the typical diabetic dyslipidemia characterized by increased triglycerides, decreased HDL-cholesterol, and increased levels of small, dense low-density lipoprotein (LDL). Diabetic dyslipidemia is present in approximately 80% of individuals with type 2 diabetes and is a major risk factor for cardiovascular disease [19]. Dyslipidemia and hyperglycemia contribute to the low-grade systemic inflammation in type 2 diabetes through aberrant immune cell activation and signaling and by increasing stress on the endoplasmic reticulum resulting in its dysfunction [20].

As explained in more detail below, I studied protein *N*-glycosylation and the anti-inflammatory effects of HDL in type 2 diabetes. Both processes are not only sensitive to metabolic and inflammatory disturbances [21-23], but may also actively induce more pro-inflammatory and metabolic alterations in the individual with type 2 diabetes [24-26]. Therefore, I hypothesized that protein *N*-glycosylation and HDL anti-inflammatory function are altered in type 2 diabetes and might contribute to the development of vascular complications.

***N*-glycosylation**

Glycosylation is the enzymatic process of attaching carbohydrate chains to lipids and proteins as a posttranslational modification. Genetic defects in glycosylation are either embryonically lethal or result in rare but severe disorders involving multiple organ systems [27,28]. In proteins, these carbohydrate chains are attached to the oxygen of the amino acids serine or threonine, referred to as *O*-glycans, or to the nitrogen of asparagine, called *N*-

glycans [24]. *N*-glycans represent the majority of glycans and their functional effects have been better studied than those of other glycans [24]. *N*-glycosylation directly influences protein function and is especially important for the interaction of proteins with cells [29]. For instance, glycans are necessary for recognizing pathogens and determine the metastatic potential of cancer cells [24]. The attachment of glycans to proteins is a complex process and is regulated by genetic, epigenetic, and environmental factors [30]. A complete *N*-glycan precursor is attached to an asparagine residue in the endoplasmic reticulum. This precursor is then extensively remodeled by glycosyltransferases and glycosidases throughout the endoplasmic reticulum and Golgi system and further remodeling occurs by glycosidases in the plasma. The final *N*-glycans on proteins can be of the high-mannose, hybrid, or complex type, of which the complex type glycans have undergone the most extensive remodeling and can contain 2 or more antennae with one or more fucose, galactose, or sialic acid groups [31].

N-glycosylation of proteins can be studied by determining the total plasma *N*-glycome (measuring all *N*-glycans from glycoproteins present in the plasma), or as the *N*-glycome of a specific glycoprotein. Patterns of the total *N*-glycome are associated with known type 2 diabetes risk factors such as BMI, lipids, smoking, and ageing [32-35]. Moreover, they have been shown to change in acute inflammation [21,36]. Immunoglobulin G (IgG) is the most common immunoglobulin in the circulation and its glycosylation has been studied extensively. Several functional effects of specific glycosylation features are known to switch its function from pro- to anti-inflammatory and vice versa [37]. Changes in the IgG *N*-glycome have been related to multiple diseases, including rheumatoid arthritis [38,39], systemic lupus erythematosus [40], inflammatory bowel disease [41], chronic kidney disease [42], and hypertension [43]. In rheumatoid arthritis, IgG *N*-glycans mediate complement activation [44], which has also been related to type 2 diabetes and its metabolic disturbances and vascular complications [45,46]. Few studies have investigated the plasma *N*-glycome in type 2 diabetes. Testa et al. showed reduced monogalactosylated, core-fucosylated diantennary *N*-glycans in type 2 diabetes [47]. Very recently, Keser et al. found increased *N*-glycan complexity in individuals at risk for type 2 diabetes [48]. These studies emphasize the need to further investigate the *N*-glycome in type 2 diabetes. New technologies have enabled high-throughput studies with detailed *N*-glycan analysis, which allows studying their associations with common multifactorial diseases in large populations [22].

HDL anti-inflammatory function

Low HDL-cholesterol levels are associated with increased risk of cardiovascular disease [49] and type 2 diabetes [50], as is well-known from epidemiological studies. However, evidence that these associations are not straightforward causal relationships is accumulating. Pharmacologically increasing HDL-cholesterol does not decrease cardiovascular disease risk [51], nor does genetically decreased HDL-cholesterol increase the risk of type

2 diabetes or cardiovascular disease [52,53]. Unlike other lipoproteins, HDL does not contain apolipoprotein(apo)-B. Instead, its main protein constituents are ApoA-I and ApoA-II [54]. HDL is defined by the density range in which it is found after ultracentrifugation: 1.063-1.21g/mL. Within this density range, different subpopulations of HDL are present which are interrelated and can interchange with ongoing metabolism [55]. Thus, HDL actually comprises a group of heterogeneous particles, which can carry a multitude of lipids and proteins, making HDL biology quite complex [56,57]. Qualities other than just HDL cholesterol content might be more important in the associations with type 2 diabetes and cardiovascular disease. For example, HDL can protect against oxidation and cell apoptosis, combat pathogenic infections, increase vasodilation, reduce inflammation, and improve glucose metabolism [58].

HDL metabolism is an ongoing process where HDL is continually remodeled in the circulation. Lipid-free ApoA-I particles are secreted by the liver and intestine and bind phospholipids and free cholesterol through adenosine-triphosphate-binding cassette protein A-I (ABCA-I). These lipid-poor ApoA-I particles attract phospholipids and free cholesterol from macrophages and other parenchymal cells in the interstitial space via ABCA-I and ABCG-I. The cholesterol is esterified by the enzyme Lecithin-cholesterol Acyltransferase (LCAT) and subsequently moves to the inner part of the particle, making the HDL particle spherical and more buoyant; this is the predominant form of HDL in the circulation. Further remodeling occurs through cholesterol ester transfer protein (CETP), which exchanges HDL-cholesterol for triglycerides from triglyceride-rich lipoproteins such as VLDL. In addition, several lipases hydrolyze phospholipids and triglycerides bound to HDL. The cholesterol and phospholipids collected in the circulation by the HDL particles are largely transferred to VLDL and LDL by CETP and phospholipid transfer protein (PLTP). Subsequently, these lipids are cleared by the liver through LDL uptake via the LDL-receptor or by the uptake of HDL itself via scavenger-receptor B-I (SR-BI). This clearance of HDL lipids generates a lipid-poor HDL particle that is available for another cycle of lipid uptake and remodeling [59,57]. The decreased levels of HDL-particles and HDL-cholesterol in type 2 diabetes are most likely caused by increased HDL catabolism due to a higher triglyceride content, increased cholesterol deposition from HDL to VLDL trough CETP, and decreased adiponectin levels [19].

Not surprisingly, the role of HDL in reverse cholesterol transport is the function that has been studied the most. However, HDL also significantly influences (vascular) inflammation through several different mechanisms. First, it decreases the expression of adhesion molecules on endothelial cells and monocytes [60,61]. Second, it decreases T-cell stimulation and monocyte activation, thereby reducing pro-inflammatory cytokine production [58]. And third, HDL reduces the migration of monocytes across the endothelium [62]. HDL also indirectly influences inflammation through anti-oxidative effects and its modulation of lipid rafts in cell membranes [63]. These mechanisms are at least partly regulated by nuclear factor

kappa B (NFκB), ABCA1, ABCG1, and SR-B1 [58,64]. Activation of immune cells and subsequent adhesion to and migration through the endothelium are early steps in atherosclerosis pathogenesis [65]. The effects of HDL on vascular inflammation could represent a pathway through which HDL modulates cardiovascular risk. HDL has been proposed to become dysfunctional in type 2 diabetes [66], as well as in other diseases in which inflammation plays a key role and cardiovascular risk is increased, such as systemic lupus erythemathosus, rheumatoid arthritis [67], and chronic kidney disease [68]. However, whether the HDL-particle is in fact dysfunctional in type 2 diabetes, what the underlying pathophysiological processes are, and how this is related to vascular complications remains to be further elucidated.

Aim of this thesis

The aim of this thesis is to gain insight in the role of *N*-glycosylation and the anti-inflammatory function of HDL as pathways that might explain part of the pathophysiology of type 2 diabetes and its complications. These insights could contribute to finding new therapeutic targets and improving prediction and prevention.

In **part II of this thesis,** I investigated the relationship between *N*-glycans and type 2 diabetes. In **chapter 2**, the DiaGene study is described: a multi-centre, prospective, extensively phenotyped type 2 diabetes cohort study with concurrent inclusion of diabetes-free individuals at baseline as controls. This study aims to integrate different omics layers for investigating the pathophysiology of type 2 diabetes and its vascular complications, of which *N*-glycomics was the first layer to be measured. in **chapter 3,** I report on the associations between the total plasma glycome and type 2 diabetes and its risk factors. And in **chapter 4,** I describe how the IgG *N*-glycome is associated with type 2 diabetes.

In **part III of this thesis**, the effect of HDL on signals of endothelial inflammation was investigated. One of the challenges in studying the effects of HDL on inflammation *in vitro*, is that HDL can be isolated with different methods and based on different properties. **Chapter 5** describes how different methods of isolating HDL affect TNF-α induced VCAM-1 expression on endothelial cells as a readout. Information on the effects of HDL on inflammation in type 2 diabetes is scarce and difficult to compare between studies. In **Chapter 6**, I have critically reviewed the literature on HDL anti-inflammatory function in type 2 diabetes, compared study results, and aimed to identify gaps in the knowledge.

Finally, in **part IV**, the main findings of this thesis are summarized and discussed. Furthermore, I discuss the methodological strengths and limitations and clinical implications of this thesis, propose directions for future research, and hypothesize on how knowledge on these processes could contribute to a decrease in the disease burden of type 2 diabetes.

References

1. Nolan CJ, Damm P, Prentki M. Type 2 diabetes across generations: from pathophysiology to prevention and management. Lancet 2011;378:169-81.
2. WHO. Global Report on Diabetes, 2016.
3. Diabetesfonds. Anonymous . (Accessed 7/13, 2017, at https://www.diabetesfonds.nl/over-diabetes/soorten-diabetes/verschil-tussen-diabetes-type-1-en-2).
4. Ligthart S, van Herpt TT, Leening MJ, et al. Lifetime risk of developing impaired glucose metabolism and eventual progression from prediabetes to type 2 diabetes: a prospective cohort study. Lancet Diabetes Endocrinol 2016;4:44-51.
5. McCarthy MI. Painting a new picture of personalised medicine for diabetes. Diabetologia 2017;60:793-9.
6. Jaacks LM, Siegel KR, Gujral UP, Narayan KM. Type 2 diabetes: A 21st century epidemic. Best Pract Res Clin Endocrinol Metab 2016;30:331-43.
7. Abate N, Chandalia M. The impact of ethnicity on type 2 diabetes. J Diabetes Complications 2003;17:39-58.
8. Kahn SE, Cooper ME, Del Prato S. Pathophysiology and treatment of type 2 diabetes: perspectives on the past, present, and future. Lancet 2014;383:1068-83.
9. Emerging Risk Factors Collaboration, Sarwar N, Gao P, et al. Diabetes mellitus, fasting blood glucose concentration, and risk of vascular disease: a collaborative meta-analysis of 102 prospective studies. Lancet 2010;375:2215-22.
10. Forbes JM, Cooper ME. Mechanisms of diabetic complications. Physiol Rev 2013;93:137-88.
11. Roy S, Kern TS, Song B, Stuebe C. Mechanistic Insights into Pathological Changes in the Diabetic Retina: Implications for Targeting Diabetic Retinopathy. Am J Pathol 2017;187:9-19.
12. Navarro-Gonzalez JF, Mora-Fernandez C, Muros de Fuentes M, Garcia-Perez J. Inflammatory molecules and pathways in the pathogenesis of diabetic nephropathy. Nat Rev Nephrol 2011;7:327-40.
13. Gaede P, Vedel P, Larsen N, Jensen GV, Parving HH, Pedersen O. Multifactorial intervention and cardiovascular disease in patients with type 2 diabetes. N Engl J Med 2003;348:383-93.
14. Holman RR, Paul SK, Bethel MA, Matthews DR, Neil HA. 10-Year Follow-Up of Intensive Glucose Control in Type 2 Diabetes. N Engl J Med 2008;359:1577-89.
15. Zoungas S, Arima H, Gerstein HC, et al. Effects of intensive glucose control on microvascular outcomes in patients with type 2 diabetes: a meta-analysis of individual participant data from randomised controlled trials. Lancet Diabetes Endocrinol 2017;5:431-7.
16. Wang X, Bao W, Liu J, et al. Inflammatory markers and risk of type 2 diabetes: a systematic review and meta-analysis. Diabetes Care 2013;36:166-75.
17. Goldberg RB. Cytokine and cytokine-like inflammation markers, endothelial dysfunction, and imbalanced coagulation in development of diabetes and its complications. J Clin Endocrinol Metab 2009;94:3171-82.
18. Hotamisligil GS. Inflammation, metaflammation and immunometabolic disorders. Nature 2017;542:177-85.
19. Verges B. Pathophysiology of diabetic dyslipidaemia: where are we? Diabetologia 2015;58:886-99.
20. Hummasti S, Hotamisligil GS. Endoplasmic reticulum stress and inflammation in obesity and diabetes. Circ Res 2010;107:579-91.
21. Novokmet M, Lukic E, Vuckovic F, et al. Changes in IgG and total plasma protein glycomes in acute systemic inflammation. Sci Rep 2014;4:4347.

22. Reiding KR, Ruhaak LR, Uh HW, et al. Human Plasma N-glycosylation as Analyzed by Matrix-Assisted Laser Desorption/Ionization-Fourier Transform Ion Cyclotron Resonance-MS Associates with Markers of Inflammation and Metabolic Health. Mol Cell Proteomics 2017;16:228-42.
23. Patel S, Puranik R, Nakhla S, et al. Acute hypertriglyceridaemia in humans increases the triglyceride content and decreases the anti-inflammatory capacity of high density lipoproteins. Atherosclerosis 2009;204:424-8.
24. Lauc G, Pezer M, Rudan I, Campbell H. Mechanisms of disease: The human N-glycome. Biochim Biophys Acta 2016;1860:1574-82.
25. Ragbir S, Farmer JA. Dysfunctional high-density lipoprotein and atherosclerosis. Curr Atheroscler Rep 2010;12:343-8.
26. Ansell BJ, Fonarow GC, Navab M, Fogelman AM. Modifying the anti-inflammatory effects of high-density lipoprotein. Curr Atheroscler Rep 2007;9:57-63.
27. Marek KW, Vijay IK, Marth JD. A recessive deletion in the GlcNAc-1-phosphotransferase gene results in peri-implantation embryonic lethality. Glycobiology 1999;9:1263-71.
28. Freeze HH, Schachter H. Chapter 42. Genetic Disorders of Glycosylation. In: Varki A, Cummings RD, Esko JD, et al, eds. Essentials of Glycobiology. Cold Spring Harbor (NY): Cold Spring Harbor Laboratory Press, 2009.
29. Wuhrer M. Glycosylation profiling in clinical proteomics: heading for glycan biomarkers. Expert Rev Proteomics 2007;4:135-6.
30. Lauc G, Rudan I, Campbell H, Rudd PM. Complex genetic regulation of protein glycosylation. Mol Biosyst 2010;6:329-35.
31. Stanley P, Schachter H, Taniguchi N. Chapter 8. N-glycans. In: Varki A, Cummings RD, Esko JD, et al, eds. Essentials of Glycobiology. 2nd edition ed. Cold Spring Harbor (NY): Cold Spring Harbor Laboratory Press, 2009.
32. Knezevic A, Gornik O, Polasek O, et al. Effects of aging, body mass index, plasma lipid profiles, and smoking on human plasma N-glycans. Glycobiology 2010;20:959-69.
33. Kristic J, Vuckovic F, Menni C, et al. Glycans are a novel biomarker of chronological and biological ages. J Gerontol A Biol Sci Med Sci 2014;69:779-89.
34. Ruhaak LR, Uh HW, Beekman M, et al. Plasma protein N-glycan profiles are associated with calendar age, familial longevity and health. J Proteome Res 2011;10:1667-74.
35. Nikolac Perkovic M, Pucic Bakovic M, Kristic J, et al. The association between galactosylation of immunoglobulin G and body mass index. Prog Neuropsychopharmacol Biol Psychiatry 2014;48:20-5.
36. Gudelj I, Baciarello M, Ugrina I, et al. Changes in total plasma and serum N-glycome composition and patient-controlled analgesia after major abdominal surgery. Sci Rep 2016;6:31234.
37. Gornik O, Pavic T, Lauc G. Alternative glycosylation modulates function of IgG and other proteins - implications on evolution and disease. Biochim Biophys Acta 2012;1820:1318-26.
38. Parekh RB, Dwek RA, Sutton BJ, et al. Association of rheumatoid arthritis and primary osteoarthritis with changes in the glycosylation pattern of total serum IgG. Nature 1985;316:452-7.
39. Parekh RB, Roitt IM, Isenberg DA, Dwek RA, Ansell BM, Rademacher TW. Galactosylation of IgG associated oligosaccharides: reduction in patients with adult and juvenile onset rheumatoid arthritis and relation to disease activity. Lancet 1988;1:966-9.
40. Vuckovic F, Kristic J, Gudelj I, et al. Association of systemic lupus erythematosus with decreased immunosuppressive potential of the IgG glycome. Arthritis Rheumatol 2015;67:2978-89.
41. Trbojevic Akmacic I, Ventham NT, Theodoratou E, et al. Inflammatory bowel disease associates with proinflammatory potential of the immunoglobulin G glycome. Inflamm Bowel Dis 2015;21:1237-47.

42. Barrios C, Zierer J, Gudelj I, et al. Glycosylation Profile of IgG in Moderate Kidney Dysfunction. J Am Soc Nephrol 2016;27:933-41.
43. Wang Y, Klaric L, Yu X, et al. The Association Between Glycosylation of Immunoglobulin G and Hypertension: A Multiple Ethnic Cross-Sectional Study. Medicine (Baltimore) 2016;95:e3379.
44. Malhotra R, Wormald MR, Rudd PM, Fischer PB, Dwek RA, Sim RB. Glycosylation changes of IgG associated with rheumatoid arthritis can activate complement via the mannose-binding protein. Nat Med 1995;1:237-43.
45. Hertle E, Stehouwer CD, van Greevenbroek MM. The complement system in human cardiometabolic disease. Mol Immunol 2014;61:135-48.
46. Mellbin LG, Bjerre M, Thiel S, Hansen TK. Complement activation and prognosis in patients with type 2 diabetes and myocardial infarction: a report from the DIGAMI 2 trial. Diabetes Care 2012;35:911-7.
47. Testa R, Vanhooren V, Bonfigli AR, et al. N-glycomic changes in serum proteins in type 2 diabetes mellitus correlate with complications and with metabolic syndrome parameters. PLoS One 2015;10:e0119983.
48. Keser T, Gornik I, Vuckovic F, et al. Increased plasma N-glycome complexity is associated with higher risk of type 2 diabetes. Diabetologia 2017;.
49. Gordon DJ, Probstfield JL, Garrison RJ, et al. High-density lipoprotein cholesterol and cardiovascular disease. Four prospective American studies. Circulation 1989;79:8-15.
50. Wilson PW, Meigs JB, Sullivan L, Fox CS, Nathan DM, D'Agostino RB S. Prediction of incident diabetes mellitus in middle-aged adults: the Framingham Offspring Study. Arch Intern Med 2007;167:1068-74.
51. Keene D, Price C, Shun-Shin MJ, Francis DP. Effect on cardiovascular risk of high density lipoprotein targeted drug treatments niacin, fibrates, and CETP inhibitors: meta-analysis of randomised controlled trials including 117,411 patients. BMJ 2014;349:g4379.
52. Haase CL, Tybjaerg-Hansen A, Qayyum AA, Schou J, Nordestgaard BG, Frikke-Schmidt R. LCAT, HDL cholesterol and ischemic cardiovascular disease: a Mendelian randomization study of HDL cholesterol in 54,500 individuals. J Clin Endocrinol Metab 2012;97:E248-56.
53. Haase CL, Tybjaerg-Hansen A, Nordestgaard BG, Frikke-Schmidt R. HDL Cholesterol and Risk of Type 2 Diabetes: A Mendelian Randomization Study. Diabetes 2015;64:3328-33.
54. Vaisar T. Proteomics investigations of HDL: challenges and promise. Curr Vasc Pharmacol 2012;10:410-21.
55. Asztalos BF, Tani M, Schaefer EJ. Metabolic and functional relevance of HDL subspecies. Curr Opin Lipidol 2011;22:176-85.
56. Gordon S.M., Hofmann S., Askew D.S., Davidson W.S. High density lipoprotein: It's not just about lipid transport anymore. Trends Endocrinol Metab 2011;22:9-15.
57. Kardassis D, Mosialou I, Kanaki M, Tiniakou I, Thymiakou E. Metabolism of HDL and its regulation. Curr Med Chem 2014;21:2864-80.
58. Kontush A. HDL-mediated mechanisms of protection in cardiovascular disease. Cardiovasc Res 2014;103:341-9.
59. Karathanasis SK, Freeman LA, Gordon SM, Remaley AT. The Changing Face of HDL and the Best Way to Measure It. Clin Chem 2017;63:196-210.
60. Cockerill GW, Rye KA, Gamble JR, Vadas MA, Barter PJ. High-density lipoproteins inhibit cytokine-induced expression of endothelial cell adhesion molecules. Arterioscler Thromb Vasc Biol 1995;15:1987-94.

61. Murphy AJ, Woollard KJ, Hoang A, et al. High-density lipoprotein reduces the human monocyte inflammatory response. Arterioscler Thromb Vasc Biol 2008;28:2071-7.
62. Navab M, Imes SS, Hama SY, et al. Monocyte transmigration induced by modification of low density lipoprotein in cocultures of human aortic wall cells is due to induction of monocyte chemotactic protein 1 synthesis and is abolished by high density lipoprotein. J Clin Invest 1991;88:2039-46.
63. Reconstituted HDL: A therapy for atherosclerosis and beyond. United Kingdom: 2009. Murphy A.J., Chin-Dusting J., Sviridov D. (Accessed 6, 4).
64. Bursill CA, Castro ML, Beattie DT, et al. High-density lipoproteins suppress chemokines and chemokine receptors in vitro and in vivo. Arterioscler Thromb Vasc Biol 2010;30:1773-8.
65. Weber C, Noels H. Atherosclerosis: current pathogenesis and therapeutic options. Nat Med 2011;17:1410-22.
66. Farbstein D, Levy AP. HDL dysfunction in diabetes: causes and possible treatments. Expert Rev Cardiovasc Ther 2012;10:353-61.
67. McMahon M, Grossman J, FitzGerald J, et al. Proinflammatory high-density lipoprotein as a biomarker for atherosclerosis in patients with systemic lupus erythematosus and rheumatoid arthritis. Arthritis Rheum 2006;54:2541-9.
68. Kaseda R, Jabs K, Hunley TE, et al. Dysfunctional high-density lipoproteins in children with chronic kidney disease. Metabolism 2015;64:263-73.

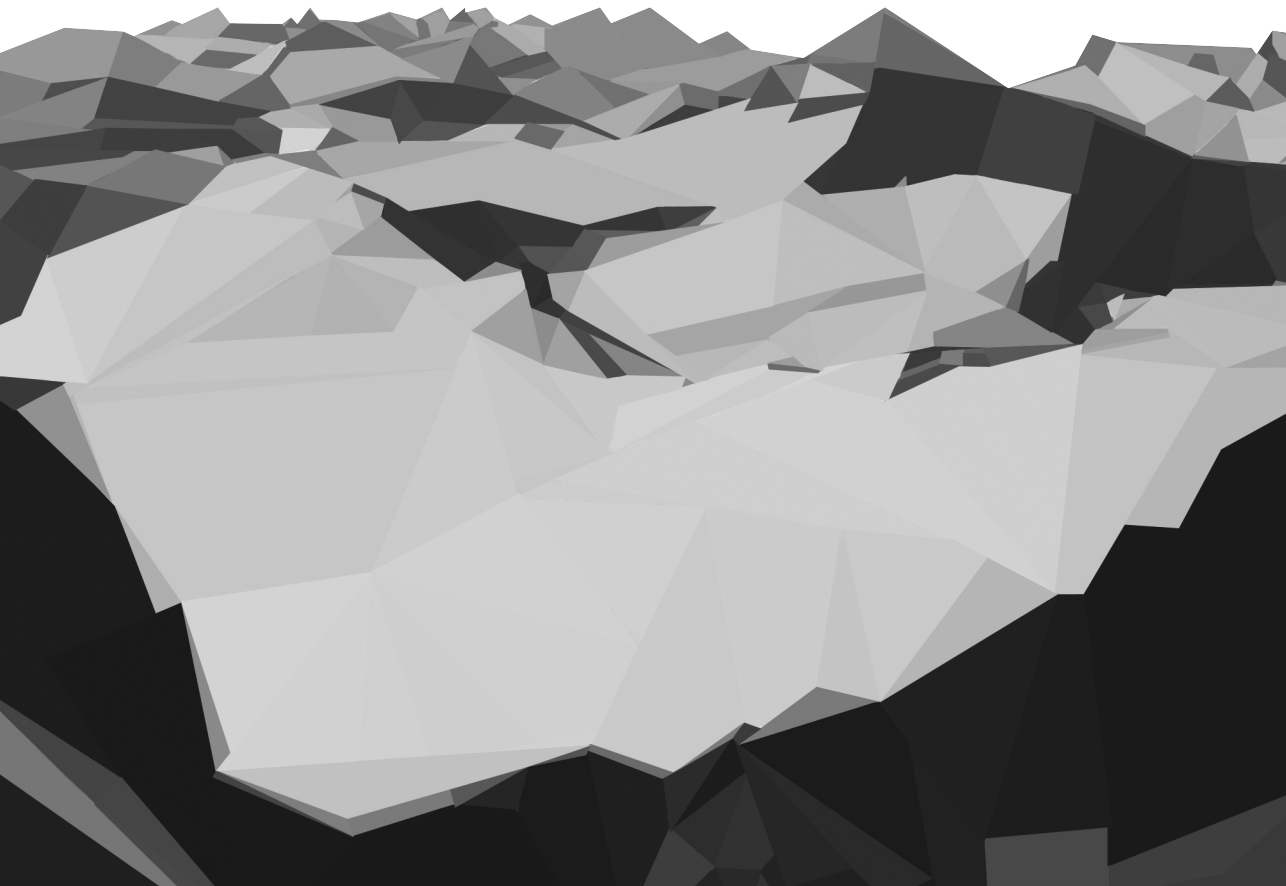

CHAPTER 2

Introduction of the DiaGene Study: clinical characteristics, pathophysiology and determinants of vascular complications of type 2 diabetes

*Thijs T.W. van Herpt, *Roosmarijn F.H. Lemmers, *Mandy van Hoek, Janneke G. Langendonk, Ronald J. Erdtsieck, Bert Bravenboer, Annelies Lucas, Monique T. Mulder, Harm R Haak, Aloysius G. Lieverse, Eric J.G. Sijbrands. *These authors contributed equally.
* These authors contributed equally

Diabetology & Metabolic Syndrome 2017;9:47,017-0245-x. eCollection 2017.

Abstract

Background: Type 2 diabetes is a major healthcare problem. Glucose-, lipid-, and blood pressure-lowering strategies decrease the risk of micro- and macrovascular complications. However, a substantial residual risk remains. To unravel the etiology of type 2 diabetes and its complications, large-scale, well-phenotyped studies with prospective follow-up are needed. This is the goal of the DiaGene study. In this manuscript, we describe the design and baseline characteristics of the study.

Methods: The DiaGene study is a multi-centre, prospective, extensively phenotyped type 2 diabetes cohort study with concurrent inclusion of diabetes-free individuals at baseline as controls in the city of Eindhoven, The Netherlands. We collected anthropometry, laboratory measurements, DNA material, and detailed information on medication usage, family history, lifestyle and past medical history. Furthermore, we assessed the prevalence and incidence of retinopathy, nephropathy, neuropathy, and diabetic feet in cases. Using logistic regression models, we analyzed the association of 11 well known genetic risk variants with type 2 diabetes in our study.

Results: In total, 1886 patients with type 2 diabetes and 854 controls were included. Cases had worse anthropometric and metabolic profiles than controls. Patients in outpatient clinics had higher prevalence of macrovascular (41.9% vs. 34.8%; P=0.002) and microvascular disease (63.8% vs. 20.7%) compared to patients from primary care. With the exception of the genetic variant in KCNJ11, all type 2 diabetes susceptibility variants had higher allele frequencies in subjects with type 2 diabetes than in controls.

Conclusions: In our study population, considerable rates of macrovascular and microvascular complications are present despite treatment. These prevalence rates are comparable to other type 2 diabetes populations. While planning genomics, we describe that 11 well-known type 2 diabetes genetic risk variants (in TCF7L2, PPARG-P12A, KCNJ11, FTO, IGF2BP2, DUSP9, CENTD2, THADA, HHEX, CDKAL1, KCNQ1) showed similar associations compared to literature. This study is well-suited for multiple omics analyses to further elucidate disease pathophysiology. Our overall goal is to increase the understanding of the underlying mechanisms of type 2 diabetes and its complications for developing new prediction, prevention, and treatment strategies.

Background

Type 2 diabetes mellitus (T2DM) is a complex metabolic disease characterized by overweight, insulin resistance and beta-cell dysfunction [1-3]. Because of ageing and the rising prevalence of obesity, the incidence and prevalence of T2DM are increasing [4-7]. T2DM accounts for a large proportion of present and future health care expenditure in Western societies [5, 7, 8]. People affected by T2DM have an increased risk of cardiovascular events [9-13], and a poor prognosis after these events [14, 15]. In addition, T2DM gives rise to microvascular complications such as retinopathy, nephropathy and neuropathy [16-19]. We have collected a new large cohort of individuals with and without T2DM with prospective follow-up in the Netherlands: the DiaGene study.

The care for T2DM in the Netherlands is organized in primary care by general practitioners and at hospital-based outpatients clinics by medical specialists. This systematic care is based on local and international treatment guidelines aiming to reduce morbidity and mortality through optimal treatment of hyperglycemia and associated metabolic complications, such as dyslipidemia, vascular dysfunction and high blood pressure [20, 21]. Treatment of these components has proven to reduce the risk of cardiovascular morbidity and mortality in T2DM [22-30]. However, a substantial residual risk remains. Improving knowledge on genetic, biochemical and environmental (lifestyle and anthropometric) determinants of T2DM and its micro– and macrovascular complications can have large implications for prevention, treatment and prognosis of T2DM [22, 23, 31]. Through high throughput sequencing, about 80 common genetic variants associated with T2DM have been discovered [31, 32]. These common variants only explain 5-10% of the overall predisposition of T2DM [33]. There clearly is a need to expand these analyses to additional populations.

In this paper, we present the DiaGene Study, a new, multicenter T2DM cohort study collected in the Netherlands in both primary and secondary care. The main purpose of the DiaGene Study is to study the analyses of genetic, biochemical and environmental determinants of T2DM and its complications. Here we describe the characteristics of our population, the prevalence of complications and future perspectives.

Methods

Study design

The DiaGene-study is a multicenter cohort study that was coordinated by the vascular section of internal medicine of the Erasmus Medical Center and the Diabetes subunit of the Máxima Medical Center, and collected in the city of Eindhoven, The Netherlands. Eindhoven is a medium-sized city with 170,668 adult (> 21 years) inhabitants in 2011.

Both hospitals in Eindhoven participated in the DiaGene study: Catherina Hospital and Máxima Medical Center. In addition, the local Primary Care Diagnostic Centre participated. Hence, virtually all diabetes patients in Eindhoven were approached for inclusion through this population-based approach. Between 2006 and 2011, physicians at all three centers included a total of 2,065 patients with T2DM. Of these, 179 patients were excluded from analysis. Reasons for exclusion where: no diabetes (n=1), Type 1 diabetes (n=30), Maturity-Onset Diabetes of the Young (n=4), Latent auto-immune diabetes in adults (n=3), double inclusion (n=77), post-pancreatitis diabetes (n=3), refusal during study period (n=2) and missing written informed consent (n=59); resulting in a total of 1,886 patients in the study population.

The control group consisted of two groups: 1. subjects recruited via advertisement in local newspapers, and 2. subjects that where included through invitation of friends and self-reported unrelated family members of participating patients. Inclusion criteria for controls was age 55 years or older. Exclusion criteria were the presence of any kind of diabetes, use of metformin or Cushing's disease. Subjects who were approached had at least 7 days of decision-time to fully reflect on research goals and methods using physician-provided information, before giving their written informed consent. Eventually, 904 diabetes-free subjects participated as controls. Of these, 50 were excluded from all analyses based on missing written informed consent (n=14), double inclusion (n=17), and suspected or confirmed diagnosis of diabetes (n=19), resulting in a total of 854 controls included in the final population. This study was approved by the Medical Ethics Committees of the Erasmus MC, Catherina Hospital and Máxima Medical Center. Written informed consent was obtained from all participants.

Definition of T2DM

Information on the diagnosis of T2DM was retrieved from the patient's medical records. In accordance with American Diabetes Association – and World Health Organization – guidelines [34, 35], diabetes was defined as a fasting plasma glucose ≥ 7.0 mmol/L and/or a non-fasting plasma glucose level ≥ 11.1 mmol/l measured at least at 2 separate time points, treatment with oral glucose-lowering medication or insulin, and/or the diagnosis of T2DM as registered by a medical specialist. Persons with the diagnosis of type 1 diabetes (as derived from medical records and patient-questionnaires) or other types of diabetes mellitus were excluded from the study. Control subjects with fasting glucose ≥ 7.0 mmol/L or glycated hemoglobin (HbA1c) ≥ 47.5mmol/mol were excluded. Information on T2DM status was checked by two investigators. If they did not reach consensus, the participant's treating physician was consulted.

Medical and family history

Each participant filled out an extensive questionnaire on their medical history (history of diabetes, metabolic disease, vascular disease, medication use and intoxications) and ethnicity of their parents. We classified a participant to be Caucasian if both parents were reported to be Caucasian. Furthermore, the participant's family history regarding diabetes and cardiovascular disease and medication usage was recorded through the questionnaire.

Sample collection

A 20cc Ethylene diamine tetra acetic (EDTA) fasting blood sample was taken from all participants. Samples were centrifuged (3000rpm; 1800G for 15 minutes at 4°C). Directly after centrifugation, the plasma and the buffy coat were separated and stored (at -80°C) for DNA analysis and future measurements.

Diabetes and complications of diabetes

Data on body mass index (BMI) (kg/m^2) and blood pressure (mmHg) were extracted from medical records at inclusion. Similarly, laboratory results were extracted around time of inclusion and contained fasting glucose, glycated hemoglobin (HbA1c), total cholesterol, low-density lipoprotein cholesterol (LDL-cholesterol), high-density lipoprotein-cholesterol (HDL-cholesterol), triglycerides, creatinin and urinary albumin/creatinine-ratio. The majority of measurements were collected within 6 months prior to or after the actual date of inclusion. To estimate kidney function, the estimated glomerular filtration rate was calculated with the Modification of Diet in Renal Disease-formula. Information on the presence of cardiovascular disease in the patients treated in the hospital-based outpatient clinics was retrieved from their medical records. Cardiovascular disease comprised myocardial infarction, percutaneous coronary intervention / coronary arterial bypass graft (PCI/CABG), cerebrovascular accident, transient ischemic attack and peripheral arterial disease. PCI/CABG was defined as any invasive intervention to treat coronary arterial disease (PCI, CABG). Peripheral arterial disease was defined as an ankle-brachial index below 0.80 or below 0.90 with typical complaints, any intervention to treat peripheral arterial disease (supervised exercise training, stenting, bypass and percutaneous transluminal angioplasty, or the self-reported presence of intermittent claudication. Information on cardiovascular disease in patients from primary care and diabetes-free controls was based on self-reporting.

Microvascular complications were subdivided into retinopathy, nephropathy and neuropathy. Diabetic foot was additionally assessed. Retinopathy was scored according to the report of an ophthalmologist as absent or present and classified as non-proliferative, proliferative, or retinopathy treated with photo coagulation or intra-vitreal injections. Neuropathy was defined by a podotherapist, neurologist or the patients' treating physician. Nephropathy was defined present when micro-albuminuria (Albumin/creatinin-ratio

(ACR)≥2.5 for men or ≥3.5 for women) was present at two of three consecutive measurements, or when high micro-albuminuria or macro-albuminuria was present at one measurement (ACR≥12.5 for men or ≥17.5 for women). Diabetic foot was established by a podotherapist or physician according to the SIMM's classification [36]. All information on laboratory data, macrovascular, and microvascular events in case and control subjects at baseline that was retrieved from medical records was separately checked by two investigators. When they did not reach consensus, the participant's physician was consulted.

Genotyping

DNA was isolated using the Invisorb® Blood Universal Kit from Stratec Molecular (Berlin, Germany). Eleven well-known T2DM genetic risk variants were genotyped: TCF7L2(rs7903146), PPARG-P12A(rs1801282) , DUSP9(rs594532), CENTD2(rs1552224), THADA(rs7578597), HHEX(rs1111875), CDKAL1(rs7754840) and KCNQ1(rs231362)which had previously been genotyped for replication in DIAGRAM [37], and KCNJ11(rs5219), IGF2BP2(rs4402960) and FTO(rs8050136). These risk variants were chosen because of their relatively large effect sizes on T2DM risk in previous studies [32, 37-42]. Genotyping was performed with TaqMan allelic discrimination assays, designed and optimized by Applied Biosystems (Foster City, CA, USA). Reactions were performed on the Taqman Prism 7900 HT platform.

Follow-up data

Currently, we are finalizing the first collection of prospective follow-up in our study population. This encompasses all anthropometric and laboratory measurements and data on metabolic, microvascular and macrovascular complications of T2DM and enables us to perform prospective analyses.

Statistical analysis

Continuous variables are expressed as median with interquartile range unless otherwise specified. Comparisons between groups were performed with Mann-Whitney U tests for continuous and X^2-tests for categorical data. Deviation from the Hardy-Weinberg equilibrium was assessed by X^2-testing. Associations of the genotypes with T2DM were tested using logistic regression models. We have calculated interaction effects of odds ratios for T2D to compare our results with previous genetic studies according to the method of Altman et al [43]. All models were adjusted for age and sex. Additionally, models were adjusted for center of inclusion as a categorical covariate. Cases and controls of non-Caucasian ethnicity were excluded from the genetic analyses. P-values smaller than 0.05 were considered to be statistically significant. Statistical analysis was performed with SPSS-software version 22.0 (SPSS, Chicago, IL, USA).

Results

General characteristics

The most relevant general characteristics of the cohort are displayed in Table 1. A total of 1886 patients with T2DM and 854 diabetes-free controls were included. Of all anthropometric measurements, 90.6% and 96.1% were performed within 6 and 12 months of inclusion, respectively. Of laboratory data, 81.8% and 93.2% were measured within 6 and 12 months of inclusion, respectively. The cases and controls were of similar age. When compared to controls, cases had higher BMI (29.5 (Interquartile range (IQR) 26.4-32.7) vs. 25.5 (IQR 23.3-27.7) kg/m^2 ; P<0.001), higher HbA1c (50.8 (IQR 43.7-57.9) vs. 37.7 (IQR 36.1-39.3) mmol/mol; P<0.001), higher creatinin (78 (IQR 66-91) vs. 72 (IQR 63-81) umol/L; P<0.001), higher triglycerides (1.4 (IQR 0.9-1.9) vs 1.2 (IQR 0.9-1.5) mmol/L; P<0.001), lower HDL-cholesterol (1.1 (IQR 0.9-1.3) vs 1.4 (IQR 1.2-1.6) mmol/L; P<0.001) and lower LDL-cholesterol (2.4 (0.8) vs. 3.6 (0.9) mmol/L; P<0.001). A larger proportion of cases had reduced estimated glomerular filtration rate (19.7% vs. 4.7%, P<0.001) and prevalent macrovascular disease (38.0% vs 8.3%, P<0.001) compared to diabetes-free controls. More cases had a first-degree relative with T2DM compared to controls (64.4% vs 33.3%, P<0.001). More baseline characteristics can be found in Table 1.

Primary care versus hospital-based outpatient clinic

Table 2 shows baseline characteristics of patients with T2DM in primary care and hospital-based outpatient clinic. Patients with T2DM from the outpatient clinic had longer median duration of diabetes compared to primary care (12.5 (IQR 7.2-17.8) vs. 4.6 (IQR 1.2-7.9) years; P<0.001) while they were diagnosed at a younger age (50.8 (10.8) vs. 58.4 (11.3) years, P<0.001). At the outpatient clinic, participants had higher BMI (30.2 (IQR 26.8-33.7) vs. 29.0 (IQR 26.0-32.0) kg/m^2; P<0.001), HDL-cholesterol (1.2 (IQR 1.0-1.4) vs.1.1 (IQR 0.9-1.3); P<0.002), HbA1c (56.3 (IQR 48.1-64.5) vs. 48.6 (43.7-53.6) mmol/mol; P<0.001) and higher creatinin (81 (67-95) vs. 76 (64-88) umol/L; P<0.001). Total cholesterol (4.3 (0.9) vs 4.2 (0.9); P=0.04) and LDL-cholesterol (2.6 (0.8) vs. 2.3 (0.8); P<0.001) was higher in primary care patients. A larger proportion of patients with T2DM at the outpatient clinic had reduced estimated glomerular filtration rate (25.5% vs. 15.2%, P<0.001), macrovascular disease (41.9% vs. 34.8%; P=0.002) and microvascular disease (63.8% vs. 20.7%) compared to patients with T2DM from primary care. We could not retrieve reliable data on neuropathy nor diabetic foot in primary care population. More patients from the outpatient clinic had a first-degree relative with T2DM compared to controls (64.4% vs. 33.3%, P<0.001).

Table 1: General baseline characteristics of participants with and without T2DM

	Cases	Controls	p-value
Number of participants	1886	854	
Female sex, n (%)	874 (46.4)	511 (59.8)	<0.001
Age, yr, median (IQR)	65.7 (58.5-72.9)	64.9 (60.4-69.4)	0.72
Age of onset diabetes, yr, median (IQR)	55 (47-63)	N/A	N/A
Duration of diabetes, yr, median (IQR)	8.1 (2.8-13.5)	N/A	N/A
BMI, kg/m^2, median (IQR)	29.5 (26.4-32.7)	25.5 (23.3-27.7)	<0.001
HbA1c, mmol/mol, median (IQR)	50.8 (43.7-57.9)	37.7 (36.1-39.3)	<0.001
Diabetes treatment, % (n / n-available / n-missing)			
No glucose-lowering medication	19.2 (340 / 1772 / 114)	N/A	N/A
Oral glucose-lowering agent	64.3 (1140 /1773 / 113)	N/A	N/A
Insulin	32.3 (572 / 1772 / 114)	N/A	N/A
Systolic blood pressure, mmHg, median (IQR)	140 (129-151)	137 (124-150)	<0.001
Diastolic blood pressure, mmHg, median (IQR)	78 (71-85)	82 (76-89)	<0.001
Total Cholesterol, mmol/L, median (IQR)	4.2 (3.6-4.8)	5.6 (4.9-6.2)	<0.001
Triglycerides, mmol/L, median (IQR)	1.4 (0.9-2.0)	1.2 (0.9-1.5)	<0.001
HDL-cholesterol, mmol/L, median (IQR)	1.1 (0.9-1.3)	1.4 (1.2-1.6)	<0.001
LDL-cholesterol, mmol/L, median (IQR)	2.3 (1.8-2.8)	3.5 (2.9-4.1)	<0.001
Creatinin, µmol/L, median (IQR)	78 (66-91)	72 (63-81)	<0.001
eGFR < 60ml/min, % (n / n-available / n-missing)	21.2 (372 / 1756 / 130)	5.0 (40 / 795 / 59)	<0.001
Cardiovascular disease, % (n / n-available / n-missing)			
Any macrovascular disease	38.0 (660 / 1738 / 148)	8.3 (68 / 824 / 30)	<0.001
Ischemic heart disease	28.0 (497 / 1778 / 108)	4.9 (41 / 842 / 12)	<0.001
Ischemic brain disease	12.0 (211 / 1757 / 129)	1.4 (12 / 840 / 14)	<0.001
Peripheral arterial disease	10.8 (193 / 1783 / 103)	2.2 (18 / 823 / 31)	<0.001
Microvascular diabetes complications, % (n / n-available / n-missing)			
Any microvascular disease	34.3 (561 / 1637 / 249)	N/A	N/A
Diabetic retinopathy	17.3 (308 / 1778 / 108)	N/A	N/A
Diabetic nephropathy	23.0 (387 / 1684 / 202)	N/A	N/A
Family history, % (n / n-available / n-missing)			
First-degree relative with T2DM	64.4 (1104 / 1714 / 172)	33.3 (269 / 809 / 45)	<0.001
First-degree relative with CVD	68.3 (1086 / 1590 / 296)	68.7 (519 / 755 / 99)	0.87
Any relative with early-onset CVD	45.0 (780 / 1732 / 154)	41.5 (342 / 825 29)	0.09
Descent:			
Caucasian descent, % (n / n-available / n-missing)	91.9 (1613 / 1755)	96.1 (810 / 843 / 11)	<0.001
Age of death father, yr, median (IQR)	73 (65-82)	75 (67-84)	<0.001
Age of death mother, yr, median (IQR)	78 (70-86)	81 (73-89)	<0.001

Table 1 shows baseline characteristics of participants from the Diagene Study. BMI, body mass index; CVD, cardiovascular disease; eGFR, estimated glomerular filtration rate calculated with the Modification of Diet in Renal Disease-formula; IQR, interquartile range; n-total, total number of participants for whom information was available; T2DM, type 2 diabetes mellitus; Yr, year.

Table 2: general baseline characteristics of participants in primary care and hospital-based outpatient clinic at inclusion.

	Primary Care	Outpatient clinic	p-value
Number of participants	1056	830	
Female sex, n (%)	494 (46.8)	380 (45.9)	0.71
Age, yr, median (IQR)	65.5 (58.1-72.9)	65.9 (58.9-72.9)	0.66
Age of onset diabetes, yr, median (IQR)	59 (51-67)	51 (44-59)	<0.001
Duration of diabetes, yr, median (IQR)	4.5 (1.2-7.9)	12.5 (7.2-17.8)	<0.001
BMI, kg/m^2, median (IQR)	29.0 (26.0-32.0)	30.2 (26.8-33.7)	<0.001
HbA1c, mmol/mol, median (IQR)	48.6 (43.7-53.6)	56.3 (48.1-64.5)	<0.001
Diabetes treatment, % (n / n-available / n-missing)			
No medication	24.7 (248 / 1004 / 52)	12.0 (92 / 768 / 62)	<0.001
Oral glucose-lowering agents	72.9 (732 / 1004 / 52)	53.1 (408 / 768 / 62)	<0.001
Insulin	8.6 (86 / 1004 / 52)	63.3 (486 / 768 / 62)	<0.001
Systolic blood pressure, mmHg, median (IQR)	146 (133-159)	134 (126-143)	<0.001
Diastolic blood pressure, mmHg, median (IQR)	79 (72-86)	75 (70-80)	<0.001
Total Cholesterol, mmol/L, median (IQR)	4.2 (3.6-4.9)	4.1 (3.6-4.6)	0.047
Triglycerides, mmol/L, median (IQR)	1.4 (0.9-1.9)	1.5 (1.0-2.0)	0.104
HDL-cholesterol, mmol/L, median (IQR)	1.1 (0.9-1.3)	1.2 (1.0-1.4)	0.002
LDL-cholesterol, mmol/L, median (IQR)	2.5 (2.0-3.1)	2.1 (1.7-2.6)	<0.001
Creatinin, µmol/L, median (IQR)	76 (64-88)	81 (67-95)	<0.001
eGFR < 60ml/min % (n / n available/ n-missing)	16.4 (160/978/78)	27.2 (212/778/52)	<0.001
Cardiovascular disease, % (n / n-available/ n-missing)			
Any macrovascular disease	34.8 (335 / 963 / 93)	41.9 (325 / 775 / 55)	0.002
Ischemic heart disease	25.2 (252 / 1000 / 56)	31.5 (245/ 778 / 52)	0.004
Ischemic brain disease	12.7 (124 / 973 / 83)	11.1 (87 / 784 / 46)	0.302
Peripheral arterial disease	9.2 (88 / 958 / 98)	12.7 (105 / 825 / 5)	0.018
Microvascular diabetes complications, % (n / n-available / n-missing)			
Any microvascular disease	20.7 (172 / 830 / 226)	48.2 (389 / 807 / 23)	<0.001
Diabetic retinopathy	6.1 (59 / 962 / 94)	30.5 (249 / 816 / 15)	<0.001
Diabetic nephropathy	15.4 (134 / 868 / 188)	31.0 (253 / 816 / 15)	<0.001
Neuropathy	Unknown	31.2 (238 / 762 / 68)	N/A
Family history, % (n / n-available / n-missing)			
First-degree relative with T2DM	61.4 (586 / 955 / 101)	68.2 (518 / 759 / 71)	0.003
First-degree relative with CVD	67.6 (608 / 899 / 157)	69.2 (478 / 691 / 139)	0.712
Any relative with early-onset CVD	45.0 (436 / 968 / 88)	45.0 (344 / 764 / 66)	1.0
Descent			
Caucasian descent, % (n / n-available / n-missing)	90.3 (892 / 988 / 132)	94.0 (721 / 767 / 63)	0.005
Age of death father, yr, median (IQR)	73 (65-82)	73 (65-82)	0.728
Age of death mother, yr, median (IQR)	79 (72-87)	77 (69-85)	0.055

Table 2 shows baseline characteristics of participants from the DiaGene Study in both primary care and hospital-based outpatient clinic. BMI, body mass index; CVD, cardiovascular disease; eGFR, estimated glomerular filtration rate calculated with the Modification of Diet in Renal Disease-formula; HDL, high-density lipoprotein; IQR, interquartile range; LDL, low-density lipoprotein; n-total, total number of participants for whom information was available; T2DM, type 2 diabetes mellitus; Yr, year.

Genetics

Table 3 shows the associations of 11 well-established genetic T2DM variants in our study population. Hardy-Weinberg's equilibrium was met for all variants. With the exception of the variant in KCNJ11, all T2DM susceptibility variants had higher allele frequencies in cases with T2DM than in controls. TCF7L2 showed the highest odds ratio for prevalent T2DM (OR 1.37 (95%CI 1.17, 1.60; P<0.001). These results were unaffected by additional correction for center of inclusion. After calculation of interaction effects, the associations of all genetic variants except for KCNJ11 did not significantly differ from the large scale meta-analyses of Morris et al. [44].

Table 3: Allele frequencies, odds ratios and 95% confidence intervals of genetic variants and risk of T2D in Diagene, original discovery studies and most recent meta-analysis of genome-wide-association studies.

		Diagene		Original discovery study results			Morris et al. 2012 [52]
Locus- Marker	Risk allele / other	Risk allele frequency Case / control / total	OR (95%CI)	Ceu-Hap Map	OR (95%CI)	Reference original study	OR (95%CI)
CDKAL1 - rs7754840	C/G	0.36 / 0.31 / 0.35	1.23 (1.06-1.44) ; p = 0.006	0.31	1.12 (1.08-1.16)	[38,39,41,42]	1.15 (1.11-1.19)
CENTD2 - rs1552224	A/C	0.86 / 0.86 / 0.86	0.95 (0.77-1.16) ; p = 0.60	0.88	1.14 (1.11-1.17)	[37]	1.13 (1.08-1.19)
DUSP9 - rs5945326	G/A	0.22 / 0.22 / 0.22	1.02 (0.88-1.18); p = 0.77	0.12	1.27 (1.18-1.37)	[37]	N/A (on X-chromosome)
FTO - rs8050136	A/C	0.40 / 0.38 / 0.39	1.06 (0.91-1.22); p = 0.45	0.45	1.15 (1.09-1.22)	[41]	1.11 (1.07-1.15)
HHEX - rs1111875	C/T	0.64 / 0.63 / 0.63	1.01 (0.87-1.16) ; p =0.95	0.56	1.13 (1.08-1.17)	[38]	1.15 (1.11-1.18)
IGFBP2 - rs4402960	T/G	0.33 / 0.32 / 0.33	1.01 (0.87-1.18) ; p = 0.89	0.29	1.17 (1.10-1.25)	[41]	1.13 (1.09-1.17)
KCNJ11 - rs5219	T/C	0.37 / 0.39 / 0.37	0.92 (0.80-1.07) ; p = 0.29	0.50	1.15 (1.09-1.21)	[38]	1.08 (1.05-1.12)
KCNQ1 - rs231362	G/A	0.53 / 0.49 / 0.52	1.16 (1.00-1.34) ; p = 0.04*	0.52	1.08 (1.06-1.10)	[40]	1.11 (1.07-1.16)*
PPARG-P12A - rs1801282	C/G	0.89 / 0.88 / 0.89	1.13 (0.91-1.42) ; p = 0.27	0.92	1.14 (1.08-1.20)	[38,39,42]	1.16 (1.11-1.22)
TCF7L2 rs7903146	T/C	0.36 / 0.28 / 0.34	1.37 (1.17-1.60) ; p <0.001	0.25	1.37 (1.28-1.47)	[41]	1.40 (1.35-1.46)
THADA rs7578597	T/C	0.91 / 0.88 / 0.90	1.36 (1.08-1.71) ; P =0.01	0.92	1.15 (1.10-1.20)	[41]	1.14 (1.08-1.22)

Table 3 shows odds ratios of association with type 2 diabetes for different known risk alleles tested in our study population. Logistic regression analysis is age, sex and center of inclusion-adjusted. CEU, Caucasian; OR, odds-ratio; CI, confidence interval. * statistically significant difference of odds ratio in association of genetic variant with T2DM when compared to Morris et al. 2012 [52].

Discussion

In this manuscript, we present the baseline characteristics and future perspectives of the DiaGene study, a new multi-centre cohort study with prospective follow-up on biochemical and genetic determinants of T2DM and its complications. We show that the population is representing both primary and secondary care and that despite treatment, considerable rates of macrovascular and microvascular complications are present. To further elucidate determinants of T2DM and its complications, multi-layer omics and prospective analyses will be of great value. Our study offers excellent opportunities to perform these analyses.

In the Netherlands, primary care practices are led by general practitioners, who are easily accessible and offer essential family medicine. Outpatient clinics of hospitals provide specialized care and require referral by the general practitioner for reimbursement by insurance companies. Therefore, complex and more severely affected patients will be referred to the hospital-based outpatient clinics. This is reflected in the higher prevalence of micro- and macrovascular complications at the outpatient clinics in our population.

The risk of microvascular disease can be reduced substantially by glycemic control and general measures to prevent cardiovascular disease such as lifestyle, blood pressure and lipid optimization [22, 23, 25]. Rates of microvascular disease in our study at baseline were 17.3%, 23.0% and 31% for retinopathy, nephropathy and neuropathy, respectively. This incidence of retinopathy in T2DM is comparable to a report from the Dutch National Institute for Public Health and the Environment [45] and in line with a worldwide meta-analyses for diabetes with a duration of less than 10 years [46], but higher than in a screening study for T2DM from the Netherlands [47]. In the latter study, the duration of T2DM was short and this probably explains the difference. For nephropathy, our rate is slightly lower than in the United Kingdom Prospective Diabetes Study (25%), also probably because of shorter follow-up [16]. Our primary care population appeared to have lower rates of nephropathy compared to studies on prevalent diabetes and newly diagnosed diabetes in patients of general practitioners in the Netherlands [47, 48]. Although the single urinary measurement-based prevalence rates in the latter could be an explanation for this discrepancy. The percentage of patients with T2DM and neuropathy in our population (31%) is lower compared to a prospective study (50%) with 25 years of follow-up from diagnosis [19] and comparable to a cross-sectional study on peripheral neuropathy in the United Kingdom [49].

The risk of macrovascular disease in T2DM can be successfully reduced by applying lifestyle interventions, lipid lowering therapies and antihypertensive treatment. The relationship with glycemic control is more complex. Even though glycemic control epidemiologically is strongly related to cardiovascular disease in T2DM, interventions applying strict glycemic control were unsuccessful [22, 50] or even showed adverse effects [51]. Macrovascular disease rates in our population with T2DM is comparable to previous reports in the Netherlands [45, 52], but lower than in an interview-based study in diabetes

patients in the USA [53]. Our population is on average 5 years older than the patients in this American study, and also contains a significant proportion of patients from outpatient clinics having further progressed disease.

T2DM and its complications are multifactorial in their pathophysiology's. Genetics, epigenetics, biological mechanisms and environmental factors are probably interacting at multiple levels. Therefore a pathway-based approach in well-defined cohorts is needed, supported by full use of information technology. High throughput research has been mainly focused on genome wide genetic associations. This has elucidated interesting associations. Yet the results only explain disease susceptibility to a small extent [31, 33]. We are planning to perform genome-wide association analysis in the near future. The quality control of this future genomic work will include analyses of the genetic-based ethnic background to definitively determine population sub-structures. Here, we restricted our analyses of well-known genetic T2DM risk variants to the sub-group of self-reported Caucasians. These DNA polymorphisms showed similar associations in our mainly Caucasian population as in previous extensive meta-analyses: most genetic variants had similar direction of their associations as earlier reported and for TCF7L2, THADA, KCNQ1 and CDKAL1 this was significant [32, 44, 54]. KCNJ11 and CENTD2 showed a slight but not statistically significant opposite association to what has previously described, with estimates close to 1 and confidence intervals embracing the estimates from literature [32]. Except for KCNJ11, all genetic variants had non-significant interaction effects for odds ratios of T2DM-risk variants compared to the latest meta-analysis [44]. The significant difference for KCNJ11 can be an effect of population-specific variance, differences in environmental factors, age or interactions of these factors with the genetic variant [44].

To study the aetiology of T2DM and its complications we need well phenotyped cohorts with prospective follow-up. Our population has these characteristics. We therefore plan to analyse several omics layers for their associations with T2DM and its complications. We are currently measuring total N-glycomics with matrix-assisted laser desorption-ionization-time of flight (MALDI-TOF), -Fourier transform ion cyclotron resonance mass spectrometry (MALDI-FTICR) [55] and IgG-glycomics with ultra-performance liquid chromatography [56]. In the near future, we aim to include lipidomics, with a focus on lipoprotein(a), metabolomics, and proteomics. Also we plan to perform genomics using the Illumina chip, for mendelian randomization and multilayer interaction analyses. The overall goal being to elucidate new pathophysiological pathways for prediction, prevention and treatment of T2DM.

Although we have performed our study with precision, we need to consider a number of limitations. A large majority of our population is of self-reported Caucasian ethnicity, which limits extending conclusions from our analyses to non-Caucasian populations. However, it also makes our analyses less vulnerable to genetic population stratification bias. Self-reported Caucasian mono-ethnicity in two generations results in a very limited risk of

misclassifying genetic admixtures [57, 58]. In addition, a small proportion of diabetes-free subjects where recruited by asking T2DM subjects to invite unrelated family members and friends. Hence, absence of family ties was self-reported, with a small possibility of hidden relatedness. In the near future, we will perform genome-wide association analysis, which will allow us to perform formal quality control and accurately account for hidden relatedness and genetic population stratification bias [59]. Another limitation of this study was our inability to retrieve information on neuropathy in primary care setting. Conclusions on neuropathy are therefore restricted to the secondary care setting. We have made extensive efforts to optimise the reliability of our data by having two independent investigators collect the data and reach consensus. This means we did have to rely on common clinical practice and adequate record keeping in primary and secondary care. For macrovascular events in primary care we had to rely on self-reported data. For validation, we have therefore checked self-reported myocardial infarction data from hospital-based participants and found that in only 6.0% of participants with self-reported myocardial infarction this diagnosis was not confirmed in hospital data. These events have therefore been scored as missing. Underestimation of the incidence of myocardial infarction based on hospital discharge data has however been described before [60]. And although the questionnaire on lifestyle, medication, clinical events and family history was straight-forward and easy to use, it is not an externally validated questionnaire. At last, our preliminary genetic results had approximately 10% missing values. We are currently collecting additional samples from the participants whose DNA was not available at the time of the current genetic analysis to improve our genetic analysis. Further strengths of our study are the meticulous hands-on medical file review for each patient by two separate physicians, which produced high-quality data that enable us to research both T2DM itself as well as its complications in great detail. Currently, we are finalizing the first collection prospective follow up on all T2DM complications. The prospective cohort setting with concurrent inclusion of diabetes-free individuals at baseline, will allow us to perform cross-sectional and prospective endpoint analyses to study aetiology and progression of type 2 diabetes and its complications.

Conclusion

In conclusion, this manuscript describes the design and baseline characteristics of the DiaGene Study, a large multi-centre prospective follow-up cohort study on environmental, biochemical and genetic risk factors of T2DM and related vascular complications. By studying both clinical and complex biochemical parameters with a current focus on glycomics, genomics and lipidomics, the DiaGene Study aims to contribute to the pathophysiological understanding of T2DM and all its vascular complications in a prospective case-control setting.

References

1. Kahn CR: Banting Lecture. Insulin action, diabetogenes, and the cause of type II diabetes. *Diabetes* 1994, 43(8):1066-1084.
2. Stumvoll M, Goldstein BJ, van Haeften TW: Type 2 diabetes: pathogenesis and treatment. *Lancet* 2008, 371(9631):2153-2156.
3. Samuel VT, Shulman GI: The pathogenesis of insulin resistance: integrating signaling pathways and substrate flux. *J Clin Invest* 2016, 126(1):12-22.
4. Chan JC, Malik V, Jia W, Kadowaki T, Yajnik CS, Yoon KH, Hu FB: Diabetes in Asia: epidemiology, risk factors, and pathophysiology. *JAMA* 2009, 301(20):2129-2140.
5. da Rocha Fernandes J, Ogurtsova K, Linnenkamp U, Guariguata L, Seuring T, Zhang P, Cavan D, Makaroff LE: IDF Diabetes Atlas estimates of 2014 global health expenditures on diabetes. *Diabetes Res Clin Pract* 2016, 117:48-54.
6. Flegal KM, Carroll MD, Ogden CL, Curtin LR: Prevalence and trends in obesity among US adults, 1999-2008. *JAMA* 2010, 303(3):235-241.
7. Narayan KM, Boyle JP, Geiss LS, Saaddine JB, Thompson TJ: Impact of recent increase in incidence on future diabetes burden: U.S., 2005-2050. *Diabetes Care* 2006, 29(9):2114-2116.
8. Herman WH: The Global Burden of Diabetes: An Overview. In: *Diabetes Mellitus in Developing Countries and Underserved Communities.* edn. Edited by Dagogo-Jack S. Cham: Springer International Publishing; 2017: 1-5.
9. Almdal T, Scharling H, Jensen JS, Vestergaard H: The independent effect of type 2 diabetes mellitus on ischemic heart disease, stroke, and death: a population-based study of 13,000 men and women with 20 years of follow-up. *Arch Intern Med* 2004, 164(13):1422-1426.
10. Emerging Risk Factors C, Sarwar N, Gao P, Seshasai SR, Gobin R, Kaptoge S, Di Angelantonio E, Ingelsson E, Lawlor DA, Selvin E *et al*: Diabetes mellitus, fasting blood glucose concentration, and risk of vascular disease: a collaborative meta-analysis of 102 prospective studies. *Lancet* 2010, 375(9733):2215-2222.
11. Kannel WB, McGee DL: Diabetes and glucose tolerance as risk factors for cardiovascular disease: the Framingham study. *Diabetes Care* 1979, 2(2):120-126.
12. Schramm TK, Gislason GH, Kober L, Rasmussen S, Rasmussen JN, Abildstrom SZ, Hansen ML, Folke F, Buch P, Madsen M *et al*: Diabetes patients requiring glucose-lowering therapy and nondiabetics with a prior myocardial infarction carry the same cardiovascular risk: a population study of 3.3 million people. *Circulation* 2008, 117(15):1945-1954.
13. Tancredi M, Rosengren A, Svensson AM, Kosiborod M, Pivodic A, Gudbjornsdottir S, Wedel H, Clements M, Dahlqvist S, Lind M: Excess Mortality among Persons with Type 2 Diabetes. *N Engl J Med* 2015, 373(18):1720-1732.
14. Ashfaq S, Ghazzal Z, Douglas JS, Morris DC, Veledar E, Weintraub WS: Impact of diabetes on five-year outcomes after vein graft interventions performed prior to the drug-eluting stent era. *J Invasive Cardiol* 2006, 18(3):100-105.
15. Chun BY, Dobson AJ, Heller RF: The impact of diabetes on survival among patients with first myocardial infarction. *Diabetes Care* 1997, 20(5):704-708.
16. Adler AI, Stevens RJ, Manley SE, Bilous RW, Cull CA, Holman RR, Ukpds G: Development and progression of nephropathy in type 2 diabetes: the United Kingdom Prospective Diabetes Study (UKPDS 64). *Kidney Int* 2003, 63(1):225-232.

17. Klein R, Klein BE, Moss SE, Davis MD, DeMets DL: The Wisconsin epidemiologic study of diabetic retinopathy. III. Prevalence and risk of diabetic retinopathy when age at diagnosis is 30 or more years. *Arch Ophthalmol* 1984, 102(4):527-532.
18. Partanen J, Niskanen L, Lehtinen J, Mervaala E, Siitonen O, Uusitupa M: Natural history of peripheral neuropathy in patients with non-insulin-dependent diabetes mellitus. *N Engl J Med* 1995, 333(2):89-94.
19. Pirart J: [Diabetes mellitus and its degenerative complications: a prospective study of 4,400 patients observed between 1947 and 1973 (author's transl)] Diabete et complications degeneratives presentation d'une etude prospective portant sur 4400 cas observes entre 1947 et 1973. (Premiere partie). *Diabete Metab* 1977, 3(2):97-107.
20. Standards of Medical Care in Diabetes-2016: Summary of Revisions. *Diabetes Care* 2016, 39 Suppl 1:S4-5.
21. Sluiter A vWH, Arntzenius A, Bots A, Dijkhorst-Oei L, van der Does F, Palmen J, Potter van Loon BJ, Schaper N, van Balen J: Dutch National Transmural Agreement (LTA) on type 2 diabetes mellitus. *Dutch national society of general practitioners* 2012, 55(1):S1-S12.
22. Intensive blood-glucose control with sulphonylureas or insulin compared with conventional treatment and risk of complications in patients with type 2 diabetes (UKPDS 33). UK Prospective Diabetes Study (UKPDS) Group. *Lancet* 1998, 352(9131):837-853.
23. Tight blood pressure control and risk of macrovascular and microvascular complications in type 2 diabetes: UKPDS 38. UK Prospective Diabetes Study Group. *BMJ* 1998, 317(7160):703-713.
24. Colhoun HM, Betteridge DJ, Durrington PN, Hitman GA, Neil HA, Livingstone SJ, Thomason MJ, Mackness MI, Charlton-Menys V, Fuller JH *et al*: Primary prevention of cardiovascular disease with atorvastatin in type 2 diabetes in the Collaborative Atorvastatin Diabetes Study (CARDS): multicentre randomised placebo-controlled trial. *Lancet* 2004, 364(9435):685-696.
25. Heart Protection Study Collaborative G: MRC/BHF Heart Protection Study of cholesterol lowering with simvastatin in 20,536 high-risk individuals: a randomised placebo-controlled trial. *Lancet* 2002, 360(9326):7-22.
26. Turnbull F, Neal B, Algert C, Chalmers J, Chapman N, Cutler J, Woodward M, MacMahon S, Blood Pressure Lowering Treatment Trialists C: Effects of different blood pressure-lowering regimens on major cardiovascular events in individuals with and without diabetes mellitus: results of prospectively designed overviews of randomized trials. *Arch Intern Med* 2005, 165(12):1410-1419.
27. Ali MK, Bullard KM, Saaddine JB, Cowie CC, Imperatore G, Gregg EW: Achievement of goals in U.S. diabetes care, 1999-2010. *N Engl J Med* 2013, 368(17):1613-1624.
28. Holman RR, Paul SK, Bethel MA, Matthews DR, Neil HA: 10-year follow-up of intensive glucose control in type 2 diabetes. *N Engl J Med* 2008, 359(15):1577-1589.
29. Xie X, Atkins E, Lv J, Bennett A, Neal B, Ninomiya T, Woodward M, MacMahon S, Turnbull F, Hillis GS *et al*: Effects of intensive blood pressure lowering on cardiovascular and renal outcomes: updated systematic review and meta-analysis. *Lancet* 2016, 387(10017):435-443.
30. Ziaeian B, Dinkler J, Guo Y, Watson K: The 2013 ACC/AHA Cholesterol Treatment Guidelines: Applicability to Patients with Diabetes. *Curr Diab Rep* 2016, 16(2):13.
31. Kwak SH, Park KS: Recent progress in genetic and epigenetic research on type 2 diabetes. *Exp Mol Med* 2016, 48:e220.
32. Billings LK, Florez JC: The genetics of type 2 diabetes: what have we learned from GWAS? *Ann N Y Acad Sci* 2010, 1212:59-77.
33. McCarthy MI: Genomics, type 2 diabetes, and obesity. *N Engl J Med* 2010, 363(24):2339-2350.

34. Alberti KG, Zimmet PZ: Definition, diagnosis and classification of diabetes mellitus and its complications. Part 1: diagnosis and classification of diabetes mellitus provisional report of a WHO consultation. *Diabet Med* 1998, 15(7):539-553.
35. American Diabetes A: Diagnosis and classification of diabetes mellitus. *Diabetes Care* 2011, 34 Suppl 1:S62-69.
36. Sims DS, Jr., Cavanagh PR, Ulbrecht JS: Risk factors in the diabetic foot. Recognition and management. *Phys Ther* 1988, 68(12):1887-1902.
37. Voight BF, Scott LJ, Steinthorsdottir V, Morris AP, Dina C, Welch RP, Zeggini E, Huth C, Aulchenko YS, Thorleifsson G *et al*: Twelve type 2 diabetes susceptibility loci identified through large-scale association analysis. *Nature Genetics* 2010, 42(7):579-589.
38. Diabetes Genetics Initiative of Broad Institute of H, Mit LU, Novartis Institutes of BioMedical R, Saxena R, Voight BF, Lyssenko V, Burtt NP, de Bakker PI, Chen H, Roix JJ *et al*: Genome-wide association analysis identifies loci for type 2 diabetes and triglyceride levels. *Science* 2007, 316(5829):1331-1336.
39. Scott LJ, Mohlke KL, Bonnycastle LL, Willer CJ, Li Y, Duren WL, Erdos MR, Stringham HM, Chines PS, Jackson AU *et al*: A genome-wide association study of type 2 diabetes in Finns detects multiple susceptibility variants. *Science* 2007, 316(5829):1341-1345.
40. Yasuda K, Miyake K, Horikawa Y, Hara K, Osawa H, Furuta H, Hirota Y, Mori H, Jonsson A, Sato Y *et al*: Variants in KCNQ1 are associated with susceptibility to type 2 diabetes mellitus. *Nature Genetics* 2008, 40(9):1092-1097.
41. Zeggini E, Scott LJ, Saxena R, Voight BF, Marchini JL, Hu T, de Bakker PI, Abecasis GR, Almgren P, Andersen G *et al*: Meta-analysis of genome-wide association data and large-scale replication identifies additional susceptibility loci for type 2 diabetes. *Nature Genetics* 2008, 40(5):638-645.
42. Zeggini E, Weedon MN, Lindgren CM, Frayling TM, Elliott KS, Lango H, Timpson NJ, Perry JR, Rayner NW, Freathy RM *et al*: Replication of genome-wide association signals in UK samples reveals risk loci for type 2 diabetes. *Science* 2007, 316(5829):1336-1341.
43. Altman DG, Bland JM: Interaction revisited: the difference between two estimates. *BMJ* 2003, 326(7382):219.
44. Morris AP, Voight BF, Teslovich TM, Ferreira T, Segre AV, Steinthorsdottir V, Strawbridge RJ, Khan H, Grallert H, Mahajan A *et al*: Large-scale association analysis provides insights into the genetic architecture and pathophysiology of type 2 diabetes. *Nature Genetics* 2012, 44(9):981-990.
45. Dutch National Institute for Public Health and the Environment (RIVM) on Health indicators in prevention and Diabetes Care. *Governmental report* 2006.
46. Yau JW, Rogers SL, Kawasaki R, Lamoureux EL, Kowalski JW, Bek T, Chen SJ, Dekker JM, Fletcher A, Grauslund J *et al*: Global prevalence and major risk factors of diabetic retinopathy. *Diabetes Care* 2012, 35(3):556-564.
47. Spijkerman AM, Dekker JM, Nijpels G, Adriaanse MC, Kostense PJ, Ruwaard D, Stehouwer CD, Bouter LM, Heine RJ: Microvascular complications at time of diagnosis of type 2 diabetes are similar among diabetic patients detected by targeted screening and patients newly diagnosed in general practice: the hoorn screening study. *Diabetes Care* 2003, 26(9):2604-2608.
48. Ubink-Veltmaat LJ, Bilo HJ, Meyboom-de Jong B: [Microalbuminuria in patients with type 2 diabetes mellitus in general practice] Microalbuminurie bij patienten met diabetes mellitus type 2 in de huisartspraktijk. *Ned Tijdschr Geneeskd* 2004, 148(41):2026-2030.
49. Young MJ, Boulton AJ, MacLeod AF, Williams DR, Sonksen PH: A multicentre study of the prevalence of diabetic peripheral neuropathy in the United Kingdom hospital clinic population. *Diabetologia* 1993, 36(2):150-154.

50. Action to Control Cardiovascular Risk in Diabetes Study G, Gerstein HC, Miller ME, Byington RP, Goff DC, Jr., Bigger JT, Buse JB, Cushman WC, Genuth S, Ismail-Beigi F *et al*: Effects of intensive glucose lowering in type 2 diabetes. *N Engl J Med* 2008, 358(24):2545-2559.
51. Group AC, Patel A, MacMahon S, Chalmers J, Neal B, Billot L, Woodward M, Marre M, Cooper M, Glasziou P *et al*: Intensive blood glucose control and vascular outcomes in patients with type 2 diabetes. *N Engl J Med* 2008, 358(24):2560-2572.
52. Spijkerman AM, Henry RM, Dekker JM, Nijpels G, Kostense PJ, Kors JA, Ruwaard D, Stehouwer CD, Bouter LM, Heine RJ: Prevalence of macrovascular disease amongst type 2 diabetic patients detected by targeted screening and patients newly diagnosed in general practice: the Hoorn Screening Study. *J Intern Med* 2004, 256(5):429-436.
53. Gregg EW, Cheng YJ, Saydah S, Cowie C, Garfield S, Geiss L, Barker L: Trends in death rates among U.S. adults with and without diabetes between 1997 and 2006: findings from the National Health Interview Survey. *Diabetes Care* 2012, 35(6):1252-1257.
54. Fuchsberger C, Flannick J, Teslovich TM, Mahajan A, Agarwala V, Gaulton KJ, Ma C, Fontanillas P, Moutsianas L, McCarthy DJ *et al*: The genetic architecture of type 2 diabetes. *Nature* 2016.
55. Wuhrer M: Glycomics using mass spectrometry. *Glycoconj J* 2013, 30(1):11-22.
56. Pucic M, Knezevic A, Vidic J, Adamczyk B, Novokmet M, Polasek O, Gornik O, Supraha-Goreta S, Wormald MR, Redzic I *et al*: High throughput isolation and glycosylation analysis of IgG-variability and heritability of the IgG glycome in three isolated human populations. *Mol Cell Proteomics* 2011, 10(10):M111 010090.
57. Mersha TB, Abebe T: Self-reported race/ethnicity in the age of genomic research: its potential impact on understanding health disparities. *Hum Genomics* 2015, 9:1.
58. Sinha M, Larkin EK, Elston RC, Redline S: Self-reported race and genetic admixture. *N Engl J Med* 2006, 354(4):421-422.
59. Price AL, Patterson NJ, Plenge RM, Weinblatt ME, Shadick NA, Reich D: Principal components analysis corrects for stratification in genome-wide association studies. *Nature Genetics* 2006, 38(8):904-909.
60. Merry AH, Boer JM, Schouten LJ, Feskens EJ, Verschuren WM, Gorgels AP, van den Brandt PA: Validity of coronary heart diseases and heart failure based on hospital discharge and mortality data in the Netherlands using the cardiovascular registry Maastricht cohort study. *Eur J Epidemiol* 2009, 24(5):237-247.

Supplementary material: Flow chart of the inclusion of cases and controls

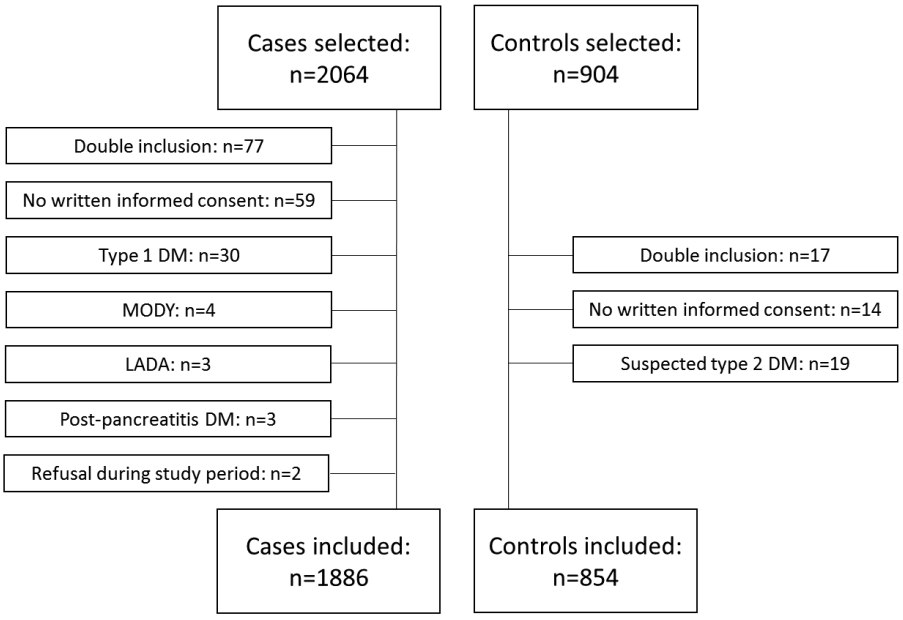

DM**,** diabetes mellitus; MODY, Maturity-Onset Diabetes of the Young; Latent Auto-immune Diabetes of the Adult

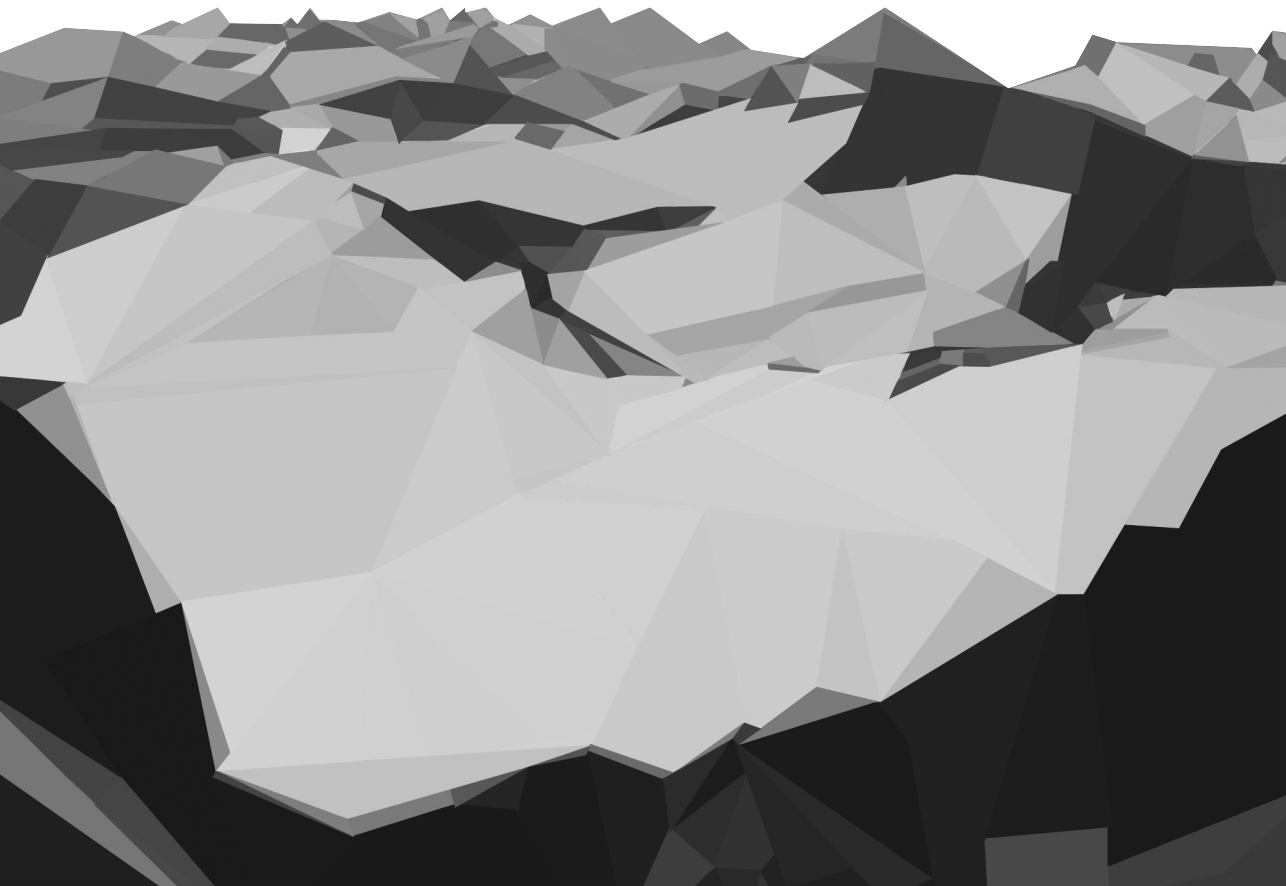

CHAPTER 3

Plasma Protein *N*-Glycan Signatures of Type 2 Diabetes

Viktoria Dotz*, Roosmarijn F.H. Lemmers*, Karli R. Reiding, Agnes L. Hipgrave Ederveen, Aloysius G. Lieverse, Monique T. Mulder, Eric J.G. Sijbrands, Manfred Wuhrer, Mandy van Hoek.

* Authors contributed equally.

Accepted for publication, Biochimica et Biophysica Acta

Abstract

Background: Little is known about enzymatic *N*-glycosylation in type 2 diabetes, a common posttranslational modification of proteins influencing their function and integrating genetic and environmental influences. We sought to gain insights into *N*-glycosylation to uncover yet unexplored pathophysiological mechanisms in type 2 diabetes.

Methods: Using a high-throughput MALDI-TOF mass spectrometry method, we measured *N*-glycans in plasma samples of the DiaGene case-control study (1583 cases and 728 controls). Associations were investigated with logistic regression and adjusted for age, sex, body mass index, high-density lipoprotein-cholesterol, non-high-density lipoprotein-cholesterol, and smoking. Findings were replicated in a nested replication cohort of 232 cases and 108 controls.

Results: Eighteen glycosylation features were significantly associated with type 2 diabetes. Fucosylation and bisection of diantennary glycans were decreased in diabetes (odds ratio (OR) = 0.81, p = 1.26E-03, and OR = 0.87, p = 2.84E-02, respectively), whereas total and, specifically, alpha2,6-linked sialylation were increased (OR = 1.38, p = 9.92E-07, and OR= 1.40, p= 5.48E-07). Alpha2,3-linked sialylation of triantennary glycans was decreased (OR = 0.60, p = 6.38E-11).

Conclusions: While some glycosylation changes were reflective of inflammation, such as increased alpha2,6-linked sialylation, our finding of decreased alpha2,3-linked sialylation in type 2 diabetes patients is contradictory to reports on acute and chronic inflammation. Thus, it might have previously unreported immunological implications in type 2 diabetes.

General significance: This study provides new insights into *N*-glycosylation patterns in type 2 diabetes, which can fuel studies on causal mechanisms and consequences of this complex disease.

Introduction

Diabetes mellitus type 2 is a disease with enormous morbidity and excess mortality [1]. Intensive therapy can reduce the burden of complications of the disease, but only to about 50% [2]. It is well-recognized as a multifactorial disease in which genetic susceptibility, numerous metabolic pathways, lifestyle and environmental factors interact at multiple levels [3]. These factors are known to also influence protein *N*-glycosylation [4-6]. Glycomics is a relatively new 'omics' approach that analyses complex sugar structures (glycans), which are among the four principal cell components besides DNA, proteins, and lipids [4]. Pathophysiological processes in type 2 diabetes are intricate and incompletely understood. 'Omics' approaches may increase our understanding of the pathophysiology and eventually advance the development of personalized diabetes medicine, early detection, and more effective treatment approaches [7].

Little is known about the enzymatic process called *N*-glycosylation in type 2 diabetes. *N*-Glycosylation is a common posttranslational modification of proteins involving the action of hundreds of different proteins such as glycosyltransferases, glycosidases, and transporters [4, 8]. Carbohydrate metabolic pathways are directly related to the biosynthesis of monosaccharides that are the substrates for glycosylation [6]. *N*-Glycans are highly diverse and have multiple functions, including important roles in protein folding, stability, and receptor-ligand interaction [4, 8]. *N*-Glycosylation is not to be confused with non-enzymatic glycation, such as in glycated hemoglobin (HbA1c) and in advanced glycation end products, which has been extensively investigated and is well-known for its detrimental effects on plasma proteins and DNA [9].

Most of the major plasma proteins are glycosylated and *N*-glycans have already been proposed as biomarkers and therapeutic targets for various inflammatory diseases and cancer [4]. In healthy individuals, plasma protein glycosylation is constant over time, but can dramatically change because of a pathological condition, especially upon inflammation [10, 11]. Furthermore, *N*-glycosylation changes have been associated with obesity, smoking, and aging [12-15], which are recognized risk factors for type 2 diabetes. However, a limited number of reports exist on plasma *N*-glycosylation in diabetes. Fucosylation of plasma *N*-glycans is partly regulated by hepatocyte nuclear factor 1-α (*HNF1A*) [16], of which rare variants cause type 3 maturity-onset diabetes of the young (MODY) [17] and of which a common genetic variant has been linked to type 2 diabetes [18]. Recently, we found decreased galactosylation and sialylation and increased bisection of fucosylated structures on immunoglobulin (Ig)G in type 2 diabetes, which corresponds with an increased inflammatory potential of IgG [19]. Reduced IgG sialylation in mice was shown to be implicated in obesity-induced insulin resistance [20]. In total plasma *N*-glycome, Testa *et al.* found that monogalactosylated, core-fucosylated diantennary *N*-glycans were reduced in individuals with type 2 diabetes compared to controls [21]. In this promising

pioneering work, a limited number of glycan structures were detected after the removal of sialic acids. Sialylation, however, has a crucial role in the functionality of *N*-glycans [22], and total plasma levels of sialic acid have been associated with incident type 2 diabetes [23, 24]. Recently, associations of increased complexity and sialylation of plasma *N*-glycan structures with a higher risk of type 2 diabetes were reported [25]. Therefore, comprehensive research of the total plasma *N*-glycome, including detailed sialylation analyses, is indicated to understand the contribution of these multifaceted structural glycan features to this complex disease. Our MALDI-TOF MS-based high-throughput approach is well suited for this purpose, as it identifies 70 glycan compositions and reveals information on not only fucosylation, bisection and sialylation [26], but also on sialic-acid linkage variants that have not been previously investigated.

In the present study, we sought to reveal differences in the detailed structural features of the plasma *N*-glycome between type 2 diabetes patients and healthy controls in a large case-control study, and performed a nested replication in a subsample of the population to gain a first insight into the possible involvement of plasma protein *N*-glycans in the pathophysiology of type 2 diabetes.

Methods

Plasma samples from the DiaGene study were used for the *N*-glycan measurements. DiaGene is a case-control study on type 2 diabetes (1886 cases and 854 controls) collected from the Eindhoven area in the Netherlands and is described in detail elsewhere [27], with basic characteristics summarized in Table 1. All samples were collected and stored according to the same protocol as described previously. The control samples were collected, stored and processed on the same location as the primary care patient samples.

All participants have given written informed consent. The study was approved by the Medical Ethical Committee of the Erasmus MC and is in compliance with the Declaration of Helsinki principles.

Total plasma N-glycome analysis

N-Glycans were analyzed after sialic-acid derivatization by a previously established MALDI-TOF MS method [26, 28], with minor modifications. Briefly, 5 µL plasma sample was denatured by the addition of 10 µL of 2% sodium dodecyl sulfate and incubation for 10 min at 60 °C. For glycan release, 10 µL of 2.5× phosphate-buffered saline containing 2% nonidet P-40 and 0.5 mU peptide-*N*-glycosidase F (Roche Diagnostics, Mannheim, Germany) were added followed by incubation for 16 h at 37 °C. Thereafter, during the derivatization procedure, α2,6-linked sialic acids were ethyl-esterified and α2,3-linked sialic acids were lactonized, facilitating mass-based discrimination of sialic-acid linkage variants. Released

Table 1. Characteristics of the study populations.

	Discovery cohort		Replication cohort	
	Cases	Controls	Cases	Controls
Total number	1583	728	232	108
Age (years)	65.2 ± 10.9	65.8 ± 7.0	65.1 ± 7.8	65.8 ± 5.0
Sex (female) (n, %)	748 (47.3)	456 (62.6)[c]	90 (38.8)	42 (38.9)
BMI (kg/m^2)	29.4 (26.6-33.0)	25.4 (23.3-27.8)[c]	30 (27.4-34)	25.8 (23.7-27.9)[c]
HDL-c (mmol/l)	1.10 (0.94-1.30)	1.42 (1.22-1.67)[c]	1.18 (1.00-1.40)	1.39 (1.19-1.64)[c]
Non-HDL-c (mmol/l)	3.00 (2.50-3.68)	4.03 (3.43-4.76)[c]	2.85 (2.4-3.46)	4.19 (3.54-4.66)[c]
Creatinine (µmol/l)	77 (67-92)	71 (63-80)[c]	77 (66-91)	77 (67-86)
Ever smoked (n, %)	1079 (74.3)	480 (68.4)[b]	158 (75.2)	64 (61.0)[a]
Currently smoking (n, %)	260 (18.1)	80 (11.4)[c]	34 (16.3)	9 (8.6)
Systolic BP (mmHg)	142 ± 19	139 ± 20[b]	142 ± 19	139 ± 18
Cardiovascular disease (n, %)	539 (37.1)	66 (9.4)[c]	89 (41.2)	0[c]
HbA1c (mmol/mol)	50.8 (45.4-59.6)	37.7 (35.5-38.8)[c]	51.9 (45.4-60.7)	36.6 (35.5-38.8)[c]
Duration of diabetes (years)	8 (3-14)	NA	10 (5-16)	NA
Insulin use (n, %)	452 (30.3)	NA	89 (40.1)	NA
Diabetic retinopathy (n, %)	223 (15.0)	NA	68 (29.4)	NA
Diabetic nephropathy (n, %)	311 (22.2)	NA	56 (25.7)	NA

Continuous data are represented as median and interquartile range or as mean ± SD in case of age and systolic blood pressure (BP). Clinical variables were compared between cases and controls with the Student's t-test or the Wilcoxon rank-sum test for normal and non-normal distributions, respectively, and with the $\chi 2$-test for binary data. All *p*-values are shown for cases *vs*. controls within the same cohort: [a] $p < 0.05$; [b] $p < 0.01$; [c] $p < 0.001$. BMI, body mass index; BP, blood pressure; HbA1c, glycated hemoglobin; HDL-c, high-density lipoprotein cholesterol; NA = not applicable.

glycans were purified using a 96-well filter plate with a GHP membrane (AcroPrep Advance 96 Filter plate, Pall Corporation, Ann Arbor, MI) on a Hamilton liquid-handling system. The derivatized sialylated glycans were detected simultaneously with nonsialylated *N*-glycans in positive-ion reflectron mode. In short, 10 µL of sample was premixed with 10 µL of 5 mg/mL super-DHB (Sigma-Aldrich, Steinheim, Germany) in 99% acetonitrile with 1 mM NaOH in a 384-well plate, 2 µL of which was spotted on plate. Mass spectra were acquired by an ultrafleXtreme MALDI-TOF mass spectrometer equipped with a Smartbeam-II laser operated by flexControl 3.4 (Build 135) (Bruker Daltonics, Bremen, Germany). A total of 20,000 shots at 1,000 Hz were accumulated per spectrum with a mass range of *m/z* 1,000–5,000. The MALDI-TOF-MS was calibrated using the Bruker Peptide Calibration Standard II. An acceleration voltage of 25 kV was applied following a 140 ns extraction delay. Using flexAnalysis 3.4 (Build 76) Batch Process, raw data were baseline-subtracted (TopHat) and smoothed (SavitzkyGolay), and .xy files were generated for further processing.

For the analyte composition list, three sum spectra were generated from selected mass spectra from cases with and cases without diabetic complications, and healthy controls,

eight mass spectra per group. In addition to the manual inspection of the peaks in the sum spectra, potential modifications for the 20 most abundant glycan compositions, including fragments, potassium adducts, and adducts from the derivatization reaction were considered, resulting in a list of 159 potential analytes with a distinct *m/z* value (Supplementary Table S1). Our in-house built software MassyTools version 0.1.8.1.2 [29] was used for area integration and internal calibration, with a list of high-intensity glycan signals distributed across the detected *m/z* range applied as calibrants: H3N4F1, H4N4F1, H5N4F1, H5N4E1F1, H6N5L1E2, H6N5L1E2F1 (Supplementary Table S1). The relative areas of the detected glycans were extracted by summing the isotopes within 80% of the isotopic envelope for each species. Furthermore, different quality parameters (see below) were calculated using MassyTools. Resulting mass errors and relative standard deviations (SD) of the calculated relative intensities of the glycan compositions are presented in Supplementary Table S1. For example, the relative SD of the main peak at *m/z* 2301 was 6.42%.

Mass spectra were excluded from further analysis if their total intensity was lower than 50,000 and their "Fraction of analyte area - background area above signal-to-noise ratio" was lower than 0.89 (corresponding to the mean minus 4-times the SD to ensure a sufficient intensity for the overall profile including minor peaks; see [29] for further details on the quality parameters). The reasoning for setting the cut-offs was confirmed by a manual inspection of several borderline spectra. After the removal of low-quality spectra, analyte compositions were removed from further analysis based on cut-offs for their signal-to-noise ratio, mass accuracy, isotopic pattern quality, and presence in a minimum percentage of the spectra within cases, healthy controls, or VisuCon-F plasma standard samples (Stago BNL, Netherlands). The cut-off values were as follows: signal-to-noise > 6, ppm error < 20, deviation from the theoretical isotopic pattern < 20 %, and present in at least 10% of spectra per group, i.e. cases, controls, or plasma standards. Only non-modified glycan compositions were further processed. The sum of the signal intensities of these remaining 70 compositions was normalized to 1, with each individual composition expressing a fraction thereof (total area normalization; see Figure 1 and Supplementary Table S1). From the 70 direct traits, 91 derived traits were calculated on the basis of their structural features (Supplementary Table S2) [25, 26, 30]. In case of ambiguity due to isomerism, for example in H5N5E1F1, bisection of diantennary glycans was assumed rather than an agalactosylated third antenna.

Experimental design and statistical analysis

In total, 2718 samples from the DiaGene cohort, 31 blanks and 155 VisuCon-F standard plasma samples were randomized over 31 96-well plates and prepared and analyzed as described above. After the removal of low-quality spectra during quality control and samples with insufficient clinical information, the discovery cohort data consisted of 1583 cases and 728 controls. For the nested replication cohort, 232 cases were randomly

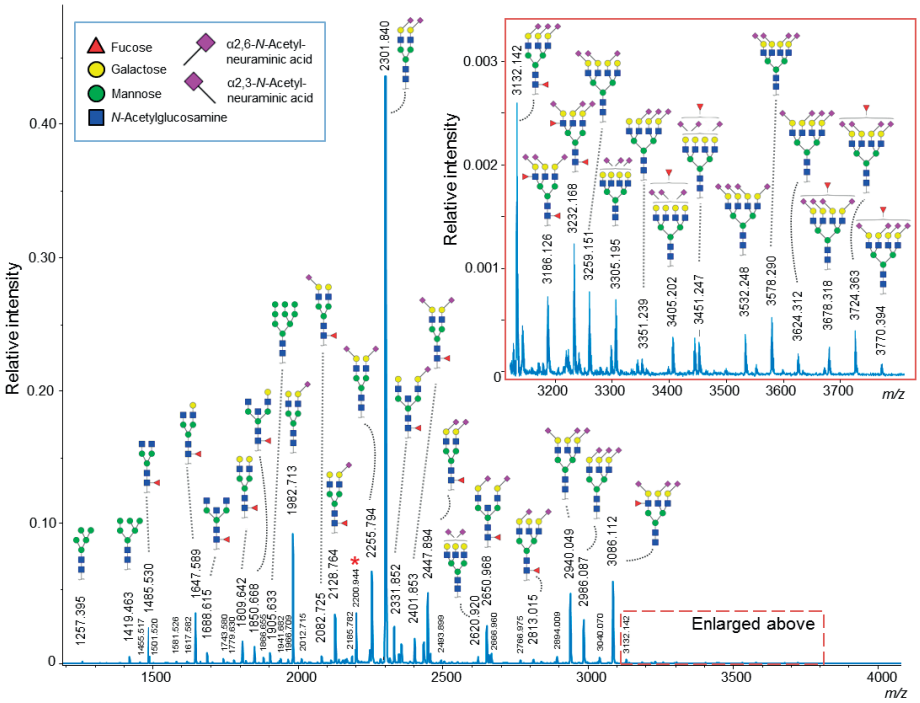

Figure 1: A typical MALDI-TOF mass spectrum of plasma protein *N*-glycans from the DiaGene cohort.

After enzymatic release of glycans, sialic acids were stabilized in linkage-specific manner and analyzed by positive-ion reflectron mode MALDI-TOF-MS. Observed *m/z* values for $[M+Na]^+$ species are depicted, with structures proposed for the most abundant species. The red asterisk marks a fragment of the species detected at *m/z* 2301.840. For the complete list of, in total, 70 quantified glycan species, see Supplementary Table S1. The inset shows the enlarged mass window of *m/z* 3130-3800.

selected using IBM SPSS Statistics (version 21.0) and 108 controls were selected matching on average age and sex frequencies as a group. A power calculation was performed using G*Power 3.1 [31]. At alpha = 0.05, we had 80% power to find odds ratios (ORs) <0.88 or >1.13 in the discovery cohort.

Statistical analyses were performed in RStudio (version 1.0.136). The distribution of the clinical variables was considered normal when Skewness and Kurtosis were within the range of -1 to +1. Clinical variables were compared between cases and controls with the Student's t-test or the Wilcoxon rank-sum test for normal and non-normal distributions, respectively. Binary data were compared with the χ2-test.

Direct and derived glycan traits were adjusted for batch effects by preparation day, MALDI plate, row and column effect using ComBat package in R. For the analyses of associations of *N*-glycans with clinical variables and diabetes, *N*-glycan relative intensities were centered by subtracting the mean and scaled by dividing by the SD. Linear regres-

sion was used for associations of *N*-glycans with continuous clinical variables, and logistic regression for associations with sex and smoking. Age, sex, and their interaction were used as covariates in a second model for the analysis of associations between *N*-glycans and clinical variables. For the sake of power, we chose to analyze the associations between *N*-glycans and clinical parameters in the entire cohort instead of stratifying for case/control status.

Associations of *N*-glycans with type 2 diabetes were assessed with logistic regression. The following covariates were included in three models: 1) age, sex, and their interaction; 2) model 1 + body mass index (BMI); and 3) model 2 + high-density lipoprotein-cholesterol (HDL-c), non-HDL-c, smoking. Outcomes of model 1 reflect the broad differences between cases and controls, while model 2 and 3 more specifically reflect the differences that are not mediated through risk factors for type 2 diabetes. The age-sex interaction was included as a covariate, since it was previously reported to affect various glycan traits [15]. Non-HDL-c was calculated as total cholesterol minus HDL-c. Smoking was divided in current smokers *vs.* former and non-smokers ('Current smoking') and in current and former smokers ('Ever having smoked') *vs.* non-smokers. Whenever values were missing per clinical variable in models 2 and 3, cases were excluded in the respective statistical analysis using the complete.cases() function in R; the exact numbers of cases and controls per analysis are stated in Table 2**.** Glycomic data was complete in all cases used for statistical analysis. Calculated ORs refer to an increase of one SD in the tested glycan traits. The Benjamini-Hochberg procedure [32] was applied to control for multiple testing, using a cutoff of q = 0.05 (5% false discovery rate).

Results

Data reliability

The complete list of the 70 quantified glycan compositions as well as additional signals from possible modifications and signals that did not pass our quality criteria is given in Supplementary Table S1. For the quantified species, relative intensities with their relative SD as extracted from technical replicates of 149 plasma standard samples that were randomized and measured together with the cohort samples demonstrate overall method repeatability on the direct-trait level. In addition, Supplementary Table S2 contains relative SD values based on our 91 derived glycan traits which were calculated from the 70 direct traits. As described before, derived glycan traits appear to have a higher technical robustness in glycomics studies compared to directly detected compositions [28]. Moreover, derived traits represent the different structural features corresponding to biosynthetic pathways in protein glycosylation as known from literature [25, 26, 30].

Subject characteristics

Detailed characteristics and numbers of the individuals included and excluded from the study are described elsewhere [27]. Details of the cohorts analyzed here for their glycomic signatures are given in Table 1 and glycomics data are shown in Figure 1 and Table S3. In both cohorts, cases had a higher BMI than controls, and a lower HDL-c and non-HDL-c. Moreover, a higher proportion of cases were smokers and had cardiovascular disease (Table 1). Additionally, in the discovery cohort, controls were more often female (62.6% *vs.* 47.3%) and had lower serum creatinine than cases.

Association of glycans with age, sex, and risk factors for type 2 diabetes

The largest effects associated with increasing age were found for decreased galactosylation and increased bisection of diantennary glycans (Supplementary Figure S2A and Table S4). With increasing age, both α2,3-linked and α2,6-linked sialylation increased for fucosylated glycans, but decreased for non-fucosylated glycans. Different glycosylation features

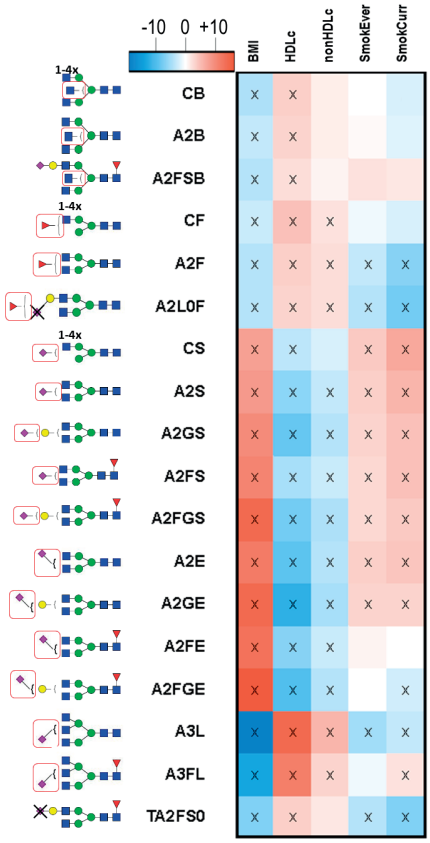

Figure 2: Associations of selected derived glycans with age, sex, BMI, HDL-cholesterol (HDLc), non-HDLc, and smoking for combined data from discovery and replication subsamples.

Associations were adjusted for age, sex, and their interaction. Colors represent the t-statistics (β / standard error); the × indicates *p*-values ≤ 0.033 (significance after FDR-adjustment). See Supplementary Table S2 for glycan derived trait description. Glycan trait abbreviations: B, bisection; C, within complex; A2, diantennary; F, fucosylation; L, α2,3-linked sialylation; S, sialylation; G, galactose; E, α2,6-linked sialylation; A3, triantennary; T, within total. Negative associations with type 2 diabetes are shown in blue, positive associations in red. Ever smoked, SmokEver; currently smoking, SmokCurr.

showed strong associations with sex, and moreover, an interaction between age and sex was observed (Supplementary Table S4 and Figure S1).

After adjustment for the covariates age, sex, and their interaction, multiple associations remained significant between glycans and BMI, HDL-c, non-HDL-c, and smoking (excerpt in Figure 2 and full version in Supplementary Figure S2B). For BMI, the strongest associations were with sialylation and sialic-acid linkage. With increasing BMI, overall sialylation increased in diantennary glycans (A2S) and decreased in tetraantennary glycans (A4S). Moreover, higher BMI was associated with lower α2,3-linked (A3L) and higher α2,6-linked sialylation (A2E). In addition, antennary fucosylation and bisection of several nonsialylated traits were positively associated with BMI, whereas bisection of mainly sialylated species and galactosylation of nonsialylated species were inversely associated. Smoking showed an association pattern similar to BMI, but additionally showed strong associations with fucosylation. For a few traits, sialic-acid linkage was associated with BMI and smoking in opposite directions, e.g. in A4F0E and A2(G)L. (Treated) HDL-c and non-HDL-c levels were similarly associated with *N*-glycans, but in the opposite direction from BMI and smoking, particularly regarding sialic-acid linkages. HDL-c and non-HDL-c were associated with low-complexity glycan traits (MM, MHy) in opposite directions (Supplementary Figure S2B).

Associations of glycans with type 2 diabetes

Multiple glycan traits were associated with type 2 diabetes in both the discovery and the replication cohort in all three models (Supplementary Table S5). Adding BMI as a covariate in model 2 affected *p*-values and effect sizes compared to model 1, but did not alter the direction of the associations and only few lost statistical significance. The replicated associations that remained significant after adjustment for additional risk factors in model 3 are shown in Table 2. The strongest associations were found for sialylated traits, particularly for di- and triantennary glycans (Figure 3). Sialylation of diantennary traits was higher in individuals with type 2 diabetes than in controls. Regarding sialic-acid linkage, diantennary α2,6-linked sialylation was increased and triantennary α2,3-linked sialylation was decreased in diabetes (A2(F)GE and A3L). In addition to sialylation changes, decreased bisection of mainly fucosylated sialylated diantennary species, and fucosylation of diantennary traits were associated with type 2 diabetes (A2FSB and A2F). Moreover, the total abundance of fucosylated nonsialylated diantennary species (TA2FS0), most likely derived from IgG [33], was decreased (Figure 3; Table 2).

Several derived traits that were associated with type 2 diabetes in the discovery cohort throughout the three models, also showed associations in the same direction in the smaller replication cohort, but lost significance after adjustment for risk factors for type 2 diabetes in model 3 (Supplementary Table S5). For instance, the abundance of diantennary *N*-glycans (CA2) was lower in type 2 diabetes while that of triantennary *N*-glycans (CA3) was higher. Galactosylation was decreased and bisection increased in traits related

Table 2. Associations between N-glycans and type 2 diabetes.

		Model 1: Age, sex, interaction				**Model 2:** Age, sex, interaction, BMI				**Model 3:** Age, sex, interaction, BMI, HDL-c, nonHDL-c, smoking			
		Discovery		Replication		Discovery		Replication		Discovery		Replication	
Sample number (cases/controls)		1583 / 728		232 / 108		1457 / 711		232 / 106		1308 / 650		206 / 100	
Trait	Description	OR	p	OR	p	OR	p	OR	p	OR	p	OR	p
Bisection (B)													
CB	in complex	0.82	2.17E-05	0.62	1.10E-04	0.86	3.37E-03	0.61	4.14E-04	0.86	1.45E-02	0.53	1.42E-03
A2B	in diantennary (A2)	0.85	3.02E-04	0.64	2.69E-04	0.87	9.80E-03	0.61	4.73E-04	0.87	2.84E-02	0.54	1.53E-03
A2FSB	in fucosylated sialylated A2	0.83	9.19E-05	0.68	1.71E-03	0.87	1.12E-02	0.67	5.53E-03	0.83	5.94E-03	0.61	1.05E-02
Fucosylation (F)													
CF	in complex	0.77	2.45E-08	0.62	1.21E-04	0.78	6.10E-06	0.60	3.61E-04	0.80	8.46E-04	0.61	9.05E-03
A2F	in diantennary (A2)	0.77	1.17E-08	0.61	6.53E-05	0.79	8.24E-06	0.59	2.33E-04	0.81	1.26E-03	0.61	1.14E-02
A2L0F	in A2 w/o α2,3-sialylation	0.77	1.49E-08	0.61	6.77E-05	0.79	4.75E-06	0.59	2.74E-04	0.80	5.54E-04	0.61	1.17E-02
Sialylation (S)													
CS	in complex	1.47	2.83E-16	1.72	1.20E-05	1.38	8.78E-10	1.54	2.10E-03	1.46	7.65E-09	1.65	8.26E-03
A2S	in diantennary (A2)	1.50	3.31E-18	1.95	2.68E-07	1.38	7.83E-10	1.80	8.54E-05	1.38	9.92E-07	1.87	1.78E-03
A2GS	per galactose in A2	1.57	2.48E-21	2.18	6.83E-09	1.40	2.66E-10	1.98	1.15E-05	1.34	7.99E-06	1.90	1.30E-03
A2FS	in fucosylated A2	1.61	9.72E-23	1.89	1.32E-06	1.46	9.88E-12	1.59	1.80E-03	1.55	4.09E-10	1.75	4.19E-03
A2FGS	per galactose in fucosylated A2	1.84	5.72E-33	2.35	1.31E-09	1.58	7.58E-16	1.94	3.4E-05	1.60	2.91E-11	1.93	9.69E-04
α2,6-sialylation (E)													
A2E	in diantennary (A2)	1.66	4.74E-26	2.15	1.53E-08	1.44	2.04E-11	1.84	7.96E-05	1.40	5.48E-07	1.96	1.18E-03
A2GE	per galactose in A2	1.76	7.36E-31	2.45	3.26E-10	1.45	6.32E-12	2.01	1.62E-05	1.36	4.91E-06	2.02	8.21E-04
A2FE	in fucosylated A2	1.63	4.82E-23	1.77	1.19E-05	1.38	7.84E-09	1.36	3.48E-02	1.45	1.51E-07	1.64	1.15E-02
A2FGE	per galactose in fucosylated A2	1.79	5.01E-30	2.09	6.37E-08	1.44	2.26E-10	1.53	5.20E-03	1.44	3.52E-07	1.79	4.26E-03
α2,3-sialylation (L)													
A3L	in triantennary (A3)	0.45	1.32E-47	0.33	2.42E-11	0.58	1.36E-18	0.50	1.42E-04	0.60	6.38E-11	0.54	1.08E-02
A3FL	in fucosylated A3	0.55	7.45E-29	0.42	4.76E-08	0.69	3.35E-10	0.60	2.85E-03	0.69	1.02E-06	0.53	5.68E-03
IgG-related													
TA2FS0	fucosylated nonsialylated A2 in total	0.69	5.90E-15	0.59	1.69E-05	0.74	8.07E-09	0.65	1.73E-03	0.70	1.13E-08	0.59	5.68E-03

Associations of *N*-glycans with type 2 diabetes were assessed with logistic regression, and the Benjamini-Hochberg procedure was applied to control for multiple testing (cut-off at 5% false discovery rate). Glycan trait abbreviations are as follows: B, bisection; C, within complex; A2, diantennary; F, fucosylation; L, α2,3-linked sialylation; S, sialylation; G, galactose; E, α2,6-linked sialylation; A3, triantennary; T, within total. Negative associations with type 2 diabetes are shown in blue, positive associations in red. BMI, body mass index; HDL-c, HDL-cholesterol; OR, odds ratio; p, p-value.

to IgG (A2FS0G and A2FS0B). In contrast, galactosylation of sialylated diantennary glycans was increased (A2SG). Alpha2,3-sialylation of tetraantennary species (A4L) was decreased in type 2 diabetes, while α2,3-sialylation of fucosylated diantennary glycans (A2F(G)L) was increased, although only in the models adjusted for BMI (models 2 and 3).

When assessing the contributions of individual glycan compositions, it becomes apparent that mainly the mono-, di-, and tri-α2,6-sialylated triantennary glycans H6N5E(1-3) drove the increase of A3E in diabetes (Supplementary Table S6). Various IgG-related compositions, such as H4N4F1, H5N4F1, and H5N5F1 showed a decrease, as well as various α2,3-sialylated species, such as H7N6(F1)E1L3 and H5N4(F1)E1L1.

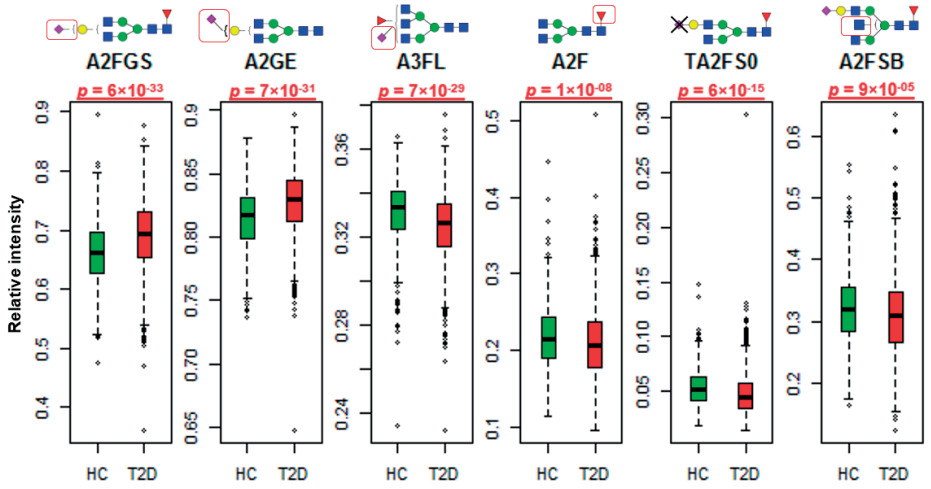

Figure 3: Selected derived glycan traits in healthy controls (HC, green) and individuals with type 2 diabetes (T2D, red) from the discovery cohort.

The 25th, 50th and 75th percentiles and whiskers at 1st quartile minus 1.5*interquartile range (Q1 - 1.5*IQR) and Q3 + 1.5*IQR of the relative intensities are shown. P-values are shown for significant, replicated associations after adjustment for age, sex, and their interaction (model 1). See Table 2 for the entire list of replicated associations and Supplementary Table S2 for details on the derived glycan traits. A2, diantennary; F, fucosylation; G, galactosylation; S, sialylation; E, α2,6-linked sialylation; A3, triantennary; L, α2,3-linked sialylation; T, in total spectrum; B, bisection.

Discussion

Here, we describe associations of multiple plasma protein *N*-glycosylation features with type 2 diabetes. We found that sialylation of diantennary glycans was higher in type 2 diabetes than in healthy controls, while fucosylation and bisection were lower. Intriguingly, diabetes was strongly associated with the type of sialic-acid linkage, with lower α2,3-linked sialylation of triantennary glycans and higher α2,6-linked sialylation of diantennary structures.

Type 2 diabetes is a complex and multifactorial disease, characterized by metabolic disturbances often accompanied by obesity and low-grade systemic inflammation [34]. Considering the large disease burden of type 2 diabetes, a deeper insight into its pathophysiology is crucial. Studying protein *N*-glycosylation as a common posttranslational modification with high complexity, diversity, and functional impact has high potential for advancing this knowledge. Associations of unspecific serum/plasma glycan markers, *i.e.* total levels of sialic acid and *N*-acetylhexosamine, with inflammation and incident type 2 diabetes have previously been described and are partly explained by an absolute increase in acute phase proteins [23, 24, 35]. Our exploration of relative shifts of *N*-glycan patterns may point at pathophysiological processes involving multiple proteins, as we discuss below.

Sialylation

We observed increased sialylation of fucosylated diantennary structures in type 2 diabetes patients, which has previously been reported for individuals at risk of developing diabetes as well as in acute (post-surgical) inflammation [11, 25, 36]. Sialic acids influence plasma protein clearance and are directly involved in activation and control of the immune system. Moreover, their functions depend on the linkage type [22, 37]. Our finding of increased sialylation in diabetes and with increasing BMI was specifically due to α2,6-sialylation, while α2,3-sialylation decreased. Beta-galactoside alpha-2,6-sialyltransferase-1 (ST6Gal1), encoded by the *ST6GAL1* gene, is the enzyme attaching α2,6-sialic acid to *N*-glycans [38]. Interestingly, polymorphisms of *ST6GAL1* have been associated with type 2 diabetes in South East Asians [39], suggesting a potential causal relation between α2,6-sialylation and type 2 diabetes. ST6Gal1 enzyme activity was increased upon inflammation in both serum and liver in rats [40]. Moreover, an inflammation-limiting role of ST6Gal1 in plasma has been proposed in a study on aging [38]. It is tempting to speculate that increased ST6Gal1 enzyme activity may be a response to the low-grade chronic inflammation in type 2 diabetes.

The majority of the α2,6-sialylated diantennary fucosylated glycans (A2FGE) and the triantennary mono-α2,6-sialylated glycan H6N5E1, which were positively associated with type 2 diabetes in our study, are thought to be derived from soluble IgM and haptoglobin, respectively [33, 41, 42]. IgM and haptoglobin function as ligands for siglec-2 (CD22) [43], a sialic-acid-binding Ig-like lectin present on immune cells and pancreatic β-cells [44]. Increased α2,6-linked sialylation of IgM and haptoglobin might augment binding to CD22, and may thus have a role in inflammation and possibly also glucose homeostasis.

In contrast to α2,6-linked sialylation, α2,3-linked sialylation of larger glycans was lower in type 2 diabetes. The opposite was found in post-surgical, acute inflammation, where highly sialylated tri- and tetraantennary fucosylated glycans increased [11, 36]. Moreover, both α2,3- and α2,6-linked sialylation of larger glycans were higher in inflammatory bowel

disease patients than in healthy controls [45]. Large, sialylated, fucosylated glycans often contain terminal sialyl-Lewis X epitopes (consisting of an antennary fucose with an α2,3-linked sialic acid), especially on acute-phase proteins [33, 35, 46]. Increased abundance of sialyl-Lewis X epitopes on plasma glycoproteins during inflammation has been postulated to exert anti-inflammatory effects through competitive binding to endothelial E-selectin and blocking of immune-cell adhesion and extravasation into tissues [47]. Thus, reduced α2,3-linked sialylation in type 2 diabetes might be a sign of either disrupted anti-inflammatory mechanisms or other processes specific to type 2 diabetes that are not related to inflammation. Since data on sialylation in disease states is scarce, it remains unclear whether reduced α2,3-linked sialylation is only seen in diabetes or also in other diseases.

Fucosylation

We observed a decrease in fucosylation of diantennary glycans (A2F) in type 2 diabetes, which has also been linked to inflammation [36], increased C-reactive protein levels, and smoking [15]. This decrease was driven by decreases of the fucosylated species H4N4F1(E1), H5N4F1(E1), H5N5F1, H3N4F1, and H4N5F1. In healthy individuals, these glycans are mostly derived from IgG, and partly from other Igs [33, 48]. Thus, the decreased fucosylation of diantennary glycans might reflect a relative decrease of IgG glycans. Accordingly, decreased absolute IgG levels have been reported in type 2 diabetes [49]. Moreover, we recently found decreased fucosylation of nonsialylated, non-bisected IgG glycans in type 2 diabetes [19], which enhances the antibody-dependent cytotoxicity of IgG [50]. In contrast, Itoh *et al.* found an increased relative amount of the core-fucosylated bisected diantennary glycan (H5N5F1) in sera of individuals with type 2 diabetes [51]. However, a low-resolution analytical technique was used, bearing the risk of an overlap of different structures, and results were not adjusted for age, sex and risk factors for diabetes.

Our MS-based glycomics technique does not reveal whether a fucose is attached to an antennary *N*-acetylglucosamine or to the core. However, chromatographic analyses indicate that diantennary glycans mostly carry core-fucoses, while tri- and tetraantennary structures are more likely to carry antennary fucoses [12, 36]. Fucosylation co-occurring with an α2,3-linked sialic acid could indicate an antennary fucose within a sialyl-Lewis X epitope, as discussed in the sialylation paragraph. As an approximation of antennary fucosylation, we used glycans bearing two fucoses, which are represented by traits A3Fa and A4Fa and imply the presence of at least one antennary fucose. These were positively associated with age, BMI and smoking, but not with diabetes. Accordingly, in a previous report, no differences were found in the proportion of antennary fucosylated triantennary glycans between type 2 diabetes and healthy controls. In contrast, individuals with MODY3 showed decreased antennary fucosylation of triantennary glycans compared to both healthy and type 2 diabetes individuals [5]. MODY3 is caused by mutations in the *HNF1A* gene, which is thought to regulate fucosyltransferase activity and to modulate

antennary fucosylation [12]. Since we found no change in antennary fucosylation in type 2 diabetes, the decreased fucosylation is more likely caused by decreased diantennary core-fucosylated (Ig-derived) glycans.

Bisection

The addition of an *N*-acetylglucosamine in β1,4-linkage to the first mannose of the *N*-glycan core by *N*-acetylglucosamine-transferase-3 is called bisection. This process is in competition with other glycosyltransferases, including fucosyltransferase-8 for core-fucosylation and *N*-acetylglucosamine-transferase-5 for branching [52]. Bisection of fucosylated sialylated diantennary glycans (A2FSB) was reduced in type 2 diabetes in our cohort, while IgG-related bisection in the non-sialylated variant (A2FS0B) tended to increase, in agreement with our previous findings in isolated IgG [19]. Also, in an independent large cohort of mostly healthy individuals, the A2FSB trait showed a positive trend (p = 0.017) with increasing glucose-to-insulin ratio [15], indicative of a higher insulin sensitivity and supporting our finding in diabetes. Interestingly, A2FSB showed a positive association with rheumatoid arthritis, which is characterized by chronic inflammation [53]. In IgG, bisection enhances antibody-dependent cytotoxicity [50]. The biological effects of bisection in IgA and IgM glycans are largely unknown. A2FSB *N*-glycans are mostly derived from IgA, IgM, and the fragment antigen-binding portion of IgG, while non-bisected A2FS are mostly attributable to a mixture of glycoproteins released by the liver (*i.e.* acute phase proteins) [33]. Therefore, the decreased A2FSB possibly also reflects a decrease in *N*-glycans derived from Igs.

Galactosylation

Various galactosylation traits in diantennary glycans (A2G) were positively associated with type 2 diabetes in the first 2 models, but lost statistical significance in the replication cohort after adjustment for risk factors for type 2 diabetes. The latter might be due either to a power issue in the smaller replication cohort or to a causal relationship of the risk factors with A2G. Very recently, increased galactosylation was associated with an increased risk of type 2 diabetes (age- and sex-adjusted), in line with our findings in model 1 and 2 [25]. Beta-1,4-galactosyltransferases are responsible for galactosylation, and their activity in plasma has been associated with aging and diabetes [38, 54]. In contrast, IgG-related galactosylation (A2FS0G) tended to decrease in diabetes, which is in line with our study on IgG [19]. While a decrease in IgG galactosylation is a well-described phenomenon in different types of inflammation and aging [55], it remains unclear which mechanisms contribute to an increase of galactosylation in non-IgG plasma *N*-glycans.

Glycan complexity

We observed a positive association of triantennary (CA3) and a negative association of diantennary glycans (CA2) with type 2 diabetes in all models, although only replicated for model 1. Similarly, increased branching was associated with type 2 diabetes risk after adjustment for age and sex [25]. However, the decreased association strength after correction for BMI and other risk factors in our study suggests that higher glycan complexity is mediated through these risk factors.

Lastly, the decreased ratio of high-mannose to hybrid glycans (MHy) in type 2 diabetes in models 1 and 2 could be due to decreased apolipoprotein B-100 levels in cases, since high-mannose plasma glycans are, for a large part, derived from this apolipoprotein [33]. This is reflected by the lower non-HDL-c in cases than controls, explained by the use of lipid-lowering treatment. Accordingly, after adjustment for lipids in model 3 this association lost significance in both cohorts.

Strengths and limitations

A major advantage of this study is that we were able to reliably identify and quantify 70 different plasma *N*-glycan structures in a large type 2 diabetes case-control study, while others have focused on fewer structures with low-resolution techniques in smaller sample sizes. Our approach with sialic-acid derivatization provided unique insights into sialic-acid linkage-specific changes. The size of our discovery cohort ensured establishing robust associations between glycans and type 2 diabetes, even after adjustment for multiple risk factors for type 2 diabetes.

Nonetheless, several limitations apply to our findings. First, the glycan species analyzed often represent isomer mixtures, except for sialic-acid linkage isomers. Second, our data are normalized to the total area of the 70 detected structures and, for this reason, are dependent on the plasma levels of the respective glycoproteins. Future glycomic investigations on a protein-specific level, as previously studied in the DiaGene study for IgG [19], combined with data on the plasma levels of these proteins will give a deeper insight into the mechanisms underlying our observations. Currently, however, this is still beyond technical capabilities for large-scale studies. Third, a separate similar cohort was not available to replicate our findings. Instead, we created a randomly selected, age- and sex-matched subcohort for replication, which was smaller and therefore some true associations may not have become significant in this cohort. Fourth, our data is cross-sectional and therefore does not allow conclusions on the causality of the associations, although recent findings in individuals at risk of type 2 diabetes [25] are supportive of our results and do point in the direction of a causal relationship. Our results are a starting point for future research in independent prospective cohorts. Last, we were not able to adjust for possible effects of diabetes treatment on *N*-glycan profiles due to the absolute association of the endpoint

(diabetes) with the treatment. Collaborations are ongoing to assess treatment effects in the future.

Conclusion

In this cross-sectional study, we found robust associations between type 2 diabetes and the plasma *N*-glycome, especially regarding sialic-acid linkages. In part, glycans in type 2 diabetes appear to reflect a pro-inflammatory state. However, not all associations seem to be explained by inflammation, such as the observed decrease in α2,3-linked sialylation. Further studies should focus on protein-specific glycosylation changes. Moreover, prospective and genetic studies including Mendelian randomization and expression levels of glycosyltransferases and glycosidases should shed light on the causality and mechanisms involved. Eventually, knowledge on altered *N*-glycosylation, an essential but understudied physiological process, has the potential to improve insight in the pathophysiology of type 2 diabetes and could contribute to decreasing the burden of this major disease.

References

[1] WHO, Global report on diabetes, World Health Organization, 2016.

[2] P. Gaede, P. Vedel, N. Larsen, G.V. Jensen, H.H. Parving, O. Pedersen, Multifactorial intervention and cardiovascular disease in patients with type 2 diabetes, The New England journal of medicine, 348 (2003) 383-393.

[3] C.J. Nolan, P. Damm, M. Prentki, Type 2 diabetes across generations: from pathophysiology to prevention and management, The Lancet, 378 (2011) 169-181.

[4] G. Lauc, M. Pezer, I. Rudan, H. Campbell, Mechanisms of disease: The human N-glycome, Biochim. Biophys. Acta, Gen. Subj. , 1860 (2016) 1574-1582.

[5] G. Thanabalasingham, J.E. Huffman, J.J. Kattla, M. Novokmet, I. Rudan, A.L. Gloyn, C. Hayward, B. Adamczyk, R.M. Reynolds, A. Muzinic, N. Hassanali, M. Pucic, A.J. Bennett, A. Essafi, O. Polasek, S.A. Mughal, I. Redzic, D. Primorac, L. Zgaga, I. Kolcic, T. Hansen, D. Gasperikova, E. Tjora, M.W.J. Strachan, T. Nielsen, J. Stanik, I. Klimes, O.B. Pedersen, P.R. Njølstad, S.H. Wild, U. Gyllensten, O. Gornik, J.F. Wilson, N.D. Hastie, H. Campbell, M.I. McCarthy, P.M. Rudd, K.R. Owen, G. Lauc, A.F. Wright, Mutations in HNF1A Result in Marked Alterations of Plasma Glycan Profile, Diabetes, 62 (2013) 1329.

[6] A.G. McDonald, J.M. Hayes, G.P. Davey, Metabolic flux control in glycosylation, Current opinion in structural biology, 40 (2016) 97-103.

[7] M.I. McCarthy, Painting a new picture of personalised medicine for diabetes, Diabetologia, 60 (2017) 793-799.

[8] A. Varki, Biological roles of glycans, Glycobiology, 27 (2017) 3-49.

[9] S. Ahmad, M.S. Khan, F. Akhter, M.S. Khan, A. Khan, J.M. Ashraf, R.P. Pandey, U. Shahab, Glycoxidation of Biological Macromolecules: A Critical Approach to Halt the Menace of Glycation, Glycobiology, 24 (2014) 979-990.

[10] R. Hennig, S. Cajic, M. Borowiak, M. Hoffmann, R. Kottler, U. Reichl, E. Rapp, Towards personalized diagnostics via longitudinal study of the human plasma N-glycome, Biochimica et biophysica acta, 1860 (2016) 1728-1738.

[11] M. Novokmet, E. Lukić, F. Vučković, Ž. –Durić, T. Keser, K. Rajšl, D. Remondini, G. Castellani, H. Gašparović, O. Gornik, G. Lauc, Changes in IgG and total plasma protein glycomes in acute systemic inflammation, Scientific Reports, 4 (2014) 4347.

[12] A. Knežević, O. Gornik, O. Polašek, M. Pučić, I. Redžić, M. Novokmet, P.M. Rudd, A.F. Wright, H. Campbell, I. Rudan, G. Lauc, Effects of aging, body mass index, plasma lipid profiles, and smoking on human plasma N-glycans, Glycobiology, 20 (2010) 959-969.

[13] J. Krištić, F. Vučković, C. Menni, L. Klarić, T. Keser, I. Beceheli, M. Pučić-Baković, M. Novokmet, M. Mangino, K. Thaqi, P. Rudan, N. Novokmet, J. Šarac, S. Missoni, I. Kolčić, O. Polašek, I. Rudan, H. Campbell, C. Hayward, Y. Aulchenko, A. Valdes, J.F. Wilson, O. Gornik, D. Primorac, V. Zoldoš, T. Spector, G. Lauc, Glycans Are a Novel Biomarker of Chronological and Biological Ages, The Journals of Gerontology: Series A, 69 (2014) 779-789.

[14] L.R. Ruhaak, H.W. Uh, M. Beekman, C.H. Hokke, R.G. Westendorp, J. Houwing-Duistermaat, M. Wuhrer, A.M. Deelder, P.E. Slagboom, Plasma protein N-glycan profiles are associated with calendar age, familial longevity and health, Journal of proteome research, 10 (2011) 1667-1674.

[15] K.R. Reiding, L.R. Ruhaak, H.-W. Uh, S. el Bouhaddani, E.B. van den Akker, R. Plomp, L.A. McDonnell, J.J. Houwing-Duistermaat, P.E. Slagboom, M. Beekman, M. Wuhrer, Human Plasma N-glycosylation as Analyzed by Matrix-Assisted Laser Desorption/Ionization-Fourier Transform Ion Cyclotron Reso-

nance-MS Associates with Markers of Inflammation and Metabolic Health, Mol. Cell. Proteomics 16 (2017) 228-242.

[16] G. Lauc, A. Essafi, J.E. Huffman, C. Hayward, A. Knežević, J.J. Kattla, O. Polašek, O. Gornik, V. Vitart, J.L. Abrahams, M. Pučić, M. Novokmet, I. Redžić, S. Campbell, S.H. Wild, F. Borovečki, W. Wang, I. Kolčić, L. Zgaga, U. Gyllensten, J.F. Wilson, A.F. Wright, N.D. Hastie, H. Campbell, P.M. Rudd, I. Rudan, Genomics Meets Glycomics—The First GWAS Study of Human N-Glycome Identifies HNF1α as a Master Regulator of Plasma Protein Fucosylation, PLOS Genetics, 6 (2010) e1001256.

[17] T.J. McDonald, S. Ellard, Maturity onset diabetes of the young: identification and diagnosis, Ann. Clin. Biochem., 50 (2013) 403-415.

[18] B.F. Voight, L.J. Scott, V. Steinthorsdottir, A.P. Morris, C. Dina, R.P. Welch, E. Zeggini, C. Huth, Y.S. Aulchenko, G. Thorleifsson, L.J. McCulloch, T. Ferreira, H. Grallert, N. Amin, G. Wu, C.J. Willer, S. Raychaudhuri, S.A. McCarroll, C. Langenberg, O.M. Hofmann, J. Dupuis, L. Qi, A.V. Segre, M. van Hoek, P. Navarro, K. Ardlie, B. Balkau, R. Benediktsson, A.J. Bennett, R. Blagieva, E. Boerwinkle, L.L. Bonnycastle, K.B. Bostrom, B. Bravenboer, S. Bumpstead, N.P. Burtt, G. Charpentier, P.S. Chines, M. Cornelis, D.J. Couper, G. Crawford, A.S.F. Doney, K.S. Elliott, A.L. Elliott, M.R. Erdos, C.S. Fox, C.S. Franklin, M. Ganser, C. Gieger, N. Grarup, T. Green, S. Griffin, C.J. Groves, C. Guiducci, S. Hadjadj, N. Hassanali, C. Herder, B. Isomaa, A.U. Jackson, P.R.V. Johnson, T. Jorgensen, W.H.L. Kao, N. Klopp, A. Kong, P. Kraft, J. Kuusisto, T. Lauritzen, M. Li, A. Lieverse, C.M. Lindgren, V. Lyssenko, M. Marre, T. Meitinger, K. Midthjell, M.A. Morken, N. Narisu, P. Nilsson, K.R. Owen, F. Payne, J.R.B. Perry, A.-K. Petersen, C. Platou, C. Proenca, I. Prokopenko, W. Rathmann, N.W. Rayner, N.R. Robertson, G. Rocheleau, M. Roden, M.J. Sampson, R. Saxena, B.M. Shields, P. Shrader, G. Sigurdsson, T. Sparso, K. Strassburger, H.M. Stringham, Q. Sun, A.J. Swift, B. Thorand, J. Tichet, T. Tuomi, R.M. van Dam, T.W. van Haeften, T. van Herpt, J.V. van Vliet-Ostaptchouk, G.B. Walters, M.N. Weedon, C. Wijmenga, J. Witteman, R.N. Bergman, S. Cauchi, F.S. Collins, A.L. Gloyn, U. Gyllensten, T. Hansen, W.A. Hide, G.A. Hitman, A. Hofman, D.J. Hunter, K. Hveem, M. Laakso, K.L. Mohlke, A.D. Morris, C.N.A. Palmer, P.P. Pramstaller, I. Rudan, E. Sijbrands, L.D. Stein, J. Tuomilehto, A. Uitterlinden, M. Walker, N.J. Wareham, R.M. Watanabe, G.R. Abecasis, B.O. Boehm, H. Campbell, M.J. Daly, A.T. Hattersley, F.B. Hu, J.B. Meigs, J.S. Pankow, O. Pedersen, H.E. Wichmann, I. Barroso, J.C. Florez, T.M. Frayling, L. Groop, R. Sladek, U. Thorsteinsdottir, J.F. Wilson, T. Illig, P. Froguel, C.M. van Duijn, K. Stefansson, D. Altshuler, M. Boehnke, M.I. McCarthy, Twelve type 2 diabetes susceptibility loci identified through large-scale association analysis, Nat. Genet., 42 (2010) 579-589.

[19] R.F.H. Lemmers, M. Vilaj, D. Urda, F. Agakov, M. Šimurina, L. Klaric, I. Rudan, H. Campbell, C. Hayward, J.F. Wilson, A.G. Lieverse, O. Gornik, E.J.G. Sijbrands, G. Lauc, M. van Hoek, IgG glycan patterns are associated with type 2 diabetes in independent European populations, Biochim. Biophys. Acta, Gen. Subj. , 1861 (2017) 2240-2249.

[20] K. Tanigaki, A. Sacharidou, J. Peng, K.L. Chambliss, I.S. Yuhanna, D. Ghosh, M. Ahmed, A.J. Szalai, W. Vongpatanasin, R.F. Mattrey, Q. Chen, P. Azadi, I. Lingvay, M. Botto, W.L. Holland, J.J. Kohler, S.R. Sirsi, K. Hoyt, P.W. Shaul, C. Mineo, Hyposialylated IgG activates endothelial IgG receptor FcgammaRIIB to promote obesity-induced insulin resistance, The Journal of clinical investigation, 10.1172/jci89333 (2017).

[21] R. Testa, V. Vanhooren, A.R. Bonfigli, M. Boemi, F. Olivieri, A. Ceriello, S. Genovese, L. Spazzafumo, V. Borelli, M.G. Bacalini, S. Salvioli, P. Garagnani, S. Dewaele, C. Libert, C. Franceschi, N-Glycomic Changes in Serum Proteins in Type 2 Diabetes Mellitus Correlate with Complications and with Metabolic Syndrome Parameters, PLOS ONE, 10 (2015) e0119983.

[22] A. Varki, P. Gagneux, Multifarious roles of sialic acids in immunity, Ann. N. Y. Acad. Sci., 1253 (2012) 16-36.

[23] M.I. Schmidt, B.B. Duncan, A.R. Sharrett, G. Lindberg, P.J. Savage, S. Offenbacher, M.I. Azambuja, R.P. Tracy, G. Heiss, Markers of inflammation and prediction of diabetes mellitus in adults (Atherosclerosis Risk in Communities study): a cohort study, The Lancet, 353 (1999) 1649-1652.

[24] A.O. Akinkuolie, A.D. Pradhan, J.E. Buring, P.M. Ridker, S. Mora, Novel Protein Glycan Side-Chain Biomarker and Risk of Incident Type 2 Diabetes Mellitus, Arterioscler., Thromb., Vasc. Biol. , 35 (2015) 1544.

[25] T. Keser, I. Gornik, F. Vuckovic, N. Selak, T. Pavic, E. Lukic, I. Gudelj, H. Gasparovic, B. Biocina, T. Tilin, A. Wennerstrom, S. Mannisto, V. Salomaa, A. Havulinna, W. Wang, J.F. Wilson, N. Charutvedi, M. Perola, H. Campbell, G. Lauc, O. Gornik, Increased plasma N-glycome complexity is associated with higher risk of type 2 diabetes, Diabetologia, 10.1007/s00125-017-4426-9 (2017).

[26] K.R. Reiding, D. Blank, D.M. Kuijper, A.M. Deelder, M. Wuhrer, High-throughput profiling of protein N-glycosylation by MALDI-TOF-MS employing linkage-specific sialic acid esterification, Analytical chemistry, 86 (2014) 5784-5793.

[27] T.T.W. van Herpt, R.F.H. Lemmers, M. van Hoek, J.G. Langendonk, R.J. Erdtsieck, B. Bravenboer, A. Lucas, M.T. Mulder, H.R. Haak, A.G. Lieverse, E.J.G. Sijbrands, Introduction of the DiaGene study: clinical characteristics, pathophysiology and determinants of vascular complications of type 2 diabetes, Diabetol. Metab. Syndr., 9 (2017) 47.

[28] M.R. Bladergroen, K.R. Reiding, A.L. Hipgrave Ederveen, G.C. Vreeker, F. Clerc, S. Holst, A. Bondt, M. Wuhrer, Y.E. van der Burgt, Automation of High-Throughput Mass Spectrometry-Based Plasma N-Glycome Analysis with Linkage-Specific Sialic Acid Esterification, Journal of proteome research, 14 (2015) 4080-4086.

[29] B.C. Jansen, K.R. Reiding, A. Bondt, A.L. Hipgrave Ederveen, M. Palmblad, D. Falck, M. Wuhrer, MassyTools: A High-Throughput Targeted Data Processing Tool for Relative Quantitation and Quality Control Developed for Glycomic and Glycoproteomic MALDI-MS, Journal of proteome research, 14 (2015) 5088-5098.

[30] F. Clerc, K.R. Reiding, B.C. Jansen, G.S.M. Kammeijer, A. Bondt, M. Wuhrer, Human plasma protein N-glycosylation, Glycoconjugate Journal, 33 (2016) 309-343.

[31] F. Faul, E. Erdfelder, A. Buchner, A.G. Lang, Statistical power analyses using G*Power 3.1: tests for correlation and regression analyses, Behavior research methods, 41 (2009) 1149-1160.

[32] Y. Benjamini, Y. Hochberg, Controlling the False Discovery Rate: A Practical and Powerful Approach to Multiple Testing, Journal of the Royal Statistical Society. Series B (Methodological), 57 (1995) 289-300.

[33] F. Clerc, K.R. Reiding, B.C. Jansen, G.S.M. Kammeijer, A. Bondt, M. Wuhrer, Human plasma protein N-glycosylation, Glycoconjugate J. , 33 (2016) 309-343.

[34] G.S. Hotamisligil, Inflammation, metaflammation and immunometabolic disorders, Nature, 542 (2017) 177-185.

[35] C. McCarthy, R. Saldova, M.R. Wormald, P.M. Rudd, N.G. McElvaney, E.P. Reeves, The Role and Importance of Glycosylation of Acute Phase Proteins with Focus on Alpha-1 Antitrypsin in Acute and Chronic Inflammatory Conditions, Journal of proteome research, 13 (2014) 3131-3143.

[36] I. Gudelj, M. Baciarello, I. Ugrina, M. De Gregori, V. Napolioni, P.M. Ingelmo, D. Bugada, S. De Gregori, L. Đerek, M. Pučić-Baković, M. Novokmet, O. Gornik, G. Saccani Jotti, T. Meschi, G. Lauc, M. Allegri, Changes in total plasma and serum N-glycome composition and patient-controlled analgesia after major abdominal surgery, Scientific Reports, 6 (2016) 31234.

[37] T.R. McCurdy, V. Bhakta, L.J. Eltringham-Smith, S. Gataiance, A.E. Fox-Robichaud, W.P. Sheffield, In Vivo Clearance of Alpha-1 Acid Glycoprotein Is Influenced by the Extent of Its N-Linked Glycosylation and by Its Interaction with the Vessel Wall, J. Biomed. Biotechnol., 2012 (2012) 11.

[38] M. Catera, V. Borelli, N. Malagolini, M. Chiricolo, G. Venturi, C.A. Reis, H. Osorio, P.M. Abruzzo, M. Capri, D. Monti, R. Ostan, C. Franceschi, F. Dall'Olio, Identification of novel plasma glycosylation-associated markers of aging, Oncotarget, 7 (2016) 7455-7468.

[39] J.S. Kooner, D. Saleheen, X. Sim, J. Sehmi, W. Zhang, P. Frossard, L.F. Been, K.-S. Chia, A.S. Dimas, N. Hassanali, T. Jafar, J.B.M. Jowett, X. Li, V. Radha, S.D. Rees, F. Takeuchi, R. Young, T. Aung, A. Basit, M. Chidambaram, D. Das, E. Grundberg, A.K. Hedman, Z.I. Hydrie, M. Islam, C.-C. Khor, S. Kowlessur, M.M. Kristensen, S. Liju, W.-Y. Lim, D.R. Matthews, J. Liu, A.P. Morris, A.C. Nica, J.M. Pinidiyapathirage, I. Prokopenko, A. Rasheed, M. Samuel, N. Shah, A.S. Shera, K.S. Small, C. Suo, A.R. Wickremasinghe, T.Y. Wong, M. Yang, F. Zhang, G.R. Abecasis, A.H. Barnett, M. Caulfield, P. Deloukas, T.M. Frayling, P. Froguel, N. Kato, P. Katulanda, M.A. Kelly, J. Liang, V. Mohan, D.K. Sanghera, J. Scott, M. Seielstad, P.Z. Zimmet, P. Elliott, Y.Y. Teo, M.I. McCarthy, J. Danesh, E.S. Tai, J.C. Chambers, Genome-wide association study in individuals of South Asian ancestry identifies six new type 2 diabetes susceptibility loci, Nat. Genet., 43 (2011) 984-989.

[40] H.A. Kaplan, B.M. Woloski, M. Hellman, J.C. Jamieson, Studies on the effect of inflammation on rat liver and serum sialyltransferase. Evidence that inflammation causes release of Gal beta 1 leads to 4GlcNAc alpha 2 leads to 6 sialyltransferase from liver, J. Biol. Chem. , 258 (1983) 11505-11509.

[41] J.N. Arnold, M.R. Wormald, D.M. Suter, C.M. Radcliffe, D.J. Harvey, R.A. Dwek, P.M. Rudd, R.B. Sim, Human serum IgM glycosylation: identification of glycoforms that can bind to mannan-binding lectin, J. Biol. Chem. , 280 (2005) 29080-29087.

[42] S. Zhang, K. Jiang, C. Sun, H. Lu, Y. Liu, Quantitative analysis of site-specific N-glycans on sera haptoglobin beta chain in liver diseases, Acta biochimica et biophysica Sinica, 45 (2013) 1021-1029.

[43] K. Hanasaki, L.D. Powell, A. Varki, Binding of Human Plasma Sialoglycoproteins by the B Cell-specific Lectin CD22: SELECTIVE RECOGNITION OF IMMUNOGLOBULIN M AND HAPTOGLOBIN, J. Biol. Chem. , 270 (1995) 7543-7550.

[44] G. Dharmadhikari, K. Stolz, M. Hauke, N.G. Morgan, A. Varki, E. de Koning, S. Kelm, K. Maedler, Siglec-7 restores β-cell function and survival and reduces inflammation in pancreatic islets from patients with diabetes, Scientific Reports, 7 (2017) 45319.

[45] F. Clerc, M. Novokmet, V. Dotz, K.R. Reiding, N. de Haan, G.S.M. Kammeijer, H. Dalebout, M.R. Bladergroen, F. Vukovic, E. Rapp, I.-B. consortium, S.R. Targan, G. Barron, N. Manetti, A. Latiano, D.P.B. McGovern, V. Annese, G. Lauc, M. Wuhrer, Plasma N-Glycan Signatures Associate With Features of Inflammatory Bowel Diseases, Gastroenterology, 10.1053/j.gastro.2018.05.030 (2018).

[46] E.C. Brinkman-van der Linden, P.F. de Haan, E.C. Havenaar, W. van Dijk, Inflammation-induced expression of sialyl LewisX is not restricted to alpha1-acid glycoprotein but also occurs to a lesser extent on alpha1-antichymotrypsin and haptoglobin, Glycoconjugate J. , 15 (1998) 177-182.

[47] H.G. Jorgensen, M.A. Elliott, R. Priest, K.D. Smith, Modulation of sialyl Lewis X dependent binding to E-selectin by glycoforms of alpha-1-acid glycoprotein expressed in rheumatoid arthritis, Biomedical chromatography : BMC, 12 (1998) 343-349.

[48] M. Colucci, H. Stöckmann, A. Butera, A. Masotti, A. Baldassarre, E. Giorda, S. Petrini, P.M. Rudd, R. Sitia, F. Emma, M. Vivarelli, Sialylation of N-Linked Glycans Influences the Immunomodulatory Effects of IgM on T Cells, J. Immunol., 194 (2014) 151.

[49] X. Guo, G. Meng, F. Liu, Q. Zhang, L. Liu, H. Wu, H. Du, H. Shi, Y. Xia, X. Liu, C. Li, X. Bao, Q. Su, Y. Gu, L. Fang, F. Yu, H. Yang, B. Yu, S. Sun, X. Wang, M. Zhou, Q. Jia, X. Chen, G. Huang, K. Song, K. Niu, Serum levels of immunoglobulins in an adult population and their relationship with type 2 diabetes, Diabetes Res. Clin. Pract., 115 (2016) 76-82.

[50] T. Shinkawa, K. Nakamura, N. Yamane, E. Shoji-Hosaka, Y. Kanda, M. Sakurada, K. Uchida, H. Anazawa, M. Satoh, M. Yamasaki, N. Hanai, K. Shitara, The absence of fucose but not the presence

of galactose or bisecting N-acetylglucosamine of human IgG1 complex-type oligosaccharides shows the critical role of enhancing antibody-dependent cellular cytotoxicity, J. Biol. Chem. , 278 (2003) 3466-3473.

[51] N. Itoh, S. Sakaue, H. Nakagawa, M. Kurogochi, H. Ohira, K. Deguchi, S.-I. Nishimura, M. Nishimura, Analysis of N-glycan in serum glycoproteins from db/db mice and humans with type 2 diabetes, Am. J. Physiol. Endocrinol. Metabolism, 293 (2007) E1069.

[52] A. Kurimoto, S. Kitazume, Y. Kizuka, K. Nakajima, R. Oka, R. Fujinawa, H. Korekane, Y. Yamaguchi, Y. Wada, N. Taniguchi, The Absence of Core Fucose Up-regulates GnT-III and Wnt Target Genes: A POSSIBLE MECHANISM FOR AN ADAPTIVE RESPONSE IN TERMS OF GLYCAN FUNCTION, J. Biol. Chem. , 289 (2014) 11704-11714.

[53] K.R. Reiding, G.C.M. Vreeker, A. Bondt, M.R. Bladergroen, J.M.W. Hazes, Y.E.M. van der Burgt, M. Wuhrer, R. Dolhain, Serum Protein N-Glycosylation Changes with Rheumatoid Arthritis Disease Activity during and after Pregnancy, Frontiers in medicine, 4 (2017) 241.

[54] L.P. Lee, A. Prasad, K.J. Bolton, J.B. McKendry, I. Hynie, Serum UDP-galactose: glycoprotein galactosyltransferase in diabetics with microangiopathy, Clin. Biochem., 10 (1977) 111-117.

[55] F. Dall'Olio, V. Vanhooren, C.C. Chen, P.E. Slagboom, M. Wuhrer, C. Franceschi, N-glycomic biomarkers of biological aging and longevity: A link with inflammaging, Ageing Res. Rev., 12 (2013) 685-698.

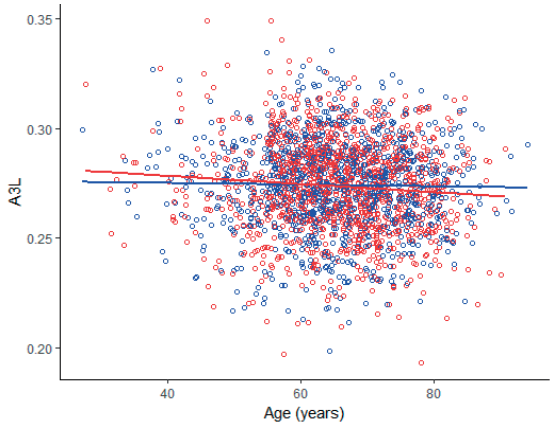

Supplementary Figure S1. Plasma N-glycosylation in dependency from age and sex.

Data from the discovery cohort are shown exemplarily for α2,3-sialylation (A3L, upper) and fucosylation of diantennary glycans (A2F, lower). Scatter points and regression lines are labeled blue for males and red for females, demonstrating an interaction between age and sex.

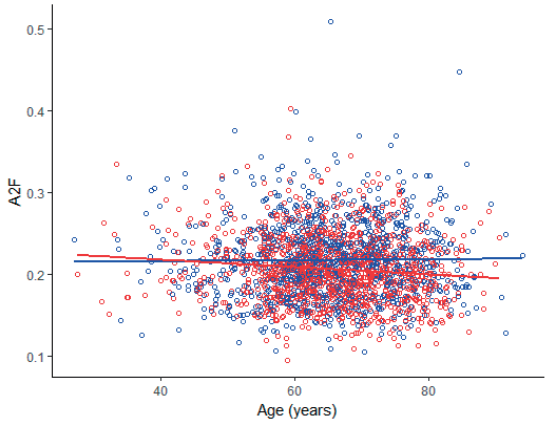

Supplementary Figure S2. Associations of derived glycan traits with age, sex, HDL-cholesterol (HDL-c), non-HDL-cholesterol (non-HDL-c), BMI, and smoking for combined data from discovery and replication subsamples.

A) Unadjusted associations. Sex was coded as male = 0, female = 1. B) Associations adjusted for age, sex, and their interaction. Colors represent the t-statistics (β / standard error); the X indicates p-values ≤ 0.033 (significance after FDR-adjustment). Association heat maps were clustered using hclust method = complete with Euclidean distance. The clustering order in both (A) and (B) is based on the unadjusted associations between glycans and clinical parameters. See Supplementary Table S2 for glycan derived trait description. Glycan trait abbreviations: B, bisection; C, within complex; A2, diantennary; F, fucosylation; L, α2,3-linked sialylation; S, sialylation; G, galactose; E, α2,6-linked sialylation; A3, triantennary; T, within total. Negative associations with type 2 diabetes are shown in blue, positive associations in red. BMI, body mass index; HDL-c, HDL-cholesterol.

Supplementary Table S1. Selected quality parameters of analytes that were quantified (A) or only detected (B).

A. Analytes quantified

Composition	Theoretical mass $[M+Na]^+$	VisuCon standard plasma (N = 149)						DiaGene controls (N = 852)			DiaGene cases (N = 1834)		
		mass error (absolute ppm)			relative intensity			mass error (absolute ppm)			mass error (absolute ppm)		
		mean	SD	count	mean	SD	RSD	mean	SD	count	mean	SD	count
H5N2	1257,423	13,68	5,00	77	0,000779	0,000238	30,51%	15,60	3,98	495	15,30	4,10	994
H6N2	1419,475	6,18	3,58	143	0,002537	0,000811	31,96%	5,98	3,17	828	6,09	2,94	1781
H3N3E1	1455,523	5,25	3,80	116	0,000676	0,000203	30,04%	5,80	4,18	666	5,60	4,27	1515
H5N3	1460,502	8,26	5,85	12	0,000188	0,000122	64,71%	7,93	4,51	250	7,83	4,87	434
H3N4F1 (calibrant)	1485,534	2,49	1,69	146	0,007087	0,001928	27,20%	2,17	1,10	839	2,18	1,32	1801
H4N4	1501,529	5,86	4,39	102	0,000881	0,000293	33,30%	5,52	3,98	653	5,59	3,93	1372
H3N5	1542,555	6,15	4,76	16	0,000278	0,000175	63,08%	6,04	4,58	191	5,92	4,35	480
H7N2	1581,528	4,00	3,31	130	0,001129	0,000453	40,13%	4,03	3,60	740	3,71	3,36	1631
H3N3F1E1	1601,581	6,51	5,30	24	0,001236	0,000727	58,85%	7,42	5,04	205	7,72	5,27	490
H4N3E1	1617,576	4,96	4,65	125	0,002477	0,001192	48,13%	4,95	4,39	661	5,36	4,42	1436
H6N3	1622,555	5,77	4,31	72	0,000618	0,000331	53,57%	5,85	4,49	570	5,72	4,41	1178
H4N4F1 (calibrant)	1647,586	2,14	1,62	146	0,018407	0,004062	22,07%	1,99	1,15	839	2,00	1,16	1803
H5N4	1663,581	4,90	4,62	134	0,000943	0,000232	24,61%	3,48	3,48	786	3,51	3,38	1710
H3N5F1	1688,613	3,60	3,33	143	0,002173	0,000533	24,52%	2,49	2,94	825	2,24	2,52	1780
H4N5	1704,608	5,83	4,68	99	0,000594	0,000240	40,36%	4,65	3,91	629	5,03	4,29	1401
H8N2	1743,581	2,93	3,13	143	0,002727	0,001019	37,37%	3,04	3,25	827	2,97	3,13	1778
H5N3E1	1779,629	5,25	4,30	93	0,001595	0,000419	26,28%	4,61	4,17	507	4,55	3,99	1201
H5N4F1 (calibrant)	1809,639	2,00	2,15	146	0,011902	0,002881	24,20%	1,73	1,41	838	1,72	1,55	1800
H4N4E1	1820,655	4,11	3,72	140	0,002577	0,000543	21,07%	3,50	3,42	821	3,32	3,24	1735
H4N5F1	1850,666	1,97	2,32	144	0,004699	0,000953	20,28%	1,90	2,37	832	1,86	2,14	1788
H5N5	1866,661	6,41	4,61	80	0,000503	0,000183	36,45%	6,03	4,78	534	5,87	4,59	1167

A. Analytes quantified (*continued*)

Composition	Theoretical mass $[M+Na]^+$	VisuCon standard plasma (N = 149)						DiaGene controls (N = 852)			DiaGene cases (N = 1834)		
		mass error (absolute ppm)			relative intensity			mass error (absolute ppm)			mass error (absolute ppm)		
		mean	SD	count	mean	SD	RSD	mean	SD	count	mean	SD	count
H9N2	1905,634	2,73	2,53	142	0,006455	0,002450	37,95%	3,05	3,33	831	2,78	2,93	1778
H5N4L1	1936,666	3,50	3,49	142	0,001787	0,000287	16,08%	3,29	3,44	824	3,14	3,13	1760
H6N3E1	1941,682	3,68	3,31	130	0,001711	0,000356	20,82%	4,02	3,88	701	3,79	3,59	1570
H4N4F1E1	1966,713	4,00	3,65	145	0,003076	0,000603	19,61%	3,55	3,32	823	3,52	3,18	1773
H5N4E1	1982,708	2,65	1,47	144	0,067861	0,005212	7,68%	2,87	1,84	836	3,07	1,92	1796
H5N5F1	2012,719	4,01	3,58	143	0,002304	0,000853	37,03%	3,58	3,23	825	3,52	3,32	1768
H4N5E1	2023,735	5,70	4,71	112	0,000809	0,000247	30,51%	5,38	4,53	617	4,94	4,17	1398
H5N4F1L1	2082,724	3,42	3,73	142	0,003170	0,000413	13,03%	2,53	2,77	832	2,46	2,73	1778
H5N4F1E1 (calibrant)	2128,766	1,46	1,46	146	0,020223	0,002141	10,59%	1,40	1,15	839	1,40	1,12	1802
H4N5F1E1	2169,793	6,30	4,65	127	0,002272	0,000526	23,15%	5,83	4,44	776	5,58	4,18	1648
H5N5E1	2185,787	4,85	4,30	133	0,004898	0,001539	31,41%	4,67	4,01	750	4,63	3,89	1625
H5N4L2	2209,751	5,44	4,85	136	0,002282	0,000421	18,43%	4,23	4,03	801	4,38	4,01	1719
H5N4E1L1	2255,793	1,62	1,87	146	0,051058	0,003677	7,20%	1,65	2,01	836	1,88	2,19	1798
H5N4E2	2301,835	3,37	3,23	144	0,510978	0,032807	6,42%	3,63	3,39	824	3,85	3,53	1757
H5N5F1E1	2331,845	2,58	2,23	145	0,011740	0,001466	12,48%	2,30	2,39	837	2,30	2,39	1796
H6N5E1	2347,840	3,60	3,04	146	0,006517	0,001040	15,96%	3,16	2,88	829	2,87	2,68	1790
H5N4F1L2	2355,809	6,88	4,55	138	0,008614	0,001859	21,58%	5,16	4,06	822	5,48	4,40	1757
H5N4F1E1L1	2401,851	2,78	2,28	146	0,012340	0,001137	9,22%	2,46	2,30	833	2,43	2,50	1796
H5N4F1E2	2447,893	2,48	1,87	146	0,030519	0,002569	8,42%	2,36	1,95	838	2,15	1,89	1799
H6N5F1E1	2493,898	6,02	4,50	135	0,001580	0,000354	22,39%	5,33	3,97	795	5,08	3,85	1721
H5N5E2	2504,914	6,28	4,62	124	0,001917	0,000317	16,53%	6,83	4,92	720	7,05	4,86	1559
H6N5L2	2574,883	7,09	5,11	46	0,000613	0,000399	65,00%	6,86	5,08	425	7,16	5,16	887

A. Analytes quantified (*continued*)

Composition	Theoretical mass $[M+Na]^+$	VisuCon standard plasma (N = 149)						DiaGene controls (N = 852)			DiaGene cases (N = 1834)		
		mass error (absolute ppm)			relative intensity			mass error (absolute ppm)			mass error (absolute ppm)		
		mean	SD	count	mean	SD	RSD	mean	SD	count	mean	SD	count
H5N5F1E1L1	2604,930	8,70	5,69	102	0,001124	0,000446	39,69%	6,79	5,09	642	6,72	4,94	1397
H6N5E1L1	2620,925	4,25	2,78	145	0,006205	0,000846	13,63%	4,17	2,81	833	3,94	2,77	1788
H5N5F1E2	2650,972	4,26	2,52	145	0,014295	0,001270	8,88%	3,56	2,07	834	3,70	2,36	1798
H6N5E2	2666,967	5,87	3,06	145	0,005395	0,000704	13,06%	5,34	3,14	831	4,93	2,90	1783
H6N5F1L2	2720,941	6,59	4,90	121	0,001205	0,000282	23,38%	5,89	4,53	726	5,71	4,58	1594
H6N5F1E1L1	2766,983	6,11	4,03	136	0,002353	0,000468	19,88%	5,83	4,00	794	5,72	3,87	1713
H6N5F1E2	2813,025	6,87	4,15	137	0,002173	0,000410	18,88%	6,66	4,11	789	6,32	3,97	1723
H6N5E1L2	2894,010	2,95	2,35	144	0,007058	0,001015	14,38%	2,84	2,75	837	2,84	2,76	1785
H6N5E2L1 (calibrant)	2940,052	1,17	1,28	146	0,052453	0,007362	14,03%	1,19	1,45	840	1,15	1,41	1799
H6N5E3	2986,094	3,73	2,45	145	0,022708	0,003057	13,46%	3,76	2,33	840	3,56	2,09	1794
H6N5F1E1L2	3040,068	3,28	3,48	147	0,004532	0,000884	19,51%	3,34	3,35	827	3,29	3,37	1785
H6N5F1E2L1 (calibrant)	3086,110	0,93	0,95	146	0,040539	0,007655	18,88%	0,92	1,10	840	0,90	1,11	1800
H6N5F1E3	3132,152	6,29	4,28	134	0,002298	0,000534	23,25%	6,48	4,41	782	6,09	4,14	1736
H6N5F2E1L2	3186,126	5,71	4,60	124	0,001104	0,000306	27,69%	6,40	5,13	529	6,13	4,86	1144
H6N5F2E2L1	3232,168	5,35	4,57	131	0,001164	0,000277	23,80%	5,46	4,70	614	5,24	4,47	1455
H7N6E1L2	3259,142	4,99	3,98	133	0,001959	0,000547	27,92%	4,89	4,15	746	4,70	4,16	1631
H7N6E2L1	3305,184	5,23	4,70	131	0,001394	0,000391	28,01%	5,08	4,25	694	5,19	4,37	1581
H7N6E3	3351,226	7,85	4,84	42	0,000359	0,000138	38,34%	7,68	5,38	179	7,61	5,40	623
H7N6F1E1L2	3405,200	7,16	5,06	107	0,000864	0,000320	37,04%	6,63	4,80	503	6,63	4,91	1174
H7N6F1E2L1	3451,242	6,59	5,15	87	0,000790	0,000243	30,76%	7,49	5,16	431	6,93	5,07	1129
H7N6E1L3	3532,227	9,57	4,76	128	0,001867	0,000543	29,09%	9,44	4,66	671	9,10	4,77	1458
H7N6E2L2	3578,269	9,61	4,34	125	0,002112	0,000595	28,18%	9,76	4,66	684	9,50	4,91	1535
H7N6E3L1	3624,311	9,61	5,15	99	0,001010	0,000289	28,59%	9,35	5,36	506	9,01	5,21	1201
H7N6F1E1L3	3678,285	10,47	5,09	99	0,000957	0,000376	39,25%	10,94	5,18	488	10,65	5,41	1060

A. Analytes quantified (*continued*)

Composition	Theoretical mass $[M+Na]^+$	VisuCon standard plasma (N = 149)						DiaGene controls (N = 852)			DiaGene cases (N = 1834)		
		mass error (absolute ppm)			relative intensity			mass error (absolute ppm)			mass error (absolute ppm)		
		mean	SD	count	mean	SD	RSD	mean	SD	count	mean	SD	count
H7N6F1E2L2	3724,327	10,97	5,52	86	0,001130	0,000395	34,95%	11,38	5,29	454	10,70	5,40	1094
H7N6F1E3L1	3770,369	9,34	5,92	40	0,000382	0,000162	42,46%	9,60	5,04	105	9,55	5,60	330
H7N6F2E2L2	3870,385	11,41	5,42	25	0,000410	0,000181	44,15%	11,16	5,97	72	11,61	5,70	202

B. Possible analytes/glycan modifications/adducts: detected, but not quantified

Composition	Theoretical mass $[M+Na+modifier]^+$	Mass error (ppm) VisuCon standard			Modifier and mass difference to theoretical $[M+Na]^+$				
		mean	SD	count	Fragment	K-Na	unidentified adduct		
					-101,048	+15.974	+132.176	+154.158	+357.180
H3N3	1136,396	not applicable	not applicable	0					
H3N3F1	1282,454	11,62	7,73	4					
H4N3	1298,449	2,84	3,49	2					
H3N4	1339,476	12,17	5,57	16					
H3N4F1sRa1	1384,486	12,08	4,48	8	X				
H3N3L1	1409,481	not applicable	not applicable	0					
H4N3F1	1444,507	6,94	5,93	3					
H4N4F1sRa1	1546,539	5,22	4,33	79	X				
H6N2sXa1	1551,652	10,72	5,98	23			X		
H3N3F1L1	1555,539	not applicable	not applicable	0					
H4N3L1	1571,534	10,07	5,46	4					
H5N3F1	1606,560	3,67	4,22	2					
H5N4F1sRa1	1708,592	5,80	4,96	68	X				
H7N2sXa1	1713,705	14,34	6,72	6			X		
H5N3L1	1733,587	12,16	2,18	2					
H4N5F1sRa1	1749,618	8,37	6,49	12	X				
H4N3E1sXa1	1749,752	6,90	6,18	2			X		
H3N3F1E1sXb1	1755,739	18,61	not applicable	1				X	

B. Possible analytes/glycan modifications/adducts: detected, but not quantified (*continued*)

Composition	Theoretical mass [M+Na+modifier]$^+$	Mass error (ppm) VisuCon standard			Modifier and mass difference to theoretical [M+Na]$^+$				
		mean	SD	count	Fragment	K-Na	unidentified adduct		
					-101,048	+15.974	+132.176	+154.158	+357.180
H4N3F1E1	1763,634	5,80	4,92	8					
H4N4L1	1774,613	15,28	4,48	2					
H4N4F1sXb1	1801,745	10,74	6,27	28				X	
H6N4	1825,634	6,70	6,65	9					
H3N4F1sXc1	1842,714	9,42	5,44	15					X
H3N5F1sXb1	1842,771	9,71	6,67	3				X	
H8N2sXa1	1875,757	10,46	5,36	34			X		
H5N4E1sRa1	1881,660	3,50	3,31	142	X				
H5N5sK1	1882,635	15,79	3,08	112		X			
H5N3E1sXa1	1911,805	18,08	not applicable	1			X		
H3N3F1L1sXc1	1912,719	not applicable	not applicable	0					X
H5N4L1sK1	1952,640	not applicable	not applicable	0		X			
H4N4E1sXa1	1952,832	13,48	4,91	5			X		
H5N3F1sXc1	1963,740	9,42	6,25	32					X
H5N4F1sXb1	1963,798	8,99	6,04	22				X	
H5N4F1E1sRa1	2027,718	4,32	3,57	98	X				
H9N2sXa1	2037,810	9,90	5,70	59			X		
H4N7	2110,767	5,97	1,25	2					
H5N4E1sXa1	2114,884	12,65	5,52	40			X		
H5N4E1L1sRa1	2154,745	4,00	3,82	138	X				
H5N5E1sK1	2201,761	13,78	2,40	131		X			
H5N5F1E1sRa1	2230,798	5,37	4,05	71	X				
H6N5E1sRa1	2246,793	6,93	5,17	117	X				
H5N4F1L2sRa1	2254,761	16,69	1,91	136	X				
H5N4F1E1sXb1	2282,924	10,63	5,59	4				X	
H5N4F1E1L1sRa1	2300,803	14,48	2,51	129	X				
H5N4E2sK1	2317,809	8,18	4,93	105		X			
H5N5E1sXa1	2317,964	12,04	6,19	8			X		

B. Possible analytes/glycan modifications/adducts: detected, but not quantified (*continued*)

Composition	Theoretical mass [M+Na+modifier]$^+$	Mass error (ppm) VisuCon standard			Modifier and mass difference to theoretical [M+Na]$^+$				
		mean	SD	count	Fragment	K-Na	unidentified adduct		
					-101,048	+15.974	+132.176	+154.158	+357.180
H4N7E1sRa1	2328,846	9,33	5,37	81	X				
H5N4E1sXc1	2339,888	6,79	4,27	12					X
H5N5E1sXb1	2339,946	12,69	7,31	5				X	
H5N4F1E2sRa1	2346,845	6,37	3,28	146	X				
H5N4E1L1sXa1	2387,969	9,43	5,36	65			X		
H4N7E1	2429,893	6,07	4,97	100					
H5N4E2sXb1	2455,993	7,24	5,15	109				X	
H6N5E1L1sRa1	2519,877	8,08	5,52	48	X				
H5N5E2sK1	2520,888	9,69	5,12	44		X			
H5N5F1E2sRa1	2549,924	10,74	6,21	82	X				
H5N4E1L1sXc1	2612,973	16,12	not applicable	1					X
H5N4E2sXc1	2659,015	6,72	5,29	57					X
H5N5E2sXb1	2659,072	12,68	5,52	41				X	
H6N5E1L2sRa1	2792,962	9,40	5,98	16	X				
H6N5E2sXa1	2799,143	6,25	3,81	21			X		
H6N5E2L1sRa1	2839,004	5,45	4,57	134	X				
H10N6	2880,004	3,54	not applicable	1					
H6N5E3sRa1	2885,046	6,29	4,48	111	X				
H6N8L1	2911,037	8,24	5,73	42					
H6N5F1E2L1sRa1	2985,062	6,05	2,68	145	X				
H5N8E1L1	3068,110	8,99	5,35	67					
H6N5E2L1sXa1	3072,228	10,35	5,38	69			X		
H6N5E3sXa1	3118,270	8,26	5,45	54			X		
H5N8F1E1L1	3214,168	7,48	4,59	16					
H6N5F1E2L1sXa1	3218,286	10,36	5,89	52			X		
H4N7F2L3	3222,137	8,05	5,50	45					
H6N5E2L1sXc1	3297,232	not applicable	not applicable	0					X
H7N6F2E1L3	3824,343	13,86	5,57	22					

B. Possible analytes/glycan modifications/adducts: detected, but not quantified (*continued*)

Composition	Theoretical mass [M+Na+modifier]$^+$	Mass error (ppm) VisuCon standard			Modifier and mass difference to theoretical [M+Na]$^+$				
		mean	SD	count	Fragment	K-Na	unidentified adduct		
					-101,048	+15.974	+132.176	+154.158	+357.180
H8N7E1L3	3897,359	19,47	not applicable	1					
H8N7E2L2	3943,401	9,65	6,54	6					
H7N6F3E1L3	3970,401	11,94	4,11	3					
H9N8E1L2	3989,407	not applicable	not applicable	0					
H8N7F1E1L3	4043,417	not applicable	not applicable	0					
H8N7F1E2L2	4089,459	not applicable	not applicable	0					
H9N8F1E1L2	4135,465	not applicable	not applicable	0					
H7N6F2E3L2	4189,511	not applicable	not applicable	0					
H8N7F2E2L2	4235,517	not applicable	not applicable	0					
H9N8E2L2	4308,533	not applicable	not applicable	0					
H10N9E1L2	4354,539	not applicable	not applicable	0					
H11N9F2E1L1	4535,623	not applicable	not applicable	0					
H10N9L4	4581,582	not applicable	not applicable	0					
H10N9E1L3	4627,624	10,29	not applicable	1					
H10N9F1L4	4727,640	not applicable	not applicable	0					

Absolute ppm error values are shown for the analytes that passed major analyte quality criteria (signal-to-noise > 6, ppm < 20). Relative intensities of the VisuCon samples after batch correction are shown as repeatability measure (see S2 for derived traits). Abbreviations for glycan compositions: H = hexose; N = N-acetylhexosamine; F = deoxyhexose (fucose); E = α2,6-linked sialic acid; L = α2,3-linked sialic acid; sRa = A0,2-cross ring fragment of reducing N-acetylglucosamine; sXa,b,c = different possible modifications derived from derivatization.

Supplementary Table S2. Derived trait description, depiction, and calculation.

Derived trait			Calculation	Relative intensity VisuCon standard plasma (N=149)		
Complexity				mean	SD	RSD
MHy	The ratio of high-mannose to hybrid glycans		MHy = (H5N2 + H6N2 + H7N2 + H8N2 + H9N2) / (H5N3 + H6N3 + H5N3E1 + H6N3E1)	3,3010	0,8767	26,56%
MM	Average number of mannoses on high mannose type glycans		MM = (5 * (H5N2) + 6 * (H6N2) + 7 * (H7N2) + 8 * (H8N2) + 9 * (H9N2) + 10 * (0)) / (H5N2 + H6N2 + H7N2 + H8N2 + H9N2)	7,8250	0,1273	1,63%
THy	Relative abundance of hybrid type glycans within total spectrum		THy = (H5N3 + H6N3 + H5N3E1 + H6N3E1) / (H5N2 + H6N2 + H3N3E1 + H5N3 + H3N4F1 + H4N4 + H3N5 + H7N2 + H3N3F1E1 + H4N3E1 + H6N3 + H4N4F1 + H5N4 + H3N5F1 + H4N5 + H8N2 + H5N3E1 + H5N4F1 + H4N4E1 + H4N5F1 + H5N5 + H9N2 + H5N4L1 + H6N3E1 + H4N4F1E1 + H5N4E1 + H5N5F1 + H4N5E1 + H5N4F1L1 + H5N4F1E1 + H4N5F1E1 + H5N5E1 + H5N4L2 + H5N4E1L1 + H5N4E2 + H5N5F1E1 + H6N5E1 + H5N4F1L2 + H5N4F1E1L1 + H5N4F1E2 + H6N5F1E1 + H5N5E2 + H6N5L2 + H5N5F1E1L1 + H6N5E1L1 + H5N5F1E2 + H6N5E2 + H6N5F1L2 + H6N5F1E1L1 + H6N5F1E2 + H6N5E1L2 + H6N5E2L1 + H6N5E3 + H6N5F1E1L2 + H6N5F1E2L1 + H6N5F1E3 + H6N5F2E1L2 + H6N5F2E2L1 + H7N6E1L2 + H7N6E2L1 + H7N6E3 + H7N6F1E1L2 + H7N6F1E2L1 + H7N6E1L3 + H7N6E2L2 + H7N6E3L1 + H7N6F1E1L3 + H7N6F1E2L2 + H7N6F1E3L1 + H7N6F2E2L2)	0,0042	0,0011	25,54%
TM	Relative abundance of high mannose type glycans within total spectrum		TM = (H5N2 + H6N2 + H7N2 + H8N2 + H9N2) / (H5N2 + H6N2 + H3N3E1 + H5N3 + H3N4F1 + H4N4 + H3N5 + H7N2 + H3N3F1E1 + H4N3E1 + H6N3 + H4N4F1 + H5N4 + H3N5F1 + H4N5 + H8N2 + H5N3E1 + H5N4F1 + H4N4E1 + H4N5F1 + H5N5 + H9N2 + H5N4L1 + H6N3E1 + H4N4F1E1 + H5N4E1 + H5N5F1 + H4N5E1 + H5N4F1L1 + H5N4F1E1 + H4N5F1E1 + H5N5E1 + H5N4L2 + H5N4E1L1 + H5N4E2 + H5N5F1E1 + H6N5E1 + H5N4F1L2 + H5N4F1E1L1 + H5N4F1E2 + H6N5F1E1 + H5N5E2 + H6N5L2 + H5N5F1E1L1 + H6N5E1L1 + H5N5F1E2 + H6N5E2 + H6N5F1L2 + H6N5F1E1L1 + H6N5F1E2 + H6N5E1L2 + H6N5E2L1 + H6N5E3 + H6N5F1E1L2 + H6N5F1E2L1 + H6N5F1E3 + H6N5F2E1L2 + H6N5F2E2L1 + H7N6E1L2 + H7N6E2L1 + H7N6E3 + H7N6F1E1L2 + H7N6F1E2L1 + H7N6E1L3 + H7N6E2L2 + H7N6E3L1 + H7N6F1E1L3 + H7N6F1E2L2 + H7N6F1E3L1 + H7N6F2E2L2)	0,0137	0,0047	34,19%

Supplementary Table S2. Derived trait description, depiction, and calculation. (*continued*)

Derived trait			Calculation	Relative intensity VisuCon standard plasma (N=149)		
CA1	Relative abundance of monoantennary glycans within complex type glycans		CA1 = (H3N3E1 + H3N3F1E1 + H4N3E1) / (H3N3E1 + H3N4F1 + H4N4 + H3N5 + H3N3F1E1 + H4N3E1 + H4N4F1 + H5N4 + H3N5F1 + H4N5 + H5N4F1 + H4N4E1 + H4N5F1 + H5N5 + H5N4L1 + H4N4F1E1 + H5N4E1 + H5N5F1 + H4N5E1 + H5N4F1L1 + H5N4F1E1 + H4N5F1E1 + H5N5E1 + H5N4L2 + H5N4E1L1 + H5N4E2 + H5N5F1E1 + H6N5E1 + H5N4F1L2 + H5N4F1E1L1 + H5N4F1E2 + H6N5F1E1 + H5N5E2 + H6N5L2 + H5N5F1E1L1 + H6N5E1L1 + H5N5F1E2 + H6N5E2 + H6N5F1L2 + H6N5F1E1L1 + H6N5F1E2 + H6N5E1L2 + H6N5E2L1 + H6N5E3 + H6N5F1E1L2 + H6N5F1E2L1 + H6N5F1E3 + H6N5F2E1L2 + H6N5F2E2L1 + H7N6E1L2 + H7N6E2L1 + H7N6E3 + H7N6F1E1L2 + H7N6F1E2L1 + H7N6E1L3 + H7N6E2L2 + H7N6E3L1 + H7N6F1E1L3 + H7N6F1E2L2 + H7N6F1E3L1 + H7N6F2E2L2)	0,0045	0,0019	42,74%
CA2	Relative abundance of diantennary glycans within complex type glycans		CA2 = (H3N4F1 + H4N4 + H3N5 + H4N4F1 + H5N4 + H3N5F1 + H4N5 + H5N4F1 + H4N4E1 + H4N5F1 + H5N5 + H5N4L1 + H4N4F1E1 + H5N4E1 + H5N5F1 + H4N5E1 + H5N4F1L1 + H5N4F1E1 + H4N5F1E1 + H5N5E1 + H5N4L2 + H5N4E1L1 + H5N4E2 + H5N5F1E1 + H6N5E1 + H5N4F1L2 + H5N4F1E1L1 + H5N4F1E2 + H5N5E2 + H5N5F1E1L1 + H5N5F1E2) / (H3N3E1 + H3N4F1 + H4N4 + H3N5 + H3N3F1E1 + H4N3E1 + H4N4F1 + H5N4 + H3N5F1 + H4N5 + H5N4F1 + H4N4E1 + H4N5F1 + H5N5 + H5N4L1 + H4N4F1E1 + H5N4E1 + H5N5F1 + H4N5E1 + H5N4F1L1 + H5N4F1E1 + H4N5F1E1 + H5N5E1 + H5N4L2 + H5N4E1L1 + H5N4E2 + H5N5F1E1 + H6N5E1 + H5N4F1L2 + H5N4F1E1L1 + H5N4F1E2 + H6N5F1E1 + H5N5E2 + H6N5L2 + H5N5F1E1L1 + H6N5E1L1 + H5N5F1E2 + H6N5E2 + H6N5F1L2 + H6N5F1E1L1 + H6N5F1E2 + H6N5E1L2 + H6N5E2L1 + H6N5E3 + H6N5F1E1L2 + H6N5F1E2L1 + H6N5F1E3 + H6N5F2E1L2 + H6N5F2E2L1 + H7N6E1L2 + H7N6E2L1 + H7N6E3 + H7N6F1E1L2 + H7N6F1E2L1 + H7N6E1L3 + H7N6E2L2 + H7N6E3L1 + H7N6F1E1L3 + H7N6F1E2L2 + H7N6F1E3L1 + H7N6F2E2L2)	0,8195	0,0243	2,96%
CA3	Relative abundance of triantennary glycans within complex type glycans		CA3 = (H6N5E1 + H6N5F1E1 + H6N5L2 + H6N5E1L1 + H6N5E2 + H6N5F1L2 + H6N5F1E1L1 + H6N5F1E2 + H6N5E1L2 + H6N5E2L1 + H6N5E3 + H6N5F1E1L2 + H6N5F1E2L1 + H6N5F1E3 + H6N5F2E1L2 + H6N5F2E2L1) / (H3N3E1 + H3N4F1 + H4N4 + H3N5 + H3N3F1E1 + H4N3E1 + H4N4F1 + H5N4 + H3N5F1 + H4N5 + H5N4F1 + H4N4E1 + H4N5F1 + H5N5 + H5N4L1 + H4N4F1E1 + H5N4E1 + H5N5F1 + H4N5E1 + H5N4F1L1 + H5N4F1E1 + H4N5F1E1 + H5N5E1 + H5N4L2 + H5N4E1L1 + H5N4E2 + H5N5F1E1 + H6N5E1 + H5N4F1L2 + H5N4F1E1L1 + H5N4F1E2 + H6N5F1E1 + H5N5E2 + H6N5L2 + H5N5F1E1L1 + H6N5E1L1 + H5N5F1E2 + H6N5E2 + H6N5F1L2 + H6N5F1E1L1 + H6N5F1E2 + H6N5E1L2 + H6N5E2L1 + H6N5E3 + H6N5F1E1L2 + H6N5F1E2L1 + H6N5F1E3 + H6N5F2E1L2 + H6N5F2E2L1 + H7N6E1L2 + H7N6E2L1 + H7N6E3 + H7N6F1E1L2 + H7N6F1E2L1 + H7N6E1L3 + H7N6E2L2 + H7N6E3L1 + H7N6F1E1L3 + H7N6F1E2L2 + H7N6F1E3L1 + H7N6F2E2L2)	0,1616	0,0213	13,16%

Supplementary Table S2. Derived trait description, depiction, and calculation. (*continued*)

Derived trait			Calculation	Relative intensity VisuCon standard plasma (N=149)		
CA4	Relative abundance of tetra-antennary glycans within complex type glycans		CA4 = (H7N6E1L2 + H7N6E2L1 + H7N6E3 + H7N6F1E1L2 + H7N6F1E2L1 + H7N6E1L3 + H7N6E2L2 + H7N6E3L1 + H7N6F1E1L3 + H7N6F1E2L2 + H7N6F1E3L1 + H7N6F2E2L2) / (H3N3E1 + H3N4F1 + H4N4 + H3N5 + H3N3F1E1 + H4N3E1 + H4N4F1 + H5N4 + H3N5F1 + H4N5 + H5N4F1 + H4N4E1 + H4N5F1 + H5N5 + H5N4L1 + H4N4F1E1 + H5N4E1 + H5N5F1 + H4N5E1 + H5N4F1L1 + H5N4F1E1 + H4N5F1E1 + H5N5E1 + H5N4L2 + H5N4E1L1 + H5N4E2 + H5N5F1E1 + H6N5E1 + H5N4F1L2 + H5N4F1E1L1 + H5N4F1E2 + H6N5F1E1 + H5N5E2 + H6N5L2 + H5N5F1E1L1 + H6N5E1L1 + H5N5F1E2 + H6N5E2 + H6N5F1L2 + H6N5F1E1L1 + H6N5F1E2 + H6N5E1L2 + H6N5E2L1 + H6N5E3 + H6N5F1E1L2 + H6N5F1E2L1 + H6N5F1E3 + H6N5F2E1L2 + H6N5F2E2L1 + H7N6E1L2 + H7N6E2L1 + H7N6E3 + H7N6F1E1L2 + H7N6F1E2L1 + H7N6E1L3 + H7N6E2L2 + H7N6E3L1 + H7N6F1E1L3 + H7N6F1E2L2 + H7N6F1E3L1 + H7N6F2E2L2)	0,0135	0,0037	27,34%
TA2FS0	Fucosylated, non-sialylated diantennary species within total glycans. Mostly derived from IgG (Clerc et al. 2015).		TA2FS0 = (H3N4F1 + H4N4F1 + H3N5F1 + H5N4F1 + H4N5F1 + H5N5F1)	0,0466	0,0101	21,74%
Fucosylation						
CF	Fucosylation within complex type glycans		CF = (H3N4F1 + H3N3F1E1 + H4N4F1 + H3N5F1 + H5N4F1 + H4N5F1 + H4N4F1E1 + H5N5F1 + H5N4F1L1 + H5N4F1E1 + H4N5F1E1 + H5N5F1E1 + H5N4F1L2 + H5N4F1E1L1 + H5N4F1E2 + H6N5F1E1 + H5N5F1E1L1 + H5N5F1E2 + H6N5F1L2 + H6N5F1E1L1 + H6N5F1E2 + H6N5F1E1L2 + H6N5F1E2L1 + H6N5F1E3 + H6N5F2E1L2 + H6N5F2E2L1 + H7N6F1E1L2 + H7N6F1E2L1 + H7N6F1E1L3 + H7N6F1E2L2 + H7N6F1E3L1 + H7N6F2E2L2) / (H3N3E1 + H3N4F1 + H4N4 + H3N5 + H3N3F1E1 + H4N3E1 + H4N4F1 + H5N4 + H3N5F1 + H4N5 + H5N4F1 + H4N4E1 + H4N5F1 + H5N5 + H5N4L1 + H4N4F1E1 + H5N4E1 + H5N5F1 + H4N5E1 + H5N4F1L1 + H5N4F1E1 + H4N5F1E1 + H5N5E1 + H5N4L2 + H5N4E1L1 + H5N4E2 + H5N5F1E1 + H6N5E1 + H5N4F1L2 + H5N4F1E1L1 + H5N4F1E2 + H6N5F1E1 + H5N5E2 + H6N5L2 + H5N5F1E1L1 + H6N5E1L1 + H5N5F1E2 + H6N5E2 + H6N5F1L2 + H6N5F1E1L1 + H6N5F1E2 + H6N5E1L2 + H6N5E2L1 + H6N5E3 + H6N5F1E1L2 + H6N5F1E2L1 + H6N5F1E3 + H6N5F2E1L2 + H6N5F2E2L1 + H7N6E1L2 + H7N6E2L1 + H7N6E3 + H7N6F1E1L2 + H7N6F1E2L1 + H7N6E1L3 + H7N6E2L2 + H7N6E3L1 + H7N6F1E1L3 + H7N6F1E2L2 + H7N6F1E3L1 + H7N6F2E2L2)	0,2220	0,0208	9,37%
A1F	Fucosylation within monoantennary glycans		A1F = (H3N3F1E1) / (H3N3E1 + H3N3F1E1 + H4N3E1)	0,2704	0,0733	27,12%

Supplementary Table S2. Derived trait description, depiction, and calculation. (*continued*)

Derived trait			Calculation	Relative intensity VisuCon standard plasma (N=149)		
A2F	Fucosylation within diantennary glycans		A2F = (H3N4F1 + H4N4F1 + H3N5F1 + H5N4F1 + H4N5F1 + H4N4F1E1 + H5N5F1 + H5N4F1L1 + H5N4F1E1 + H4N5F1E1 + H5N5F1E1 + H5N4F1L2 + H5N4F1E1L1 + H5N4F1E2 + H5N5F1E1L1 + H5N5F1E2) / (H3N4F1 + H4N4 + H3N5 + H4N4F1 + H5N4 + H3N5F1 + H4N5 + H5N4F1 + H4N4E1 + H4N5F1 + H5N5 + H5N4L1 + H4N4F1E1 + H5N4E1 + H5N5F1 + H4N5E1 + H5N4F1L1 + H5N4F1E1 + H4N5F1E1 + H5N5E1 + H5N4L2 + H5N4E1L1 + H5N4E2 + H5N5F1E1 + H5N4F1L2 + H5N4F1E1L1 + H5N4F1E2 + H5N5E2 + H5N5F1E1L1 + H5N5F1E2)	0,1925	0,0201	10,46%
A3F	Fucosylation within triantennary glycans		A3F = (H6N5F1E1 + H6N5F1L2 + H6N5F1E1L1 + H6N5F1E2 + H6N5F1E1L2 + H6N5F1E2L1 + H6N5F1E3 + H6N5F2E1L2 + H6N5F2E2L1) / (H6N5E1 + H6N5F1E1 + H6N5L2 + H6N5E1L1 + H6N5E2 + H6N5F1L2 + H6N5F1E1L1 + H6N5F1E2 + H6N5E1L2 + H6N5E2L1 + H6N5E3 + H6N5F1E1L2 + H6N5F1E2L1 + H6N5F1E3 + H6N5F2E1L2 + H6N5F2E2L1)	0,3593	0,0265	7,36%
A4F	Fucosylation within tetra-antennary glycans	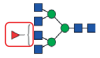	A4F = (H7N6F1E1L2 + H7N6F1E2L1 + H7N6F1E1L3 + H7N6F1E2L2 + H7N6F1E3L1 + H7N6F2E2L2) / (H7N6E1L2 + H7N6E2L1 + H7N6E3 + H7N6F1E1L2 + H7N6F1E2L1 + H7N6E1L3 + H7N6E2L2 + H7N6E3L1 + H7N6F1E1L3 + H7N6F1E2L2 + H7N6F1E3L1 + H7N6F2E2L2)	0,3396	0,0286	8,42%
A2SF	Fucosylation within sialylated diantennary glycans		A2SF = (H4N4F1E1 + H5N4F1L1 + H5N4F1E1 + H4N5F1E1 + H5N5F1E1 + H5N4F1L2 + H5N4F1E1L1 + H5N4F1E2 + H5N5F1E1L1 + H5N5F1E2) / (H4N4E1 + H5N4L1 + H4N4F1E1 + H5N4E1 + H4N5E1 + H5N4F1L1 + H5N4F1E1 + H4N5F1E1 + H5N5E1 + H5N4L2 + H5N4E1L1 + H5N4E2 + H5N5F1E1 + H5N4F1L2 + H5N4F1E1L1 + H5N4F1E2 + H5N5E2 + H5N5F1E1L1 + H5N5F1E2)	0,1431	0,0129	9,02%
A2S0F	Fucosylation within non-sialylated diantennary glycans		A2S0F = (H3N4F1 + H4N4F1 + H3N5F1 + H5N4F1 + H4N5F1 + H5N5F1) / (H3N4F1 + H4N4 + H3N5 + H4N4F1 + H5N4 + H3N5F1 + H4N5 + H5N4F1 + H4N5F1 + H5N5 + H5N5F1)	0,9334	0,0131	1,41%
A2EF	Fucosylation within diantennary glycans with α2,6-linked sialic acid		A2EF = (H4N4F1E1 + H5N4F1E1 + H4N5F1E1 + H5N5F1E1 + H5N4F1E1L1 + H5N4F1E2 + H5N5F1E1L1 + H5N5F1E2) / (H4N4E1 + H4N4F1E1 + H5N4E1 + H4N5E1 + H5N4F1E1 + H4N5F1E1 + H5N5E1 + H5N4E1L1 + H5N4E2 + H5N5F1E1 + H5N4F1E1L1 + H5N4F1E2 + H5N5E2 + H5N5F1E1L1 + H5N5F1E2)	0,1302	0,0121	9,30%
A2E0F	Fucosylation within diantennary glycans without α2,6-linked sialic acid	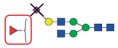	A2E0F = (H3N4F1 + H4N4F1 + H3N5F1 + H5N4F1 + H4N5F1 + H5N5F1 + H5N4F1L1 + H5N4F1L2) / (H3N4F1 + H4N4 + H3N5 + H4N4F1 + H5N4 + H3N5F1 + H4N5 + H5N4F1 + H4N5F1 + H5N5 + H5N4L1 + H5N5F1 + H5N4F1L1 + H5N4L2 + H5N4F1L2)	0,8873	0,0136	1,53%
A2LF	Fucosylation within diantennary glycans with α2,3-linked sialic acid		A2LF = (H5N4F1L1 + H5N4F1L2 + H5N4F1E1L1 + H5N5F1E1L1) / (H5N4L1 + H5N4F1L1 + H5N4L2 + H5N4E1L1 + H5N4F1L2 + H5N4F1E1L1 + H5N5F1E1L1)	0,3133	0,0173	5,51%

Supplementary Table S2. Derived trait description, depiction, and calculation. (*continued*)

Derived trait			Calculation	Relative intensity VisuCon standard plasma (N=149)		
A2L0F	Fucosylation within diantennary glycans without α2,3-linked sialic acid		A2L0F = (H3N4F1 + H4N4F1 + H3N5F1 + H5N4F1 + H4N5F1 + H4N4F1E1 + H5N5F1 + H5N4F1E1 + H4N5F1E1 + H5N5F1E1 + H5N4F1E2 + H5N5F1E2) / (H3N4F1 + H4N4 + H3N5 + H4N4F1 + H5N4 + H3N5F1 + H4N5 + H5N4F1 + H4N4E1 + H4N5F1 + H5N5 + H4N4F1E1 + H5N4E1 + H5N5F1 + H4N5E1 + H5N4F1E1 + H4N5F1E1 + H5N5E1 + H5N4E2 + H5N5F1E1 + H5N4F1E2 + H5N5E2 + H5N5F1E2)	0,1788	0,0212	11,83%
A3EF	Fucosylation within triantennary glycans with α2,6-linked sialic acid		A3EF = (H6N5F1E1 + H6N5F1E1L1 + H6N5F1E2 + H6N5F1E1L2 + H6N5F1E2L1 + H6N5F1E3 + H6N5F2E1L2 + H6N5F2E2L1) / (H6N5E1 + H6N5F1E1 + H6N5E1L1 + H6N5E2 + H6N5F1E1L1 + H6N5F1E2 + H6N5E1L2 + H6N5E2L1 + H6N5E3 + H6N5F1E1L2 + H6N5F1E2L1 + H6N5F1E3 + H6N5F2E1L2 + H6N5F2E2L1)	0,3558	0,0267	7,52%
A3E0F	Fucosylation within triantennary glycans without α2,6-linked sialic acid		A3E0F = (H6N5F1L2) / (H6N5L2 + H6N5F1L2)	0,6817	0,0969	14,22%
A3LF	Fucosylation within triantennary glycans with α2,3-linked sialic acid		A3LF = (H6N5F1L2 + H6N5F1E1L1 + H6N5F1E1L2 + H6N5F1E2L1 + H6N5F2E1L2 + H6N5F2E2L1) / (H6N5L2 + H6N5E1L1 + H6N5F1L2 + H6N5F1E1L1 + H6N5E1L2 + H6N5E2L1 + H6N5F1E1L2 + H6N5F1E2L1 + H6N5F2E1L2 + H6N5F2E2L1)	0,4326	0,0334	7,71%
A3L0F	Fucosylation within triantennary glycans without α2,3-linked sialic acid		A3L0F = (H6N5F1E1 + H6N5F1E2 + H6N5F1E3) / (H6N5E1 + H6N5F1E1 + H6N5E2 + H6N5F1E2 + H6N5E3 + H6N5F1E3)	0,1487	0,0173	11,65%
A4LF	Fucosylation within tetra-antennary glycans with α2,3-linked sialic acid		A4LF = (H7N6F1E1L2 + H7N6F1E2L1 + H7N6F1E1L3 + H7N6F1E2L2 + H7N6F1E3L1 + H7N6F2E2L2) / (H7N6E1L2 + H7N6E2L1 + H7N6F1E1L2 + H7N6F1E2L1 + H7N6E1L3 + H7N6E2L2 + H7N6E3L1 + H7N6F1E1L3 + H7N6F1E2L2 + H7N6F1E3L1 + H7N6F2E2L2)	0,3493	0,0298	8,54%

Supplementary Table S2. Derived trait description, depiction, and calculation. (*continued*)

Derived trait			Calculation	Relative intensity VisuCon standard plasma (N=149)		
Antennary fucosylation						
CFa	Relative abundance of species with 2 fucoses (i.e. at least one antennary fucose) within all complex type glycans	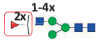	CFa = (H6N5F2E1L2 + H6N5F2E2L1 + H7N6F2E2L2) / (H3N3E1 + H3N4F1 + H4N4 + H3N5 + H3N3F1E1 + H4N3E1 + H4N4F1 + H5N4 + H3N5F1 + H4N5 + H5N4F1 + H4N4E1 + H4N5F1 + H5N5 + H5N4L1 + H4N4F1E1 + H5N4E1 + H5N5F1 + H4N5E1 + H5N4F1L1 + H5N4F1E1 + H4N5F1E1 + H5N5E1 + H5N4L2 + H5N4E1L1 + H5N4E2 + H5N5F1E1 + H6N5E1 + H5N4F1L2 + H5N4F1E1L1 + H5N4F1E2 + H6N5F1E1 + H5N5E2 + H6N5L2 + H5N5F1E1L1 + H6N5E1L1 + H5N5F1E2 + H6N5E2 + H6N5F1L2 + H6N5F1E1L1 + H6N5F1E2 + H6N5E1L2 + H6N5E2L1 + H6N5E3 + H6N5F1E1L2 + H6N5F1E2L1 + H6N5F1E3 + H6N5F2E1L2 + H6N5F2E2L1 + H7N6E1L2 + H7N6E2L1 + H7N6E3 + H7N6F1E1L2 + H7N6F1E2L1 + H7N6E1L3 + H7N6E2L2 + H7N6E3L1 + H7N6F1E1L3 + H7N6F1E2L2 + H7N6F1E3L1 + H7N6F2E2L2)	0,0027	0,0007	25,42%
A3Fa	Relative abundance of species with 2 fucoses (i.e. at least one antennary fucose) within triantennary glycans		A3Fa = (H6N5F2E1L2 + H6N5F2E2L1) / (H6N5E1 + H6N5F1E1 + H6N5L2 + H6N5E1L1 + H6N5E2 + H6N5F1L2 + H6N5F1E1L1 + H6N5F1E2 + H6N5E1L2 + H6N5E2L1 + H6N5E3 + H6N5F1E1L2 + H6N5F1E2L1 + H6N5F1E3 + H6N5F2E1L2 + H6N5F2E2L1)	0,0143	0,0029	20,10%
A4Fa	Relative abundance of species with 2 fucoses (i.e. at least one antennary fucose) within tetra-antennary glycans	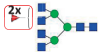	A4Fa = (H7N6F2E2L2) / (H7N6E1L2 + H7N6E2L1 + H7N6E3 + H7N6F1E1L2 + H7N6F1E2L1 + H7N6E1L3 + H7N6E2L2 + H7N6E3L1 + H7N6F1E1L3 + H7N6F1E2L2 + H7N6F1E3L1 + H7N6F2E2L2)	0,0310	0,0099	32,10%
Bisection						
CB	Relative abundance of species with a bisecting GlcNAc within all complex glycans		CB = (H3N5 + H3N5F1 + H4N5 + H4N5F1 + H5N5 + H5N5F1 + H4N5E1 + H4N5F1E1 + H5N5E1 + H5N5F1E1 + H5N5E2 + H5N5F1E1L1 + H5N5F1E2) / (H3N3E1 + H3N4F1 + H4N4 + H3N5 + H3N3F1E1 + H4N3E1 + H4N4F1 + H5N4 + H3N5F1 + H4N5 + H5N4F1 + H4N4E1 + H4N5F1 + H5N5 + H5N4L1 + H4N4F1E1 + H5N4E1 + H5N5F1 + H4N5E1 + H5N4F1L1 + H5N4F1E1 + H4N5F1E1 + H5N5E1 + H5N4L2 + H5N4E1L1 + H5N4E2 + H5N5F1E1 + H6N5E1 + H5N4F1L2 + H5N4F1E1L1 + H5N4F1E2 + H6N5F1E1 + H5N5E2 + H6N5L2 + H5N5F1E1L1 + H6N5E1L1 + H5N5F1E2 + H6N5E2 + H6N5F1L2 + H6N5F1E1L1 + H6N5F1E2 + H6N5E1L2 + H6N5E2L1 + H6N5E3 + H6N5F1E1L2 + H6N5F1E2L1 + H6N5F1E3 + H6N5F2E1L2 + H6N5F2E2L1 + H7N6E1L2 + H7N6E2L1 + H7N6E3 + H7N6F1E1L2 + H7N6F1E2L1 + H7N6E1L3 + H7N6E2L2 + H7N6E3L1 + H7N6F1E1L3 + H7N6F1E2L2 + H7N6F1E3L1 + H7N6F2E2L2)	0,0490	0,0057	11,71%

Supplementary Table S2. Derived trait description, depiction, and calculation. (*continued*)

Derived trait			Calculation	Relative intensity VisuCon standard plasma (N=149)		
A2B	Relative abundance of species with a bisecting GlcNAc within diantennary glycans		A2B = (H3N5 + H3N5F1 + H4N5 + H4N5F1 + H5N5 + H5N5F1 + H4N5E1 + H4N5F1E1 + H5N5E1 + H5N5F1E1 + H5N5E2 + H5N5F1E1L1 + H5N5F1E2) / (H3N4F1 + H4N4 + H3N5 + H4N4F1 + H5N4 + H3N5F1 + H4N5 + H5N4F1 + H4N4E1 + H4N5F1 + H5N5 + H5N4L1 + H4N4F1E1 + H5N4E1 + H5N5F1 + H4N5E1 + H5N4F1L1 + H5N4F1E1 + H4N5F1E1 + H5N5E1 + H5N4L2 + H5N4E1L1 + H5N4E2 + H5N5F1E1 + H5N4F1L2 + H5N4F1E1L1 + H5N4F1E2 + H5N5E2 + H5N5F1E1L1 + H5N5F1E2)	0,0599	0,0075	12,57%
A2FB	Relative abundance of species with a bisecting GlcNAc within fucosylated diantennary glycans		A2FB = (H3N5F1 + H4N5F1 + H5N5F1 + H4N5F1E1 + H5N5F1E1 + H5N5F1E1L1 + H5N5F1E2) / (H3N4F1 + H4N4F1 + H3N5F1 + H5N4F1 + H4N5F1 + H4N4F1E1 + H5N5F1 + H5N4F1L1 + H5N4F1E1 + H4N5F1E1 + H5N5F1E1 + H5N4F1L2 + H5N4F1E1L1 + H5N4F1E2 + H5N5F1E1L1 + H5N5F1E2)	0,2511	0,0113	4,51%
A2F0B	Relative abundance of species with a bisecting GlcNAc within non-fucosylated diantennary glycans		A2F0B = (H3N5 + H4N5 + H5N5 + H4N5E1 + H5N5E1 + H5N5E2) / (H4N4 + H3N5 + H5N4 + H4N5 + H4N4E1 + H5N5 + H5N4L1 + H5N4E1 + H4N5E1 + H5N5E1 + H5N4L2 + H5N4E1L1 + H5N4E2 + H5N5E2)	0,0142	0,0036	25,46%
A2SB	Relative abundance of species with a bisecting GlcNAc within sialylated diantennary glycans		A2SB = (H4N5E1 + H4N5F1E1 + H5N5E1 + H5N5F1E1 + H5N5E2 + H5N5F1E1L1 + H5N5F1E2) / (H4N4E1 + H5N4L1 + H4N4F1E1 + H5N4E1 + H4N5E1 + H5N4F1L1 + H5N4F1E1 + H4N5F1E1 + H5N5E1 + H5N4L2 + H5N4E1L1 + H5N4E2 + H5N5F1E1 + H5N4F1L2 + H5N4F1E1L1 + H5N4F1E2 + H5N5E2 + H5N5F1E1L1 + H5N5F1E2)	0,0498	0,0061	12,20%
A2S0B	Relative abundance of species with a bisecting GlcNAc within non-sialylated diantennary glycans		A2S0B = (H3N5 + H3N5F1 + H4N5 + H4N5F1 + H5N5 + H5N5F1) / (H3N4F1 + H4N4 + H3N5 + H4N4F1 + H5N4 + H3N5F1 + H4N5 + H5N4F1 + H4N5F1 + H5N5 + H5N5F1)	0,2134	0,0186	8,70%
A2FSB	Relative abundance of species with a bisecting GlcNAc within fucosylated sialylated diantennary glycans		A2FSB = (H4N5F1E1 + H5N5F1E1 + H5N5F1E1L1 + H5N5F1E2) / (H4N4F1E1 + H5N4F1L1 + H5N4F1E1 + H4N5F1E1 + H5N5F1E1 + H5N4F1L2 + H5N4F1E1L1 + H5N4F1E2 + H5N5F1E1L1 + H5N5F1E2)	0,2739	0,0128	4,67%
A2FS0B	Relative abundance of species with a bisecting GlcNAc within fucosylated non-sialylated diantennary glycans		A2FS0B = (H3N5F1 + H4N5F1 + H5N5F1) / (H3N4F1 + H4N4F1 + H3N5F1 + H5N4F1 + H4N5F1 + H5N5F1)	0,1976	0,0160	8,10%

Supplementary Table S2. Derived trait description, depiction, and calculation. (*continued*)

Derived trait			Calculation	Relative intensity VisuCon standard plasma (N=149)		
A2F0SB	Relative abundance of species with a bisecting GlcNAc within non-fucosylated sialylated diantennary glycans		A2F0SB = (H4N5E1 + H5N5E1 + H5N5E2) / (H4N4E1 + H5N4L1 + H5N4E1 + H4N5E1 + H5N5E1 + H5N4L2 + H5N4E1L1 + H5N4E2 + H5N5E2)	0,0120	0,0031	25,79%
A2F0S0B	Relative abundance of species with a bisecting GlcNAc within non-fucosylated non-sialylated diantennary glycans	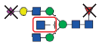	A2F0S0B = (H3N5 + H4N5 + H5N5) / (H4N4 + H3N5 + H5N4 + H4N5 + H5N5)	0,4293	0,0531	12,36%
Galactosylation per antenna						
CG	Galactosylation within all complex glycans		CG = (H3N3E1 + H4N4 + H3N3F1E1 + H4N3E1 + H4N4F1 + H5N4 + H4N5 + H5N4F1 + H4N4E1 + H4N5F1 + H5N5 + H5N4L1 + H4N4F1E1 + H5N4E1 + H5N5F1 + H4N5E1 + H5N4F1L1 + H5N4F1E1 + H4N5F1E1 + H5N5E1 + H5N4L2 + H5N4E1L1 + H5N4E2 + H5N5F1E1 + H6N5E1 + H5N4F1L2 + H5N4F1E1L1 + H5N4F1E2 + H6N5F1E1 + H5N5E2 + H6N5L2 + H5N5F1E1L1 + H6N5E1L1 + H5N5F1E2 + H6N5E2 + H6N5F1L2 + H6N5F1E1L1 + H6N5F1E2 + H6N5E1L2 + H6N5E2L1 + H6N5E3 + H6N5F1E1L2 + H6N5F1E2L1 + H6N5F1E3 + H6N5F2E1L2 + H6N5F2E2L1 + H7N6E1L2 + H7N6E2L1 + H7N6E3 + H7N6F1E1L2 + H7N6F1E2L1 + H7N6E1L3 + H7N6E2L2 + H7N6E3L1 + H7N6F1E1L3 + H7N6F1E2L2 + H7N6F1E3L1 + H7N6F2E2L2) / (H3N3E1 + H3N4F1 + H4N4 + H3N5 + H3N3F1E1 + H4N3E1 + H4N4F1 + H5N4 + H3N5F1 + H4N5 + H5N4F1 + H4N4E1 + H4N5F1 + H5N5 + H5N4L1 + H4N4F1E1 + H5N4E1 + H5N5F1 + H4N5E1 + H5N4F1L1 + H5N4F1E1 + H4N5F1E1 + H5N5E1 + H5N4L2 + H5N4E1L1 + H5N4E2 + H5N5F1E1 + H6N5E1 + H5N4F1L2 + H5N4F1E1L1 + H5N4F1E2 + H6N5F1E1 + H5N5E2 + H6N5L2 + H5N5F1E1L1 + H6N5E1L1 + H5N5F1E2 + H6N5E2 + H6N5F1L2 + H6N5F1E1L1 + H6N5F1E2 + H6N5E1L2 + H6N5E2L1 + H6N5E3 + H6N5F1E1L2 + H6N5F1E2L1 + H6N5F1E3 + H6N5F2E1L2 + H6N5F2E2L1 + H7N6E1L2 + H7N6E2L1 + H7N6E3 + H7N6F1E1L2 + H7N6F1E2L1 + H7N6E1L3 + H7N6E2L2 + H7N6E3L1 + H7N6F1E1L3 + H7N6F1E2L2 + H7N6F1E3L1 + H7N6F2E2L2)	0,9900	0,0025	0,26%

Supplementary Table S2. Derived trait description, depiction, and calculation. (*continued*)

Derived trait			Calculation	Relative intensity VisuCon standard plasma (N=149)		
A2G	Galactosylation per antenna within diantennary glycans		A2G = (0/2 * (H3N4F1 + H3N5 + H3N5F1) + 1/2 * (H4N4 + H4N4F1 + H4N5 + H4N4E1 + H4N5F1 + H4N4F1E1 + H4N5E1 + H4N5F1E1) + 2/2 * (H5N4 + H5N4F1 + H5N5 + H5N4L1 + H5N4E1 + H5N5F1 + H5N4F1L1 + H5N4F1E1 + H5N5E1 + H5N4L2 + H5N4E1L1 + H5N4E2 + H5N5F1E1 + H5N4F1L2 + H5N4F1E1L1 + H5N4F1E2 + H5N5E2 + H5N5F1E1L1 + H5N5F1E2)) / (H3N4F1 + H4N4 + H3N5 + H4N4F1 + H5N4 + H3N5F1 + H4N5 + H5N4F1 + H4N4E1 + H4N5F1 + H5N5 + H5N4L1 + H4N4F1E1 + H5N4E1 + H5N5F1 + H4N5E1 + H5N4F1L1 + H5N4F1E1 + H4N5F1E1 + H5N5E1 + H5N4L2 + H5N4E1L1 + H5N4E2 + H5N5F1E1 + H5N4F1L2 + H5N4F1E1L1 + H5N4F1E2 + H5N5E2 + H5N5F1E1L1 + H5N5F1E2)	0,9667	0,0069	0,72%
A2FG	Galactosylation per antenna within fucosylated diantennary glycans		A2FG = (0/2 * (H3N4F1 + H3N5F1) + 1/2 * (H4N4F1 + H4N5F1 + H4N4F1E1 + H4N5F1E1) + 2/2 * (H5N4F1 + H5N5F1 + H5N4F1L1 + H5N4F1E1 + H5N5F1E1 + H5N4F1L2 + H5N4F1E1L1 + H5N4F1E2 + H5N5F1E1L1 + H5N5F1E2)) / (H3N4F1 + H4N4F1 + H3N5F1 + H5N4F1 + H4N5F1 + H4N4F1E1 + H5N5F1 + H5N4F1L1 + H5N4F1E1 + H4N5F1E1 + H5N5F1E1 + H5N4F1L2 + H5N4F1E1L1 + H5N4F1E2 + H5N5F1E1L1 + H5N5F1E2)	0,8476	0,0209	2,46%
A2F0G	Galactosylation per antenna within non-fucosylated diantennary glycans		A2F0G = (0/2 * (H3N5) + 1/2 * (H4N4 + H4N5 + H4N4E1 + H4N5E1) + 2/2 * (H5N4 + H5N5 + H5N4L1 + H5N4E1 + H5N5E1 + H5N4L2 + H5N4E1L1 + H5N4E2 + H5N5E2)) / (H4N4 + H3N5 + H5N4 + H4N5 + H4N4E1 + H5N5 + H5N4L1 + H5N4E1 + H4N5E1 + H5N5E1 + H5N4L2 + H5N4E1L1 + H5N4E2 + H5N5E2)	0,9956	0,0011	0,11%
A2SG	Galactosylation per antenna within sialylated diantennary glycans		A2SG = (0/2 * (0) + 1/2 * (H4N4E1 + H4N4F1E1 + H4N5E1 + H4N5F1E1) + 2/2 * (H5N4L1 + H5N4E1 + H5N4F1L1 + H5N4F1E1 + H5N5E1 + H5N4L2 + H5N4E1L1 + H5N4E2 + H5N5F1E1 + H5N4F1L2 + H5N4F1E1L1 + H5N4F1E2 + H5N5E2 + H5N5F1E1L1 + H5N5F1E2)) / (H4N4E1 + H5N4L1 + H4N4F1E1 + H5N4E1 + H4N5E1 + H5N4F1L1 + H5N4F1E1 + H4N5F1E1 + H5N5E1 + H5N4L2 + H5N4E1L1 + H5N4E2 + H5N5F1E1 + H5N4F1L2 + H5N4F1E1L1 + H5N4F1E2 + H5N5E2 + H5N5F1E1L1 + H5N5F1E2)	0,9941	0,0011	0,11%
A2S0G	Galactosylation per antenna within non-sialylated diantennary glycans		A2S0G = (0/2 * (H3N4F1 + H3N5 + H3N5F1) + 1/2 * (H4N4 + H4N4F1 + H4N5 + H4N5F1) + 2/2 * (H5N4 + H5N4F1 + H5N5 + H5N5F1)) / (H3N4F1 + H4N4 + H3N5 + H4N4F1 + H5N4 + H3N5F1 + H4N5 + H5N4F1 + H4N5F1 + H5N5 + H5N5F1)	0,5604	0,0210	3,75%
A2FSG	Galactosylation per antenna within fucosylated sialylated diantennary glycans		A2FSG = (0/2 * (0) + 1/2 * (H4N4F1E1 + H4N5F1E1) + 2/2 * (H5N4F1L1 + H5N4F1E1 + H5N5F1E1 + H5N4F1L2 + H5N4F1E1L1 + H5N4F1E2 + H5N5F1E1L1 + H5N5F1E2)) / (H4N4F1E1 + H5N4F1L1 + H5N4F1E1 + H4N5F1E1 + H5N5F1E1 + H5N4F1L2 + H5N4F1E1L1 + H5N4F1E2 + H5N5F1E1L1 + H5N5F1E2)	0,9749	0,0043	0,45%
A2F0SG	Galactosylation per antenna within non-fucosylated sialylated diantennary glycans		A2F0SG = (0/2 * (0) + 1/2 * (H4N4E1 + H4N5E1) + 2/2 * (H5N4L1 + H5N4E1 + H5N5E1 + H5N4L2 + H5N4E1L1 + H5N4E2 + H5N5E2)) / (H4N4E1 + H5N4L1 + H5N4E1 + H4N5E1 + H5N5E1 + H5N4L2 + H5N4E1L1 + H5N4E2 + H5N5E2)	0,9973	0,0006	0,06%

Supplementary Table S2. Derived trait description, depiction, and calculation. (*continued*)

Derived trait			Calculation	Relative intensity VisuCon standard plasma (N=149)		
A2FS0G	Galactosylation per antenna within fucosylated non-sialylated diantennary glycans		A2FS0G = (0/2 * (H3N4F1 + H3N5F1) + 1/2 * (H4N4F1 + H4N5F1) + 2/2 * (H5N4F1 + H5N5F1)) / (H3N4F1 + H4N4F1 + H3N5F1 + H5N4F1 + H4N5F1 + H5N5F1)	0,5525	0,0218	3,95%
A2F0S0G	Galactosylation per antenna within non-fucosylated, non-sialylated diantennary glycans		A2F0S0G = (0/2 * (H3N5) + 1/2 * (H4N4 + H4N5) + 2/2 * (H5N4 + H5N5)) / (H4N4 + H3N5 + H5N4 + H4N5 + H5N5)	0,6800	0,0466	6,85%
A4F0G	Galactosylation per antenna within non-fucosylated tetra-antennary glycans	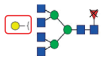	A4F0G = (0/4 * (0) + 1/4 * (0) + 2/4 * (0) + 3/4 * (0) + 4/4 * (H7N6E1L2 + H7N6E2L1 + H7N6E3 + H7N6E1L3 + H7N6E2L2 + H7N6E3L1)) / (H7N6E1L2 + H7N6E2L1 + H7N6E3 + H7N6F1E1L2 + H7N6F1E2L1 + H7N6E1L3 + H7N6E2L2 + H7N6E3L1 + H7N6F1E1L3 + H7N6F1E2L2 + H7N6F1E3L1 + H7N6F2E2L2)	0,6598	0,0288	4,37%
Sialylation per antenna						
CS	Sialylation per antenna within all complex glycans	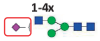	CS = (H3N3E1 + H3N3F1E1 + H4N3E1 + H4N4E1 + H5N4L1 + H4N4F1E1 + H5N4E1 + H4N5E1 + H5N4F1L1 + H5N4F1E1 + H4N5F1E1 + H5N5E1 + H5N4L2 + H5N4E1L1 + H5N4E2 + H5N5F1E1 + H6N5E1 + H5N4F1L2 + H5N4F1E1L1 + H5N4F1E2 + H6N5F1E1 + H5N5E2 + H6N5L2 + H5N5F1E1L1 + H6N5E1L1 + H5N5F1E2 + H6N5E2 + H6N5F1L2 + H6N5F1E1L1 + H6N5F1E2 + H6N5E1L2 + H6N5E2L1 + H6N5E3 + H6N5F1E1L2 + H6N5F1E2L1 + H6N5F1E3 + H6N5F2E1L2 + H6N5F2E2L1 + H7N6E1L2 + H7N6E2L1 + H7N6E3 + H7N6F1E1L2 + H7N6F1E2L1 + H7N6E1L3 + H7N6E2L2 + H7N6E3L1 + H7N6F1E1L3 + H7N6F1E2L2 + H7N6F1E3L1 + H7N6F2E2L2) / (H3N3E1 + H3N4F1 + H4N4 + H3N5 + H3N3F1E1 + H4N3E1 + H4N4F1 + H5N4 + H3N5F1 + H4N5 + H5N4F1 + H4N4E1 + H4N5F1 + H5N5 + H5N4L1 + H4N4F1E1 + H5N4E1 + H5N5F1 + H4N5E1 + H5N4F1L1 + H5N4F1E1 + H4N5F1E1 + H5N5E1 + H5N4L2 + H5N4E1L1 + H5N4E2 + H5N5F1E1 + H6N5E1 + H5N4F1L2 + H5N4F1E1L1 + H5N4F1E2 + H6N5F1E1 + H5N5E2 + H6N5L2 + H5N5F1E1L1 + H6N5E1L1 + H5N5F1E2 + H6N5E2 + H6N5F1L2 + H6N5F1E1L1 + H6N5F1E2 + H6N5E1L2 + H6N5E2L1 + H6N5E3 + H6N5F1E1L2 + H6N5F1E2L1 + H6N5F1E3 + H6N5F2E1L2 + H6N5F2E2L1 + H7N6E1L2 + H7N6E2L1 + H7N6E3 + H7N6F1E1L2 + H7N6F1E2L1 + H7N6E1L3 + H7N6E2L2 + H7N6E3L1 + H7N6F1E1L3 + H7N6F1E2L2 + H7N6F1E3L1 + H7N6F2E2L2)	0,9483	0,0120	1,26%

Supplementary Table S2. Derived trait description, depiction, and calculation. (*continued*)

Derived trait			Calculation	Relative intensity VisuCon standard plasma (N=149)		
A2S	Sialylation per antenna within diantennary glycans		A2S = (0/2 * (H3N4F1 + H4N4 + H3N5 + H4N4F1 + H5N4 + H3N5F1 + H4N5 + H5N4F1 + H4N5F1 + H5N5 + H5N5F1) + 1/2 * (H4N4E1 + H5N4L1 + H4N4F1E1 + H5N4E1 + H4N5E1 + H5N4F1L1 + H5N4F1E1 + H4N5F1E1 + H5N5E1 + H5N5F1E1) + 2/2 * (H5N4L2 + H5N4E1L1 + H5N4E2 + H5N4F1L2 + H5N4F1E1L1 + H5N4F1E2 + H5N5E2 + H5N5F1E1L1 + H5N5F1E2)) / (H3N4F1 + H4N4 + H3N5 + H4N4F1 + H5N4 + H3N5F1 + H4N5 + H5N4F1 + H4N4E1 + H4N5F1 + H5N5 + H5N4L1 + H4N4F1E1 + H5N4E1 + H5N5F1 + H4N5E1 + H5N4F1L1 + H5N4F1E1 + H4N5F1E1 + H5N5E1 + H5N4L2 + H5N4E1L1 + H5N4E2 + H5N5F1E1 + H5N4F1L2 + H5N4F1E1L1 + H5N4F1E2 + H5N5E2 + H5N5F1E1L1 + H5N5F1E2)	0,8630	0,0192	2,23%
A3S	Sialylation per antenna within triantennary glycans		A3S = (0/3 * (0) + 1/3 * (H6N5E1 + H6N5F1E1) + 2/3 * (H6N5L2 + H6N5E1L1 + H6N5E2 + H6N5F1L2 + H6N5F1E1L1 + H6N5F1E2) + 3/3 * (H6N5E1L2 + H6N5E2L1 + H6N5E3 + H6N5F1E1L2 + H6N5F1E2L1 + H6N5F1E3 + H6N5F2E1L2 + H6N5F2E2L1)) / (H6N5E1 + H6N5F1E1 + H6N5L2 + H6N5E1L1 + H6N5E2 + H6N5F1L2 + H6N5F1E1L1 + H6N5F1E2 + H6N5E1L2 + H6N5E2L1 + H6N5E3 + H6N5F1E1L2 + H6N5F1E2L1 + H6N5F1E3 + H6N5F2E1L2 + H6N5F2E2L1)	0,9269	0,0083	0,89%
A4S	Sialylation per antenna within tetra-antennary glycans		A4S = (0/4 * (0) + 1/4 * (0) + 2/4 * (0) + 3/4 * (H7N6E1L2 + H7N6E2L1 + H7N6E3 + H7N6F1E1L2 + H7N6F1E2L1) + 4/4 * (H7N6E1L3 + H7N6E2L2 + H7N6E3L1 + H7N6F1E1L3 + H7N6F1E2L2 + H7N6F1E3L1 + H7N6F2E2L2)) / (H7N6E1L2 + H7N6E2L1 + H7N6E3 + H7N6F1E1L2 + H7N6F1E2L1 + H7N6E1L3 + H7N6E2L2 + H7N6E3L1 + H7N6F1E1L3 + H7N6F1E2L2 + H7N6F1E3L1 + H7N6F2E2L2)	0,8983	0,0063	0,70%
A2FS	Sialylation per antenna within fucosylated diantennary glycans		A2FS = (0/2 * (H3N4F1 + H4N4F1 + H3N5F1 + H5N4F1 + H4N5F1 + H5N5F1) + 1/2 * (H4N4F1E1 + H5N4F1L1 + H5N4F1E1 + H4N5F1E1 + H5N5F1E1) + 2/2 * (H5N4F1L2 + H5N4F1E1L1 + H5N4F1E2 + H5N5F1E1L1 + H5N5F1E2)) / (H3N4F1 + H4N4F1 + H3N5F1 + H5N4F1 + H4N5F1 + H4N4F1E1 + H5N5F1 + H5N4F1L1 + H5N4F1E1 + H4N5F1E1 + H5N5F1E1 + H5N4F1L2 + H5N4F1E1L1 + H5N4F1E2 + H5N5F1E1L1 + H5N5F1E2)	0,5673	0,0398	7,01%
A2F0S	Sialylation per antenna within non-fucosylated diantennary glycans		A2F0S = (0/2 * (H4N4 + H3N5 + H5N4 + H4N5 + H5N5) + 1/2 * (H4N4E1 + H5N4L1 + H5N4E1 + H4N5E1 + H5N5E1) + 2/2 * (H5N4L2 + H5N4E1L1 + H5N4E2 + H5N5E2)) / (H4N4 + H3N5 + H5N4 + H4N5 + H4N4E1 + H5N5 + H5N4L1 + H5N4E1 + H4N5E1 + H5N5E1 + H5N4L2 + H5N4E1L1 + H5N4E2 + H5N5E2)	0,9342	0,0068	0,72%

Supplementary Table S2. Derived trait description, depiction, and calculation. (*continued*)

Derived trait			Calculation	Relative intensity VisuCon standard plasma (N=149)		
A3FS	Sialylation per antenna within fucosylated triantennary glycans		A3FS = (0/3 * (0) + 1/3 * (H6N5F1E1) + 2/3 * (H6N5F1L2 + H6N5F1E1L1 + H6N5F1E2) + 3/3 * (H6N5F1E1L2 + H6N5F1E2L1 + H6N5F1E3 + H6N5F2E1L2 + H6N5F2E2L1)) / (H6N5F1E1 + H6N5F1L2 + H6N5F1E1L1 + H6N5F1E2 + H6N5F1E1L2 + H6N5F1E2L1 + H6N5F1E3 + H6N5F2E1L2 + H6N5F2E2L1)	0,9471	0,0066	0,70%
A3F0S	Sialylation per antenna within non-fucosylated triantennary glycans		A3F0S = (0/3 * (0) + 1/3 * (H6N5E1) + 2/3 * (H6N5L2 + H6N5E1L1 + H6N5E2) + 3/3 * (H6N5E1L2 + H6N5E2L1 + H6N5E3)) / (H6N5E1 + H6N5L2 + H6N5E1L1 + H6N5E2 + H6N5E1L2 + H6N5E2L1 + H6N5E3)	0,9156	0,0107	1,17%
A4FS	Sialylation per antenna within fucosylated tetra-antennary glycans	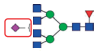	A4FS = (0/4 * (0) + 1/4 * (0) + 2/4 * (0) + 3/4 * (H7N6F1E1L2 + H7N6F1E2L1) + 4/4 * (H7N6F1E1L3 + H7N6F1E2L2 + H7N6F1E3L1 + H7N6F2E2L2)) / (H7N6E1L2 + H7N6E2L1 + H7N6E3 + H7N6F1E1L2 + H7N6F1E2L1 + H7N6E1L3 + H7N6E2L2 + H7N6E3L1 + H7N6F1E1L3 + H7N6F1E2L2 + H7N6F1E3L1 + H7N6F2E2L2)	0,3085	0,0262	8,48%
A4F0S	Sialylation per antenna within non-fucosylated tetra-antennary glycans	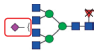	A4F0S = (0/4 * (0) + 1/4 * (0) + 2/4 * (0) + 3/4 * (H7N6E1L2 + H7N6E2L1 + H7N6E3) + 4/4 * (H7N6E1L3 + H7N6E2L2 + H7N6E3L1)) / (H7N6E1L2 + H7N6E2L1 + H7N6E3 + H7N6F1E1L2 + H7N6F1E2L1 + H7N6E1L3 + H7N6E2L2 + H7N6E3L1 + H7N6F1E1L3 + H7N6F1E2L2 + H7N6F1E3L1 + H7N6F2E2L2)	0,5896	0,0270	4,59%
Sialylation per galactose						
A2GS	Sialylation per galactose within diantennary glycans		A2GS = ((0/2 * (H3N4F1 + H4N4 + H3N5 + H4N4F1 + H5N4 + H3N5F1 + H4N5 + H5N4F1 + H4N5F1 + H5N5 + H5N5F1) + 1/2 * (H4N4E1 + H5N4L1 + H4N4F1E1 + H5N4E1 + H4N5E1 + H5N4F1L1 + H5N4F1E1 + H4N5F1E1 + H5N5E1 + H5N5F1E1) + 2/2 * (H5N4L2 + H5N4E1L1 + H5N4E2 + H5N4F1L2 + H5N4F1E1L1 + H5N4F1E2 + H5N5E2 + H5N5F1E1L1 + H5N5F1E2)) / (H3N4F1 + H4N4 + H3N5 + H4N4F1 + H5N4 + H3N5F1 + H4N5 + H5N4F1 + H4N4E1 + H4N5F1 + H5N5 + H5N4L1 + H4N4F1E1 + H5N4E1 + H5N5F1 + H4N5E1 + H5N4F1L1 + H5N4F1E1 + H4N5F1E1 + H5N5E1 + H5N4L2 + H5N4E1L1 + H5N4E2 + H5N5F1E1 + H5N4F1L2 + H5N4F1E1L1 + H5N4F1E2 + H5N5E2 + H5N5F1E1L1 + H5N5F1E2)) / ((0/2 * (H3N4F1 + H3N5 + H3N5F1) + 1/2 * (H4N4 + H4N4F1 + H4N5 + H4N4E1 + H4N5F1 + H4N4F1E1 + H4N5E1 + H4N5F1E1) + 2/2 * (H5N4 + H5N4F1 + H5N5 + H5N4L1 + H5N4E1 + H5N5F1 + H5N4F1L1 + H5N4F1E1 + H5N5E1 + H5N4L2 + H5N4E1L1 + H5N4E2 + H5N5F1E1 + H5N4F1L2 + H5N4F1E1L1 + H5N4F1E2 + H5N5E2 + H5N5F1E1L1 + H5N5F1E2)) / (H3N4F1 + H4N4 + H3N5 + H4N4F1 + H5N4 + H3N5F1 + H4N5 + H5N4F1 + H4N4E1 + H4N5F1 + H5N5 + H5N4L1 + H4N4F1E1 + H5N4E1 + H5N5F1 + H4N5E1 + H5N4F1L1 + H5N4F1E1 + H4N5F1E1 + H5N5E1 + H5N4L2 + H5N4E1L1 + H5N4E2 + H5N5F1E1 + H5N4F1L2 + H5N4F1E1L1 + H5N4F1E2 + H5N5E2 + H5N5F1E1L1 + H5N5F1E2))	0,8924	0,0144	1,61%

Supplementary Table S2. Derived trait description, depiction, and calculation. (*continued*)

Derived trait			Calculation	Relative intensity VisuCon standard plasma (N=149)		
A2FGS	Sialylation per galactose within fucosylated diantennary glycans		A2FGS = ((0/2 * (H3N4F1 + H4N4F1 + H3N5F1 + H5N4F1 + H4N5F1 + H5N5F1) + 1/2 * (H4N4F1E1 + H5N4F1L1 + H5N4F1E1 + H4N5F1E1 + H5N5F1E1) + 2/2 * (H5N4F1L2 + H5N4F1E1L1 + H5N4F1E2 + H5N5F1E1L1 + H5N5F1E2)) / (H3N4F1 + H4N4F1 + H3N5F1 + H5N4F1 + H4N5F1 + H4N4F1E1 + H5N5F1 + H5N4F1L1 + H5N4F1E1 + H4N5F1E1 + H5N5F1E1 + H5N4F1L2 + H5N4F1E1L1 + H5N4F1E2 + H5N5F1E1L1 + H5N5F1E2)) / ((0/2 * (H3N4F1 + H3N5F1) + 1/2 * (H4N4F1 + H4N5F1 + H4N4F1E1 + H4N5F1E1) + 2/2 * (H5N4F1 + H5N5F1 + H5N4F1L1 + H5N4F1E1 + H5N5F1E1 + H5N4F1L2 + H5N4F1E1L1 + H5N4F1E2 + H5N5F1E1L1 + H5N5F1E2)) / (H3N4F1 + H4N4F1 + H3N5F1 + H5N4F1 + H4N5F1 + H4N4F1E1 + H5N5F1 + H5N4F1L1 + H5N4F1E1 + H4N5F1E1 + H5N5F1E1 + H5N4F1L2 + H5N4F1E1L1 + H5N4F1E2 + H5N5F1E1L1 + H5N5F1E2))	0,6681	0,0340	5,09%
A2F0GS	Sialylation per galactose within non-fucosylated diantennary glycans		A2F0GS = ((0/2*(H4N4 + H3N5 + H5N4 + H4N5 + H5N5) + 1/2 * (H4N4E1 + H5N4L1 + H5N4E1 + H4N5E1 + H5N5E1) + 2/2 * (H5N4L2 + H5N4E1L1 + H5N4E2 + H5N5E2)) / (H4N4 + H3N5 + H5N4 + H4N5 + H4N4E1 + H5N5 + H5N4L1 + H5N4E1 + H4N5E1 + H5N5E1 + H5N4L2 + H5N4E1L1 + H5N4E2 + H5N5E2)) / ((0/2 * (H3N5) + 1/2 * (H4N4 + H4N5 + H4N4E1 + H4N5E1) + 2/2 * (H5N4 + H5N5 + H5N4L1 + H5N4E1 + H5N5E1 + H5N4L2 + H5N4E1L1 + H5N4E2 + H5N5E2)) / (H4N4 + H3N5 + H5N4 + H4N5 + H4N4E1 + H5N5 + H5N4L1 + H5N4E1 + H4N5E1 + H5N5E1 + H5N4L2 + H5N4E1L1 + H5N4E2 + H5N5E2))	0,9383	0,0062	0,66%
A4FGS	Sialylation per galactose within fucosylated tetra-antennary glycans	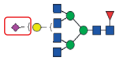	A4FGS = ((0/4 * (0) + 1/4 * (0) + 2/4 * (0) + 3/4 * (H7N6F1E1L2 + H7N6F1E2L1) + 4/4 * (H7N6F1E1L3 + H7N6F1E2L2 + H7N6F1E3L1 + H7N6F2E2L2)) / (H7N6E1L2 + H7N6E2L1 + H7N6E3 + H7N6F1E1L2 + H7N6F1E2L1 + H7N6E1L3 + H7N6E2L2 + H7N6E3L1 + H7N6F1E1L3 + H7N6F1E2L2 + H7N6F1E3L1 + H7N6F2E2L2)) / ((0/4 * (0) + 1/4 * (0) + 2/4 * (0) + 3/4 * (0) + 4/4 * (H7N6F1E1L2 + H7N6F1E2L1 + H7N6F1E1L3 + H7N6F1E2L2 + H7N6F1E3L1 + H7N6F2E2L2)) / (H7N6E1L2 + H7N6E2L1 + H7N6E3 + H7N6F1E1L2 + H7N6F1E2L1 + H7N6E1L3 + H7N6E2L2 + H7N6E3L1 + H7N6F1E1L3 + H7N6F1E2L2 + H7N6F1E3L1 + H7N6F2E2L2))	0,9084	0,0091	1,00%

Supplementary Table S2. Derived trait description, depiction, and calculation. (*continued*)

Derived trait			Calculation	Relative intensity VisuCon standard plasma (N=149)		
α2,3-sialylation per antenna						
A2L	α2,3-sialylation per antenna within diantennary glycans		A2L = (0/2 * (H3N4F1 + H4N4 + H3N5 + H4N4F1 + H5N4 + H3N5F1 + H4N5 + H5N4F1 + H4N4E1 + H4N5F1 + H5N5 + H4N4F1E1 + H5N4E1 + H5N5F1 + H4N5E1 + H5N4F1E1 + H4N5F1E1 + H5N5E1 + H5N4E2 + H5N5F1E1 + H5N4F1E2 + H5N5E2 + H5N5F1E2) + 1/2 * (H5N4L1 + H5N4F1L1 + H5N4E1L1 + H5N4F1E1L1 + H5N5F1E1L1) + 2/2 * (H5N4L2 + H5N4F1L2)) / (H3N4F1 + H4N4 + H3N5 + H4N4F1 + H5N4 + H3N5F1 + H4N5 + H5N4F1 + H4N4E1 + H4N5F1 + H5N5 + H5N4L1 + H4N4F1E1 + H5N4E1 + H5N5F1 + H4N5E1 + H5N4F1L1 + H5N4F1E1 + H4N5F1E1 + H5N5E1 + H5N4L2 + H5N4E1L1 + H5N4E2 + H5N5F1E1 + H5N4F1L2 + H5N4F1E1L1 + H5N4F1E2 + H5N5E2 + H5N5F1E1L1 + H5N5F1E2)	0,0568	0,0044	7,70%
A2FL	α2,3-sialylation per antenna within fucosylated diantennary glycans		A2FL = (0/2 * (H3N4F1 + H4N4F1 + H3N5F1 + H5N4F1 + H4N5F1 + H4N4F1E1 + H5N5F1 + H5N4F1E1 + H4N5F1E1 + H5N5F1E1 + H5N4F1E2 + H5N5F1E2) + 1/2 * (H5N4F1L1 + H5N4F1E1L1 + H5N5F1E1L1) + 2/2 * (H5N4F1L2)) / (H3N4F1 + H4N4F1 + H3N5F1 + H5N4F1 + H4N5F1 + H4N4F1E1 + H5N5F1 + H5N4F1E1 + H4N5F1E1 + H5N5F1E1 + H5N4F1L1 + H5N4F1E1 + H4N5F1E1 + H5N5F1E1 + H5N4F1L2 + H5N4F1E1L1 + H5N4F1E2 + H5N5F1E1L1 + H5N5F1E2)	0,1087	0,0105	9,67%
A2F0L	α2,3-sialylation per antenna within non-fucosylated diantennary glycans		A2F0L = (0/2 * (H4N4 + H3N5 + H5N4 + H4N5 + H4N4E1 + H5N5 + H5N4E1 + H4N5E1 + H5N5E1 + H5N4E2 + H5N5E2) + 1/2 * (H5N4L1 + H5N4E1L1) + 2/2 * (H5N4L2)) / (H4N4 + H3N5 + H5N4 + H4N5 + H4N4E1 + H5N5 + H5N4L1 + H5N4E1 + H4N5E1 + H5N5E1 + H5N4L2 + H5N4E1L1 + H5N4E2 + H5N5E2)	0,0443	0,0038	8,65%
A3L	α2,3-sialylation per antenna within triantennary glycans		A3L = (0/3 * (H6N5E1 + H6N5F1E1 + H6N5E2 + H6N5F1E2 + H6N5E3 + H6N5F1E3) + 1/3 * (H6N5E1L1 + H6N5F1E1L1 + H6N5E2L1 + H6N5F1E2L1 + H6N5F2E2L1) + 2/3 * (H6N5L2 + H6N5F1L2 + H6N5E1L2 + H6N5F1E1L2 + H6N5F2E1L2) + 3/3 * (0)) / (H6N5E1 + H6N5F1E1 + H6N5L2 + H6N5E1L1 + H6N5E2 + H6N5F1L2 + H6N5F1E1L1 + H6N5F1E2 + H6N5E1L2 + H6N5E2L1 + H6N5E3 + H6N5F1E1L2 + H6N5F1E2L1 + H6N5F1E3 + H6N5F2E1L2 + H6N5F2E2L1)	0,2779	0,0052	1,86%
A3FL	α2,3-sialylation per antenna within fucosylated triantennary glycans		A3FL = (0/3 * (H6N5F1E1 + H6N5F1E2 + H6N5F1E3) + 1/3 * (H6N5F1E1L1 + H6N5F1E2L1 + H6N5F2E2L1) + 2/3 * (H6N5F1L2 + H6N5F1E1L2 + H6N5F2E1L2) + 3/3 * (0)) / (H6N5F1E1 + H6N5F1L2 + H6N5F1E1L1 + H6N5F1E2 + H6N5F1E1L2 + H6N5F1E2L1 + H6N5F1E3 + H6N5F2E1L2 + H6N5F2E2L1)	0,3375	0,0040	1,18%

Supplementary Table S2. Derived trait description, depiction, and calculation. (*continued*)

Derived trait			Calculation	Relative intensity VisuCon standard plasma (N=149)		
A3F0L	α2,3-sialylation per antenna within non-fucosylated triantennary glycans		A3F0L = (0/3 * (H6N5E1 + H6N5E2 + H6N5E3) + 1/3 * (H6N5E1L1 + H6N5E2L1) + 2/3 * (H6N5L2 + H6N5E1L2) + 3/3 * (0)) / (H6N5E1 + H6N5L2 + H6N5E1L1 + H6N5E2 + H6N5E1L2 + H6N5E2L1 + H6N5E3)	0,2442	0,0075	3,08%
A4L	α2,3-sialylation per antenna within tetra-antennary glycans	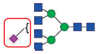	A4L = (0/4 * (H7N6E3) + 1/4 * (H7N6E2L1 + H7N6F1E2L1 + H7N6E3L1 + H7N6F1E3L1) + 2/4 * (H7N6E1L2 + H7N6F1E1L2 + H7N6E2L2 + H7N6F1E2L2 + H7N6F2E2L2) + 3/4 * (H7N6E1L3 + H7N6F1E1L3) + 4/4 * (0)) / (H7N6E1L2 + H7N6E2L1 + H7N6E3 + H7N6F1E1L2 + H7N6F1E2L1 + H7N6E1L3 + H7N6E2L2 + H7N6E3L1 + H7N6F1E1L3 + H7N6F1E2L2 + H7N6F1E3L1 + H7N6F2E2L2)	0,4712	0,0103	2,18%
A4FL	α2,3-sialylation per antenna within fucosylated tetra-antennary glycans	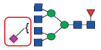	A4FL = (0/4 * (0) + 1/4 * (H7N6F1E2L1 + H7N6F1E3L1) + 2/4 * (H7N6F1E1L2 + H7N6F1E2L2 + H7N6F2E2L2) + 3/4 * (H7N6F1E1L3) + 4/4 * (0)) / (H7N6E1L2 + H7N6E2L1 + H7N6E3 + H7N6F1E1L2 + H7N6F1E2L1 + H7N6E1L3 + H7N6E2L2 + H7N6E3L1 + H7N6F1E1L3 + H7N6F1E2L2 + H7N6F1E3L1 + H7N6F2E2L2)	0,1654	0,0146	8,85%
A4F0L	α2,3-sialylation per antenna within non-fucosylated tetra-antennary glycans	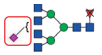	A4F0L = (0/4 * (H7N6E3) + 1/4 * (H7N6E2L1 + H7N6E3L1) + 2/4 * (H7N6E1L2 + H7N6E2L2) + 3/4 * (H7N6E1L3) + 4/4 * (0)) / (H7N6E1L2 + H7N6E2L1 + H7N6E3 + H7N6F1E1L2 + H7N6F1E2L1 + H7N6E1L3 + H7N6E2L2 + H7N6E3L1 + H7N6F1E1L3 + H7N6F1E2L2 + H7N6F1E3L1 + H7N6F2E2L2)	0,3057	0,0171	5,60%
α2,6-sialylation per antenna						
A2E	α2,6-sialylation per antenna within diantennary glycans		A2E = (0/2 * (H3N4F1 + H4N4 + H3N5 + H4N4F1 + H5N4 + H3N5F1 + H4N5 + H5N4F1 + H4N5F1 + H5N5 + H5N4L1 + H5N5F1 + H5N4F1L1 + H5N4L2 + H5N4F1L2) + 1/2 * (H4N4E1 + H4N4F1E1 + H5N4E1 + H4N5E1 + H5N4F1E1 + H4N5F1E1 + H5N5E1 + H5N4E1L1 + H5N5F1E1 + H5N4F1E1L1 + H5N5F1E1L1) + 2/2 * (H5N4E2 + H5N4F1E2 + H5N5E2 + H5N5F1E2)) / (H3N4F1 + H4N4 + H3N5 + H4N4F1 + H5N4 + H3N5F1 + H4N5 + H5N4F1 + H4N4E1 + H4N5F1 + H5N5 + H5N4L1 + H4N4F1E1 + H5N4E1 + H5N5F1 + H4N5E1 + H5N4F1L1 + H5N4F1E1 + H4N5F1E1 + H5N5E1 + H5N4L2 + H5N4E1L1 + H5N4E2 + H5N5F1E1 + H5N4F1L2 + H5N4F1E1L1 + H5N4F1E2 + H5N5E2 + H5N5F1E1L1 + H5N5F1E2)	0,8062	0,0200	2,47%
A2FE	α2,6-sialylation per antenna within fucosylated diantennary glycans		A2FE = (0/2 * (H3N4F1 + H4N4F1 + H3N5F1 + H5N4F1 + H4N5F1 + H5N5F1 + H5N4F1L1 + H5N4F1L2) + 1/2 * (H4N4F1E1 + H5N4F1E1 + H4N5F1E1 + H5N5F1E1 + H5N4F1E1L1 + H5N5F1E1L1) + 2/2 * (H5N4F1E2 + H5N5F1E2)) / (H3N4F1 + H4N4F1 + H3N5F1 + H5N4F1 + H4N5F1 + H4N4F1E1 + H5N5F1 + H5N4F1L1 + H5N4F1E1 + H4N5F1E1 + H5N5F1E1 + H5N4F1L2 + H5N4F1E1L1 + H5N4F1E2 + H5N5F1E1L1 + H5N5F1E2)	0,4563	0,0313	6,86%

Supplementary Table S2. Derived trait description, depiction, and calculation. (*continued*)

Derived trait			Calculation	Relative intensity VisuCon standard plasma (N=149)		
A2F0E	α2,6-sialylation per antenna within non-fucosylated diantennary glycans		A2F0E = (0/2 * (H4N4 + H3N5 + H5N4 + H4N5 + H5N5 + H5N4L1 + H5N4L2) + 1/2 * (H4N4E1 + H5N4E1 + H4N5E1 + H5N5E1 + H5N4E1L1) + 2/2 * (H5N4E2 + H5N5E2)) / (H4N4 + H3N5 + H5N4 + H4N5 + H4N4E1 + H5N5 + H5N4L1 + H5N4E1 + H4N5E1 + H5N5E1 + H5N4L2 + H5N4E1L1 + H5N4E2 + H5N5E2)	0,8898	0,0089	1,00%
A3E	α2,6-sialylation per antenna within triantennary glycans		A3E = (0/3 * (H6N5L2 + H6N5F1L2) + 1/3 * (H6N5E1 + H6N5F1E1 + H6N5E1L1 + H6N5F1E1L1 + H6N5E1L2 + H6N5F1E1L2 + H6N5F2E1L2) + 2/3 * (H6N5E2 + H6N5F1E2 + H6N5E2L1 + H6N5F1E2L1 + H6N5F2E2L1) + 3/3 * (H6N5E3 + H6N5F1E3)) / (H6N5E1 + H6N5F1E1 + H6N5L2 + H6N5E1L1 + H6N5E2 + H6N5F1L2 + H6N5F1E1L1 + H6N5F1E2 + H6N5E1L2 + H6N5E2L1 + H6N5E3 + H6N5F1E1L2 + H6N5F1E2L1 + H6N5F1E3 + H6N5F2E1L2 + H6N5F2E2L1)	0,6490	0,0072	1,11%
A3FE	α2,6-sialylation per antenna within fucosylated triantennary glycans		A3FE = (0/3 * (H6N5F1L2) + 1/3 * (H6N5F1E1 + H6N5F1E1L1 + H6N5F1E1L2 + H6N5F2E1L2) + 2/3 * (H6N5F1E2 + H6N5F1E2L1 + H6N5F2E2L1) + 3/3 * (H6N5F1E3)) / (H6N5F1E1 + H6N5F1L2 + H6N5F1E1L1 + H6N5F1E2 + H6N5F1E1L2 + H6N5F1E2L1 + H6N5F1E3 + H6N5F2E1L2 + H6N5F2E2L1)	0,6094	0,0057	0,94%
A3F0E	α2,6-sialylation per antenna within non-fucosylated triantennary glycans		A3F0E = (0/3 * (H6N5L2) + 1/3 * (H6N5E1 + H6N5E1L1 + H6N5E1L2) + 2/3 * (H6N5E2 + H6N5E2L1) + 3/3 * (H6N5E3)) / (H6N5E1 + H6N5L2 + H6N5E1L1 + H6N5E2 + H6N5E1L2 + H6N5E2L1 + H6N5E3)	0,6713	0,0079	1,18%
A4E	α2,6-sialylation per antenna within tetra-antennary glycans	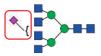	A4E = (0/4 * (0) + 1/4 * (H7N6E1L2 + H7N6F1E1L2 + H7N6E1L3 + H7N6F1E1L3) + 2/4 * (H7N6E2L1 + H7N6F1E2L1 + H7N6E2L2 + H7N6F1E2L2 + H7N6F2E2L2) + 3/4 * (H7N6E3 + H7N6E3L1 + H7N6F1E3L1) + 4/4 * (0)) / (H7N6E1L2 + H7N6E2L1 + H7N6E3 + H7N6F1E1L2 + H7N6F1E2L1 + H7N6E1L3 + H7N6E2L2 + H7N6E3L1 + H7N6F1E1L3 + H7N6F1E2L2 + H7N6F1E3L1 + H7N6F2E2L2)	0,4272	0,0082	1,93%
A4FE	α2,6-sialylation per antenna within fucosylated tetra-antennary glycans	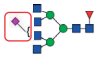	A4FE = (0/4 * (0) + 1/4 * (H7N6F1E1L2 + H7N6F1E1L3) + 2/4 * (H7N6F1E2L1 + H7N6F1E2L2 + H7N6F2E2L2) + 3/4 * (H7N6F1E3L1) + 4/4 * (0)) / (H7N6E1L2 + H7N6E2L1 + H7N6E3 + H7N6F1E1L2 + H7N6F1E2L1 + H7N6E1L3 + H7N6E2L2 + H7N6E3L1 + H7N6F1E1L3 + H7N6F1E2L2 + H7N6F1E3L1 + H7N6F2E2L2)	0,1431	0,0129	9,04%

Supplementary Table S2. Derived trait description, depiction, and calculation. (*continued*)

Derived trait			Calculation	Relative intensity VisuCon standard plasma (N=149)		
A4F0E	α2,6-sialylation per antenna within non-fucosylated tetra-antennary glycans		A4F0E = (0/4 * (0) + 1/4 * (H7N6E1L2 + H7N6E1L3) + 2/4 * (H7N6E2L1 + H7N6E2L2) + 3/4 * (H7N6E3 + H7N6E3L1) + 4/4 * (0)) / (H7N6E1L2 + H7N6E2L1 + H7N6E3 + H7N6F1E1L2 + H7N6F1E2L1 + H7N6E1L3 + H7N6E2L2 + H7N6E3L1 + H7N6F1E1L3 + H7N6F1E2L2 + H7N6F1E3L1 + H7N6F2E2L2)	0,2839	0,0129	4,56%
α2,3-sialylation per galactose						
A2GL	α2,3-sialylation per galactose within diantennary glycans		A2GL = ((0/2 * (H3N4F1 + H4N4 + H3N5 + H4N4F1 + H5N4 + H3N5F1 + H4N5 + H5N4F1 + H4N4E1 + H4N5F1 + H5N5 + H4N4F1E1 + H5N4E1 + H5N5F1 + H4N5E1 + H5N4F1E1 + H4N5F1E1 + H5N5E1 + H5N4E2 + H5N5F1E1 + H5N4F1E2 + H5N5E2 + H5N5F1E2) + 1/2 * (H5N4L1 + H5N4F1L1 + H5N4E1L1 + H5N4F1E1L1 + H5N5F1E1L1) + 2/2 * (H5N4L2 + H5N4F1L2)) / (H3N4F1 + H4N4 + H3N5 + H4N4F1 + H5N4 + H3N5F1 + H4N5 + H5N4F1 + H4N4E1 + H4N5F1 + H5N5 + H5N4L1 + H4N4F1E1 + H5N4E1 + H5N5F1 + H4N5E1 + H5N4F1L1 + H5N4F1E1 + H4N5F1E1 + H5N5E1 + H5N4L2 + H5N4E1L1 + H5N4E2 + H5N5F1E1 + H5N4F1L2 + H5N4F1E1L1 + H5N4F1E2 + H5N5E2 + H5N5F1E1L1 + H5N5F1E2)) / ((0/2 * (H3N4F1 + H3N5 + H3N5F1) + 1/2 * (H4N4 + H4N4F1 + H4N5 + H4N4E1 + H4N5F1 + H4N4F1E1 + H4N5E1 + H4N5F1E1) + 2/2 * (H5N4 + H5N4F1 + H5N5 + H5N4L1 + H5N4E1 + H5N5F1 + H5N4F1L1 + H5N4F1E1 + H5N5E1 + H5N4L2 + H5N4E1L1 + H5N4E2 + H5N5F1E1 + H5N4F1L2 + H5N4F1E1L1 + H5N4F1E2 + H5N5E2 + H5N5F1E1L1 + H5N5F1E2)) / (H3N4F1 + H4N4 + H3N5 + H4N4F1 + H5N4 + H3N5F1 + H4N5 + H5N4F1 + H4N4E1 + H4N5F1 + H5N5 + H5N4L1 + H4N4F1E1 + H5N4E1 + H5N5F1 + H4N5E1 + H5N4F1L1 + H5N4F1E1 + H4N5F1E1 + H5N5E1 + H5N4L2 + H5N4E1L1 + H5N4E2 + H5N5F1E1 + H5N4F1L2 + H5N4F1E1L1 + H5N4F1E2 + H5N5E2 + H5N5F1E1L1 + H5N5F1E2))	0,0587	0,0046	7,75%
A2FGL	α2,3-sialylation per galactose within fucosylated diantennary glycans		A2FGL = ((0/2 * (H3N4F1 + H4N4F1 + H3N5F1 + H5N4F1 + H4N5F1 + H4N4F1E1 + H5N5F1 + H5N4F1E1 + H4N5F1E1 + H5N5F1E1 + H5N4F1E2 + H5N5F1E2) + 1/2 * (H5N4F1L1 + H5N4F1E1L1 + H5N5F1E1L1) + 2/2 * (H5N4F1L2)) / (H3N4F1 + H4N4F1 + H3N5F1 + H5N4F1 + H4N5F1 + H4N4F1E1 + H5N5F1 + H5N4F1L1 + H5N4F1E1 + H4N5F1E1 + H5N5F1E1 + H5N4F1L2 + H5N4F1E1L1 + H5N4F1E2 + H5N5F1E1L1 + H5N5F1E2)) / ((0/2 * (H3N4F1 + H3N5F1) + 1/2 * (H4N4F1 + H4N5F1 + H4N4F1E1 + H4N5F1E1) + 2/2 * (H5N4F1 + H5N5F1 + H5N4F1L1 + H5N4F1E1 + H5N5F1E1 + H5N4F1L2 + H5N4F1E1L1 + H5N4F1E2 + H5N5F1E1L1 + H5N5F1E2)) / (H3N4F1 + H4N4F1 + H3N5F1 + H5N4F1 + H4N5F1 + H4N4F1E1 + H5N5F1 + H5N4F1L1 + H5N4F1E1 + H4N5F1E1 + H5N5F1E1 + H5N4F1L2 + H5N4F1E1L1 + H5N4F1E2 + H5N5F1E1L1 + H5N5F1E2))	0,1278	0,0101	7,88%

Supplementary Table S2. Derived trait description, depiction, and calculation. (*continued*)

Derived trait			Calculation	Relative intensity VisuCon standard plasma (N=149)		
A2F0GL	α2,3-sialylation per galactose within non-fucosylated diantennary glycans	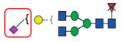	A2F0GL = ((0/2 * (H4N4 + H3N5 + H5N4 + H4N5 + H4N4E1 + H5N5 + H5N4E1 + H4N5E1 + H5N5E1 + H5N4E2 + H5N5E2) + 1/2 * (H5N4L1 + H5N4E1L1) + 2/2 * (H5N4L2)) / (H4N4 + H3N5 + H5N4 + H4N5 + H4N4E1 + H5N5 + H5N4L1 + H5N4E1 + H4N5E1 + H5N5E1 + H5N4L2 + H5N4E1L1 + H5N4E2 + H5N5E2)) / ((0/2 * (H3N5) + 1/2 * (H4N4 + H4N5 + H4N4E1 + H4N5E1) + 2/2 * (H5N4 + H5N5 + H5N4L1 + H5N4E1 + H5N5E1 + H5N4L2 + H5N4E1L1 + H5N4E2 + H5N5E2)) / (H4N4 + H3N5 + H5N4 + H4N5 + H4N4E1 + H5N5 + H5N4L1 + H5N4E1 + H4N5E1+H5N5E1+H5N4L2+ H5N4E1L1 + H5N4E2 + H5N5E2))	0,0445	0,0039	8,67%
A4FGL	α2,3-sialylation per galactose within fucosylated tetra-antennary glycans	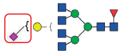	A4FGL = ((0/4 * (0) + 1/4 * (H7N6F1E2L1 + H7N6F1E3L1) + 2/4 * (H7N6F1E1L2 + H7N6F1E2L2 + H7N6F2E2L2) + 3/4 * (H7N6F1E1L3) + 4/4 * (0)) / (H7N6E1L2 + H7N6E2L1 + H7N6E3 + H7N6F1E1L2 + H7N6F1E2L1 + H7N6E1L3 + H7N6E2L2 + H7N6E3L1 + H7N6F1E1L3 + H7N6F1E2L2 + H7N6F1E3L1 + H7N6F2E2L2)) / ((0/4 * (0) + 1/4 * (0) + 2/4 * (0) + 3/4 * (0) + 4/4 * (H7N6F1E1L2 + H7N6F1E2L1 + H7N6F1E1L3 + H7N6F1E2L2 + H7N6F1E3L1 + H7N6F2E2L2)) / (H7N6E1L2 + H7N6E2L1 + H7N6E3 + H7N6F1E1L2 + H7N6F1E2L1 + H7N6E1L3 + H7N6E2L2 + H7N6E3L1 + H7N6F1E1L3 + H7N6F1E2L2 + H7N6F1E3L1 + H7N6F2E2L2))	0,4869	0,0142	2,92%
A4F0GL	α2,3-sialylation per galactose within non-fucosylated tetra-antennary glycans	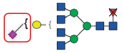	A4F0GL = ((0/4 * (H7N6E3) + 1/4 * (H7N6E2L1 + H7N6E3L1) + 2/4 * (H7N6E1L2 + H7N6E2L2) + 3/4 * (H7N6E1L3) + 4/4 * (0)) / (H7N6E1L2 + H7N6E2L1 + H7N6E3 + H7N6F1E1L2 + H7N6F1E2L1 + H7N6E1L3 + H7N6E2L2 + H7N6E3L1 + H7N6F1E1L3 + H7N6F1E2L2 + H7N6F1E3L1 + H7N6F2E2L2)) / ((0/4 * (0) + 1/4 * (0) + 2/4 * (0) + 3/4 * (0) + 4/4 * (H7N6E1L2 + H7N6E2L1 + H7N6E3 + H7N6E1L3 + H7N6E2L2 + H7N6E3L1)) / (H7N6E1L2 + H7N6E2L1 + H7N6E3 + H7N6F1E1L2 + H7N6F1E2L1 + H7N6E1L3 + H7N6E2L2 + H7N6E3L1 + H7N6F1E1L3 + H7N6F1E2L2 + H7N6F1E3L1 + H7N6F2E2L2))	0,4629	0,0120	2,58%

Supplementary Table S2. Derived trait description, depiction, and calculation. (*continued*)

Derived trait			Calculation	Relative intensity VisuCon standard plasma (N=149)		
α2,6-sialylation per galactose						
A2GE	α2,6-sialylation per galactose within diantennary glycans	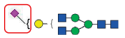	A2GE = ((0/2 * (H3N4F1 + H4N4 + H3N5 + H4N4F1 + H5N4 + H3N5F1 + H4N5 + H5N4F1 + H4N5F1 + H5N5 + H5N4L1 + H5N5F1 + H5N4F1L1 + H5N4L2 + H5N4F1L2) + 1/2 * (H4N4E1 + H4N4F1E1 + H5N4E1 + H4N5E1 + H5N4F1E1 + H4N5F1E1 + H5N5E1 + H5N4E1L1 + H5N5F1E1 + H5N4F1E1L1 + H5N5F1E1L1) + 2/2 * (H5N4E2 + H5N4F1E2 + H5N5E2 + H5N5F1E2)) / (H3N4F1 + H4N4 + H3N5 + H4N4F1 + H5N4 + H3N5F1 + H4N5 + H5N4F1 + H4N4E1 + H4N5F1 + H5N5 + H5N4L1 + H4N4F1E1 + H5N4E1 + H5N5F1 + H4N5E1 + H5N4F1L1 + H5N4F1E1 + H4N5F1E1 + H5N5E1 + H5N4L2 + H5N4E1L1 + H5N4E2 + H5N5F1E1 + H5N4F1L2 + H5N4F1E1L1 + H5N4F1E2 + H5N5E2 + H5N5F1E1L1 + H5N5F1E2)) / ((0/2 * (H3N4F1 + H3N5 + H3N5F1) + 1/2 * (H4N4 + H4N4F1 + H4N5 + H4N4E1 + H4N5F1 + H4N4F1E1 + H4N5E1 + H4N5F1E1) + 2/2 * (H5N4 + H5N4F1 + H5N5 + H5N4L1 + H5N4E1 + H5N5F1 + H5N4F1L1 + H5N4F1E1 + H5N5E1 + H5N4L2 + H5N4E1L1 + H5N4E2 + H5N5F1E1 + H5N4F1L2 + H5N4F1E1L1 + H5N4F1E2 + H5N5E2 + H5N5F1E1L1 + H5N5F1E2)) / (H3N4F1 + H4N4 + H3N5 + H4N4F1 + H5N4 + H3N5F1 + H4N5 + H5N4F1 + H4N4E1 + H4N5F1 + H5N5 + H5N4L1 + H4N4F1E1 + H5N4E1 + H5N5F1 + H4N5E1 + H5N4F1L1 + H5N4F1E1 + H4N5F1E1 + H5N5E1 + H5N4L2 + H5N4E1L1 + H5N4E2 + H5N5F1E1 + H5N4F1L2 + H5N4F1E1L1 + H5N4F1E2 + H5N5E2 + H5N5F1E1L1 + H5N5F1E2))	0,8335	0,0159	1,91%
A2FGE	α2,6-sialylation per galactose within fucosylated diantennary glycans	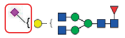	A2FGE = ((0/2 * (H3N4F1 + H4N4F1 + H3N5F1 + H5N4F1 + H4N5F1 + H5N5F1 + H5N4F1L1 + H5N4F1L2) + 1/2 * (H4N4F1E1 + H5N4F1E1 + H4N5F1E1 + H5N5F1E1 + H5N4F1E1L1 + H5N5F1E1L1) + 2/2 * (H5N4F1E2 + H5N5F1E2)) / (H3N4F1 + H4N4F1 + H3N5F1 + H5N4F1 + H4N5F1 + H4N4F1E1 + H5N5F1 + H5N4F1L1 + H5N4F1E1 + H4N5F1E1 + H5N5F1E1 + H5N4F1L2 + H5N4F1E1L1 + H5N4F1E2 + H5N5F1E1L1 + H5N5F1E2)) / ((0/2 * (H3N4F1 + H3N5F1) + 1/2 * (H4N4F1 + H4N5F1 + H4N4F1E1 + H4N5F1E1) + 2/2 * (H5N4F1 + H5N5F1 + H5N4F1L1 + H5N4F1E1 + H5N5F1E1 + H5N4F1L2 + H5N4F1E1L1 + H5N4F1E2 + H5N5F1E1L1 + H5N5F1E2)) / (H3N4F1 + H4N4F1 + H3N5F1 + H5N4F1 + H4N5F1 + H4N4F1E1 + H5N5F1 + H5N4F1L1 + H5N4F1E1 + H4N5F1E1 + H5N5F1E1 + H5N4F1L2 + H5N4F1E1L1 + H5N4F1E2 + H5N5F1E1L1 + H5N5F1E2))	0,5375	0,0269	5,00%

Supplementary Table S2. Derived trait description, depiction, and calculation. (*continued*)

Derived trait			Calculation	Relative intensity VisuCon standard plasma (N=149)		
A2F0GE	α2,6-sialylation per galactose within non-fucosylated diantennary glycans		A2F0GE = ((0/2 * (H4N4 + H3N5 + H5N4 + H4N5 + H5N5 + H5N4L1 + H5N4L2) + 1/2 * (H4N4E1 + H5N4E1 + H4N5E1 + H5N5E1 + H5N4E1L1) + 2/2 * (H5N4E2 + H5N5E2)) / (H4N4 + H3N5 + H5N4 + H4N5 + H4N4E1 + H5N5 + H5N4L1 + H5N4E1 + H4N5E1 + H5N5E1 + H5N4L2 + H5N4E1L1 + H5N4E2 + H5N5E2)) / ((0/2 * (H3N5) + 1/2 * (H4N4 + H4N5 + H4N4E1 + H4N5E1) + 2/2 * (H5N4 + H5N5 + H5N4L1 + H5N4E1 + H5N5E1 + H5N4L2 + H5N4E1L1 + H5N4E2 + H5N5E2)) / (H4N4 + H3N5 + H5N4 + H4N5 + H4N4E1 + H5N5 + H5N4L1 + H5N4E1 + H4N5E1 + H5N5E1 + H5N4L2 + H5N4E1L1 +H5N4E2+H5N5E2))	0,8937	0,0085	0,95%
A4FGE	α2,6-sialylation per galactose within fucosylated tetra-antennary glycans	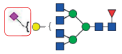	A4FGE = ((0/4 * (0) + 1/4 * (H7N6F1E1L2 + H7N6F1E1L3) + 2/4 * (H7N6F1E2L1 + H7N6F1E2L2 + H7N6F2E2L2) + 3/4 * (H7N6F1E3L1) + 4/4 * (0)) / (H7N6E1L2 + H7N6E2L1 + H7N6E3 + H7N6F1E1L2 + H7N6F1E2L1 + H7N6E1L3 + H7N6E2L2 + H7N6E3L1 + H7N6F1E1L3 + H7N6F1E2L2 + H7N6F1E3L1 + H7N6F2E2L2)) / ((0/4 * (0) + 1/4 * (0) + 2/4 * (0) + 3/4 * (0) + 4/4 * (H7N6F1E1L2 + H7N6F1E2L1 + H7N6F1E1L3 + H7N6F1E2L2 + H7N6F1E3L1 + H7N6F2E2L2)) / (H7N6E1L2 + H7N6E2L1 + H7N6E3 + H7N6F1E1L2 + H7N6F1E2L1 + H7N6E1L3 + H7N6E2L2 + H7N6E3L1 + H7N6F1E1L3 + H7N6F1E2L2 + H7N6F1E3L1 + H7N6F2E2L2))	0,4216	0,0114	2,70%
A4F0GE	α2,6-sialylation per galactose within non-fucosylated tetra-antennary glycans	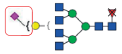	A4F0GE = ((0/4 * (0) + 1/4 * (H7N6E1L2 + H7N6E1L3) + 2/4 * (H7N6E2L1 + H7N6E2L2) + 3/4 * (H7N6E3 + H7N6E3L1) + 4/4 * (0)) / (H7N6E1L2 + H7N6E2L1 + H7N6E3 + H7N6F1E1L2 + H7N6F1E2L1 + H7N6E1L3 + H7N6E2L2 + H7N6E3L1 + H7N6F1E1L3 + H7N6F1E2L2 + H7N6F1E3L1 + H7N6F2E2L2)) / ((0/4 * (0) + 1/4 * (0) + 2/4 * (0) + 3/4 * (0) + 4/4 * (H7N6E1L2 + H7N6E2L1 + H7N6E3 + H7N6E1L3 + H7N6E2L2 + H7N6E3L1)) / (H7N6E1L2 + H7N6E2L1 + H7N6E3 + H7N6F1E1L2 + H7N6F1E2L1 + H7N6E1L3 + H7N6E2L2 + H7N6E3L1 + H7N6F1E1L3 + H7N6F1E2L2 + H7N6F1E3L1 + H7N6F2E2L2))	0,4305	0,0103	2,38%

Within the depictions, divisions have been indicated by braces, exclusions by a cross, whereas numerical values indicate compositional limitations (i.e. 5-9 as the possible number of mannoses, 1-4 N-acetylhexosamines, or 2 fucoses). Trait abbreviations: M = mannose; Hy = hybrid species; T = within total spectrum; C = within complex species; F = deoxyhexose (fucose); G = galactose; S = N-acetylneuraminic acid (sialic acid); E = α2,6-linked sialic acid; L = α2,3-linked sialic acid; H = hexose (mannose or galactose) ; N = N-acetylhexosamine (N-acetylglucosamine: GlcNAc). Additional calculated traits whose values were '0' or '1' in all samples are listed in Table S2 .

Supplementary Table S3. Medians and interquartile ranges of direct and derived glycan traits.

Exact mass $[M+Na]^+$	Discovery cohort								Replication cohort							
	Cases	n=1583			Controls	n=728			Cases	n=232			Controls	n=108		
	Derived traits								Derived traits							
	Trait	25%	median	75%	name	25%	median	75%	Trait	25%	median	75%	name	25%	median	75%
1257,423	H5N2	0,000682	0,000845	0,001060	H5N2	0,000806	0,000977	0,001207	H5N2	0,000687	0,000852	0,001094	H5N2	0,000837	0,001010	0,001194
1419,475	H6N2	0,001978	0,002473	0,003117	H6N2	0,002118	0,002601	0,003250	H6N2	0,001929	0,002435	0,003107	H6N2	0,002065	0,002675	0,003331
1455,523	H3N3E1	0,000537	0,000645	0,000770	H3N3E1	0,000518	0,000618	0,000725	H3N3E1	0,000529	0,000630	0,000751	H3N3E1	0,000506	0,000623	0,000757
1460,502	H5N3	0,000101	0,000151	0,000215	H5N3	0,000131	0,000185	0,000265	H5N3	0,000107	0,000148	0,000218	H5N3	0,000136	0,000206	0,000272
1485,534	H3N4F1	0,005462	0,007705	0,010820	H3N4F1	0,005912	0,008221	0,011126	H3N4F1	0,005300	0,007512	0,010818	H3N4F1	0,005711	0,008084	0,011111
1501,529	H4N4	0,000566	0,000738	0,000989	H4N4	0,000659	0,000876	0,001143	H4N4	0,000537	0,000690	0,000945	H4N4	0,000710	0,000894	0,001069
1542,555	H3N5	0,000187	0,000276	0,000392	H3N5	0,000189	0,000279	0,000390	H3N5	0,000194	0,000287	0,000379	H3N5	0,000193	0,000291	0,000431
1581,528	H7N2	0,000621	0,000857	0,001160	H7N2	0,000649	0,000873	0,001202	H7N2	0,000601	0,000857	0,001185	H7N2	0,000741	0,000934	0,001182
1601,581	H3N3F1E1	0,000628	0,000858	0,001163	H3N3F1E1	0,000656	0,000917	0,001224	H3N3F1E1	0,000653	0,000843	0,001168	H3N3F1E1	0,000672	0,000951	0,001212
1617,576	H4N3E1	0,001854	0,002335	0,003010	H4N3E1	0,001898	0,002378	0,003014	H4N3E1	0,001934	0,002370	0,002948	H4N3E1	0,001997	0,002440	0,003123
1622,555	H6N3	0,000367	0,000499	0,000665	H6N3	0,000412	0,000551	0,000748	H6N3	0,000379	0,000511	0,000684	H6N3	0,000429	0,000536	0,000697
1647,586	H4N4F1	0,011771	0,015611	0,020506	H4N4F1	0,015156	0,019597	0,024379	H4N4F1	0,012071	0,015522	0,020864	H4N4F1	0,014891	0,019750	0,026875
1663,581	H5N4	0,000664	0,000842	0,001071	H5N4	0,000770	0,000964	0,001207	H5N4	0,000669	0,000843	0,001053	H5N4	0,000754	0,000970	0,001180
1688,613	H3N5F1	0,002303	0,003050	0,003920	H3N5F1	0,002270	0,002986	0,003840	H3N5F1	0,002366	0,003079	0,004100	H3N5F1	0,002406	0,002915	0,004080
1704,608	H4N5	0,000404	0,000532	0,000700	H4N5	0,000432	0,000561	0,000722	H4N5	0,000382	0,000511	0,000687	H4N5	0,000438	0,000568	0,000724
1743,581	H8N2	0,001618	0,002107	0,002758	H8N2	0,001828	0,002340	0,003004	H8N2	0,001618	0,002134	0,002702	H8N2	0,001822	0,002286	0,003139
1779,629	H5N3E1	0,001443	0,001800	0,002251	H5N3E1	0,001512	0,001848	0,002300	H5N3E1	0,001535	0,001830	0,002268	H5N3E1	0,001500	0,001866	0,002309
1809,639	H5N4F1	0,006610	0,009165	0,012574	H5N4F1	0,008493	0,011435	0,014682	H5N4F1	0,006570	0,009194	0,012583	H5N4F1	0,008629	0,011961	0,016603
1820,655	H4N4E1	0,002335	0,002780	0,003349	H4N4E1	0,002672	0,003172	0,003828	H4N4E1	0,002368	0,002731	0,003325	H4N4E1	0,002690	0,003101	0,003754
1850,666	H4N5F1	0,004340	0,005461	0,007003	H4N5F1	0,004791	0,005912	0,007298	H4N5F1	0,004446	0,005436	0,006686	H4N5F1	0,005000	0,006314	0,007728
1866,661	H5N5	0,000390	0,000488	0,000621	H5N5	0,000433	0,000544	0,000664	H5N5	0,000394	0,000483	0,000607	H5N5	0,000444	0,000565	0,000687
1905,634	H9N2	0,003823	0,004903	0,006359	H9N2	0,004140	0,005222	0,006797	H9N2	0,003618	0,005159	0,006435	H9N2	0,004184	0,005304	0,006678

Supplementary Table S3. Medians and interquartile ranges of direct and derived glycan traits. (*continued*)

Exact mass $[M+Na]^+$	Discovery cohort								Replication cohort							
	Cases	n=1583			Controls	n=728			Cases	n=232			Controls	n=108		
	Derived traits								Derived traits							
	Trait	25%	median	75%	name	25%	median	75%	Trait	25%	median	75%	name	25%	median	75%
1936,666	H5N4L1	0,001722	0,001984	0,002316	H5N4L1	0,001887	0,002162	0,002482	H5N4L1	0,001719	0,001987	0,002289	H5N4L1	0,001902	0,002168	0,002392
1941,682	H6N3E1	0,001580	0,001908	0,002357	H6N3E1	0,001600	0,001887	0,002267	H6N3E1	0,001644	0,001974	0,002417	H6N3E1	0,001586	0,001883	0,002332
1966,713	H4N4F1E1	0,002221	0,002648	0,003180	H4N4F1E1	0,002432	0,002878	0,003464	H4N4F1E1	0,002116	0,002632	0,003163	H4N4F1E1	0,002506	0,002872	0,003566
1982,708	H5N4E1	0,064318	0,072431	0,081987	H5N4E1	0,067267	0,075272	0,083591	H5N4E1	0,064200	0,071731	0,079920	H5N4E1	0,067357	0,073062	0,082484
2012,719	H5N5F1	0,001842	0,002303	0,002950	H5N5F1	0,002126	0,002593	0,003239	H5N5F1	0,001893	0,002262	0,002870	H5N5F1	0,002283	0,002837	0,003456
2023,735	H4N5E1	0,000463	0,000650	0,000863	H4N5E1	0,000497	0,000669	0,000872	H4N5E1	0,000456	0,000637	0,000856	H4N5E1	0,000497	0,000654	0,000893
2082,724	H5N4F1L1	0,003461	0,003988	0,004585	H5N4F1L1	0,003849	0,004323	0,004866	H5N4F1L1	0,003536	0,004042	0,004574	H5N4F1L1	0,003912	0,004451	0,004871
2128,766	H5N4F1E1	0,016185	0,019746	0,023805	H5N4F1E1	0,018962	0,022678	0,026982	H5N4F1E1	0,015750	0,019157	0,023426	H5N4F1E1	0,020083	0,023857	0,029556
2169,793	H4N5F1E1	0,001930	0,002335	0,002863	H4N5F1E1	0,001999	0,002387	0,002932	H4N5F1E1	0,001858	0,002310	0,002818	H4N5F1E1	0,002079	0,002526	0,003110
2185,787	H5N5E1	0,003412	0,004189	0,005254	H5N5E1	0,003783	0,004586	0,005782	H5N5E1	0,003442	0,004245	0,005260	H5N5E1	0,003795	0,004962	0,006136
2209,751	H5N4L2	0,002284	0,002595	0,002976	H5N4L2	0,002344	0,002644	0,003037	H5N4L2	0,002224	0,002598	0,003034	H5N4L2	0,002348	0,002665	0,002950
2255,793	H5N4E1L1	0,046011	0,051741	0,057504	H5N4E1L1	0,049930	0,055470	0,062131	H5N4E1L1	0,045339	0,050916	0,057505	H5N4E1L1	0,049957	0,055064	0,059480
2301,835	H5N4E2	0,471182	0,498384	0,526727	H5N4E2	0,460228	0,487200	0,514241	H5N4E2	0,477608	0,508732	0,534336	H5N4E2	0,463153	0,491258	0,516871
2331,845	H5N5F1E1	0,011387	0,014675	0,018706	H5N5F1E1	0,013118	0,016740	0,021410	H5N5F1E1	0,010903	0,014190	0,018271	H5N5F1E1	0,013890	0,018108	0,024627
2347,840	H6N5E1	0,005728	0,006887	0,008288	H6N5E1	0,005196	0,006026	0,007117	H6N5E1	0,005852	0,006844	0,008270	H6N5E1	0,004974	0,006121	0,007031
2355,809	H5N4F1L2	0,007918	0,009250	0,010944	H5N4F1L2	0,008341	0,009505	0,010875	H5N4F1L2	0,007760	0,009411	0,011029	H5N4F1L2	0,008263	0,009615	0,010922
2401,851	H5N4F1E1L1	0,007770	0,009825	0,012586	H5N4F1E1L1	0,008456	0,010496	0,013685	H5N4F1E1L1	0,007833	0,009850	0,013306	H5N4F1E1L1	0,009090	0,010663	0,014712
2447,893	H5N4F1E2	0,028010	0,033976	0,041845	H5N4F1E2	0,025681	0,031214	0,037344	H5N4F1E2	0,027474	0,033651	0,041429	H5N4F1E2	0,026672	0,030771	0,036732
2493,898	H6N5F1E1	0,001502	0,001849	0,002221	H6N5F1E1	0,001574	0,001869	0,002245	H6N5F1E1	0,001530	0,001808	0,002214	H6N5F1E1	0,001705	0,001910	0,002369
2504,914	H5N5E2	0,001627	0,001894	0,002194	H5N5E2	0,001549	0,001790	0,002078	H5N5E2	0,001609	0,001876	0,002185	H5N5E2	0,001546	0,001792	0,002076
2574,883	H6N5L2	0,000473	0,000593	0,000717	H6N5L2	0,000507	0,000627	0,000757	H6N5L2	0,000479	0,000584	0,000707	H6N5L2	0,000513	0,000598	0,000709
2604,930	H5N5F1E1L1	0,000861	0,001069	0,001334	H5N5F1E1L1	0,000888	0,001094	0,001371	H5N5F1E1L1	0,000865	0,001037	0,001304	H5N5F1E1L1	0,000963	0,001187	0,001412

Supplementary Table S3. Medians and interquartile ranges of direct and derived glycan traits. (*continued*)

Exact mass [M+Na]$^+$	Discovery cohort								Replication cohort							
	Cases	n=1583			Controls	n=728			Cases	n=232			Controls	n=108		
	Derived traits								Derived traits							
	Trait	25%	median	75%	name	25%	median	75%	Trait	25%	median	75%	name	25%	median	75%
2620,925	H6N5E1L1	0,005373	0,006730	0,008293	H6N5E1L1	0,005552	0,006907	0,008272	H6N5E1L1	0,005290	0,006544	0,007902	H6N5E1L1	0,005273	0,006407	0,007712
2650,972	H5N5F1E2	0,013004	0,017293	0,022676	H5N5F1E2	0,013632	0,017557	0,022538	H5N5F1E2	0,013224	0,016238	0,021741	H5N5F1E2	0,013667	0,018473	0,023018
2666,967	H6N5E2	0,004885	0,006132	0,007630	H6N5E2	0,004163	0,005072	0,006118	H6N5E2	0,004984	0,006168	0,007741	H6N5E2	0,003853	0,004680	0,005738
2720,941	H6N5F1L2	0,001027	0,001215	0,001414	H6N5F1L2	0,001122	0,001275	0,001493	H6N5F1L2	0,001047	0,001207	0,001389	H6N5F1L2	0,001108	0,001362	0,001503
2766,983	H6N5F1E1L1	0,001428	0,001881	0,002555	H6N5F1E1L1	0,001481	0,001965	0,002571	H6N5F1E1L1	0,001448	0,001900	0,002646	H6N5F1E1L1	0,001562	0,002000	0,002656
2813,025	H6N5F1E2	0,001649	0,002090	0,002619	H6N5F1E2	0,001502	0,001873	0,002300	H6N5F1E2	0,001617	0,002051	0,002644	H6N5F1E2	0,001512	0,001836	0,002334
2894,010	H6N5E1L2	0,004837	0,006539	0,008614	H6N5E1L2	0,005602	0,007365	0,009560	H6N5E1L2	0,004736	0,005978	0,008126	H6N5E1L2	0,005355	0,007003	0,009025
2940,052	H6N5E2L1	0,039075	0,053032	0,067712	H6N5E2L1	0,039286	0,053494	0,067288	H6N5E2L1	0,037219	0,049304	0,066024	H6N5E2L1	0,035336	0,047984	0,060209
2986,094	H6N5E3	0,017536	0,020991	0,025096	H6N5E3	0,014842	0,017551	0,020703	H6N5E3	0,017481	0,021254	0,025289	H6N5E3	0,013976	0,016587	0,019018
3040,068	H6N5F1E1L2	0,002588	0,003317	0,004349	H6N5F1E1L2	0,002801	0,003569	0,004529	H6N5F1E1L2	0,002574	0,003278	0,004153	H6N5F1E1L2	0,002908	0,003680	0,004599
3086,110	H6N5F1E2L1	0,020087	0,028186	0,038865	H6N5F1E2L1	0,019895	0,027458	0,036277	H6N5F1E2L1	0,020660	0,028377	0,039341	H6N5F1E2L1	0,021587	0,027743	0,038604
3132,152	H6N5F1E3	0,001658	0,002131	0,002728	H6N5F1E3	0,001375	0,001773	0,002209	H6N5F1E3	0,001639	0,002133	0,002806	H6N5F1E3	0,001405	0,001782	0,002195
3186,126	H6N5F2E1L2	0,000398	0,000618	0,000961	H6N5F2E1L2	0,000429	0,000673	0,000986	H6N5F2E1L2	0,000437	0,000643	0,000958	H6N5F2E1L2	0,000439	0,000712	0,001067
3232,168	H6N5F2E2L1	0,000609	0,000928	0,001338	H6N5F2E2L1	0,000511	0,000749	0,001046	H6N5F2E2L1	0,000605	0,000980	0,001351	H6N5F2E2L1	0,000535	0,000758	0,001100
3259,142	H7N6E1L2	0,001118	0,001525	0,002034	H7N6E1L2	0,001178	0,001591	0,002064	H7N6E1L2	0,001066	0,001428	0,002024	H7N6E1L2	0,001039	0,001503	0,001946
3305,184	H7N6E2L1	0,000877	0,001139	0,001511	H7N6E2L1	0,000778	0,001030	0,001349	H7N6E2L1	0,000884	0,001155	0,001457	H7N6E2L1	0,000717	0,000942	0,001189
3351,226	H7N6E3	0,000234	0,000310	0,000413	H7N6E3	0,000208	0,000274	0,000354	H7N6E3	0,000243	0,000307	0,000409	H7N6E3	0,000193	0,000253	0,000333
3405,200	H7N6F1E1L2	0,000383	0,000535	0,000757	H7N6F1E1L2	0,000384	0,000539	0,000752	H7N6F1E1L2	0,000380	0,000573	0,000779	H7N6F1E1L2	0,000424	0,000544	0,000806
3451,242	H7N6F1E2L1	0,000409	0,000558	0,000741	H7N6F1E2L1	0,000389	0,000511	0,000682	H7N6F1E2L1	0,000433	0,000545	0,000737	H7N6F1E2L1	0,000435	0,000574	0,000709
3532,227	H7N6E1L3	0,000884	0,001252	0,001737	H7N6E1L3	0,001032	0,001417	0,002010	H7N6E1L3	0,000835	0,001065	0,001646	H7N6E1L3	0,001023	0,001481	0,002104
3578,269	H7N6E2L2	0,001164	0,001575	0,002086	H7N6E2L2	0,001191	0,001607	0,002147	H7N6E2L2	0,001059	0,001477	0,001996	H7N6E2L2	0,001078	0,001590	0,002089
3624,311	H7N6E3L1	0,000592	0,000748	0,000957	H7N6E3L1	0,000555	0,000702	0,000878	H7N6E3L1	0,000568	0,000704	0,000985	H7N6E3L1	0,000537	0,000685	0,000948

Supplementary Table S3. Medians and interquartile ranges of direct and derived glycan traits. (*continued*)

Exact mass $[M+Na]^+$	Discovery cohort								Replication cohort							
	Cases	n=1583			Controls	n=728			Cases	n=232			Controls	n=108		
	Derived traits								Derived traits							
	Trait	25%	median	75%	name	25%	median	75%	Trait	25%	median	75%	name	25%	median	75%
3678,285	H7N6F1E1L3	0,000406	0,000570	0,000761	H7N6F1E1L3	0,000473	0,000630	0,000871	H7N6F1E1L3	0,000406	0,000534	0,000726	H7N6F1E1L3	0,000529	0,000622	0,000880
3724,327	H7N6F1E2L2	0,000490	0,000674	0,000924	H7N6F1E2L2	0,000494	0,000678	0,000918	H7N6F1E2L2	0,000490	0,000681	0,000871	H7N6F1E2L2	0,000529	0,000693	0,000952
3770,369	H7N6F1E3L1	0,000152	0,000228	0,000317	H7N6F1E3L1	0,000149	0,000216	0,000290	H7N6F1E3L1	0,000168	0,000240	0,000330	H7N6F1E3L1	0,000160	0,000220	0,000296
3870,385	H7N6F2E2L2	0,000126	0,000204	0,000325	H7N6F2E2L2	0,000119	0,000194	0,000305	H7N6F2E2L2	0,000144	0,000210	0,000329	H7N6F2E2L2	0,000143	0,000230	0,000327
	A1F	0,182283	0,216837	0,257032	A1F	0,189860	0,224401	0,267777	A1F	0,176613	0,212800	0,254379	A1F	0,188358	0,221179	0,262313
	A2B	0,057886	0,070078	0,083979	A2B	0,062855	0,073927	0,087048	A2B	0,056778	0,067350	0,080420	A2B	0,067587	0,077538	0,089939
	A2E	0,779045	0,800767	0,819879	A2E	0,765095	0,784897	0,803197	A2E	0,782572	0,801058	0,821649	A2E	0,761281	0,781120	0,800850
	A2E0F	0,863641	0,882420	0,899251	A2E0F	0,870376	0,887713	0,901794	A2E0F	0,865930	0,884449	0,899289	A2E0F	0,867819	0,889836	0,909281
	A2EF	0,120194	0,142111	0,167063	A2EF	0,126171	0,146060	0,167228	A2EF	0,116160	0,138024	0,161105	A2EF	0,133570	0,149181	0,177535
	A2F	0,176646	0,205324	0,236174	A2F	0,190278	0,214474	0,243263	A2F	0,170848	0,200713	0,231636	A2F	0,198658	0,221248	0,260926
	A2F0B	0,010715	0,012975	0,015914	A2F0B	0,011366	0,013567	0,016820	A2F0B	0,010840	0,012963	0,015081	A2F0B	0,011717	0,014192	0,016801
	A2F0E	0,872248	0,883675	0,894108	A2F0E	0,864485	0,876622	0,886895	A2F0E	0,876519	0,885288	0,895121	A2F0E	0,868563	0,879791	0,885427
	A2F0G	0,994611	0,995599	0,996393	A2F0G	0,994080	0,995055	0,995929	A2F0G	0,994871	0,995659	0,996412	A2F0G	0,993957	0,994970	0,995916
	A2F0GE	0,876411	0,887532	0,897645	A2F0GE	0,869699	0,880703	0,890798	A2F0GE	0,880892	0,889678	0,898901	A2F0GE	0,872610	0,883779	0,888775
	A2F0GL	0,041060	0,045997	0,051096	A2F0GL	0,044256	0,049444	0,055155	A2F0GL	0,040447	0,045173	0,050119	A2F0GL	0,044826	0,048789	0,053574
	A2F0GS	0,926464	0,934291	0,941837	A2F0GS	0,922902	0,930998	0,938401	A2F0GS	0,927927	0,936283	0,941813	A2F0GS	0,923396	0,931778	0,938535
	A2F0L	0,040874	0,045796	0,050849	A2F0L	0,044028	0,049171	0,054906	A2F0L	0,040294	0,044977	0,049886	A2F0L	0,044552	0,048585	0,053344
	A2F0S	0,921313	0,930105	0,938320	A2F0S	0,917768	0,926467	0,934181	A2F0S	0,923425	0,932351	0,937924	A2F0S	0,918517	0,927335	0,935186
	A2F0S0B	0,403744	0,452531	0,500629	A2F0S0B	0,386079	0,434852	0,478097	A2F0S0B	0,405287	0,459833	0,501079	A2F0S0B	0,397624	0,437991	0,478773
	A2F0S0G	0,642811	0,678446	0,711449	A2F0S0G	0,652998	0,683603	0,716868	A2F0S0G	0,651615	0,682393	0,709797	A2F0S0G	0,657219	0,684629	0,708730
	A2F0SB	0,008915	0,010810	0,013331	A2F0SB	0,009364	0,011303	0,013942	A2F0SB	0,008977	0,010610	0,012735	A2F0SB	0,009833	0,011882	0,014135
	A2F0SG	0,996657	0,997244	0,997702	A2F0SG	0,996253	0,996899	0,997437	A2F0SG	0,996788	0,997291	0,997654	A2F0SG	0,996283	0,996925	0,997441

Supplementary Table S3. Medians and interquartile ranges of direct and derived glycan traits. (*continued*)

Exact mass [M+Na]$^+$	Discovery cohort								Replication cohort							
	Cases	n=1583			Controls	n=728			Cases	n=232			Controls	n=108		
	Derived traits								Derived traits							
	Trait	25%	median	75%	name	25%	median	75%	Trait	25%	median	75%	name	25%	median	75%
	A2FB	0,259264	0,289859	0,323549	A2FB	0,261713	0,292255	0,322402	A2FB	0,257489	0,284624	0,315429	A2FB	0,269542	0,292925	0,332122
	A2FE	0,437228	0,476849	0,517671	A2FE	0,414829	0,451372	0,486744	A2FE	0,435027	0,475065	0,512241	A2FE	0,397670	0,441998	0,488530
	A2FG	0,823132	0,849840	0,874882	A2FG	0,819495	0,843551	0,865481	A2FG	0,822457	0,850235	0,870407	A2FG	0,818329	0,850111	0,869303
	A2FGE	0,525147	0,564456	0,600964	A2FGE	0,502611	0,533793	0,568875	A2FGE	0,526760	0,561444	0,596503	A2FGE	0,487956	0,529824	0,563899
	A2FGL	0,101677	0,121371	0,142657	A2FGL	0,103241	0,120648	0,138550	A2FGL	0,103884	0,126270	0,145438	A2FGL	0,102303	0,113247	0,133832
	A2FGS	0,654075	0,693091	0,730467	A2FGS	0,626858	0,661936	0,695877	A2FGS	0,655297	0,691341	0,727362	A2FGS	0,610782	0,653440	0,687333
	A2FL	0,085967	0,101963	0,121576	A2FL	0,085851	0,101979	0,116334	A2FL	0,088082	0,105342	0,124906	A2FL	0,086298	0,096998	0,113134
	A2FS	0,541435	0,587735	0,631733	A2FS	0,517361	0,556438	0,597405	A2FS	0,543278	0,581613	0,625438	A2FS	0,499056	0,551069	0,598046
	A2FS0B	0,217576	0,250731	0,288983	A2FS0B	0,202002	0,227721	0,260010	A2FS0B	0,215530	0,250436	0,291934	A2FS0B	0,207529	0,233348	0,267185
	A2FS0G	0,461594	0,507469	0,554429	A2FS0G	0,487015	0,529091	0,563893	A2FS0G	0,467169	0,507122	0,547658	A2FS0G	0,493857	0,530898	0,569197
	A2FSB	0,267275	0,308271	0,347664	A2FSB	0,284094	0,320675	0,356391	A2FSB	0,264228	0,297984	0,343040	A2FSB	0,289636	0,323919	0,361640
	A2FSG	0,975089	0,978283	0,981286	A2FSG	0,974587	0,977686	0,980467	A2FSG	0,975299	0,978248	0,980987	A2FSG	0,974630	0,978051	0,980709
	A2G	0,957300	0,965824	0,972917	A2G	0,954830	0,962516	0,969502	A2G	0,956692	0,965677	0,973046	A2G	0,949970	0,964066	0,968718
	A2GE	0,812917	0,829888	0,845135	A2GE	0,798734	0,816847	0,830632	A2GE	0,817882	0,831411	0,845244	A2GE	0,798251	0,813688	0,827756
	A2GL	0,054554	0,059773	0,065427	A2GL	0,057687	0,062898	0,069132	A2GL	0,053526	0,058697	0,065212	A2GL	0,058585	0,063133	0,066687
	A2GS	0,874931	0,891011	0,903825	A2GS	0,865744	0,879958	0,893610	A2GS	0,877829	0,892520	0,905193	A2GS	0,859884	0,875877	0,890905
	A2L	0,052750	0,057561	0,063134	A2L	0,055359	0,060409	0,066408	A2L	0,051798	0,056410	0,063095	A2L	0,055906	0,060073	0,064425
	A2L0F	0,163025	0,193663	0,226257	A2L0F	0,177597	0,204552	0,233077	A2L0F	0,158015	0,189544	0,221997	A2L0F	0,184749	0,207706	0,252647
	A2LF	0,269345	0,302088	0,341387	A2LF	0,266209	0,295631	0,336330	A2LF	0,273996	0,302763	0,340559	A2LF	0,276160	0,307339	0,343064
	A2S	0,837437	0,859584	0,877474	A2S	0,827574	0,845998	0,864348	A2S	0,839623	0,859956	0,881197	A2S	0,822269	0,840304	0,861106
	A2S0B	0,231944	0,264976	0,301988	A2S0B	0,214048	0,241786	0,273983	A2S0B	0,226643	0,265770	0,305097	A2S0B	0,218887	0,249848	0,282551

Supplementary Table S3. Medians and interquartile ranges of direct and derived glycan traits. (*continued*)

Exact mass $[M+Na]^+$	Discovery cohort								Replication cohort							
	Cases	n=1583			Controls	n=728			Cases	n=232			Controls	n=108		
	Derived traits								Derived traits							
	Trait	25%	median	75%	name	25%	median	75%	Trait	25%	median	75%	name	25%	median	75%
	A2S0F	0,920764	0,936403	0,948076	A2S0F	0,923768	0,938325	0,949158	A2S0F	0,924416	0,938683	0,949149	A2S0F	0,924012	0,937007	0,952881
	A2S0G	0,475291	0,519360	0,564048	A2S0G	0,497458	0,537197	0,573042	A2S0G	0,477094	0,519279	0,556306	A2S0G	0,502333	0,542320	0,578566
	A2SB	0,046432	0,057965	0,070540	A2SB	0,050766	0,061469	0,073321	A2SB	0,045546	0,054836	0,066482	A2SB	0,053527	0,065131	0,074752
	A2SF	0,134889	0,157079	0,180592	A2SF	0,142244	0,160563	0,182127	A2SF	0,130198	0,152897	0,175368	A2SF	0,148169	0,164581	0,191444
	A2SG	0,993238	0,994298	0,995130	A2SG	0,992852	0,993754	0,994648	A2SG	0,993389	0,994360	0,995253	A2SG	0,992538	0,993712	0,994705
	A3E	0,634365	0,645206	0,655834	A3E	0,623481	0,633758	0,643142	A3E	0,634807	0,645893	0,657771	A3E	0,623296	0,631058	0,639971
	A3E0F	0,622009	0,669837	0,716077	A3E0F	0,622256	0,668152	0,716780	A3E0F	0,626119	0,664732	0,711335	A3E0F	0,636057	0,679027	0,720257
	A3EF	0,216246	0,289437	0,383592	A3EF	0,217288	0,290070	0,388786	A3EF	0,237992	0,304849	0,387423	A3EF	0,245724	0,328346	0,402120
	A3F	0,223443	0,295075	0,387902	A3F	0,223181	0,294954	0,392891	A3F	0,242856	0,309595	0,391707	A3F	0,252205	0,333984	0,406445
	A3F0E	0,650036	0,664271	0,678621	A3F0E	0,639434	0,651101	0,663991	A3F0E	0,649704	0,665966	0,680394	A3F0E	0,640676	0,648594	0,662122
	A3F0L	0,218804	0,242589	0,263847	A3F0L	0,239466	0,260474	0,277432	A3F0L	0,212316	0,238227	0,259118	A3F0L	0,238576	0,261598	0,275130
	A3F0S	0,890859	0,907890	0,921696	A3F0S	0,897348	0,913081	0,925319	A3F0S	0,889526	0,903750	0,919207	A3F0S	0,889612	0,909576	0,924065
	A3Fa	0,007210	0,010998	0,015490	A3Fa	0,006739	0,010308	0,014735	A3Fa	0,007840	0,011814	0,016240	A3Fa	0,007182	0,011331	0,015965
	A3FE	0,592303	0,602343	0,611573	A3FE	0,582089	0,593306	0,602805	A3FE	0,593100	0,603827	0,613107	A3FE	0,581456	0,593203	0,601835
	A3FL	0,316038	0,326153	0,334900	A3FL	0,323764	0,333482	0,340498	A3FL	0,315174	0,325299	0,334337	A3FL	0,325471	0,334677	0,340931
	A3FS	0,913601	0,928829	0,940948	A3FS	0,912281	0,927020	0,938674	A3FS	0,912007	0,928954	0,939337	A3FS	0,912604	0,927451	0,939668
	A3L	0,256547	0,269540	0,283249	A3L	0,271854	0,284225	0,295388	A3L	0,254754	0,268495	0,279716	A3L	0,274847	0,284944	0,293060
	A3L0F	0,129660	0,151252	0,178235	A3L0F	0,136626	0,161921	0,188365	A3L0F	0,130784	0,153577	0,176196	A3L0F	0,149293	0,172063	0,199104
	A3LF	0,254078	0,351337	0,471984	A3LF	0,248988	0,339109	0,463374	A3LF	0,284414	0,373965	0,480784	A3LF	0,277016	0,388840	0,484072
	A3S	0,904283	0,915024	0,926076	A3S	0,908089	0,918097	0,927491	A3S	0,902004	0,914966	0,923737	A3S	0,906379	0,917081	0,925422
	A4E	0,417852	0,430795	0,444789	A4E	0,408563	0,420553	0,433850	A4E	0,421388	0,434556	0,445905	A4E	0,409676	0,420727	0,433178
	A4F	0,231298	0,295441	0,377398	A4F	0,228998	0,297720	0,373632	A4F	0,241049	0,312324	0,386025	A4F	0,244009	0,323153	0,391510

Supplementary Table S3. Medians and interquartile ranges of direct and derived glycan traits. (*continued*)

Exact mass [M+Na]$^+$	Discovery cohort								Replication cohort							
	Cases	n=1583			Controls	n=728			Cases	n=232			Controls	n=108		
	Derived traits								Derived traits							
	Trait	25%	median	75%	name	25%	median	75%	Trait	25%	median	75%	name	25%	median	75%
	A4F0E	0,273478	0,304156	0,331274	A4F0E	0,268838	0,296091	0,321933	A4F0E	0,270545	0,299551	0,326927	A4F0E	0,259302	0,289394	0,314174
	A4F0G	0,622575	0,703641	0,767657	A4F0G	0,626092	0,700796	0,769319	A4F0G	0,614750	0,685393	0,757490	A4F0G	0,609073	0,677602	0,748134
	A4F0GE	0,421021	0,435640	0,452293	A4F0GE	0,411855	0,424312	0,439420	A4F0GE	0,423715	0,438472	0,454918	A4F0GE	0,412138	0,424830	0,436250
	A4F0GL	0,428991	0,449762	0,469583	A4F0GL	0,448315	0,468491	0,483147	A4F0GL	0,425130	0,443888	0,465252	A4F0GL	0,451789	0,470961	0,483595
	A4F0L	0,273910	0,313978	0,352315	A4F0L	0,286581	0,328620	0,364663	A4F0L	0,267208	0,304564	0,345339	A4F0L	0,274794	0,315472	0,354833
	A4F0S	0,549205	0,623562	0,681640	A4F0S	0,559634	0,628177	0,686660	A4F0S	0,539827	0,606016	0,670319	A4F0S	0,550123	0,602017	0,667529
	A4Fa	0,013030	0,021490	0,034168	A4Fa	0,011816	0,020355	0,032346	A4Fa	0,014000	0,024286	0,036134	A4Fa	0,014768	0,022936	0,031279
	A4FE	0,095889	0,124470	0,158882	A4FE	0,094236	0,121995	0,155682	A4FE	0,102354	0,133425	0,161753	A4FE	0,100674	0,132898	0,166033
	A4FGE	0,406193	0,419248	0,433879	A4FGE	0,399983	0,411888	0,427000	A4FGE	0,411755	0,423698	0,434294	A4FGE	0,400154	0,411501	0,423220
	A4FGL	0,464638	0,481016	0,496992	A4FGL	0,476056	0,492245	0,507023	A4FGL	0,462408	0,476038	0,492183	A4FGL	0,476565	0,492709	0,505633
	A4FGS	0,893222	0,901512	0,909530	A4FGS	0,897318	0,904729	0,912398	A4FGS	0,891145	0,900500	0,908111	A4FGS	0,897235	0,905383	0,913422
	A4FL	0,110962	0,142585	0,180552	A4FL	0,112661	0,147732	0,183850	A4FL	0,115728	0,150926	0,187308	A4FL	0,121457	0,159820	0,190690
	A4FS	0,207759	0,265396	0,340672	A4FS	0,207599	0,268576	0,339048	A4FS	0,215013	0,284134	0,347710	A4FS	0,219703	0,296222	0,353159
	A4L	0,443105	0,459807	0,476236	A4L	0,459209	0,476200	0,489446	A4L	0,441776	0,454890	0,472896	A4L	0,464465	0,475600	0,492848
	A4LF	0,239541	0,306001	0,391478	A4LF	0,235272	0,304949	0,384398	A4LF	0,250044	0,325411	0,398545	A4LF	0,258243	0,332346	0,402476
	A4S	0,883065	0,891182	0,899041	A4S	0,889477	0,896145	0,903169	A4S	0,882341	0,889533	0,898401	A4S	0,891059	0,898467	0,904784
	CA1	0,003208	0,003985	0,005022	CA1	0,003333	0,004085	0,005132	CA1	0,003319	0,004080	0,004894	CA1	0,003494	0,004110	0,005319
	CA2	0,809540	0,832460	0,853527	CA2	0,818307	0,838463	0,858716	CA2	0,809036	0,833916	0,857745	CA2	0,824953	0,843671	0,864452
	CA3	0,132702	0,151524	0,173136	CA3	0,128014	0,145232	0,164142	CA3	0,128920	0,151149	0,173594	CA3	0,121071	0,138321	0,157610
	CA4	0,008012	0,009867	0,012333	CA4	0,007943	0,009983	0,012553	CA4	0,007664	0,009462	0,012102	CA4	0,007781	0,009877	0,012550
	CB	0,047884	0,058095	0,070102	CB	0,052054	0,061555	0,072435	CB	0,046847	0,055516	0,067070	CB	0,056137	0,065165	0,077732
	CF	0,193889	0,221653	0,252566	CF	0,200674	0,229288	0,262120	CF	0,189706	0,220743	0,249539	CF	0,213550	0,230780	0,276869

Supplementary Table S3. Medians and interquartile ranges of direct and derived glycan traits. (*continued*)

Exact mass $[M+Na]^+$	Discovery cohort								Replication cohort							
	Cases	n=1583			Controls	n=728			Cases	n=232			Controls	n=108		
	Derived traits								Derived traits							
	Trait	25%	median	75%	name	25%	median	75%	Trait	25%	median	75%	name	25%	median	75%
	CFa	0,001249	0,001844	0,002686	CFa	0,001184	0,001697	0,002373	CFa	0,001261	0,001882	0,002595	CFa	0,001260	0,001772	0,002518
	CG	0,984105	0,988275	0,991318	CG	0,983762	0,987602	0,990731	CG	0,983485	0,988047	0,991347	CG	0,984266	0,987427	0,990789
	CS	0,935995	0,950434	0,961230	CS	0,929101	0,942475	0,953763	CS	0,936875	0,949414	0,962151	CS	0,921417	0,942849	0,953884
	MHy	1,996119	2,545918	3,227351	MHy	2,103293	2,638946	3,329389	MHy	1,946251	2,466116	3,125511	MHy	2,167154	2,728980	3,271214
	MM	7,575929	7,689729	7,795024	MM	7,557682	7,684143	7,794574	MM	7,568869	7,680626	7,796233	MM	7,581945	7,662232	7,773899
	TA2FS0	0,035029	0,044932	0,057676	TA2FS0	0,041719	0,051602	0,063871	TA2FS0	0,034880	0,046047	0,057794	TA2FS0	0,042330	0,052121	0,072055
	THy	0,003754	0,004478	0,005536	THy	0,003940	0,004650	0,005583	THy	0,003787	0,004627	0,005622	THy	0,003866	0,004677	0,005911
	TM	0,009132	0,011332	0,014443	TM	0,010036	0,012078	0,015170	TM	0,008859	0,011732	0,014313	TM	0,010135	0,012145	0,015240

Values represent detected relative intensities for direct traits and calculated values for derived traits as described in Table S2. Abbreviations for direct traits: H = hexose; N = N-acetylhexosamine; F = deoxyhexose (fucose); E = α2,6-linked sialic acid; L = α2,3-linked sialylation. See Table S2 for description of derived traits. Additional traits that were calculated, but not taken into further consideration, since their values were 1 (equivalent to, e.g., full galactosylation for the G□traits): A1G, A3G, A4G, A1(G)S, A1(G)E.

Supplementary Table S4. Associations between derived glycan traits and clinical risk factors for type 2 diabetes.

Age			Sex			BMI			HDLc			non-HDLc			Ever having smoked			Current smoking		
trait	t-statistic	p-value	trait	t-statistic	p-value	trait	t-statistic	p-value	trait	t-statistic	p-value	trait	t-statistic	p-value	trait	t-statistic	p-value	trait	t-statistic	p-value
A2FS0G	-21,7284	1,81E-96	A4FL	-16,0272	8,25E-58	A3L	-18,4549	2,10E-71	A3E	-16,9612	3,65E-61	A3FE	-5,0283	5,30E-07	A4F0L	-7,8082	5,80E-15	A4F0L	-8,2021	2,36E-16
A2S0G	-21,1929	3,30E-92	A3F	-15,9230	4,39E-57	A4L	-16,6388	4,81E-59	A3F0E	-15,2473	2,90E-50	A3E	-4,9384	8,40E-07	A3F0L	-7,6335	2,29E-14	A4F0S	-8,0903	5,95E-16
A2F0SG	-12,3138	6,35E-34	A3EF	-15,8766	9,21E-57	A4F0GL	-15,7053	4,37E-53	A3FE	-12,7122	6,37E-36	A3F0E	-4,7692	1,96E-06	A4F0S	-7,2165	5,33E-13	A4F0G	-7,8971	2,85E-15
CG	-10,6720	4,62E-26	A4FS	-15,7406	7,97E-56	A2GL	-14,7607	2,42E-47	A2F0GE	-12,5107	7,04E-35	A4F0GE	-4,4739	8,02E-06	A4F0G	-6,9245	4,37E-12	A3F0L	-7,5638	3,92E-14
A2FG	-10,3821	8,87E-25	A4F	-15,5673	1,21E-54	A4S	-14,2133	3,77E-44	A2F0E	-12,5062	7,43E-35	A2GE	-4,4491	9,00E-06	A4F0GL	-6,6803	2,38E-11	A2L0F	-7,0744	1,50E-12
A2F0G	-10,2123	4,84E-24	A4LF	-15,4248	1,12E-53	A2L	-14,1874	5,31E-44	A4E	-11,3803	2,71E-29	A2FGS	-4,4446	9,19E-06	A4L	-5,5383	3,06E-08	A4F0E	-6,9519	3,60E-12
A2F0S0G	-9,7433	4,60E-22	A3LF	-15,3989	1,66E-53	A3FL	-14,0905	1,90E-43	A4F0GE	-10,9672	2,28E-27	A2F0S0B	-4,4429	9,26E-06	A4F0E	-5,3653	8,08E-08	TA2FS0	-6,4374	1,22E-10
A2SG	-9,1260	1,37E-19	A4FE	-15,0895	1,90E-51	A2F0GL	-12,8702	9,43E-37	A2GE	-10,7690	1,82E-26	A4E	-4,3339	1,52E-05	A3L	-4,5516	5,32E-06	A4F0GL	-6,2695	3,62E-10
A2F0S	-8,5936	1,42E-17	A2LF	-14,7435	3,39E-49	A2F0L	-12,8016	2,17E-36	A2F0SG	-9,5016	4,66E-21	A2GS	-3,8332	1,30E-04	A2F0GL	-4,4060	1,05E-05	A2E0F	-5,9216	3,19E-09
A2F0GS	-8,0775	9,94E-16	A3L0F	-12,9651	1,93E-38	A3F0L	-12,4324	1,78E-34	A2F0S	-8,8596	1,49E-18	A2S0B	-3,7238	2,01E-04	A2F0L	-4,3961	1,10E-05	A2F	-5,7645	8,19E-09
A2FSG	-7,7079	1,80E-14	A3Fa	-12,5863	2,51E-36	A4FGL	-10,6801	4,55E-26	A2F0GS	-8,7144	5,22E-18	A2F0GE	-3,6987	2,21E-04	A3F0S	-4,0330	5,51E-05	A2EF	-4,9853	6,19E-07
MHy	-7,1832	8,81E-13	A4Fa	-12,0497	1,95E-33	CA2	-9,5206	3,90E-21	A2E	-8,2059	3,62E-16	A2FS0B	-3,5619	3,75E-04	A4FGL	-3,6513	2,61E-04	A4L	-4,8557	1,20E-06
A2G	-6,3942	1,90E-10	CA2	-11,3265	9,71E-30	A4FGS	-7,6136	3,75E-14	A4FGE	-8,0972	8,69E-16	A2F0E	-3,5414	4,05E-04	A4S	-2,9849	2,84E-03	A2S0F	-4,8460	1,26E-06
A2F0E	-6,0323	1,84E-09	CF	-10,9107	1,02E-27	TA2FS0	-7,2296	6,41E-13	A2GS	-7,6546	2,75E-14	A2FGE	-3,4745	5,20E-04	A2L0F	-2,5034	1,23E-02	A2SF	-4,3665	1,26E-05
A2F0GE	-5,5062	4,02E-08	CFa	-8,4796	2,26E-17	A3L0F	-6,6746	3,04E-11	A2FGE	-7,5681	5,29E-14	A2E	-3,3680	7,69E-04	A2S0F	-2,4378	1,48E-02	A3F0S	-4,1475	3,36E-05
A3F0S	-4,8596	1,24E-06	A4S	-7,1993	6,05E-13	A2S0G	-6,6322	4,04E-11	A2F0G	-6,6867	2,80E-11	A3LF	-2,8652	4,20E-03	TA2FS0	-2,4068	1,61E-02	A4FGL	-3,5159	4,38E-04
MM	-4,8314	1,43E-06	A3FL	-7,1126	1,14E-12	A2FS0G	-6,5980	5,07E-11	A2FGS	-6,2690	4,26E-10	A2FS	-2,8043	5,08E-03	A2E0F	-1,9016	5,72E-02	CA2	-3,5120	4,45E-04
A2E0F	-4,8072	1,62E-06	A3FS	-6,8736	6,26E-12	CB	-5,2366	1,77E-07	A2SG	-6,0300	1,88E-09	A4FGE	-2,7251	6,47E-03	A2F	-1,5209	1,28E-01	A2F0GL	-3,4722	5,16E-04
A2S0F	-4,6428	3,61E-06	A2F0GE	-6,7668	1,32E-11	A2FSB	-5,1929	2,24E-07	A2S	-5,5389	3,36E-08	A4FE	-2,7016	6,95E-03	CA4	-1,1751	2,40E-01	A2F0L	-3,4431	5,75E-04
A4F0G	-4,3946	1,15E-05	A2E0F	-6,7417	1,57E-11	A2FGL	-4,6398	3,67E-06	A2FE	-5,3766	8,29E-08	A2S	-2,6954	7,08E-03	A2FGE	-0,9538	3,40E-01	THy	-3,4081	6,54E-04
A1F	-4,3353	1,51E-05	A2F0E	-6,5351	6,36E-11	A4F0L	-4,5722	5,06E-06	MM	-5,1660	2,58E-07	A3FS	-2,5836	9,83E-03	A2EF	-0,9425	3,46E-01	A4S	-3,0736	2,12E-03
A4F0S	-4,2481	2,23E-05	A4FGS	-6,4283	1,29E-10	A2F0S0G	-4,4527	8,85E-06	A2FS	-4,0011	6,49E-05	A4LF	-2,5287	1,15E-02	CA1	-0,7791	4,36E-01	A3L	-3,0364	2,39E-03
A4F0E	-4,1851	2,94E-05	A2F	-5,9641	2,46E-09	A2B	-4,1795	3,02E-05	A2F0S0B	-3,8235	1,35E-04	A4F	-2,4381	1,48E-02	A2F0S0G	-0,6850	4,93E-01	A2FGE	-2,8775	4,01E-03
A4F0L	-3,8545	1,19E-04	A2F0GS	-5,8493	4,94E-09	A2F	-4,0705	4,84E-05	A3FS	-3,6823	2,36E-04	A4Fa	-2,3837	1,72E-02	A2SF	-0,5694	5,69E-01	CB	-2,8141	4,89E-03
A3S	-3,8073	1,44E-04	TA2FS0	-5,7377	9,60E-09	A2SB	-4,0686	4,88E-05	A2FS0B	-3,4858	4,99E-04	A4FS	-2,3619	1,83E-02	A3S	-0,5588	5,76E-01	A2B	-2,4555	1,41E-02

Supplementary Table S4. Associations between derived glycan traits and clinical risk factors for type 2 diabetes. (*continued*)

Age			Sex			BMI			HDLc			non-HDLc			Ever having smoked			Current smoking		
trait	t-statistic	p-value	trait	t-statistic	p-value	trait	t-statistic	p-value	trait	t-statistic	p-value	trait	t-statistic	p-value	trait	t-statistic	p-value	trait	t-statistic	p-value
A3F0L	-3,8037	1,46E-04	A2SF	-5,5654	2,62E-08	A2FL	-4,0491	5,30E-05	A2S0B	-3,4315	6,10E-04	A2F0GS	-2,2834	2,25E-02	A2GL	-0,4102	6,82E-01	A2SB	-2,4514	1,42E-02
TM	-3,3572	7,98E-04	A2F0S	-5,5242	3,31E-08	A2F0B	-3,9598	7,71E-05	CFa	-3,0510	2,30E-03	A2FE	-2,2551	2,42E-02	CA2	-0,3796	7,04E-01	TM	-2,3861	1,70E-02
CA3	-3,3206	9,10E-04	A3E0F	-5,4321	5,57E-08	A2F0SB	-3,8626	1,15E-04	A4Fa	-3,0047	2,68E-03	A2F0S	-2,1303	3,32E-02	TM	-0,2641	7,92E-01	A4FGS	-2,0907	3,66E-02
A2L0F	-3,2892	1,02E-03	A3F0E	-5,1260	2,96E-07	A2L0F	-3,6478	2,70E-04	A4F0E	-2,8691	4,15E-03	CFa	-2,1234	3,38E-02	A2F0SB	-0,1909	8,49E-01	A2F0B	-2,0112	4,43E-02
A2EF	-3,2071	1,36E-03	A2EF	-5,0997	3,40E-07	CF	-3,4435	5,84E-04	A3Fa	-2,6121	9,05E-03	A3EF	-2,0591	3,96E-02	A2L	-0,1165	9,07E-01	A2F0SB	-1,7582	7,87E-02
A2SF	-2,4809	1,32E-02	A4F0GE	-5,0857	3,66E-07	THy	-3,0360	2,42E-03	A2LF	-2,5582	1,06E-02	A3F	-2,0127	4,43E-02	THy	-0,1034	9,18E-01	CF	-1,3005	1,93E-01
A2F	-2,4184	1,57E-02	A2FL	-4,6665	3,06E-06	A4FL	-3,0217	2,54E-03	A4FE	-2,4339	1,50E-02	A4FL	-1,9783	4,80E-02	A2F0B	-0,0602	9,52E-01	CA1	-1,1837	2,37E-01
A3L	-2,2750	2,30E-02	A2FGL	-4,5268	5,99E-06	A1F	-2,9915	2,80E-03	A3LF	-2,3358	1,96E-02	A3Fa	-1,8048	7,12E-02	A4FGS	0,0177	9,86E-01	A2F0S0B	-0,8255	4,09E-01
A2FE	-1,7073	8,79E-02	A2FS0G	-4,3407	1,42E-05	A3F0S	-2,2550	2,42E-02	A2E0F	-2,1685	3,02E-02	A2FGL	-1,6929	9,06E-02	MM	0,1295	8,97E-01	A2FE	-0,2312	8,17E-01
A2E	-1,6777	9,35E-02	A2L0F	-4,1234	3,73E-05	A2FB	-2,1635	3,06E-02	MHy	-1,6161	1,06E-01	A2LF	-1,6368	1,02E-01	MHy	0,2279	8,20E-01	MHy	-0,0581	9,54E-01
TA2FS0	-1,2741	2,03E-01	A2S0G	-4,0485	5,15E-05	A2E0F	-1,9935	4,63E-02	CS	-1,5863	1,13E-01	A2FL	-1,3213	1,87E-01	A2FE	0,2749	7,83E-01	A2FSB	0,2638	7,92E-01
CA4	-1,2509	2,11E-01	A4E	-3,7261	1,94E-04	A3F	-1,9140	5,57E-02	A4LF	-1,5856	1,13E-01	A2F0SB	-1,1733	2,41E-01	A1F	0,3511	7,26E-01	CA4	0,8277	4,08E-01
A2F0L	-1,2109	2,26E-01	A4FGE	-3,2453	1,17E-03	A3S	-1,7984	7,22E-02	A2S0F	-1,3951	1,63E-01	A2F0B	-1,1456	2,52E-01	A3FL	0,3952	6,93E-01	A3S	0,8724	3,83E-01
A2F0GL	-1,1245	2,61E-01	A2S0F	-3,1195	1,81E-03	A3EF	-1,7532	7,97E-02	A4F	-1,3029	1,93E-01	CS	-1,1403	2,54E-01	A2SB	0,4151	6,78E-01	A1F	0,8882	3,74E-01
A2S	-0,8977	3,69E-01	A2FSG	-2,6515	8,01E-03	A2SF	-1,7451	8,11E-02	A4FS	-1,2511	2,11E-01	A3E0F	-0,7772	4,37E-01	CA3	0,5792	5,62E-01	A3L0F	0,9630	3,36E-01
A3E	-0,8649	3,87E-01	A3FE	-2,6115	9,01E-03	A3E0F	-1,6272	1,04E-01	A2FSG	-1,2315	2,18E-01	A2FB	-0,3791	7,05E-01	A2FSB	0,7864	4,32E-01	A2F0S0G	0,9812	3,26E-01
A4F0GL	-0,7193	4,72E-01	A2F0SG	-2,1914	2,84E-02	A4FS	-1,5790	1,14E-01	A3EF	-1,0781	2,81E-01	A2SG	-0,3321	7,40E-01	A2FSG	0,8329	4,05E-01	A2F0GS	1,4290	1,53E-01
CF	-0,6174	5,37E-01	CB	-2,1418	3,22E-02	CA1	-1,4106	1,58E-01	A3F	-0,9694	3,32E-01	CA1	-0,2035	8,39E-01	CB	0,8795	3,79E-01	MM	1,4793	1,39E-01
A4FGL	-0,4857	6,27E-01	THy	-1,7653	7,75E-02	A4F	-1,2812	2,00E-01	CA3	-0,9053	3,65E-01	CA4	-0,1976	8,43E-01	A2B	0,9027	3,67E-01	A2F0S	1,7226	8,50E-02
A4L	-0,3357	7,37E-01	A2FG	-1,3340	1,82E-01	TM	-1,1771	2,39E-01	A3S	-0,7968	4,26E-01	A1F	-0,1060	9,16E-01	A2F0G	1,2525	2,10E-01	A3FL	2,2047	2,75E-02
A3FE	0,2081	8,35E-01	A2GL	-1,3286	1,84E-01	A4LF	-0,8457	3,98E-01	A3E0F	-0,7438	4,57E-01	CA3	-0,0263	9,79E-01	A2FS0G	1,3083	1,91E-01	A2GL	2,3583	1,84E-02
A2GE	0,5973	5,50E-01	A3L	-1,2263	2,20E-01	A2EF	-0,7977	4,25E-01	A4FL	-0,1097	9,13E-01	CA2	0,0900	9,28E-01	A2S0G	1,3633	1,73E-01	A2FB	2,5515	1,07E-02
A3F0E	0,6638	5,07E-01	A2L	-1,0606	2,89E-01	A2LF	-0,6749	5,00E-01	A2G	-0,0630	9,50E-01	A2F0SG	0,1056	9,16E-01	A2SG	1,5396	1,24E-01	A3E0F	2,5541	1,06E-02
A3L0F	0,8311	4,06E-01	CA1	-0,9984	3,18E-01	A4F0S	-0,2345	8,15E-01	A3F0S	0,4694	6,39E-01	A2F0G	0,1071	9,15E-01	A2F0S0B	1,5996	1,10E-01	A4FGE	2,7755	5,51E-03
CS	1,0358	3,00E-01	A1F	-0,8546	3,93E-01	A2S0F	-0,1681	8,67E-01	CA2	0,4957	6,20E-01	A2G	0,1908	8,49E-01	CF	1,7360	8,26E-02	A2F0GE	2,7992	5,12E-03

Supplementary Table S4. Associations between derived glycan traits and clinical risk factors for type 2 diabetes. (*continued*)

Age			Sex			BMI			HDLc			non-HDLc			Ever having smoked			Current smoking		
trait	t-statistic	p-value	trait	t-statistic	p-value	trait	t-statistic	p-value	trait	t-statistic	p-value	trait	t-statistic	p-value	trait	t-statistic	p-value	trait	t-statistic	p-value
A4E	1,1293	2,59E-01	A2B	-0,7099	4,78E-01	A4FE	-0,0063	9,95E-01	CF	0,7083	4,79E-01	THy	0,3302	7,41E-01	A2F0SG	1,9446	5,18E-02	A2F0E	2,9571	3,11E-03
A4F0GE	1,1846	2,36E-01	A2SB	-0,7003	4,84E-01	A3LF	0,0208	9,83E-01	TM	0,8968	3,70E-01	CF	0,5021	6,16E-01	A3E0F	1,9944	4,61E-02	A2GE	2,9973	2,72E-03
A2FS	1,2773	2,02E-01	A2F0S0G	-0,5886	5,56E-01	CG	0,6298	5,29E-01	A2EF	1,0011	3,17E-01	A2FSG	0,5478	5,84E-01	A2FGS	2,0107	4,44E-02	A2FGS	3,0503	2,29E-03
A4S	1,2972	1,95E-01	A4FGL	-0,5616	5,74E-01	A4Fa	1,0111	3,12E-01	TA2FS0	1,2341	2,17E-01	A2B	0,5823	5,60E-01	A3L0F	2,0628	3,91E-02	A2L	3,1014	1,93E-03
A4FGE	1,4508	1,47E-01	A2F0G	-0,5317	5,95E-01	A4F0G	1,2018	2,30E-01	A4F0G	1,2673	2,05E-01	A2E0F	0,5954	5,52E-01	CS	2,3580	1,84E-02	A2FSG	3,5968	3,22E-04
A4FGS	1,5129	1,30E-01	A4L	-0,3333	7,39E-01	CA4	2,0938	3,64E-02	CA1	1,2721	2,03E-01	CB	0,6056	5,45E-01	A2GE	2,5025	1,23E-02	CA3	3,6838	2,30E-04
A3FS	1,5648	1,18E-01	A2F0B	-0,3289	7,42E-01	A3Fa	2,2115	2,71E-02	A2SF	1,4717	1,41E-01	A4FGS	0,6670	5,05E-01	A2FS	2,6016	9,28E-03	A2F0G	3,9972	6,41E-05
CFa	1,7297	8,38E-02	A2F0SB	-0,1238	9,01E-01	A2FSG	2,2442	2,49E-02	A2F	1,5204	1,29E-01	A4F0E	0,7524	4,52E-01	CG	2,6189	8,82E-03	A2FS0G	4,1065	4,02E-05
CA1	2,0241	4,31E-02	A2SG	-0,0015	9,99E-01	MHy	2,3638	1,82E-02	A4FGS	1,5247	1,27E-01	A2S0F	0,7532	4,51E-01	A2GS	2,6776	7,42E-03	A2S0G	4,1990	2,68E-05
A2GS	2,0296	4,25E-02	A3S	0,1551	8,77E-01	A2FG	2,5200	1,18E-02	A2L0F	1,5772	1,15E-01	TA2FS0	0,8834	3,77E-01	A2G	2,7125	6,68E-03	A2GS	4,2422	2,21E-05
A3FL	2,0717	3,84E-02	A2FS	0,8338	4,04E-01	A3FS	3,8004	1,48E-04	A2FG	1,7278	8,42E-02	A2FSB	0,9007	3,68E-01	A2F0S	2,7899	5,27E-03	A4E	4,2890	1,79E-05
A2FGE	2,6082	9,15E-03	A2GS	1,0283	3,04E-01	A2G	4,2843	1,90E-05	THy	1,7330	8,32E-02	A2SB	1,0258	3,05E-01	A2FG	2,7977	5,15E-03	A3E	4,3714	1,23E-05
A3Fa	2,6687	7,66E-03	MM	1,3138	1,89E-01	MM	5,5396	3,35E-08	A4F0S	1,8559	6,36E-02	A2FG	1,2916	1,97E-01	A2F0GS	2,8635	4,19E-03	A2E	4,6467	3,37E-06
A2L	3,0235	2,52E-03	A2GE	1,4706	1,41E-01	A2F0GS	5,7723	8,79E-09	A2FGL	2,1342	3,29E-02	A2EF	1,3839	1,67E-01	A2FB	2,8646	4,18E-03	A2FS	4,6910	2,72E-06
CA2	3,0971	1,97E-03	A2S	1,5483	1,22E-01	CFa	5,7984	7,54E-09	A2FL	2,3578	1,85E-02	A2SF	1,5319	1,26E-01	A2E	2,8744	4,05E-03	A2F0SG	4,8051	1,55E-06
THy	3,1161	1,85E-03	TM	1,7460	8,08E-02	A4F0E	6,0965	1,25E-09	CA4	2,4444	1,46E-02	A2F	1,6260	1,04E-01	A2S	2,9985	2,71E-03	A4F0GE	5,4335	5,53E-08
A2F0SB	3,3835	7,26E-04	CG	1,7526	7,97E-02	A2FS0B	6,2681	4,29E-10	A2FB	2,5963	9,48E-03	A3FL	1,7376	8,24E-02	A4FGE	4,3130	1,61E-05	A2S	5,6884	1,28E-08
A4Fa	3,5779	3,53E-04	A2F0S0B	1,7545	7,93E-02	A2F0S	6,2876	3,79E-10	A1F	2,7084	6,81E-03	A3L0F	1,7581	7,88E-02	A2F0E	4,4431	8,87E-06	A3Fa	5,8447	5,07E-09
A2GL	3,6496	2,68E-04	A3E	1,7991	7,20E-02	A2S0B	6,5369	7,58E-11	CG	2,8670	4,18E-03	A2L0F	1,7783	7,55E-02	A3FS	4,4994	6,81E-06	A2FG	5,8949	3,75E-09
A3E0F	3,6698	2,48E-04	A2E	1,8492	6,44E-02	A2SG	6,6959	2,64E-11	CB	3,0453	2,35E-03	CG	1,8164	6,94E-02	A2F0GE	4,5480	5,42E-06	A2SG	6,1705	6,81E-10
A3EF	3,7369	1,90E-04	A2FGS	1,8885	5,90E-02	A2F0S0B	7,0965	1,66E-12	A2B	3,1489	1,66E-03	A4F0G	2,3551	1,86E-02	A3E	5,1510	2,59E-07	CS	6,3631	1,98E-10
A3F	3,7846	1,57E-04	A2G	2,3487	1,88E-02	CS	7,6810	2,25E-14	A2SB	3,8138	1,40E-04	A3S	2,4573	1,41E-02	A4E	5,2459	1,55E-07	CG	6,4511	1,11E-10
A3LF	3,9768	7,17E-05	A4F0GL	2,3520	1,87E-02	A4FGE	8,3852	8,34E-17	A2FSB	4,1753	3,08E-05	A4FGL	2,5870	9,74E-03	A3FE	5,4675	4,56E-08	A3FE	6,5645	5,22E-11
A2F0B	4,2533	2,18E-05	A2FE	3,0065	2,64E-03	A2F0G	8,5746	1,71E-17	A2F0B	4,4157	1,05E-05	A4F0S	2,6343	8,48E-03	A4Fa	5,4755	4,36E-08	A3FS	6,5852	4,54E-11
A4FE	4,3548	1,38E-05	MHy	3,2157	1,30E-03	A2S	8,6606	8,26E-18	A3L0F	4,4509	8,93E-06	A4S	2,9939	2,78E-03	A2FGL	5,6376	1,72E-08	A2S0B	6,6354	3,24E-11

Supplementary Table S4. Associations between derived glycan traits and clinical risk factors for type 2 diabetes. (*continued*)

Age			Sex			BMI			HDLc			non-HDLc			Ever having smoked			Current smoking		
trait	t-statistic	p-value	trait	t-statistic	p-value	trait	t-statistic	p-value	trait	t-statistic	p-value	trait	t-statistic	p-value	trait	t-statistic	p-value	trait	t-statistic	p-value
A4LF	4,3645	1,32E-05	A2FSB	4,3862	1,15E-05	A2GS	9,8187	2,36E-22	A2F0SB	4,7386	2,27E-06	A2GL	3,2014	1,38E-03	A4F0GE	5,7705	7,90E-09	A4Fa	6,6742	2,49E-11
A2SB	4,3715	1,28E-05	A2F0GL	4,4043	1,06E-05	A2F0SG	10,0415	2,74E-23	A4F0L	4,9855	6,60E-07	A2L	3,2246	1,28E-03	A2S0B	5,8615	4,59E-09	A2FS0B	6,7818	1,19E-11
A4F	4,4810	7,75E-06	A2F0L	4,4050	1,06E-05	CA3	10,1441	1,00E-23	A4S	5,0434	4,90E-07	A2S0G	3,5779	3,53E-04	A2FS0B	5,9582	2,55E-09	A3F0E	7,0425	1,89E-12
A4FS	4,5120	6,70E-06	A2FGE	4,4524	8,49E-06	A2FS	10,3744	1,02E-24	A2F0S0G	5,0670	4,34E-07	A2FS0G	3,5998	3,25E-04	A2FL	5,9787	2,25E-09	A2G	7,1687	7,57E-13
A4FL	4,5517	5,56E-06	A2FS0B	5,0024	5,66E-07	A2F0GE	10,7983	1,34E-26	A2FS0G	5,2878	1,35E-07	A2F0S0G	3,6286	2,91E-04	A3Fa	6,0458	1,49E-09	A2LF	7,1883	6,56E-13
A2LF	4,9068	9,82E-07	A2S0B	5,0873	3,63E-07	A2F0E	10,9686	2,25E-27	A2S0G	5,4368	5,95E-08	A4F0L	3,6750	2,43E-04	CFa	6,2007	5,62E-10	CFa	7,3123	2,63E-13
A2B	5,7588	9,45E-09	A2FB	5,1493	2,61E-07	A2E	12,1210	6,69E-33	A4FGL	7,4375	1,40E-13	A2F0GL	3,8246	1,34E-04	A4FL	6,5288	6,63E-11	A4FL	7,3676	1,74E-13
CB	5,9292	3,44E-09	CS	5,6164	1,95E-08	A4F0GE	12,1915	2,97E-33	A3FL	8,5614	1,92E-17	A2F0L	3,8279	1,32E-04	A4FS	6,8720	6,33E-12	A3F	7,6571	1,90E-14
A2FL	6,9768	3,80E-12	A3F0S	6,2177	5,05E-10	A4E	12,5931	2,65E-35	A3F0L	10,3630	1,14E-24	A3F0S	4,0170	6,07E-05	A4F	6,9143	4,70E-12	A3EF	7,6937	1,43E-14
A2FGS	7,5006	8,62E-14	A3F0L	7,6603	1,85E-14	A2FGS	12,7132	6,28E-36	A4F0GL	10,9337	3,25E-27	A4L	4,7859	1,80E-06	A3F	7,0323	2,03E-12	A4FS	7,7346	1,04E-14
A2FGL	9,3226	2,32E-20	CA4	7,7296	1,08E-14	A2FE	13,2763	6,37E-39	A2L	11,0636	8,22E-28	A4F0GL	5,0042	6,00E-07	A4LF	7,0651	1,60E-12	A4F	7,8707	3,53E-15
A2FSB	9,5731	2,29E-21	CA3	11,3231	1,01E-29	A2GE	14,0763	2,29E-43	A2GL	11,1625	2,86E-28	MM	5,1101	3,46E-07	A3EF	7,0654	1,60E-12	A4FE	7,9431	1,97E-15
A2F0S0B	10,1573	8,34E-24	A4F0L	13,2583	4,04E-40	A2FGE	15,9101	2,27E-54	A2F0L	11,2835	7,77E-29	A3L	5,7866	8,08E-09	A4FE	7,0889	1,35E-12	A4LF	7,9610	1,71E-15
A2FB	12,0429	1,47E-32	A4F0S	14,8325	9,04E-50	A3F0E	16,6245	5,96E-59	A4L	11,2936	6,97E-29	A3F0L	5,8860	4,49E-09	A3F0E	7,2934	3,02E-13	A3LF	8,1782	2,88E-16
A2FS0B	12,2965	7,77E-34	A4F0E	15,1973	3,69E-52	A3FE	18,2448	6,32E-70	A2F0GL	11,3371	4,35E-29	MHy	7,1672	1,00E-12	A2LF	7,3214	2,45E-13	A2FGL	10,1586	3,03E-24
A2S0B	12,7724	2,69E-36	A4F0G	15,5251	2,35E-54	A3E	21,5442	1,39E-94	A3L	12,7670	3,29E-36	TM	7,3633	2,42E-13	A3LF	7,5677	3,80E-14	A2FL	10,9415	7,30E-28

Glycan values were centered and scaled, therefore the effect sizes are indicative of 1 standard deviation change in glycan value. Shown are the regression coefficient β (for continuous variables) or the odds ratio (for binary variables), the standard error, the t-statistic as calculated by β/SE, and the corresponding p-value per association. All associations are unadjusted for additional covariates. The associations that remained statistically significant after correction for multiple comparisons are highlighted in green. Red indicates a positive association, blue a negative association. A2, diantennary; A3, triantennary; A4, tetraantennary; F, fucosylation; B, bisection; E, α2,6-linked sialylation; G, galactosylation; L, α2,3-linked sialylation; S, sialylation. FDR, false discovery rate; BMI, body mass index; HDL-c, high-density lipoprotein-cholesterol; non-HDLc is the calculated difference between total cholesterol and HDL-c.

Supplementary Table S5. Regression results for type 2 diabetes.

Model 1						Model 2						Model 3					
Discovery cohort			Replication cohort			Discovery cohort			Replication cohort			Discovery cohort			Replication cohort		
number of tests: 91			number of tests: 70			number of tests: 91			number of tests: 67			number of tests: 91			number of tests: 55		
FDR (Q)	0,05		FDR (Q)	0,05		FDR (Q)	0,05		FDR (Q)	0,05		FDR (Q)	0,05		FDR (Q)	0,05	
FDR α	0,0385		FDR α	0,0407		FDR α	0,0368		FDR α	0,0373		FDR α	0,0302		FDR α	0,0164	
trait	OR	p	trait	OR	p	trait	OR	p	trait	OR	p	trait	OR	p	trait	OR	p
A3L	0,4494	1,32E-47	**A3L**	0,3270	2,42E-11	**A3L**	0,5814	1,36E-18	A3L	0,5008	0,000142	A3L	0,5993	6,38E-11	A3L	0,5439	1,08E-02
A4L	0,5232	4,12E-36	**A4L**	0,3965	7,28E-10	**A4L**	0,6616	1,01E-12	A4L	0,5853	0,001352	A4L	0,6640	2,42E-08	**A4L**	0,7346	1,74E-01
A4F0GL	0,5404	2,77E-32	**A4F0GL**	0,4249	5,92E-09	**A4F0GL**	0,6814	3,39E-11	A4F0GL	0,6264	0,003636	A4F0GL	0,6908	3,76E-07	**A4F0GL**	0,7838	2,55E-01
A3FL	0,5463	7,45E-29	**A3FL**	0,4218	4,76E-08	**A3FL**	0,6874	3,35E-10	A3FL	0,6003	0,00285	A3FL	0,6919	1,02E-06	A3FL	0,5279	5,68E-03
TA2FS0	0,6880	5,90E-15	**TA2FS0**	0,5862	1,69E-05	**TA2FS0**	0,7353	8,07E-09	TA2FS0	0,6452	0,001727	TA2FS0	0,6977	1,13E-08	TA2FS0	0,5930	5,68E-03
A4S	0,5970	1,31E-25	**A4S**	0,4732	9,57E-08	**A4S**	0,7337	3,12E-08	A4S	0,695	0,02107	A4S	0,7166	1,80E-06	**A4S**	0,8864	5,62E-01
A3F0L	0,5661	9,74E-27	**A3F0L**	0,4785	3,58E-07	**A3F0L**	0,7003	8,28E-10	A3F0L	0,6633	0,009135	A3F0L	0,7416	3,83E-05	**A3F0L**	0,7476	1,65E-01
A4FGL	0,6391	1,16E-19	**A4FGL**	0,5323	5,98E-06	**A4FGL**	0,7537	2,52E-07	A4FGL	0,6961	0,023322	A4FGL	0,7448	1,47E-05	**A4FGL**	0,8641	4,92E-01
A2E0F	0,7977	2,05E-06	**A2E0F**	0,7301	1,45E-02	**A2E0F**	0,7862	1,23E-05	A2E0F	0,6852	0,010867	A2E0F	0,7609	7,27E-05	**A2E0F**	0,7155	1,00E-01
A4FGS	0,7133	2,51E-12	**A4FGS**	0,7519	2,62E-02	**A4FGS**	0,8107	1,06E-04	**A4FGS**	0,9674	8,25E-01	A4FGS	0,7668	7,43E-05	**A4FGS**	1,1016	6,06E-01
A3L0F	0,6767	1,08E-15	**A3L0F**	0,5862	2,67E-05	**A3L0F**	0,7221	5,94E-09	A3L0F	0,6747	0,005699	A3L0F	0,7790	1,90E-04	**A3L0F**	0,8124	2,91E-01
A2L0F	0,7708	1,49E-08	**A2L0F**	0,6107	6,77E-05	**A2L0F**	0,7852	4,75E-06	A2L0F	0,5921	0,000274	A2L0F	0,7960	5,54E-04	A2L0F	0,6125	1,17E-02
CF	0,7685	2,45E-08	**CF**	0,6179	1,21E-04	**CF**	0,7822	6,10E-06	CF	0,5961	0,000361	CF	0,8016	8,46E-04	CF	0,6105	9,05E-03
A2F	0,7685	1,17E-08	**A2F**	0,6092	6,53E-05	**A2F**	0,7892	8,24E-06	A2F	0,5876	0,000233	A2F	0,8085	1,26E-03	A2F	0,6119	1,14E-02
A3S	0,8389	1,51E-04	**A3S**	0,8431	1,53E-01	**A3S**	0,8595	4,36E-03	**A3S**	0,9323	6,11E-01	A3S	0,8276	4,78E-03	**A3S**	0,8560	3,85E-01
CA2	0,7304	1,18E-10	**CA2**	0,7240	1,15E-02	**CA2**	0,8182	2,86E-04	**CA2**	0,8463	2,44E-01	CA2	0,8302	6,32E-03	**CA2**	0,8871	5,54E-01
A2FSB	0,8345	9,19E-05	**A2FSB**	0,6815	1,71E-03	**A2FSB**	0,8715	1,12E-02	A2FSB	0,6735	0,005527	A2FSB	0,8319	5,94E-03	A2FSB	0,6097	1,05E-02
A1F	0,8355	7,23E-05	**A1F**	0,8303	1,17E-01	**A1F**	0,8804	1,45E-02	**A1F**	0,8553	2,57E-01	A1F	0,8413	7,62E-03	**A1F**	0,8988	5,41E-01
A2F0GL	0,6428	7,43E-21	**A2F0GL**	0,5913	3,19E-05	**A2F0GL**	0,7882	1,32E-05	**A2F0GL**	0,8245	1,95E-01	A2F0GL	0,8431	1,06E-02	**A2F0GL**	0,7564	1,74E-01
A2F0L	0,6446	1,26E-20	**A2F0L**	0,5932	3,50E-05	**A2F0L**	0,7900	1,60E-05	**A2F0L**	0,8267	2,01E-01	A2F0L	0,8454	1,19E-02	**A2F0L**	0,7595	1,80E-01
A2FS0G	0,6759	1,51E-13	**A2FS0G**	0,6059	1,70E-04	**A2FS0G**	0,7831	6,08E-05	A2FS0G	0,6959	0,014901	A2FS0G	0,8479	2,67E-02	**A2FS0G**	0,8085	2,61E-01
A3F0S	0,8303	8,95E-05	**A3F0S**	0,8030	7,03E-02	**A3F0S**	0,8553	3,35E-03	**A3F0S**	0,8881	3,95E-01	A3F0S	0,8480	1,35E-02	**A3F0S**	0,8555	3,81E-01
CB	0,8249	2,17E-05	**CB**	0,6226	1,10E-04	**CB**	0,8568	3,37E-03	CB	0,609	0,000414	CB	0,8573	1,45E-02	CB	0,5334	1,42E-03
A2F0B	0,8726	2,37E-03	**A2F0B**	0,7174	4,72E-03	**A2F0B**	0,8959	3,61E-02	A2F0B	0,7452	0,029431	A2F0B	0,8614	1,60E-02	**A2F0B**	0,7170	6,45E-02

Supplementary Table S5. Regression results for type 2 diabetes. (*continued*)

Model 1						Model 2						Model 3					
Discovery cohort			Replication cohort			Discovery cohort			Replication cohort			Discovery cohort			Replication cohort		
number of tests: 91			number of tests: 70			number of tests: 91			number of tests: 67			number of tests: 91			number of tests: 55		
FDR (Q)	0,05		FDR (Q)	0,05		FDR (Q)	0,05		FDR (Q)	0,05		FDR (Q)	0,05		FDR (Q)	0,05	
FDR α	0,0385		FDR α	0,0407		FDR α	0,0368		FDR α	0,0373		FDR α	0,0302		FDR α	0,0164	
trait	OR	p	trait	OR	p	trait	OR	p	trait	OR	p	trait	OR	p	trait	OR	p
A2S0G	0,6867	9,69E-13	A2S0G	0,6169	2,71E-04	A2S0G	0,7968	1,79E-04	A2S0G	0,712	0,021663	A2S0G	0,8643	4,86E-02	A2S0G	0,8228	3,02E-01
A2B	0,8496	3,02E-04	A2B	0,6420	2,69E-04	A2B	0,8726	9,80E-03	A2B	0,6089	0,000473	A2B	0,8708	2,84E-02	A2B	0,5377	1,53E-03
A3F	0,8713	4,49E-03	A3F	0,8658	2,33E-01	A3F	0,8794	2,15E-02	A3F	0,8758	3,35E-01	A3F	0,8730	5,09E-02	A3F	0,8345	3,14E-01
A3EF	0,8765	6,51E-03	A3EF	0,8731	2,61E-01	A3EF	0,8824	2,51E-02	A3EF	0,8800	3,52E-01	A3EF	0,8743	5,32E-02	A3EF	0,8375	3,23E-01
A2SB	0,8403	1,08E-04	A2SB	0,6382	2,14E-04	A2SB	0,8656	5,78E-03	A2SB	0,5952	0,000269	A2SB	0,8797	4,12E-02	A2SB	0,5614	2,90E-03
A2F0SB	0,8860	6,73E-03	A2F0SB	0,7380	9,32E-03	A2F0SB	0,9172	9,76E-02	A2F0SB	0,7612	4,25E-02	A2F0SB	0,8870	5,17E-02	A2F0SB	0,7360	8,86E-02
A4FL	0,8540	1,17E-03	A4FL	0,8408	1,56E-01	A4FL	0,8915	3,92E-02	A4FL	0,8517	2,51E-01	A4FL	0,8974	1,20E-01	A4FL	0,8039	2,29E-01
A2S0F	0,8909	1,46E-02	A2S0F	0,8873	3,39E-01	A2S0F	0,8923	3,21E-02	A2S0F	0,8398	2,20E-01	A2S0F	0,9007	1,08E-01	A2S0F	0,8589	4,37E-01
A2EF	0,8696	2,16E-03	A2EF	0,6801	1,40E-03	A2EF	0,8632	5,04E-03	A2EF	0,607	0,000445	A2EF	0,9102	1,44E-01	A2EF	0,6806	4,96E-02
A2GL	0,6559	3,82E-19	A2GL	0,6541	6,23E-04	A2GL	0,8356	1,09E-03	A2GL	0,9272	6,17E-01	A2GL	0,9134	1,86E-01	A2GL	0,8627	4,71E-01
TM	0,8277	2,09E-05	TM	0,7994	5,37E-02	TM	0,8109	4,09E-05	TM	0,7296	0,025335	TM	0,9159	1,61E-01	TM	0,8769	4,75E-01
A3LF	0,9616	4,18E-01	A3LF	0,9812	8,75E-01	A3LF	0,9437	2,99E-01	A3LF	0,9491	7,05E-01	A3LF	0,9216	2,41E-01	A3LF	0,8846	4,96E-01
A2SF	0,8573	7,47E-04	A2SF	0,6748	1,15E-03	A2SF	0,8665	6,43E-03	A2SF	0,6102	0,000537	A2SF	0,9226	2,10E-01	A2SF	0,6816	5,11E-02
A4F0L	0,8451	4,91E-04	A4F0L	0,8148	8,85E-02	A4F0L	0,9218	1,38E-01	A4F0L	0,9513	7,19E-01	A4F0L	0,9227	2,38E-01	A4F0L	1,0862	6,41E-01
A4FS	0,9119	5,65E-02	A4FS	0,9218	5,00E-01	A4FS	0,9299	1,93E-01	A4FS	0,9023	4,62E-01	A4FS	0,9298	2,96E-01	A4FS	0,8309	3,12E-01
A4F	0,9243	1,03E-01	A4F	0,9308	5,52E-01	A4F	0,9379	2,50E-01	A4F	0,9016	4,59E-01	A4F	0,9385	3,62E-01	A4F	0,8260	2,96E-01
A2L	0,6754	5,42E-17	A2L	0,6721	1,25E-03	A2L	0,8598	5,84E-03	A2L	0,9537	7,53E-01	A2L	0,9448	4,07E-01	A2L	0,9015	6,07E-01
A4LF	0,9405	2,04E-01	A4LF	0,9513	6,78E-01	A4LF	0,9466	3,24E-01	A4LF	0,9152	5,26E-01	A4LF	0,9457	4,22E-01	A4LF	0,8326	3,15E-01
MHy	0,9080	3,32E-02	MHy	0,8142	7,89E-02	MHy	0,8485	1,42E-03	MHy	0,7166	0,017749	MHy	0,9485	4,06E-01	MHy	0,8393	3,52E-01
A3E0F	0,9617	3,94E-01	A3E0F	0,8822	2,88E-01	A3E0F	0,9599	4,44E-01	A3E0F	0,8753	3,54E-01	A3E0F	0,9661	6,00E-01	A3E0F	0,7919	2,34E-01
A4FE	0,9782	6,47E-01	A4FE	1,0186	8,79E-01	A4FE	0,9741	6,39E-01	A4FE	0,9651	8,01E-01	A4FE	0,9672	6,32E-01	A4FE	0,8672	4,44E-01
A3FS	1,0790	9,32E-02	A3FS	1,0878	4,67E-01	A3FS	1,0158	7,65E-01	A3FS	1,0278	8,41E-01	A3FS	0,9735	6,85E-01	A3FS	0,8907	4,93E-01
THy	0,9285	9,79E-02	THy	0,9428	6,14E-01	THy	0,9583	4,10E-01	THy	0,9931	9,59E-01	THy	0,9741	6,86E-01	THy	0,9871	9,43E-01
A2FB	1,0082	8,62E-01	A2FB	0,8204	9,49E-02	A2FB	1,0251	6,50E-01	A2FB	0,7966	9,94E-02	A2FB	0,9789	7,52E-01	A2FB	0,6896	4,56E-02
CA1	0,9744	5,65E-01	CA1	0,9416	6,06E-01	CA1	0,9788	6,83E-01	CA1	0,9715	8,25E-01	CA1	0,9835	7,95E-01	CA1	0,9257	6,40E-01

Supplementary Table S5. Regression results for type 2 diabetes. (*continued*)

Model 1						Model 2						Model 3					
Discovery cohort			Replication cohort			Discovery cohort			Replication cohort			Discovery cohort			Replication cohort		
number of tests: 91			number of tests: 70			number of tests: 91			number of tests: 67			number of tests: 91			number of tests: 55		
FDR (Q)	0,05		FDR (Q)	0,05		FDR (Q)	0,05		FDR (Q)	0,05		FDR (Q)	0,05		FDR (Q)	0,05	
FDR α	0,0385		FDR α	0,0407		FDR α	0,0368		FDR α	0,0373		FDR α	0,0302		FDR α	0,0164	
trait	OR	p	trait	OR	p	trait	OR	p	trait	OR	p	trait	OR	p	trait	OR	p
CA4	1,0568	2,33E-01	CA4	0,9717	8,07E-01	CA4	1,0533	3,29E-01	CA4	0,9478	6,95E-01	CA4	0,9895	8,71E-01	CA4	0,9590	8,19E-01
A4Fa	1,0346	4,80E-01	A4Fa	1,1398	2,98E-01	A4Fa	1,0281	6,22E-01	A4Fa	1,1373	3,91E-01	A4Fa	0,9951	9,43E-01	A4Fa	1,1707	4,60E-01
A3Fa	1,0262	5,88E-01	A3Fa	1,0428	7,25E-01	A3Fa	0,9810	7,29E-01	A3Fa	0,9712	8,35E-01	A3Fa	0,9987	9,85E-01	A3Fa	1,0382	8,43E-01
A4F0S	1,0224	6,45E-01	A4F0S	1,0019	9,88E-01	A4F0S	1,0368	5,14E-01	A4F0S	1,0684	6,33E-01	A4F0S	1,0319	6,49E-01	A4F0S	1,1789	3,59E-01
A2LF	1,0076	8,77E-01	A2LF	0,9533	6,89E-01	A2LF	1,0035	9,49E-01	A2LF	0,8566	2,66E-01	A2LF	1,0354	6,08E-01	A2LF	0,8946	5,57E-01
MM	1,0649	1,66E-01	MM	1,0601	6,21E-01	MM	0,9633	4,74E-01	MM	0,9172	5,38E-01	MM	1,0395	5,48E-01	MM	0,9908	9,63E-01
A2F0S0G	0,8590	1,23E-03	A2F0S0G	0,8781	2,77E-01	A2F0S0G	0,9559	3,99E-01	A2F0S0G	1,0079	9,55E-01	A2F0S0G	1,0570	4,00E-01	A2F0S0G	1,2979	1,69E-01
A4F0G	1,0820	1,03E-01	A4F0G	1,0775	5,35E-01	A4F0G	1,0719	2,14E-01	A4F0G	1,1074	4,64E-01	A4F0G	1,0696	3,34E-01	A4F0G	1,1993	3,17E-01
CFa	1,1547	2,92E-03	CFa	1,1491	2,51E-01	CFa	1,0658	2,59E-01	CFa	1,0117	9,34E-01	CFa	1,0712	3,19E-01	CFa	0,9990	9,96E-01
A2F0GS	1,2296	7,11E-06	A2F0GS	1,4368	3,32E-03	A2F0GS	1,1406	1,32E-02	A2F0GS	1,3843	0,024587	A2F0GS	1,0765	2,49E-01	A2F0GS	1,4073	7,43E-02
A2F0S	1,2584	6,37E-07	A2F0S	1,4718	1,79E-03	A2F0S	1,1618	4,87E-03	A2F0S	1,397	0,020658	A2F0S	1,1047	1,20E-01	A2F0S	1,4293	6,25E-02
A2F0S0B	1,3535	2,94E-10	A2F0S0B	1,3959	6,54E-03	A2F0S0B	1,2003	8,65E-04	A2F0S0B	1,1369	3,70E-01	A2F0S0B	1,1445	4,62E-02	A2F0S0B	1,0725	7,16E-01
A2FSG	1,0940	4,83E-02	A2FSG	1,1179	3,41E-01	A2FSG	1,0963	7,95E-02	A2FSG	1,1085	4,61E-01	A2FSG	1,1555	2,37E-02	A2FSG	1,2337	2,50E-01
A2F0GE	1,4772	1,43E-16	A2F0GE	1,7609	1,18E-05	A2F0GE	1,2601	2,13E-05	A2F0GE	1,432	0,016141	A2F0GE	1,1650	2,10E-02	A2F0GE	1,5422	3,55E-02
CG	1,0311	5,08E-01	CG	1,1194	3,29E-01	CG	1,0880	1,21E-01	CG	1,1323	3,54E-01	CG	1,1838	1,06E-02	CG	1,3168	1,37E-01
A2F0E	1,4945	2,07E-17	A2F0E	1,7776	8,82E-06	A2F0E	1,2751	8,12E-06	A2F0E	1,4419	0,014116	A2F0E	1,1877	9,42E-03	A2F0E	1,5562	3,19E-02
A4FGE	1,3869	1,42E-11	A4FGE	1,8973	3,86E-06	A4FGE	1,2303	1,43E-04	A4FGE	1,5501	0,004474	A4FGE	1,2075	5,17E-03	A4FGE	1,3303	1,64E-01
A4F0E	1,3476	1,06E-09	A4F0E	1,3822	9,29E-03	A4F0E	1,2333	2,19E-04	A4F0E	1,2797	9,01E-02	A4F0E	1,2263	4,35E-03	A4F0E	1,3383	1,32E-01
CA3	1,3943	1,12E-11	CA3	1,4547	3,76E-03	CA3	1,2320	1,68E-04	CA3	1,2290	1,53E-01	CA3	1,2278	2,66E-03	CA3	1,1568	4,76E-01
A2FGL	1,0504	2,94E-01	A2FGL	1,2932	4,11E-02	A2FGL	1,1786	2,67E-03	A2FGL	1,5302	0,003591	A2FGL	1,2356	3,14E-03	A2FGL	1,3662	1,22E-01
A2SG	1,3541	5,04E-11	A2SG	1,5064	7,45E-04	A2SG	1,2669	6,72E-06	A2SG	1,4691	0,007856	A2SG	1,2741	1,42E-04	A2SG	1,5884	2,28E-02
A2FG	1,1203	1,36E-02	A2FG	1,0924	4,51E-01	A2FG	1,1430	1,27E-02	A2FG	1,0352	7,98E-01	A2FG	1,2787	2,58E-04	A2FG	1,2378	2,38E-01
A2FL	1,0692	1,52E-01	A2FL	1,2909	4,24E-02	A2FL	1,1974	9,54E-04	A2FL	1,4988	0,00536	A2FL	1,2885	4,17E-04	A2FL	1,3951	1,00E-01
A3F0E	1,8903	5,80E-32	A3F0E	2,4801	6,16E-09	A3F0E	1,4387	9,04E-10	A3F0E	1,6904	0,001654	A3F0E	1,2942	4,75E-04	A3F0E	1,3053	2,61E-01
A2F0SG	1,4624	1,16E-15	A2F0SG	1,5448	3,82E-04	A2F0SG	1,2766	5,45E-06	A2F0SG	1,2858	7,22E-02	A2F0SG	1,2969	4,98E-05	A2F0SG	1,3654	1,01E-01

Supplementary Table S5. Regression results for type 2 diabetes. (*continued*)

Model 1						Model 2						Model 3					
Discovery cohort			Replication cohort			Discovery cohort			Replication cohort			Discovery cohort			Replication cohort		
number of tests: 91			number of tests: 70			number of tests: 91			number of tests: 67			number of tests: 91			number of tests: 55		
FDR (Q)	0,05		FDR (Q)	0,05		FDR (Q)	0,05		FDR (Q)	0,05		FDR (Q)	0,05		FDR (Q)	0,05	
FDR α	0,0385		FDR α	0,0407		FDR α	0,0368		FDR α	0,0373		FDR α	0,0302		FDR α	0,0164	
trait	OR	p	trait	OR	p	trait	OR	p	trait	OR	p	trait	OR	p	trait	OR	p
A3FE	1,7942	1,13E-32	**A3FE**	1,9135	1,69E-06	**A3FE**	1,4066	1,31E-09	A3FE	1,4036	0,020748	A3FE	1,3027	1,44E-04	**A3FE**	1,1748	3,63E-01
A4F0GE	1,6592	3,60E-23	**A4F0GE**	1,8668	4,66E-06	**A4F0GE**	1,3769	2,28E-08	A4F0GE	1,3673	3,72E-02	A4F0GE	1,3343	5,80E-05	**A4F0GE**	1,1830	3,98E-01
A2GS	1,5673	2,48E-21	**A2GS**	2,1827	6,83E-09	**A2GS**	1,3980	2,66E-10	A2GS	1,9758	1,15E-05	A2GS	1,3375	7,99E-06	A2GS	1,8964	1,30E-03
A2F0G	1,4145	1,30E-13	**A2F0G**	1,5993	1,76E-04	**A2F0G**	1,2913	1,38E-06	A2F0G	1,3543	0,027814	A2F0G	1,3407	4,01E-06	**A2F0G**	1,4732	2,97E-02
A2G	1,2561	4,56E-07	**A2G**	1,4016	4,20E-03	**A2G**	1,2605	1,11E-05	A2G	1,3558	0,025544	A2G	1,3513	4,57E-06	**A2G**	1,5282	2,35E-02
A4E	1,6699	2,04E-24	**A4E**	2,0552	2,07E-07	**A4E**	1,3909	6,89E-09	A4E	1,5241	0,006332	A4E	1,3545	2,43E-05	**A4E**	1,3179	1,82E-01
A2GE	1,7609	7,36E-31	**A2GE**	2,4462	3,26E-10	**A2GE**	1,4549	6,32E-12	A2GE	2,0057	1,62E-05	A2GE	1,3589	4,91E-06	A2GE	2,0179	8,21E-04
A2S	1,5028	3,31E-18	**A2S**	1,9521	2,68E-07	**A2S**	1,3849	7,83E-10	A2S	1,8014	8,54E-05	A2S	1,3786	9,92E-07	A2S	1,8656	1,78E-03
A2E	1,6643	4,74E-26	**A2E**	2,1473	1,53E-08	**A2E**	1,4365	2,04E-11	A2E	1,8408	7,96E-05	A2E	1,3973	5,48E-07	A2E	1,9618	1,18E-03
A2FGE	1,7890	5,01E-30	**A2FGE**	2,0898	6,37E-08	**A2FGE**	1,4368	2,26E-10	A2FGE	1,532	0,005204	A2FGE	1,4443	3,52E-07	A2FGE	1,7890	4,26E-03
A2FE	1,6346	4,82E-23	**A2FE**	1,7704	1,19E-05	**A2FE**	1,3822	7,84E-09	A2FE	1,3628	0,034847	A2FE	1,4535	1,51E-07	A2FE	1,6434	1,15E-02
CS	1,4656	2,83E-16	**CS**	1,7198	1,20E-05	**CS**	1,3796	8,78E-10	CS	1,5387	0,002104	CS	1,4582	7,65E-09	CS	1,6531	8,26E-03
A3E	2,1908	2,82E-48	**A3E**	3,1552	2,94E-12	**A3E**	1,6319	4,69E-16	A3E	2,0948	3,41E-05	A3E	1,4802	2,34E-07	**A3E**	1,6836	3,82E-02
A2FS	1,6129	9,72E-23	**A2FS**	1,8914	1,32E-06	**A2FS**	1,4557	9,88E-12	A2FS	1,5929	0,001803	A2FS	1,5466	4,09E-10	A2FS	1,7548	4,19E-03
A2S0B	1,7392	2,20E-25	**A2S0B**	1,4968	1,65E-03	**A2S0B**	1,5831	9,39E-15	A2S0B	1,3794	0,027312	A2S0B	1,5683	1,54E-09	**A2S0B**	1,0642	7,51E-01
A2FS0B	1,7335	2,37E-25	**A2FS0B**	1,4843	2,05E-03	**A2FS0B**	1,5909	3,86E-15	A2FS0B	1,375	0,029161	A2FS0B	1,5809	6,51E-10	**A2FS0B**	1,0356	8,58E-01
A2FGS	1,8384	5,72E-33	**A2FGS**	2,3461	1,31E-09	**A2FGS**	1,5810	7,58E-16	A2FGS	1,94	3,4E-05	A2FGS	1,6002	2,91E-11	A2FGS	1,9350	9,69E-04

Glycan values were centered and scaled, therefore the effect sizes are indicative of 1 standard deviation change in glycan value. Shown are the regression coefficient β (for continuous variables) or the odds ratio (for binary variables), the standard error, the t-statistic as calculated by β/SE, and the corresponding p-value per association. All associations with type 2 diabetes that were statistically significant after correction for multiple comparisons are highlighted in green. The associations are adjusted for the following covariates: model 1) age, sex, and their interaction; model 2) age, sex, their interaction, and BMI; and model 3) age, sex, their interaction, BMI, HDL-c, non-HDL-c, and smoking (ever and current). A2, diantennary; A3, triantennary; A4, tetraantennary; F, fucosylation; B, bisection; E, α2,6-linked sialylation; G, galactosylation; L, α2,3-linked sialylation; S, sialylation. FDR, false discovery rate; BMI, body mass index; HDL-c, high-density lipoprotein-cholesterol; non-HDLc is the calculated difference between total cholesterol and HDL-c.

Supplementary Table S6. Regression results of detected glycan compositions for type 2 diabetes in the discovery cohort.

Trait	OR	p	Trait	OR	p
H4N4F1	0,6500	2,30E-10	H6N5L2	1,0128	8,49E-01
H5N4F1	0,7011	7,96E-08	H7N6E2L2	1,0155	8,16E-01
H5N4F1E1	0,7141	7,89E-07	H7N2	1,0192	7,60E-01
H4N4	0,7640	2,53E-05	H7N6F1E2L1	1,0199	7,66E-01
H4N4F1E1	0,7695	3,00E-05	H5N4E1	1,0225	7,30E-01
H4N4E1	0,7962	4,39E-04	H7N6E1L2	1,0228	7,29E-01
H4N5	0,8027	5,94E-04	H7N6F1E3L1	1,0472	5,03E-01
H5N3	0,8076	8,20E-04	H6N5E2L1	1,1017	1,57E-01
H5N5F1	0,8088	1,08E-03	H7N6E3L1	1,1235	8,31E-02
H3N4F1	0,8132	1,56E-03	H6N5F1E2	1,1389	6,60E-02
H5N4	0,8136	1,17E-03	H5N4L2	1,1539	3,02E-02
H7N6F1E1L3	0,8288	3,86E-03	H5N4E2	1,1566	2,68E-02
H4N5E1	0,8291	2,64E-03	H5N4F1L2	1,1570	3,07E-02
H4N5F1	0,8348	2,41E-03	H6N5E1L1	1,1624	2,98E-02
H6N3	0,8373	4,29E-03	H6N3E1	1,1726	2,35E-02
H5N4E1L1	0,8391	9,21E-03	H7N6E3	1,1899	1,49E-02
H5N5E1	0,8417	5,95E-03	H5N5E2	1,1993	1,07E-02
H5N5	0,8556	1,51E-02	H7N6E2L1	1,2399	2,89E-03
H5N4F1E1L1	0,8564	2,35E-02	H5N4F1E2	1,2683	1,33E-03
H6N5F1E1L2	0,8588	2,45E-02	H6N5F2E2L1	1,2812	9,44E-04
H7N6E1L3	0,8655	2,21E-02	H3N3E1	1,3295	5,27E-05
H5N2	0,8689	2,47E-02	H6N5F1E3	1,3857	1,72E-05
H3N5	0,8778	3,65E-02	H6N5E1	1,6844	2,09E-11
H5N5F1E2	0,8991	9,29E-02	H6N5E3	1,7103	6,54E-11
H6N5E1L2	0,9010	1,20E-01	H6N5E2	1,9926	2,22E-14
H6N5F2E1L2	0,9013	1,18E-01			
H8N2	0,9050	1,08E-01			
H6N2	0,9058	1,09E-01			
H3N3F1E1	0,9097	1,37E-01			
H5N5F1E1	0,9123	1,31E-01			
H9N2	0,9220	2,00E-01			
H6N5F1E1	0,9464	3,95E-01			
H6N5F1E1L1	0,9546	4,86E-01			
H5N3E1	0,9550	4,67E-01			
H3N5F1	0,9561	5,05E-01			
H5N5F1E1L1	0,9600	5,30E-01			
H7N6F1E2L2	0,9662	6,06E-01			
H7N6F1E1L2	0,9675	6,21E-01			
H4N5F1E1	0,9684	6,15E-01			

H6N5F1E2L1	0,9738	6,99E-01
H7N6F2E2L2	0,9774	7,32E-01
H4N3E1	0,9799	7,47E-01
H5N4L1	0,9807	7,68E-01
H6N5F1L2	0,9943	9,30E-01
H5N4F1L1	0,9959	9,52E-01

Glycan values were centered and scaled, therefore the effect sizes are indicative of 1 standard deviation change in glycan value. Shown are the odds ratio and p-value for each direct trait after adjustment for age, sex, their interaction, BMI, HDL-cholesterol, non-HDL-cholesterol, and smoking (ever and current). H = hexose; N = N-acetylhexosamine; F = deoxyhexose (fucose); S = N-acetylneuraminic acid (sialic acid); E, α2,6-linked sialic acid; L, α2,3-linked sialic acid.

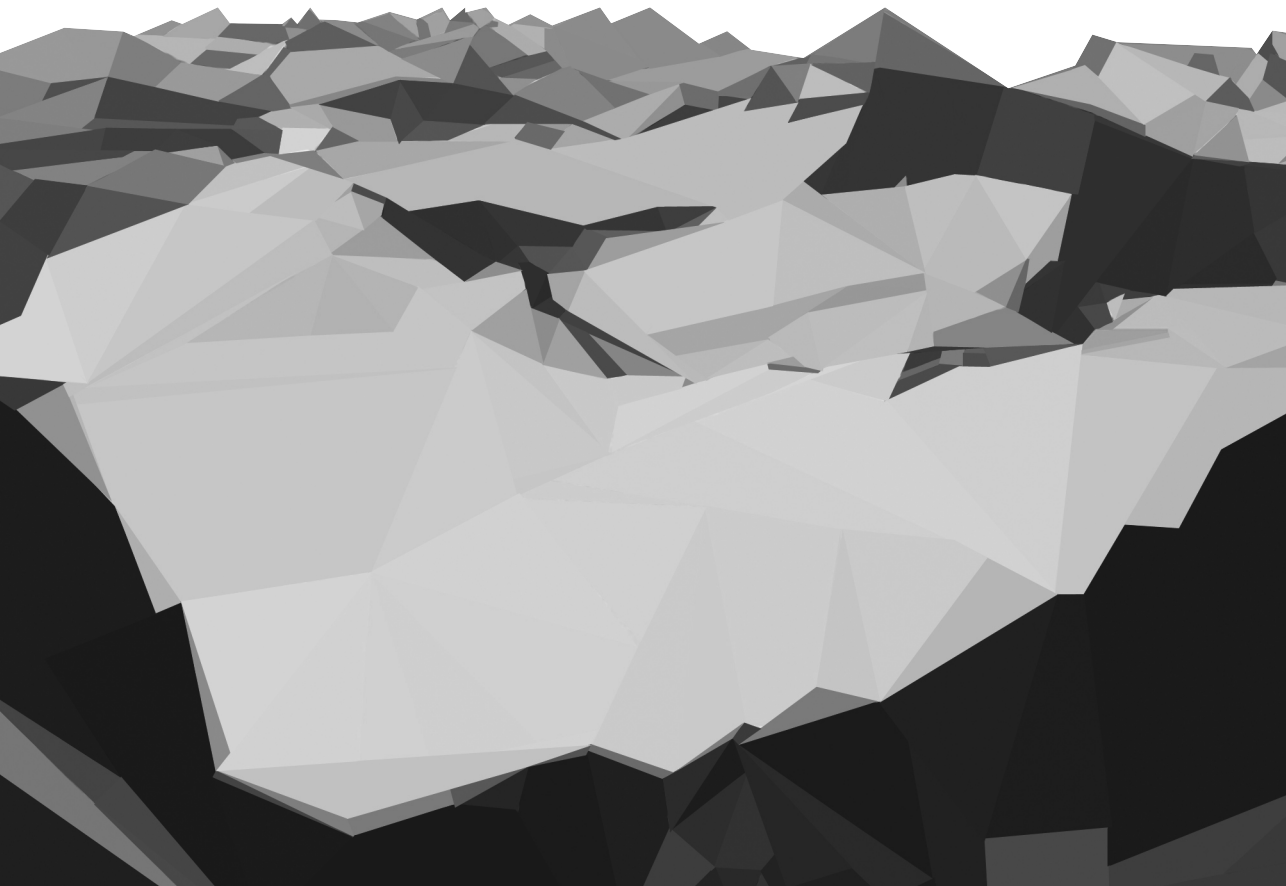

CHAPTER 4

IgG glycan patterns are associated with type 2 diabetes in independent European populations

Roosmarijn F.H. Lemmers, *Marija Vilaj, *Daniel Urda, Felix Agakov, Mirna Šimurina, Lucija Klaric, Igor Rudan, Harry Campbell, Caroline Hayward, Jim F. Wilson, Aloysius G. Lieverse, Olga Gornik, Eric J.G. Sijbrands, Gordan Lauc, Mandy van Hoek.
*These authors contributed equally

Biochimica et Biophysica Acta 2017;1861:2240-9

Abstract

Background; Type 2 diabetes results from interplay between genetic and acquired factors. Glycans on proteins reflect genetic, metabolic and environmental factors. However, associations of IgG glycans with type 2 diabetes have not been described. We compared IgG N-glycan patterns in type 2 diabetes with healthy subjects.

Methods; In the DiaGene study, a population-based case-control study, (1886 cases and 854 controls) 58 IgG glycan traits were analyzed. Findings were replicated in the population-based CROATIA-Korcula-CROATIA-Vis-ORCADES studies (162 cases and 3162 controls), and meta-analyzed. AUCs of ROC-curves were calculated using 10-fold cross-validation for clinical characteristics, IgG glycans and their combination.

Results; After correction for extensive clinical covariates, 5 IgG glycans and 13 derived traits significantly associated with type 2 diabetes in meta-analysis (after Bonferroni correction). Adding IgG glycans to age and sex increased the AUC from 0.542 to 0.734. Adding them to the extensive model did not substantially improve the AUC. The AUC for IgG glycans alone was 0.729.

Conclusions; Several IgG glycans and traits firmly associate with type 2 diabetes, reflecting a pro-inflammatory and biologically-aged state. IgG glycans showed limited improvement of AUCs. However, IgG glycans showed good prediction alone, indicating they may capture information of combined covariates. The associations found may yield insights in type 2 diabetes pathophysiology.

General significance; This work shows that IgG glycomic changes have biomarker potential and may yield important insights into pathophysiology of complex public health diseases, illustrated here for the first time in type 2 diabetes.

Introduction

Type 2 diabetes is an extremely challenging health issue in the 21st century [1]. It is a multifactorial disease, resulting from intricate interplay between environmental and genetic factors. Although many environmental and genetic risk factors have been identified, the underlying mechanisms of the disease remain largely unknown.

Genetic factors identified so far explain up to 5-10% of disease risk [2]. It is likely that epigenetic and posttranscriptional modifications play a substantial role in disease pathophysiology. Glycosylation of proteins is one of the most common posttranslational modifications. *N*-glycans are present on most proteins and are generated through interplays between hundreds of enzymes [3, 4]. They play structural, functional, and regulatory roles and reflect genetic, metabolic, and environmental factors [3]. These unique qualities raises interest for the role and use of *N*-glycans in complex disease such as type 2 diabetes. Total *N*-glycomic changes have been reported once in a relatively large type 2 diabetes population and showed significant changes. However, total *N*-glycomic changes do not inform us on the exact underlying proteins and processes involved and results are influenced by the relative abundance of proteins in the circulation.

Type 2 diabetes is characterized by a pro-inflammatory state and elevated levels of inflammatory markers, such as C-reactive protein and interleukin-6, that have been associated with risk of developing type 2 diabetes [5]. IgG *N*-glycome changes have been linked to clinical risk factors for type 2 diabetes, such as age, BMI, smoking, and dyslipidemia [6-9]. IgG is a tetramer protein complex consisting of Fc and Fab regions. IgG glycosylation is particularly interesting, as *N*-glycans attached to the Fc part of IgG can modulate and switch its function from pro- to anti-inflammatory and vice versa [3, 10, 11]. However, IgG *N*-glycosylation patterns in type 2 diabetes compared to the non-diabetic state have not been described in current literature. Knowledge on specific IgG *N*-glycosylation profiles in type 2 diabetes could shed light on underlying inflammatory pathophysiological processes and on drug target and biomarker potential.

We hypothesized that characteristic IgG *N*-glycan profiles are present in type 2 diabetes. In this study, we investigated the association of IgG *N*-glycan profiles with type 2 diabetes in a large population-based case control cohort, followed by replication in independent European samples. Moreover, we evaluate the AUC under the Receiver Operator Characteristic (ROC) curves for models including clinical characteristics, IgG glycans, and both.

Research design and Methods

Subjects

Discovery cohort:

The discovery cohort was the DiaGene study. Characteristics of the DiaGene population have been described elsewhere [12]. Briefly, the DiaGene study is a case-control cohort collected in and around the city of Eindhoven, the Netherlands. All hospitals in this area participated, as well as the center for primary care diagnostics. Type 2 diabetes was diagnosed according the ADA and WHO criteria [13, 14]. Patients with other types of diabetes, diabetes secondary to Cushing's syndrome or to corticosteroid use were excluded. Controls were recruited by advertising in local newspapers (aged 55 years or older) and through unrelated friends/family of the cases. Controls with diabetes mellitus, impaired glucose tolerance or Cushing's disease were excluded. In total, 1886 patients and 854 controls were included. All participants gave written informed consent. The study has been approved by the Medical Ethical Committee of the Erasmus MC.

Replication cohort:

We validated the results of our discovery analyses in three family-based cohorts from isolated islands: the Orkney Complex Disease Study (ORCADES), CROATIA-Vis, and CROATIA-Korcula. The ORCADES study was collected between 2005 and 2011 from the Orkney isles in Scotland. The CROATIA-Vis and CROATIA-Korcula cohorts were collected from the Croatian islands Vis and Korcula in 2003-2004 and 2007, respectively. Type 2 diabetes status was self-reported. These three deeply phenotyped cohorts have been described in more detail elsewhere [15-18]. Procedures used for extraction and preprocessing of glycomic profiles were harmonized for the discovery and replication cohorts. After quality control, the total number of samples in the combined replication cohorts was n=3324 (162 cases with type 2 diabetes and 3162 controls).

IgG N-glycosylation

In the DiaGene study, 1837 cases and 852 controls had plasma available for IgG glycosylation analyses. Twenty nine samples failed quality control. The remaining 1815 cases and 845 controls were included in the analyses. IgG glycan isolation, release and labeling in the DiaGene study were executed as described previously [19]. In total, 24 IgG glycan peaks were measured. The same peaks were measured in the CROATIA-Vis, CROATIA-Korcula and ORCADES samples as more extensively described by Pucic et al [19]. Figure 1 shows the glycan structures of the most abundant glycans per peak; a more detailed description can be found in supplementary table S1.

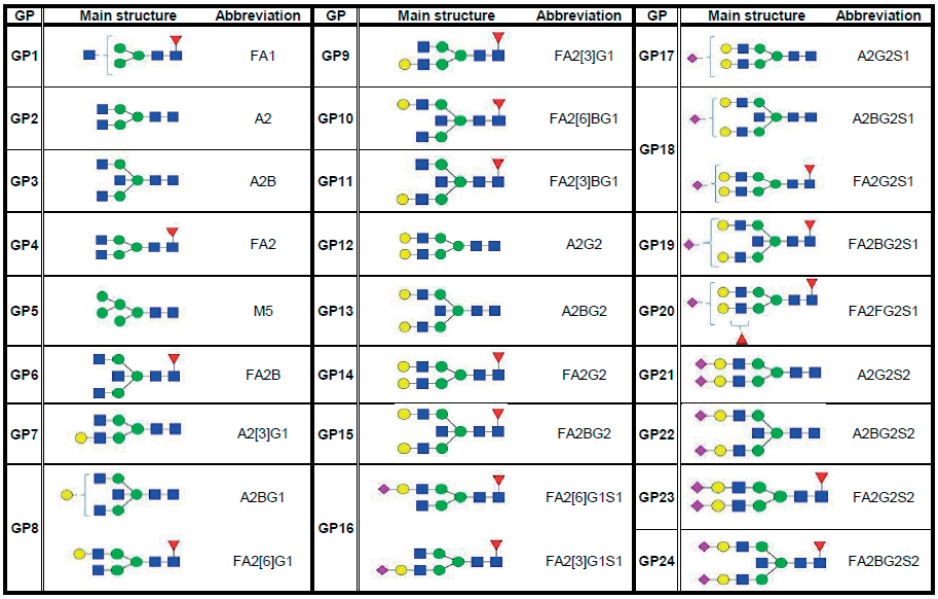

Figure 1. The 24 IgG glycan peaks as measured with ultra-performance liquid chromatography.

Shown are the structure of the main IgG glycan component(s) per peak and their structure abbreviation. Structure abbreviations: F, α-1,6-linked core fucose; A, number of antenna's attached to the core sequence (existing of two N-Acetylglucosamine (GlcNAc) and three mannose residues); B, bisecting GlcNac β1-4 linked to β1-3 mannose; M, number of mannose residues; G, number of β1-4 linked galactoses; [3]G1, galactose on the antenna of the α1-3 linked mannose; [6]G1, galactose on the antenna of the α1-6 linked mannose; S, sialic acid linked to galactose. Structural schemes are defined as follows: blue square, GlcNac; green circle, mannose; red triangle, core fucose; yellow circle, galactose; purple rhomb, sialic acid.

Table 1. Characteristics of the discovery and replication cohorts.

	DiaGene Study			CROATIA-Vis, CROATIA-Korcula, ORCADES		
	Cases (n=1815)	Controls (845)	p-value cases vs controls	Cases (n=162)	Controls (n=3162)	p-value cases vs controls
Age (yr.)	65.2 (±10.5)	65.7 (±6.8)	0.198	66.6 (±10.6)	54.5 (±14.9)	<0.001
Sex (% male)	53.7	40.2	<0.001	45.7	38.5	0.082
BMI (kg/m^2)	30.5 (±5.5)	25.8 (±3.7)	<0.001	30.1 (±4.7)	27.6 (±4.5)	<0.001
HDL-cholesterol (mmol/L)	1.17 (±0.32)	1.46 (±0.36)	<0.001	1.38 (±0.37)	1.52 (±0.39)	<0.001
nonHDL-cholesterol (mmol/L)	3.12 (±0.90)	4.10 (±0.98)	<0.001	4.12 (±1.12)	4.17 (±1.15)	0.535
Current smoking (%)	17.8	10.9		14.8	16.3	
Former smoking (%)	56.1	56.1	<0.001*	31.5	30	0.852*
Creatinine (umol/L)	83.35 (±0.69)	73.00 (±0.49)	<0.001	86.77 (±27.54)	79.86 (±16.95)	0.002

Unless stated otherwise, mean (±SD) are given. BMI, body mass index; HDL, high-density lipoprotein. * p-value for trend across categories.

In short, for both the discovery and the replication cohorts, IgG was isolated from plasma using 96-well protein G monolithic plates, eluted with 0.1M formic acid, and neutralized with 1M ammonium bicarbonate. Dried IgG samples (150-200ug) were denatured (with 30µl SDS), incubated at 65°C for 10 minutes and cooled to room temperature, followed by addition of 10µl of Igepal-CA630 (ϕ=4%). *N*-glycans were released with the addition of 1.2U of PNGase F in 10µL 5x PBS and incubation at 37°C for 18 hours. Released *N*-glycans were labeled with 2-AB. The samples were cleaned by using hydrophilic interaction liquid chromatography solid phase extraction (HILIC-SPE) and stored at -20°C until ultra-performance liquid chromatography (UPLC). Finally, 24 IgG glycan peaks (GPs) were measured by Waters Acquity UPLC instrument as described previously [19]. All chromatograms were separated in the same manner into 24 peaks and the amount of glycans in each peak was expressed as percentage of total integrated area.

An additional 34 derived IgG glycan traits were calculated from the 24 directly measured peaks as described previously [6, 19]. These traits represent specific IgG glycosylation features (such as galactosylation, fucosylation and sialylation); a detailed description can be found in supplementary table S1.

Harmonization

Twelve glycan profiles were removed after visual inspection of the chromatograms. In all cohorts, preprocessing of the data followed the same protocol, where: (i) IgG glycan expressions were normalized by the total area under the expression peaks, followed by log-transformation, and (ii) batch effects were removed by applying ComBat modified to correct for outliers (using R Package sva). Measurement error of each of the 24 glycan structures was estimated based on the correlation between replicated samples (n=69 out of 2688 samples) and variation of standard sample measurements (n=153), which are shown in supplementary figure S1 and S2, respectively. No samples were excluded based on measurement error. After the preprocessing, ORCADES, CROATIA-Vis and CROATIA-Korcula cohorts were pooled, to form a joint validation dataset.

Statistical analyses

The distribution of the IgG glycan peaks was analyzed by visual inspection of QQ plots and showed no major deviations from normality. Pairwise dependencies between the 24 IgG glycan peaks and age, BMI, cholesterol traits, and creatinine in the discovery population were evaluated by Pearson's correlation coefficients; significance was assessed by the correlation test for bivariate normal distributions. Associations of smoking and sex with the IgG glycan peaks were evaluated with ANOVA. Non-HDL cholesterol was calculated as the difference between total cholesterol and HDL-cholesterol. These clinical variables were selected because they are risk factors for type 2 diabetes [20] and/or associated with

N-glycosylation [6, 8, 21]. Student's t-tests and chi-squared tests were applied to test differences between cases and controls for continuous and categorical variables respectively.

Logistic regression models were used to investigate the associations of directly measured IgG glycan peaks and derived traits with type 2 diabetes. Three models were considered: model 1) adjusted for age and sex; model 2) adjusted for age, sex, and BMI; and model 3) adjusted for age, sex, BMI, HDL-cholesterol, non-HDL-cholesterol, smoking and creatinine. All analyses described above were performed in the discovery population using 'binary logistic regression' in SPSS Statistics, version 21. Covariates were entered without forward or backward selection.

All analyses in the validation cohort were done in R, using the packages glm, pROC, and ROCR [22]. The likelihood-ratio test was used to compare the performance of logistic regression models with and without IgG glycans. The same clinical and demographic variables were applied in the models of the validation cohort. All analyses in the validation cohort were additionally adjusted for the covariate denoting their original cohort.

Results of the association analyses in the discovery and replication sets were meta-analyzed using the weighted z-transform method [23]. This method takes into account the regression coefficients, standard errors, and number of participants per study, and sets the weight of each study to the square root of the sample size. Bonferroni correction for multiple testing was applied for 58 tests (24 direct and 34 derived measurements). P-values < $8.62E^{-4}$ were considered statistically significant.

For prediction analyses, we fitted logistic regression models using 10-fold cross-validation. In this method, the original sample is partitioned in 10 non-overlapping subsamples of equal size, where 1 sample serves as a test set and the other 9 samples serve as training sets, and models are fitted repeatedly for all training/test fold partitions. We first computed the average AUC across the test folds, and finally the aggregated AUC, where predictions on 10 independent subsets were merged into a single vector. This method limits the danger of overfitting and estimates how well the model can be generalized to independent datasets. We compared model AUCs that included the above-mentioned clinical variables with those that additionally contained the 24 directly measured IgG glycans. All continuous variables were standardized before they were included in the models for AUC calculation.

The term prediction is used in the statistical sense, *i.e.* the inference of an outcome given the covariates. Specifically, we do not refer to forecasting of prospective outcomes, and our predictions in the considered case-control setting refer to the time of the measurements.

Results

Cohort characteristics

Characteristics of the cohorts are shown in Table 2. In the DiaGene study, patients with type 2 diabetes were more often male (53.7 vs 40.2% for cases and controls, respectively), had higher BMI and creatinine levels, lower HDL-cholesterol and non-HDL cholesterol levels, and were more often smokers than healthy controls. In the replication cohort, cases were older (66.6 vs. 54.5y), had a lower HDL-cholesterol, and higher BMI and creatinine.

Table 2: Correlations (continuous variables) and direction of effect in ANOVA (categorical variables) of clinical traits with IgG glycan peaks in the discovery population.

Glycan peak	Glycan structure	Age	Sex	BMI	Smoking	HDLc	NonHDLc	Creatinine
GP1	FA1	0.26	NS	NS	NS	NS	NS	0.15
GP2	A2	0.19	↑	NS	NS	NS	NS	NS
GP3	A2B	0.20	NS	0.12	NS	-0.08	NS	0.10
GP4	FA2	0.37	↑	0.15	↓	-0.10	-0.07	0.16
GP5	M5	0.11	NS	NS	NS	NS	NS	NS
GP6	FA2B	0.37	↑	0.16	↑	-0.12	-0.11	0.16
GP7	A2[3]G1	NS	NS	-0.10	NS	0.08	NS	NS
GP8	A2BG1 FA2[6]G1	-0.23	NS	-0.19	NS	0.17	0.13	-0.04
GP9	FA2[3]G1	-0.15	↓	-0.11	↓	0.10	0.10	-0.16
GP10	FA2[6]BG1	NS	NS	NS	↑	NS	NS	NS
GP11	FA2[3]BG1	0.14	NS	0.08	↑	NS	NS	0.08
GP12	A2G2	-0.12	NS	-0.08	↑	NS	NS	NS
GP13	A2BG2	-0.10	NS	-0.07	↑	NS	NS	NS
GP14	FA2G2	-0.45	↓	-0.11	↑	NS	NS	-0.16
GP15	FA2BG2	-0.25	↓	NS	↑	NS	NS	NS
GP16	FA2[6]G1S1 FA2[3]G1S1	-0.09	↓	NS	NS	NS	NS	NS
GP17	A2G2S1	NS	NS	NS	NS	NS	NS	NS
GP18	A2BG2S1 FA2G2S1	-0.41	↓	-0.08	NS	NS	NS	-0.14
GP19	FA2BG2S1	NS	NS	-0.15	NS	NS	NS	NS
GP20	FA2FG2S1	-0.10	NS	NS	NS	NS	NS	NS
GP21	A2G2S2	NS	NS	-0.08	NS	NS	NS	NS
GP22	A2BG2S2	NS	NS	NS	NS	NS	NS	NS
GP23	FA2G2S2	-0.23	↓	-0.09	↓	NS	0.07	-0.12
GP24	FA2BG2S2	NS	NS	-0.11	NS	0.07	NS	-0.08

βs are shown for continuous variables. Sex: ↑, higher in females; ↓, lower in females. Smoking: ↑, higher in current/former smokers; ↓, lower in current/former smokers. A p-value < 8.62E-4 was considered statistically significant. NS, not significant. Structure abbreviations: F, α-1,6-linked core fucose; A, number of antenna's; B, bisecting GlcNac β1-4 linked to β1-3 mannose; M, number of mannose residues; Gx, number of β1-4 linked galactoses; [3]G1, galactose on the antenna of the α1-3 linked mannose; [6]G1, galactose on the antenna of the α1-6 linked mannose; Sx, number of sialic acids linked to galactose. Red background, positive association; blue background, negative association.

Clinical traits associated with type 2 diabetes or N-glycosylation

Correlations of clinical traits associated with type 2 diabetes or N-glycosylation with the 24 IgG glycan peaks are shown in table 2. IgG glycan peaks show significant univariate associations with more than one clinical trait and vice versa.

IgG glycan associations with type 2 diabetes

Illustrative IgG glycan profiles for type 2 diabetes and the non-diabetic state are shown in figure 2; median and interquartile ranges of all peaks in both cohorts are shown in supplementary table S2. Table 3 shows glycans that were significantly associated with type 2 diabetes after meta-analyses in the discovery and validation cohorts, adjusted for age and sex. The strongest associations are for glycan peaks GP6, GP8 and GP9 (P meta-analyses <2.22E-16). Additional adjustment for BMI did not substantially change significant associations (complete data on all outcomes in all models are shown in Supplementary tables S3-S5).

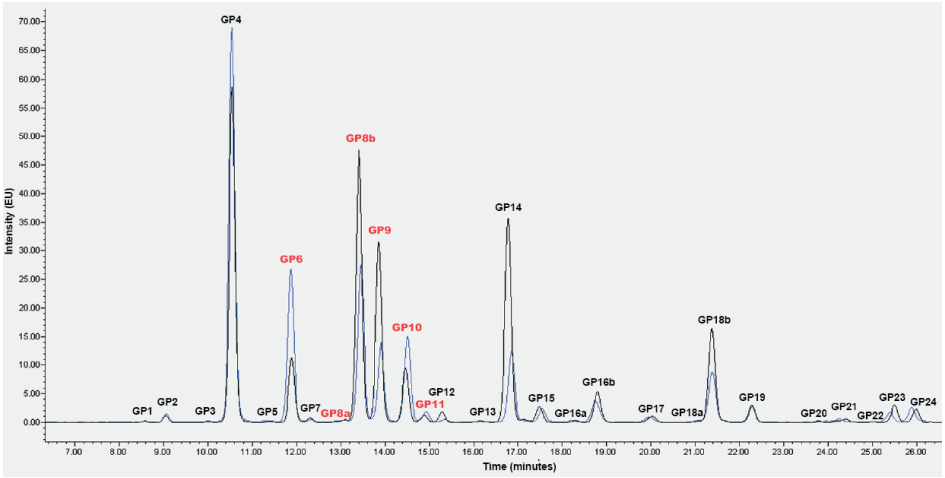

Figure 2. UPLC chromatogram of one individual with and one individual without type 2 diabetes.

The 24 IgG glycan peaks are numbered and peaks associated with type 2 diabetes in the full model are highlighted in red. Black line, healthy control; blue line, individual with type 2 diabetes.

The associations with type 2 diabetes remained statistically significant for glycan peaks GP6, GP8, GP9, GP10, and GP11 in the full model (adjusted for age, sex, BMI, HDL-cholesterol, non-HDL-cholesterol, smoking and creatinine). Figure 3 shows boxplots for these IgG glycan peaks; β- and p-values adjusted for the full model are shown in table 4. Excluding participants using medication indicative of auto-immune, malignant, or inflammatory conditions from the analyses did not change our results (data not shown). These glycans

Table 3. Statistically significant associations of IgG glycan traits for the discovery and replication cohorts and meta-analyses, adjusted for age and sex.

		Discovery		Replication		Meta-analysis
Glycan peaks		**β**	**p-value**	**β**	**p-value**	**p-value**
GP3	A2B	4.81	5.90E-05	3.24	0.04	1.05E-05
GP4	FA2	0.06	2.05E-14	0.01	0.73	8.97E-08
GP6	FA2B	0.39	1.21E-39	0.27	3.13E-06	<2.22e-16
GP8	A2BG1	-0.35	1.88E-41	-0.20	1.09E-05	<2.22e-16
GP9	FA2[3]G1	-0.32	1.01E-23	-0.23	1.40E-03	<2.22e-16
GP10	FA2[6]BG1	0.20	2.86E-08	0.33	8.02E-05	3.15E-11
GP11	FA2[3]BG1	1.93	2.76E-10	1.23	8.63E-03	7.05E-10
GP14	FA2G2	-0.11	3.32E-12	-0.01	0.88	1.95E-06
GP19	FA2BG2S1	-0.51	2.00E-06	-0.23	0.18	3.31E-05
GP23	FA2G2S2	-0.63	3.08E-09	-0.37	0.02	1.37E-08
Derived traits						
FBGS/(FBG+FBGS)	Sialylation of fucosylated galactosylated structures with bisecting GlcNAc	-0.04	3.74E-08	-0.05	1.00E-03	9.35E-10
FBGS/(FB+FBG+FBGS)	Sialylation of fucosylated structures with bisecting GlcNAc	-0.09	1.54E-19	-0.06	2.80E-04	<2.22e-16
FG1S1/(FG1+FG1S1)	S1 of fucosylated G1 structures	0.21	1.26E-10	0.04	0.34	5.87E-07
FG2S1/(FG2+FG2S1+FG2S2)	S1 of fucosylated G2 structures	0.10	8.30E-09	0.03	0.44	9.87E-06
FBG2S1/(FBG2+FBG2S1+FBG2S2)	S1 of fucosylated G2 structures with bisecting GlcNAc	-0.06	3.00E-06	-0.05	0.02	1.52E-06
FS1/FS2	Ratio of fucosylated S1 and S2 structures	0.09	2.77E-04	0.14	1.00E-03	1.08E-06
FBS2/FS2	Ratio of fucosylated S2 structures with and without bisecting GlcNAc	0.86	5.11E-10	0.62	3.10E-03	2.16E-10
FBS2/(FS2+FBS2)	B in all fucosylated S2 structures	4.71	2.24E-10	4.17	5.30E-03	2.83E-10
G0n	G0 structures in total neutral glycans	0.07	1.56E-24	0.02	0.13	2.22E-15
G1n	G1 structures in total neutral glycans	-0.19	3.55E-39	-0.08	5.80E-04	<2.22e-16
G2n	G2 structures in total neutral glycans	-0.06	9.67E-10	0.01	0.79	1.06E-04

Table 3. Statistically significant associations of IgG glycan traits for the discovery and replication cohorts and meta-analyses, adjusted for age and sex. (*continued*)

		Discovery		Replication		Meta-analysis
Derived traits		**β**	**p-value**	**β**	**p-value**	**p-value**
Fn	F in neutral glycans (without bisecting GlcNAc)	-0.12	4.55E-20	-0.11	8.10E-06	<2.22e-16
FG0n/G0n	F in neutral G0 structures	-0.06	3.18E-09	-0.08	1.86E-05	9.38E-13
FG1n/G1n	F in neutral G1 structures	-0.13	1.93E-24	-0.13	2.03E-07	<2.22e-16
FG2n/G2n	F in neutral G2 structures	-0.10	1.19E-12	-0.02	0.21	1.39E-08
FBn	F in neutral structures with bisecting GlcNAc	0.16	1.72E-26	0.18	8.74E-09	<2.22e-16
FBG0n/G0n	F in neutral G0 structures with bisecting GlcNAc	0.09	1.10E-14	0.13	3.99E-07	<2.22e-16
FBG1n/G1n	F in neutral G1 structures with bisecting GlcNAc	0.14	1.34E-26	0.16	1.78E-09	<2.22e-16
FBG2n/G2n	F in neutral G2 structures with bisecting GlcNAc	0.22	8.01E-21	0.06	0.06	2.09E-14
FBn/Fn	Ratio of fucosylated neutral glycans with and without bisecting GlcNAc	0.10	2.73E-25	0.12	2.14E-06	<2.22e-16
FBn/Fn total	Ratio of bisecting GlcNAc in all fucosylated structures within neutral glycans	0.15	1.63E-25	0.16	2.45E-08	<2.22e-16

A p-value <8.62E-4 was considered statistically significant. Structure abbreviations: F, core fucose; A, number of antenna's; B, bisecting GlcNAc; M, number of mannose residues; Gx, number of galactoses; [3]G1, galactose on the α1-3 antenna; [6]G1, galactose on the α1-6 antenna; Sx, number of sialic acids linked to galactose; n, neutral glycans. Red: positive association with type 2 diabetes; blue: negative association.

Table 4. Associations of IgG glycan traits for the discovery and replication cohorts and meta-analyses, adjusted for age, sex, BMI, HDL-cholesterol, non-HDL cholesterol, smoking and serum creatinine.

		Discovery cohort		Replication cohort		Meta-analysis
Glycan peaks		**β**	**p-value**	**β**	**p-value**	**p-value**
GP6	FA2B	0.23	2.45E-08	0.24	3.89E-05	1.84E-11
GP8	A2BG1	-0.22	1.59E-09	-0.20	2.10E-05	1.10E-12
GP9	FA2[3]G1	-0.19	4.30E-05	-0.22	3.15E-03	1.08E-06
GP10	FA2[6]BG1	0.14	6.56E-03	0.30	4.93E-04	9.96E-06
GP11	FA2[3]BG1	1.28	3.10E-03	1.10	0.03	3.28E-04
Derived traits						
FBGS/(FB+FBG+FBGS)	Sialylation of fucosylated structures with bisecting GlcNAc	-0.03	0.06	-0.05	1.89E-03	3.28E-04
FBS2/FS2	Ratio of fucosylated S2 structures with and without bisecting GlcNAc	0.68	7.42E-04	0.59	5.89E-03	1.96E-05
FBS2/(FS2+FBS2)	Bisecting GlcNAc in all fucosylated S2 structures	3.72	6.27E-04	4.02	8.62E-03	2.67E-05
G1n	G1 structures in total neutral glycans	-0.10	1.00E-06	-0.07	2.70E-03	7.40E-08
Fn	F in neutral glycans (without bisecting GlcNAc)	-0.08	6.00E-06	-0.02	2.37E-05	8.90E-10
FG0n/G0n	F in neutral G0 structures	-0.05	4.06E-04	-0.08	2.76E-05	4.16E-08
FG1n/G1n	F in neutral G1 structures	-0.08	2.00E-06	-0.12	1.92E-06	2.36E-11
FBn	F in neutral structures with bisecting GlcNAc	0.11	2.09E-07	0.17	9.07E-08	1.13E-13
FBG0n/G0n	F in neutral G0 structures with bisecting GlcNAc	0.08	1.00E-05	0.13	5.62E-07	2.65E-11
FBG1n/G1n	F in neutral G1 structures with bisecting GlcNAc	0.09	9.91E-07	0.16	4.08E-08	2.04E-13
FBG2n/G2n	F in neutral G2 structures with bisecting GlcNAc	0.13	8.10E-05	0.06	0.08	1.24E-04
FBn/Fn	Ratio of fucosylated neutral glycans with and without bisecting GlcNAc	0.07	3.79E-07	0.11	1.54E-05	5.25E-11
FBn/Fn total	Ratio of bisecting GlcNAc in all fucosylated structures within neutral glycans	0.10	3.42E-07	0.16	1.80E-07	3.63E-13

A p-value <8.62E-4 was considered statistically significant. Structure abbreviations: F, core fucose; A, number of antenna's; B, bisecting GlcNAc; M, number of mannose residues; Gx, number of galactoses; [3]G1, galactose on the α1-3 antenna; [6]G1, galactose on the α1-6 antenna; Sx, number of sialic acids linked to galactose; n, neutral glycans. Red: positive association with type 2 diabetes; blue: negative association.

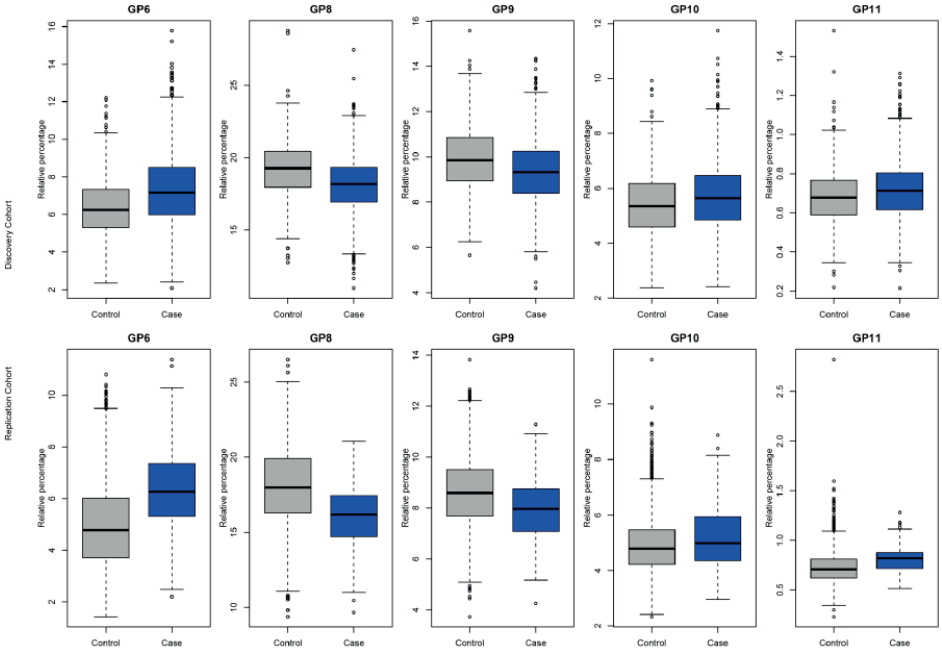

Figure 3. Distribution of IgG glycan peaks associated with type 2 diabetes after adjustment for the full model.

Upper half: distribution of glycan peaks in the discovery cohort. Bottom half: distribution of glycan peaks in the replication cohort. Shown are the relative percentages of each peak for controls (grey) and cases (blue). GP, glycan peak.

are reflective of increased presence of agalactosylated (GP6) and monogalactosylated (GP10, GP11) FA2 glycans with bisecting *N*-Acetylglucosamine (GlcNAc) and decreased presence of FA2[6] (GP8) and FA2[3] (GP9) monogalactosylated glycans. The derived traits associated with type 2 diabetes show a decrease in the percentage of sialylation of all fucosylated structures with bisecting GlcNAc (FBGS/(FB+FBG+FBGS)) and an increase of bisecting GlcNAc in fucosylated disialylated structures (FBS2/FS2 and FBS2/(FS2+FBS2)). There was a decrease in monogalactosylated structures (G1n). Furthermore, there was a decrease in fucosylated structures without bisecting GlcNAc in neutral glycans (Fn) and in agalactosylated (FG0n/G0n) and monogalactosylated (FG1n/G1n) structures. Finally, there was an increase in fucosylated structures with bisecting GlcNAc (FBn, FBG0n/G0n, FBG1n/G1n, FBG2n/G2n, FBn/Fn, FBn/Fntotal).

Area under the ROC curves for type 2 diabetes

The average AUCs for 24 IgG glycans without clinical variables was 0.73 and 0.75 for the discovery and validation populations, respectively. Figure 4 shows ROC curves for the

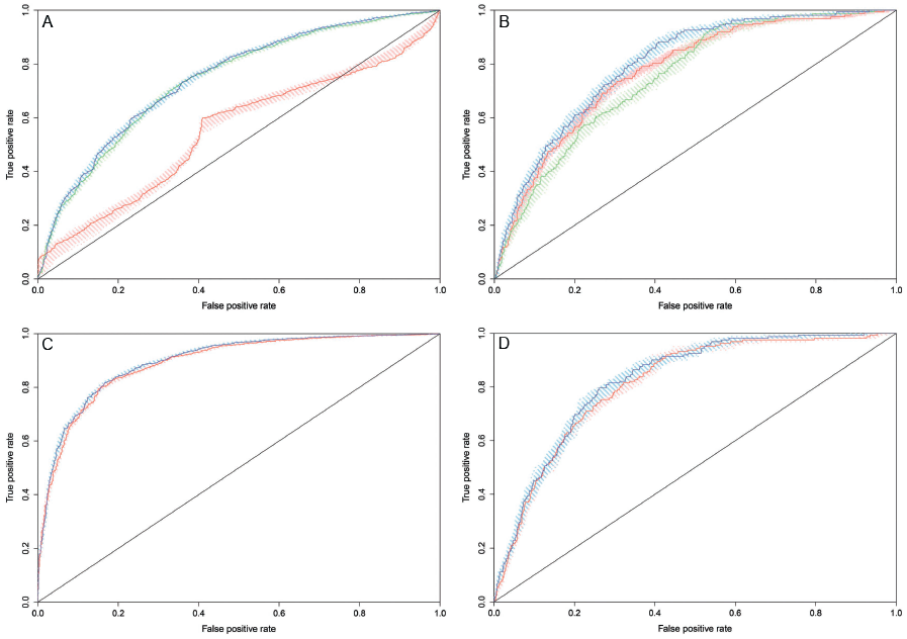

Figure 4. ROC curves for type 2 diabetes.

The AUC is shown for 1) IgG glycans alone (green); 2) age and sex (red); 3) age, sex, and IgG glycans (blue) in A for the discovery cohort and in B for the replication cohort. AUCs for 4) the full model (red); and 5) the full model with IgG glycans (blue) are shown in C for the discovery cohort and in D for the replication cohort. AUC, area under the curve.

predictive capacity of clinical variables with and without glycans for type 2 diabetes in the case-control setting.

As shown in table 5, adding the 24 IgG glycans to clinical variables led to improvement of the AUC in all models. This improvement was most extensive in the model containing age and sex (AUC 0.542 vs 0.734 for age and sex vs age, sex, and 24 IgG glycans). Similar results were found in our validation cohort. Augmented AUCs were similar and differences with average AUCs were negligible (data not shown).

Table 5. Ten-fold cross validated AUCs standardized.

Model	AUC without 24 IgG glycans	AUC with 24 IgG glycans
DiaGene study		
Glycans only		0.73
Age, sex	0.54	0.73
Age, sex, BMI	0.78	0.82
Age, sex, BMI, HDL-c, non-HDL-c, smoking	0.89	0.89
Age, sex, BMI, HDL-c, non-HDL-c, creatinine, smoking	0.89	0.90
CROATIA-Vis, CROATIA-Korcula, ORCADES population[a]		
Glycans only		0.75
Age, sex	0.77	0.80
Age, sex, BMI	0.79	0.82
Age, sex, BMI, HDL-c, non-HDL-c, smoking	0.81	0.82
Age, sex, BMI, HDL-c, non-HDL-c, creatinine, smoking	0.81	0.82

All analyses in CROATIA-Vis, CROATIA-Korcula and ORCADES were adjusted for cohort ID. BMI, body mass index; HDL-c, high-density lipoprotein-cholesterol; non-HDL-c, non-high-density lipoprotein cholesterol.

Discussion

In the present study, we are the first to describe the association and predictive potential of IgG *N*-glycans in type 2 diabetes versus healthy individuals in a large case-control study. We have found significant and replicated associations for GP6, GP8, GP9, GP10, and GP11 and several derived IgG glycan traits associated with decreased galactosylation and sialyation, an increase in fucosylated structures with bisecting GlcNAc and a decrease in fucosylated structures without bisecting GlcNAc. AUCs showed slight improvement for predicting type 2 diabetes in the case-control setting when IgG glycan peaks were added to models with clinical characteristics. Remarkably, the AUC for IgG glycans by themselves for type 2 diabetes was 0.73.

Type 2 diabetes is a multifactorial disorder in which genetics, environmental, and metabolic influences interact at multiple levels. Glycans reflect all these influences, which makes them attractive biomarkers for multifactorial diseases. In this study, the IgG glycan profile showed significant associations with age, sex, BMI, lipid profile, smoking, and kidney function. These associations are largely in line with previous reports on IgG glycosylation and total *N*-glycome in these traits [6-8, 21, 24].

The associations we found in type 2 diabetes are reflective of an overall pro-inflammatory state and biological aging [3, 7, 11, 25-28]. In the most extensive model, the associations were in concordance with a decrease in galactosylation and sialylation, an increase in fucosylated structures with bisecting GlcNac, and a decrease in fucosylated structures without bisecting GlcNAc.

Galactosylation has been shown to influence the inflammatory potential of IgG [25]. Lack of galactosylation is associated with a pro-inflammatory state of IgG through activation of the complement cascade [27]. Previous studies found a decrease in galactosylation in rheumatoid arthritis (RA) [29, 30], systemic lupus erythematosus (SLE) [31], inflammatory bowel disease (IBD) [32]), chronic kidney disease (CKD) [21], hypertension [9], colorectal cancer [33], and with increasing age [7] and BMI [6]. Contrarily, in Parkinson's disease, galactosylation increased [34]. The decreased IgG galactosylation found in most studies followed the same patterns as in type 2 diabetes and thus seems a general feature of pro-inflammatory disease. A possible explanation for this decreased galactosylation are posttranslational modifications of the enzyme β4-galactosyltransferase-1 [35]. Interestingly, Ercan et al. recently showed that estrogen increases galactosylation in IgG and accounts for a difference between men and premenopausal women [24]. As the majority of individuals in our discovery and replication cohorts were older than 50 and all models were adjusted for sex, this is not expected to influence the findings in our study.

Sialylation also plays an important role in the inflammatory potential of IgG. Addition of sialic acid to IgG converts its function from pro- to anti-inflammatory by decreased binding to Fcγ receptors [11]. It should be noted that a lack of galactose also leads to a lack of sialic acid, as sialic acid mainly binds to terminal galactose [35]. Similar to our findings, a reduction in sialylation was recently described in SLE [31], IBD [32], CKD [21], and colorectal cancer [33], while sialylation increased in hypertension [9]. Interestingly, in our study, decreased sialylation was present in fucosylated bisecting structures mainly due to decreased GP19 (FA2BG2S1). In contrast, in SLE and IBD, sialylation decreased in general while GP19 increased [31, 32]; in CKD, sialylation was decreased in fucosylated non-bisecting structures due to a decrease in GP18 (FA2G2S1; analysis adjusted for diabetes). Decreased sialylation was seen in roughly the same glycan peaks in individuals with colorectal cancer patients as in our study, although different derived traits were calculated. Thus, although decreased IgG sialylation is seen in more diseases than type 2 diabetes, the desialylated glycan structures differ and could thus be disease-specific changes.

Finally, core-fucosylation and bisecting GlcNAc exert important effects on IgG function. Core fucosylation prevents antibody-dependent cytotoxicity [26, 28, 36], while the presence of bisecting GlcNAc is thought to have the opposite effect [37]. We observed decreased fucosylation in structures without bisecting GlcNAc and increased fucosylation in structures with bisecting GlcNAc. Moreover, we found increased bisection in fucosylated glycans, especially when sialylated. These changes indicate a higher antibody dependent cytotoxic potential of IgG in type 2 diabetes. Similar associations have been found in increasing age, CKD [21], SLE.[31], colorectal cancer [33], and hypertension [9], although small differences existed. In CKD, the strongest association with bisection was in fucosylated monosialylated structures, while in type 2 diabetes this was the case for fucosylated disialylated structures. Furthermore, bisection of neutral structures was positively associ-

ated with type 2 diabetes, while it was negatively associated with colorectal cancer [33] and not at all with CKD [21]. If and how these differences in bisection and fucosylation affect the efficacy of IgG in antibody-dependent cytotoxicity is unknown and should be subject of future studies. A potential gene of interest for studying this is *MGAT-3*, which encodes N-acetylglycosaminyltransferase 3, a glycosyltransferase that adds bisecting GlcNAc to IgG glycans, and is associated with IgG bisecting [38].

Recently, Testa et al described the total *N*-glycome in type 2 diabetes [39] and found a reduction in monogalactosylation on the 3- and 6-arm of fucosylated diantennary glycans, which is in line with our findings. In contrast with our findings, Itoh et al found [40] a small increase in an *N*-glycan with α1,6-core fucose in the total *N*-glycome in type 2 diabetes. Findings of both studies are difficult to compare to ours, due to the different quantification techniques for *N*-glycans. The method of Testa et al. does not allow for measurement of sialylation and has lower resolution. Itoh et al. measured exact bi-antennary glycan structures as single molecules, while our method divides IgG glycans in groups, reflecting major structural characteristics (such as total core fucosylation, outer arm fucosylation, degree of sialylation, etc.).In both studies, total *N*-glycome was measured, quantifying glycans from all plasma proteins, while we quantified IgG-specific glycans. Total plasma N-glycome not only reflects *N*-glycosylation, but also the relative abundance of proteins in the circulation.

Due to the case-control nature of our study it remains unclear whether the IgG glycan associations are a cause or a consequence of the disease. Notably, for RA it was shown that a decrease in galactosylation precedes a flare of the disease rather than the other way around [41]. In addition, the IgG glycans associated with type 2 diabetes in our study showed high heritabilities in previous studies (35-76%) [19, 42]. Genome wide association studies (GWAS) have identified several loci influencing *N*-glycosylation. Of interest, the *HNF1A* gene, known for its causal role in monogenic types of diabetes and its common variants associated with type 2 diabetes [12], is a genetic locus of significant association with total plasma *N*-glycome as a regulator of fucosylation [43]. Moreover, *HNF1A* regulates expression of *FUT8* [43], a fucosyltransferase gene associated with IgG core fucosylation [38], which was associated with type 2 diabetes in our study. In addition, GWAS on IgG glycosylation found associations with the *ST6GAL1* gene [38], which was previously associated with type 2 diabetes in South Asians [44]. *ST6GAL1*, as well as *B4GALT1 (*encoding sialyltransferase 6 and beta1,4-galactosyltransferase 1, respectively), are associated with IgG sialylation [38] and could therefore be candidate genes for future studies on the role of IgG sialylation in type 2 diabetes pathophysiology. Besides these genetic links between glycosylation and type 2 diabetes, the associations found between risk factors for type 2 diabetes and IgG glycans support the hypothesis that pro-inflammatory IgG could already at an early stage contribute to pathophysiology. Possibly, pro-inflammatory IgG could contribute to the pro-inflammatory state seen in obesity and type 2 diabetes [45],

which leads to β-cell destruction and insulin resistance [46, 47]. A potential mechanism is through complement activation, which has been shown to be associated with type 2 diabetes incidence and complications [48, 49] and is activated by agalactosylated IgG. Taken together, these findings are supportive of the hypothesis that IgG glycans play a role in type 2 diabetes disease pathophysiology, rather than just reflective of changes the disease brought on.

As glycan profiles are associated with genetic, metabolic and environmental influences, this adds to their predictive potential. We observed a modest improvement when adding the IgG glycan profiles to clinical risk factors. However, the AUC of IgG glycans alone was substantial compared to combined clinical risk factors, indicating that the IgG glycan profile captures much of the combined risk of these factors. This underlines its potential as a biomarker of the complex inflammatory pathophysiological changes in type 2 diabetes. Future studies in prospective cohorts should be conducted to investigate whether this biomarker potential could be used for personalized approaches in prevention and treatment of the disease as well as its role in diabetes complications. Of note, because of the case-control setting, the predictive capacity of clinical risk factors was high in both cohorts, especially in the replication cohort where the cases were considerably older than the controls. The discovery population was quite well-matched for age. A consideration in the interpretation of our findings is that we have only looked at the glycan profile of IgG. As many more glycoproteins are present in the circulation, the total *N*-glycome or a combination of several glycoprotein profiles may give better results for prediction of type 2 diabetes.

Strengths of our study are the robust manner in which IgG *N*-glycans were measured, the large size of our populations, and the fact that we included an independent replication cohort. Also, we have calculated our AUC using 10-fold cross validation to limit overfitting and get an accurate idea on how the models will perform in independent datasets. A limitation is the lack of prospective follow-up for the outcome type 2 diabetes. Therefore, no causal claims can be made and AUCs are to be interpreted in a case-control setting of patients already treated for their disease. The case-control setting in general may lead to overestimation, while the fact that patients are being treated for their disease may reduce the contrast between the groups. The current setup does allow comparing how IgG glycans add to the models and how important their relative contribution is on their own, but does not give an absolute reflection of their predictive potential. Second, simple predictive models (logistic regression) were used. Residual confounding by yet unknown factors involved in type 2 diabetes pathophysiology and the IgG glycome cannot be excluded. Third, we cannot exclude an effect of glucose-lowering treatment on the associations between IgG glycans and type 2 diabetes. In the discovery cohort, 19.2% was treated with diet alone, 64.9% took oral glucose-lowering agents, and 31.6 used insulin (alone or in combination with oral medication); we do not have this data for the replication cohort. Collaborations

to create larger sample sizes with glycomic and treatment information, preferably with a prospective setup, will enable us to research these effects in future. Fourth, the method used to measure IgG glycans does not allow to distinguish between Fc and Fab associated glycans. As only 15%-20% of the Fab part of IgG is glycosylated, the associations are more likely to be driven by differences in Fc glycans [50]. However, a contribution of changes in Fab N-glycosylation cannot be excluded.

To conclude, we found robust associations of IgG glycan peaks and traits with the presence of type 2 diabetes that reflect a pro-inflammatory and biologically aged state. Future studies should be directed at in-depth pathophysiological insights that can be derived from IgG glycan associations with type 2 diabetes. Also, prospective follow-up studies and genetic studies can shed light on the causality, its potential as a biomarker for complex inflammatory processes, and true predictive capacity of IgG and other glycans in type 2 diabetes.

References

[1] WHO (2016) Diabetes mellitus. Fact sheet N°138

[2] Morris AP, Voight BF, Teslovich TM, et al. (2012) Large-scale association analysis provides insights into the genetic architecture and pathophysiology of type 2 diabetes. Nat Genet 44: 981-990

[3] Gornik O, Pavic T, Lauc G (2012) Alternative glycosylation modulates function of IgG and other proteins - implications on evolution and disease. Biochim Biophys Acta 1820: 1318-1326

[4] Lauc G, Rudan I, Campbell H, Rudd PM (2010) Complex genetic regulation of protein glycosylation. Mol Biosyst 6: 329-335

[5] Wang X, Bao W, Liu J, et al. (2013) Inflammatory markers and risk of type 2 diabetes: a systematic review and meta-analysis. Diabetes Care 36: 166-175

[6] Nikolac Perkovic M, Pucic Bakovic M, Kristic J, et al. (2014) The association between galactosylation of immunoglobulin G and body mass index. Prog Neuropsychopharmacol Biol Psychiatry 48: 20-25

[7] Kristic J, Vuckovic F, Menni C, et al. (2014) Glycans are a novel biomarker of chronological and biological ages. J Gerontol A Biol Sci Med Sci 69: 779-789

[8] Knezevic A, Gornik O, Polasek O, et al. (2010) Effects of aging, body mass index, plasma lipid profiles, and smoking on human plasma N-glycans. Glycobiology 20: 959-969

[9] Wang Y, Klaric L, Yu X, et al. (2016) The Association Between Glycosylation of Immunoglobulin G and Hypertension: A Multiple Ethnic Cross-Sectional Study. Medicine (Baltimore) 95: e3379

[10] Anthony RM, Nimmerjahn F, Ashline DJ, Reinhold VN, Paulson JC, Ravetch JV (2008) Recapitulation of IVIG anti-inflammatory activity with a recombinant IgG Fc. Science 320: 373-376

[11] Kaneko Y, Nimmerjahn F, Ravetch JV (2006) Anti-inflammatory activity of immunoglobulin G resulting from Fc sialylation. Science 313: 670-673

[12] Voight BF, Scott LJ, Steinthorsdottir V, et al. (2010) Twelve type 2 diabetes susceptibility loci identified through large-scale association analysis. Nat Genet 42: 579-589

[13] Alberti KG, Zimmet PZ (1998) Definition, diagnosis and classification of diabetes mellitus and its complications. Part 1: diagnosis and classification of diabetes mellitus provisional report of a WHO consultation. Diabet Med 15: 539-553

[14] American Diabetes A (2011) Diagnosis and classification of diabetes mellitus. Diabetes Care 34 Suppl 1: S62-69

[15] McQuillan R, Leutenegger AL, Abdel-Rahman R, et al. (2008) Runs of homozygosity in European populations. Am J Hum Genet 83: 359-372

[16] Rudan I, Campbell H, Rudan P (1999) Genetic epidemiological studies of eastern Adriatic Island isolates, Croatia: objective and strategies. Coll Antropol 23: 531-546

[17] Polašek O, Marušić A, Rotim K, et al. (2009) Genome-wide Association Study of Anthropometric Traits in Korčula Island, Croatia. Croatian Medical Journal 50: 7-16

[18] Vitart V, Rudan I, Hayward C, et al. (2008) SLC2A9 is a newly identified urate transporter influencing serum urate concentration, urate excretion and gout 40: 437-442

[19] Pucic M, Knezevic A, Vidic J, et al. (2011) High throughput isolation and glycosylation analysis of IgG-variability and heritability of the IgG glycome in three isolated human populations. Mol Cell Proteomics 10: M111 010090

[20] Jaacks LM, Siegel KR, Gujral UP, Narayan KMV (2016) Type 2 diabetes: A 21st century epidemic. Best Practice & Research Clinical Endocrinology & Metabolism 30: 331-343

[21] Barrios C, Zierer J, Gudelj I, et al. (2016) Glycosylation Profile of IgG in Moderate Kidney Dysfunction. J Am Soc Nephrol 27: 933-941

[22] RDC T (2008) A language and environment for statistical computing. Available from http://www.R-project.org.
[23] Zaykin DV (2011) Optimally weighted Z-test is a powerful method for combining probabilities in meta-analysis. J Evol Biol 24: 1836-1841
[24] Ercan A, Kohrt WM, Cui J, et al. (2017) Estrogens regulate glycosylation of IgG in women and men. JCI Insight 2
[25] Karsten CM, Pandey MK, Figge J, et al. (2012) Anti-inflammatory activity of IgG1 mediated by Fc galactosylation and association of FcgammaRIIB and dectin-1. Nat Med 18: 1401-1406
[26] Masuda K, Kubota T, Kaneko E, et al. (2007) Enhanced binding affinity for FcgammaRIIIa of fucose-negative antibody is sufficient to induce maximal antibody-dependent cellular cytotoxicity. Mol Immunol 44: 3122-3131
[27] Mihai S, Nimmerjahn F (2013) The role of Fc receptors and complement in autoimmunity. Autoimmun Rev 12: 657-660
[28] Nimmerjahn F, Ravetch JV (2008) Fcgamma receptors as regulators of immune responses. Nat Rev Immunol 8: 34-47
[29] Parekh RB, Roitt IM, Isenberg DA, Dwek RA, Ansell BM, Rademacher TW (1988) Galactosylation of IgG associated oligosaccharides: reduction in patients with adult and juvenile onset rheumatoid arthritis and relation to disease activity. Lancet 1: 966-969
[30] Parekh RB, Dwek RA, Sutton BJ, et al. (1985) Association of rheumatoid arthritis and primary osteoarthritis with changes in the glycosylation pattern of total serum IgG. Nature 316: 452-457
[31] Vuckovic F, Kristic J, Gudelj I, et al. (2015) Association of systemic lupus erythematosus with decreased immunosuppressive potential of the IgG glycome. Arthritis Rheumatol 67: 2978-2989
[32] Trbojevic Akmacic I, Ventham NT, Theodoratou E, et al. (2015) Inflammatory bowel disease associates with proinflammatory potential of the immunoglobulin G glycome. Inflamm Bowel Dis 21: 1237-1247
[33] Vučković F, Theodoratou E, Thaçi K, et al. (2016) IgG Glycome in Colorectal Cancer. Clinical Cancer Research 22: 3078-3086
[34] Russell AC, Šimurina M, Garcia MT, et al. (2017) The N-glycosylation of immunoglobulin G as a novel biomarker of Parkinson's disease. Glycobiology 27: 501-510
[35] Dall'Olio F, Vanhooren V, Chen CC, Slagboom PE, Wuhrer M, Franceschi C (2013) N-glycomic biomarkers of biological aging and longevity: A link with inflammaging. Ageing Research Reviews 12: 685-698
[36] Ferrara C, Stuart F, Sondermann P, Brunker P, Umana P (2006) The carbohydrate at FcgammaRIIIa Asn-162. An element required for high affinity binding to non-fucosylated IgG glycoforms. J Biol Chem 281: 5032-5036
[37] Davies J, Jiang L, Pan LZ, LaBarre MJ, Anderson D, Reff M (2001) Expression of GnTIII in a recombinant anti-CD20 CHO production cell line: Expression of antibodies with altered glycoforms leads to an increase in ADCC through higher affinity for FC gamma RIII. Biotechnol Bioeng 74: 288-294
[38] Lauc G, Huffman JE, Pucic M, et al. (2013) Loci associated with N-glycosylation of human immunoglobulin G show pleiotropy with autoimmune diseases and haematological cancers. PLoS Genet 9: e1003225
[39] Testa R, Vanhooren V, Bonfigli AR, et al. (2015) N-glycomic changes in serum proteins in type 2 diabetes mellitus correlate with complications and with metabolic syndrome parameters. PLoS One 10: e0119983
[40] Itoh N, Sakaue S, Nakagawa H, et al. (2007) Analysis of N-glycan in serum glycoproteins from db/db mice and humans with type 2 diabetes. Am J Physiol Endocrinol Metab 293: E1069-1077

[41] Ercan A, Cui J, Chatterton DE, et al. (2010) Aberrant IgG galactosylation precedes disease onset, correlates with disease activity, and is prevalent in autoantibodies in rheumatoid arthritis. Arthritis Rheum 62: 2239-2248

[42] Menni C, Keser T, Mangino M, et al. (2013) Glycosylation of immunoglobulin g: role of genetic and epigenetic influences. PLoS One 8: e82558

[43] Lauc G, Essafi A, Huffman JE, et al. (2010) Genomics meets glycomics-the first GWAS study of human N-Glycome identifies HNF1alpha as a master regulator of plasma protein fucosylation. PLoS Genet 6: e1001256

[44] Kooner JS, Saleheen D, Sim X, et al. (2011) Genome-wide association study in individuals of South Asian ancestry identifies six new type 2 diabetes susceptibility loci. Nat Genet 43: 984-989

[45] Hotamisligil GS (2010) Endoplasmic Reticulum Stress and the Inflammatory Basis of Metabolic Disease. Cell 140: 900-917

[46] Donath MY, Shoelson SE (2011) Type 2 diabetes as an inflammatory disease 11: 98-107

[47] Goldberg RB (2009) Cytokine and Cytokine-Like Inflammation Markers, Endothelial Dysfunction, and Imbalanced Coagulation in Development of Diabetes and Its Complications. The Journal of Clinical Endocrinology & Metabolism 94: 3171-3182

[48] Hertle E, Stehouwer CDA, van Greevenbroek MMJ (2014) The complement system in human cardiometabolic disease. Molecular Immunology 61: 135-148

[49] Ghosh P, Sahoo R, Vaidya A, Chorev M, Halperin JA (2015) Role of Complement and Complement Regulatory Proteins in the Complications of Diabetes. Endocrine Reviews 36: 272-288

[50] Holland M, Yagi H, Takahashi N, et al. (2006) Differential glycosylation of polyclonal IgG, IgG-Fc and IgG-Fab isolated from the sera of patients with ANCA-associated systemic vasculitis. Biochim Biophys Acta 1760: 669-677

Supplementary table S1. Description of direct glycan peaks and derived traits measured in this study.

GROUP	Zagreb_Code		DESCRIPTION	FORMULA
Total IgG glycans (neutral + charged)	GP1	FA1	The percentage of FA1 glycan in total IgG glycans	GP1 / GP * 100
	GP2	A2	The percentage of A2 glycan in total IgG glycans	GP2 / GP * 100
	GP3	A2B	The percentage of A2B glycan in total IgG glycans	GP3 / GP * 100
	GP4	FA2	The percentage of FA2 glycan in total IgG glycans	GP4 / GP * 100
	GP5	M5	The percentage of M5 glycan in total IgG glycans	GP5 / GP * 100
	GP6	FA2B	The percentage of FA2B glycan in total IgG glycans	GP6 / GP * 100
	GP7	A2[3]G1	The percentage of A2G1 glycan in total IgG glycans	GP7 / GP * 100
	GP8	A2BG1 FA2[6]G1	The percentage of FA2[6]G1 glycan in total IgG glycans	GP8 / GP * 100
	GP9	FA2[3]G1	The percentage of FA2[3]G1 glycan in total IgG glycans	GP9 / GP * 100
	GP10	FA2[6]BG1	The percentage of FA2[6]BG1 glycan in total IgG glycans	GP10 / GP * 100
	GP11	FA2[3]BG1	The percentage of FA2[3]BG1 glycan in total IgG glycans	GP11 / GP * 100
	GP12	A2G2	The percentage of A2G2 glycan in total IgG glycans	GP12 / GP * 100
	GP13	A2BG2	The percentage of A2BG2 glycan in total IgG glycans	GP13 / GP * 100
	GP14	FA2G2	The percentage of FA2G2 glycan in total IgG glycans	GP14 / GP * 100
	GP15	FA2BG2	The percentage of FA2BG2 glycan in total IgG glycans	GP15 / GP * 100
	GP16	FA2[6]G1S1 FA2[3]G1S1	The percentage of FA2G1S1 glycan in total IgG glycans	GP16 / GP * 100
	GP17	A2G2S1	The percentage of A2G2S1 glycan in total IgG glycans	GP17/ GP * 100
	GP18	A2BG2S1 FA2G2S1	The percentage of FA2G2S1 glycan in total IgG glycans	GP18 / GP * 100
	GP19	FA2BG2S1	The percentage of FA2BG2S1 glycan in total IgG glycans	GP19 / GP * 100
	GP20*	FA2FG2S1	The percentage of FA2FG2S1 in total IgG glycans*	GP20 / GP * 100
	GP21	A2G2S2	The percentage of A2G2S2 glycan in total IgG glycans	GP21 / GP * 100
	GP22	A2BG2S2	The percentage of A2BG2S2 glycan in total IgG glycans	GP22 / GP * 100
	GP23	FA2G2S2	The percentage of FA2G2S2 glycan in total IgG glycans	GP23 / GP * 100
	GP24	FA2BG2S2	The percentage of FA2BG2S2 glycan in total IgG glycans	GP24 / GP * 100

Supplementary table S1. Description of direct glycan peaks and derived traits measured in this study. *(continued)*

GROUP	Zagreb_Code	DESCRIPTION	FORMULA
Total IgG glycans - derived parameters	FGS/(FG+FGS)	The percentage of sialylation of fucosylated galactosylated structures without bisecting GlcNAc in total IgG glycans	SUM(GP16 + GP18 + GP23) / SUM(GP16 + GP18 + GP23 + GP8 + GP9 + GP14) * 100
	FBGS/(FBG+FBGS)	The percentage of sialylation of fucosylated galactosylated structures with bisecting GlcNAc in total IgG glycans	SUM(GP19 + GP24) / SUM(GP19 + GP24 + GP10 + GP11 + GP15) * 100
	FGS/(F+FG+FGS)	The percentage of sialylation of all fucosylated structures without bisecting GlcNAc in total IgG glycans	SUM(GP16 + GP18 + GP23) / SUM(GP16 + GP18 + GP23 + GP4 + GP8 + GP9 + GP14) * 100
	FBGS/(FB+FBG+FBGS)	The percentage of sialylation of all fucosylated structures with bisecting GlcNAc in total IgG glycans	SUM(GP19 + GP24) / SUM(GP19 + GP24 + GP6 + GP10 + GP11 + GP15) * 100
	FG1S1/(FG1+FG1S1)	The percentage of monosialylation of fucosylated monogalactosylated structures without bisecting GlcNAc in total IgG glycans	GP16 / SUM(GP16 + GP8 + GP9) * 100
	FG2S1/(FG2+FG2S1+FG2S2)	The percentage of monosialylation of fucosylated digalactosylated structures without bisecting GlcNAc in total IgG glycans	GP18 / SUM(GP18 + GP14 + GP23) * 100
	FG2S2/(FG2+FG2S1+FG2S2)	The percentage of disialylation of fucosylated digalactosylated structures without bisecting GlcNAc in total IgG glycans	GP23 / SUM(GP23 + GP14 + GP18) * 100
	FBG2S1/ (FBG2+FBG2S1+FBG2S2)	The percentage of monosialylation of fucosylated digalactosylated structures with bisecting GlcNAc in total IgG glycans	GP19 / SUM(GP19 + GP15 + GP24) * 100
	FBG2S2/ (FBG2+FBG2S1+FBG2S2)	The percentage of disialylation of fucosylated digalactosylated structures with bisecting GlcNAc in total IgG glycans	GP24 / SUM(GP24 + GP15 + GP19) * 100
	$F^{total}S1/F^{total}S2$	Ratio of all fucosylated monosialylated and disialylated structures (+/- bisecting GlcNAc) in total IgG glycans	SUM(GP16 + GP18 + GP19) / SUM(GP23 + GP24)
	FS1/FS2	Ratio of fucosylated monosialylated and disialylated structures (without bisecting GlcNAc) in total IgG glycans	SUM(GP16 + GP18) / GP23
	FBS1/FBS2	Ratio of fucosylated monosialylated and disialylated structures (with bisecting GlcNAc) in total IgG glycans	GP19 / GP24
	FBS^{total}/FS^{total}	Ratio of all fucosylated sialylated structures with and without bisecting GlcNAc in total IgG glycans	SUM(GP19 + GP24) / SUM(GP16 + GP18 + GP23)
	FBS1/FS1	Ratio of fucosylated monosialylated structures with and without bisecting GlcNAc in total IgG glycans	GP19 / SUM(GP16 + GP18)
	FBS1/(FS1+FBS1)	The incidence of bisecting GlcNAc in all fucosylated monosialylated structures in total IgG glycans in total IgG glycans	GP19 / SUM(GP16 + GP18 + GP19)
	FBS2/FS2	Ratio of fucosylated disialylated structures with and without bisecting GlcNAc in total IgG glycans	GP24 / GP23
	FBS2/(FS2+FBS2)	The incidence of bisecting GlcNAc in all fucosylated disialylated structures in total IgG glycans	GP24 / SUM(GP23 + GP24)
			GP = SUM(GP1:GP24)

Supplementary table S1. Description of direct glycan peaks and derived traits measured in this study. *(continued)*

GROUP	Zagreb_Code	DESCRIPTION	FORMULA
Neutral IgG glycans	$GP1^n$	The percentage of FA1 glycan in total neutral IgG glycans (GP^n)	GP1 / GP^n* 100
	$GP2^n$	The percentage of A2 glycan in total neutral IgG glycans (GP^n)	GP2 / GP^n* 100
	$GP4^n$	The percentage of FA2 glycan in total neutral IgG glycans (GP^n)	GP4 / GP^n* 100
	$GP5^n$	The percentage of M5 glycan in total neutral IgG glycans (GP^n)	GP5 / GP^n* 100
	$GP6^n$	The percentage of FA2B glycan in total neutral IgG glycans (GP^n)	GP6 / GP^n* 100
	$GP7^n$	The percentage of A2G1 glycan in total neutral IgG glycans (GP^n)	GP7 / GP^n* 100
	$GP8^n$	The percentage of FA2[6]G1 glycan in total neutral IgG glycans (GP^n)	GP8 / GP^n* 100
	$GP9^n$	The percentage of FA2[3]G1 glycan in total neutral IgG glycans (GP^n)	GP9 / GP^n* 100
	$GP10^n$	The percentage of FA2[6]BG1 glycan in total neutral IgG glycans (GP^n)	GP10 / GP^n* 100
	$GP11^n$	The percentage of FA2[3]BG1 glycan in total neutral IgG glycans (GP^n)	GP11 / GP^n* 100
	$GP12^n$	The percentage of A2G2 glycan in total neutral IgG glycans (GP^n)	GP12 / GP^n* 100
	$GP13^n$	The percentage of A2BG2 glycan in total neutral IgG glycans (GP^n)	GP13 / GP^n* 100
	$GP14^n$	The percentage of FA2G2 glycan in total neutral IgG glycans (GP^n)	GP14 / GP^n* 100
	$GP15^n$	The percentage of FA2BG2 glycan in total neutral IgG glycans (GP^n)	GP15 / GP^n* 100

Supplementary table S1. Description of direct glycan peaks and derived traits measured in this study. *(continued)*

GROUP	Zagreb_Code	DESCRIPTION	FORMULA
Neutral IgG glycans - derived parameters	$G0^{n,}$	The percentage of agalactosylated structures in total neutral IgG glycans	SUM($GP1^n$: $GP4^n$ + $GP6^n$)
	$G1^n$	The percentage of monogalactosylated structures in total neutral IgG glycans	SUM($GP7^n$: $GP11^n$)
	$G2^n$	The percentage of digalactosylated structures in total neutral IgG glycans	SUM($GP12^n$: $GP15^n$),
	$F^{n\ total}$	The percentage of all fucosylated structures (+/- bisecting GlcNAc) in total neutral IgG glycans	SUM($GP1^n$+ $GP4^n$+ $GP6^n$+ $GP8^n$+ $GP9^n$+ $GP10^n$+ $GP11^n$+ $GP14^n$+ $GP15^n$)
	$FG0^{n\ total}/G0^n$	The percentage of fucosylation of agalactosylated structures in total neutral IgG glycans	SUM($GP1^n$+ $GP4^n$+ $GP6^n$) / $G0^n$ * 100
	$FG1^{n\ total}/G1^n$	The percentage of fucosylation of monogalactosylated structures in total neutral IgG glycans	SUM($GP8^n$+ $GP9^n$+ $GP10^n$+ $GP11^n$) / $G1^n$ * 100
	$FG2^{n\ total}/G2^n$	The percentage of fucosylation of digalactosylated structures in total neutral IgG glycans	SUM($GP14^n$+ GP15) / $G2^n$ * 100
	F^n	The percentage of fucosylated structures (without bisecting GlcNAc) in total neutral IgG glycans	SUM($GP1^n$+ $GP4^n$+ $GP8^n$+ $GP9^n$+ $GP14^n$)
	$FG0^n/G0^n$	The percentage of fucosylation of agalactosylated structures (without bisecting GlcNAc) in total neutral IgG glycans	SUM($GP1^n$+ $GP4^n$) / $G0^n$ * 100
	$FG1^n/G1^n$	The percentage of fucosylation of monogalactosylated structures (without bisecting GlcNAc) in total neutral IgG glycans	SUM($GP8^n$+ $GP9^n$) / $G1^n$ * 100
	$FG2^n/G2^n$	The percentage of fucosylation of digalactosylated structures (without bisecting GlcNAc) in total neutral IgG glycans	$GP14^n$/ $G2^n$ * 100
	FB^n	The percentage of fucosylated structures (with bisecting GlcNAc) in total neutral IgG glycans	SUM($GP6^n$ + $GP10^n$ + $GP11^n$ + $GP15^n$)
	$FBG0^n/G0^n$	The percentage of fucosylation of agalactosylated structures (with bisecting GlcNAc) in total neutral IgG glycans	$GP6^n$/ $G0^n$ * 100
	$FBG1^n/G1^n$	The percentage of fucosylation of monogalactosylated structures (with bisecting GlcNAc) in total neutral IgG glycans	SUM($GP10^n$ + $GP11^n$) / $G1^n$ * 100
	$FBG2^n/G2^n$	The percentage of fucosylation of digalactosylated structures (with bisecting GlcNAc) in total neutral IgG glycans	$GP15^n$ / $G2^n$ * 100
	FB^n/F^n	Ratio of fucosylated structures with and without bisecting GlcNAc in total neutral IgG glycans	FB^n/ F^n * 100
	$FB^n/F^{n\ total}$	The incidence of bisecting GlcNAc in all fucosylated structures in total neutral IgG glycans	FB^n/ $F^{n\ total}$ * 100
			GP^n = SUM($GP1^n$:$GP15^n$)
*GP20	FA2FG2S1	The presence of this glycan structure in GP20 remains to be confirmed (Russel et al., Glycobiology, 2017, vol. 27, no. 5, 501–510)	

Structure abbreviations are as follows: F, α-1,6-linked core fucose; A, number of antenna's; B, bisecting GlcNac β1-4 linked to β1-3 mannose; M, number of mannose residues; Gx, number of β1-4 linked galactoses; [3]G1, galactose on the antenna of the α1-3 linked mannose; [6]G1, galactose on the antenna of the α1-6 linked mannose; Sx, number of sialic acids linked to galactose.

Supplementary table S2. Median and interquartile ranges of glycan peaks for cases and controls in the discovery and replication cohort.

	Discovery cohort				Replication cohort			
	Case		Control		Case		Control	
	Median	IQR	Median	IQR	Median	IQR	Median	IQR
GP1	0.092	0.074-0.117	0.094	0.075-0.118	0.155	0.109-0.242	0.119	0.080-0.119
GP2	0.750	0.506-1.064	0.759	0.514-1.073	0.821	0.530-1.202	0.548	0.352-0.851
GP3	0.119	0.098-0.145	0.112	0.096-0.138	0.319*	0.253-0.402*	0.258*	0.206-0.321*
GP4	26.430	22.380-30.534	24.709	21.501-28.223	22.672	18.760-26.673	19.116	15.288-23.656
GP5	0.129	0.105-0.154	0.132	0.108-0.154	0.285	0.226-0.348	0.252	0.209-0.313
GP6	7.159	5.979-8.486	6.244	5.307-7.338	6.252	5.320-7.342	4.781	3.701-6.016
GP7	0.337	0.239-0.479	0.376	0.269-0.516	0.604	0.446-0.918	0.561	0.397-0.801
GP8	18.162	16.911-19.300	19.260	17.948-20.412	16.185	14.741-17.452	17.978	16.304-19.897
GP9	9.328	8.392-10.235	9.854	8.940-10.862	7.967	7.103-8.751	8.594	7.699-9.510
GP10	5.634	4.840-6.470	5.358	4.594-6.170	4.979	4.352-5.927	4.796	4.229-5.474
GP11	0.713	0.617-0.805	0.678	0.588-0.766	0.819	0.720-0.877	0.709	0.619-0.810
GP12	0.501	0.341-0.731	0.535	0.372-0.742	0.849	0.598-1.192	0.799	0.552-1.115
GP13	0.185	0.157-0.215	0.190	0.165-0.218	0.276	0.215-0.341	0.311	0.239-0.383
GP14	11.004	9.133-13.092	11.841	10.016-13.515	10.294	8.551-12.104	12.880	10.108-15.950
GP15	1.622	1.401-1.884	1.618	1.433-1.835	1.454	1.288-1.685	1.524	1.298-1.785
GP16	2.805	2.502-3.117	2.840	2.532-3.141	3.179	2.900-3.471	3.259	2.953-3.604
GP17	0.758	0.671-0.868	0.751	0.678-0.855	2.270	1.209-3.317	1.235	0.863-2.615
GP18	7.319	6.171-8.696	1.572	6.546-8.840	8.144	7.027-9.284	9.777	8.021-12.030
GP19	1.759	1.548-2.013	1.834	1.602-2.107	2.310	2.022-2.719	2.233	1.959-2.591
GP20	0.203	0.170-0.243	0.211	0.177-0.247	0.464	0.339-0.667	0.408	0.315-0.579
GP21	0.475	0.422-0.539	0.495	0.448-0.562	2.979	1.025-4.471	0.978	0.695-3.432
GP22	0.087	0.070-0.111	0.088	0.071-0.109	0.301	0.177-0.381	0.186	0.118-0.339
GP23	1.299	1.051-1.574	1.373	1.148-1.651	1.808	1.420-2.285	1.975	1.577-2.389
GP24	1.667	1.444-1.932	1.701	1.460-1.956	2.525	2.175-3.057	2.341	1.924-2.804

GP, glycan peak; IQR, interquartile range. * In the replication cohort, GP3 was only measured in the ORCADES study but not in the CROATIA-Vis or -Korcula studies. These values thus only represent GP3 in the ORCADES study.

Supplementary table S3. Associations of IgG glycans and derived traits adjusted for age and sex.

Direct glycan peaks		Discovery population			Replication population			Meta-analysis
Glycan peak	Glycan structure	p-value	β	S.E.	p-value	β	S.E.	p-value
GP1	FA1	7.00E-01	-0.42	1.10	6.28E-01	0.28	0.58	9.17E-01
GP2	A2	2.27E-01	0.10	0.09	3.02E-01	0.11	0.11	1.15E-01
GP3	**A2B**	**5.90E-05**	4.81	1.20	4.22E-02	3.24	1.60	**1.05E-05**
GP4	**FA2**	**2.05E-14**	0.06	0.01	7.39E-01	0.01	0.02	**8.97E-08**
GP5	M5	3.39E-01	-1.01	1.05	5.31E-01	-0.53	0.84	2.69E-01
GP6	**FA2B**	**1.21E-39**	0.39	0.03	**3.13E-06**	0.27	0.06	**<2.22E-16**
GP7	A2[3]G1	2.05E-03	-0.62	0.20	5.71E-01	-0.14	0.24	1.32E-02
GP8	**A2BG1** **FA2[6]G1**	**1.88E-41**	-0.35	0.03	**1.09E-05**	-0.20	0.05	**<2.22E-16**
GP9	**FA2[3]G1**	**1.01E-23**	-0.32	0.03	1.43E-03	-0.23	0.07	**<2.22E-16**
GP10	**FA2[6]BG1**	**2.86E-08**	0.20	0.04	**8.02E-05**	0.33	0.08	**3.15E-11**
GP11	**FA2[3]BG1**	**2.76E-10**	1.93	0.31	8.63E-03	1.23	0.47	**7.05E-10**
GP12	A2G2	1.05E-01	-0.18	0.11	6.51E-01	0.09	0.20	4.57E-01
GP13	A2BG2	9.44E-03	-2.38	0.92	1.43E-01	1.43	0.98	5.23E-01
GP14	**FA2G2**	**3.32E-12**	-0.11	0.02	8.76E-01	-0.01	0.03	**1.95E-06**
GP15	FA2BG2	8.78E-01	-0.02	0.13	1.63E-02	0.64	0.27	9.13E-02
GP16	FA2[6]G1S1 FA2[3]G1S1	8.89E-03	-0.25	0.09	8.08E-02	-0.32	0.18	2.32E-03
GP17	A2G2S1	5.16E-01	0.15	0.23	6.59E-01	0.03	0.06	4.46E-01
GP18	A2BG2S1 FA2G2S1	**1.40E-05**	-0.10	0.02	9.90E-01	0.00	0.04	3.86E-03
GP19	**FA2BG2S1**	**2.00E-06**	-0.51	0.11	1.80E-01	-0.23	0.17	**3.31E-05**
GP20	FA2FG2S1	**3.22E-04**	-2.50	0.70	4.50E-01	-0.22	0.30	3.07E-03
GP21	A2G2S2	**1.40E-05**	-1.48	0.34	5.42E-01	0.02	0.04	1.46E-02
GP22	A2BG2S2	6.76E-01	0.41	0.97	8.63E-01	0.13	0.73	6.83E-01
GP23	**FA2G2S2**	**3.08E-09**	-0.63	0.11	2.06E-02	-0.37	0.16	**1.37E-08**
GP24	FA2BG2S2	1.32E-01	-0.15	0.10	4.75E-01	-0.10	0.13	1.24E-01

	Discovery population			Replication population			Meta-analysis
Derived traits	**p-value**	**β**	**S.E.**	**p-value**	**β**	**S.E.**	**p-value**
FGS/(FG+FGS)	1.99E-03	0.051	0.016	5.21E-01	0.017	0.027	1.11E-02
FBGS/(FBG+FBGS)	**3.74E-08**	-0.040	0.007	1.00E-03	-0.045	0.014	**9.35E-10**
FGS/(F+FG+FGS)	8.92E-04	-0.050	0.015	9.10E-01	-0.003	0.025	2.15E-02
FBGS/(FB+FBG+FBGS)	**1.54E-19**	-0.086	0.009	**2.75E-04**	-0.058	0.016	**<2.22E-16**
FG1S1/(FG1+FG1S1)	**1.26E-10**	0.206	0.032	3.42E-01	0.044	0.047	**5.87E-07**
FG2S1/(FG2+FG2S1+FG2S2)	**8.30E-09**	0.099	0.017	4.37E-01	0.026	0.034	**9.87E-06**
FG2S2/(FG2+FG2S1+FG2S2)	8.16E-01	-0.005	0.024	4.75E-02	-0.068	0.034	1.03E-01
FBG2S1/(FBG2+FBG2S1+FBG2S2)	**3.00E-06**	-0.060	0.013	2.31E-02	-0.054	0.024	**1.52E-06**
FBG2S2/(FBG2+FBG2S1+FBG2S2)	1.38E-01	0.017	0.011	3.40E-01	-0.018	0.019	7.81E-01
FtotalS1/FtotalS2	8.97E-01	-0.007	0.058	5.53E-02	0.168	0.088	1.80E-01
FS1/FS2	**2.77E-04**	0.086	0.024	9.98E-04	0.141	0.043	**1.08E-06**
FBS1/FBS2	**6.80E-05**	-1.149	0.288	5.93E-01	-0.293	0.547	2.26E-03
FBStotal/FStotal	3.21E-02	1.227	0.572	9.41E-01	0.065	0.882	1.38E-01
FBS1/FS1	6.43E-01	0.390	0.843	6.80E-01	-0.574	1.393	9.99E-01
FBS1/(FS1+FBS1)	6.21E-01	0.606	1.227	7.09E-01	-0.833	2.235	9.59E-01
FBS2/FS2	**5.11E-10**	0.861	0.138	3.08E-03	0.623	0.210	**2.16E-10**
FBS2/(FS2+FBS2)	**2.24E-10**	4.713	0.743	5.29E-03	4.172	1.496	**2.83E-10**
G0n	**1.56E-24**	0.068	0.007	1.36E-01	0.018	0.012	**2.22E-15**
G1n	**3.55E-39**	-0.195	0.015	**5.83E-04**	-0.085	0.025	**<2.22E-16**
G2n	**9.67E-10**	-0.063	0.010	7.90E-01	0.005	0.019	**1.06E-04**
Fn total	3.49E-01	0.033	0.035	9.52E-01	-0.003	0.050	5.62E-01
FG0n total/G0n	2.43E-02	0.067	0.030	4.30E-01	-0.033	0.042	3.61E-01
FG1n total/G1n	2.06E-01	0.088	0.069	5.21E-01	0.045	0.071	1.86E-01
FG2n total/G2n	1.70E-01	-0.025	0.018	8.16E-01	-0.006	0.027	2.77E-01
Fn	**4.55E-20**	-0.116	0.013	**8.07E-06**	-0.106	0.024	**<2.22E-16**
FG0n/G0n	**3.18E-09**	-0.059	0.010	**1.86E-05**	-0.079	0.018	**9.38E-13**
FG1n/G1n	**1.93E-24**	-0.126	0.012	**2.03E-07**	-0.129	0.025	**<2.22E-16**
FG2n/G2n	**1.19E-12**	-0.105	0.015	2.09E-01	-0.025	0.020	**1.39E-08**
FBn	**1.72E-26**	0.157	0.015	**8.74E-09**	0.182	0.032	**<2.22E-16**
FBG0n/G0n	**1.10E-14**	0.092	0.012	**3.99E-07**	0.126	0.025	**<2.22E-16**
FBG1n/G1n	**1.34E-26**	0.137	0.013	**1.78E-09**	0.164	0.027	**<2.22E-16**
FBG2n/G2n	**8.01E-21**	0.218	0.023	5.93E-02	0.062	0.033	**2.09E-14**
FBn/Fn	**2.73E-25**	0.097	0.009	**2.14E-06**	0.119	0.025	**<2.22E-16**
FBn/Fn total	**1.63E-25**	0.147	0.014	**2.45E-08**	0.164	0.029	**<2.22E-16**

Glycan peaks and derived traits that were significantly associated with type 2 diabetes in the meta-analysis are in bold font. Structure abbreviations are as follows: F, α-1,6-linked core fucose; A, number of antenna's; B, bisecting GlcNac β1-4 linked to β1-3 mannose; M, number of mannose residues; Gx, number of β1-4 linked galactoses; [3]G1, galactose on the antenna of the α1-3 linked mannose; [6]G1, galactose on the antenna of the α1-6 linked mannose; Sx, number of sialic acids linked to galactose. Red: positive association between glycan and clinical trait; blue: negative association.

Supplementary Table S4. Associations of IgG glycans and derived traits adjusted for age, sex and BMI.

Direct glycan peaks		Discovery population			Replication population			Meta-analysis
Glycan peak	**Glycan structure**	**p-value**	**β**	**S.E.**	**p-value**	**β**	**S.E.**	**p-value**
GP1	FA1	1.25E-01	-1.924	1.255	6.70E-01	0.237	0.557	4.93E-01
GP2	A2	4.73E-01	0.070	0.098	4.42E-01	0.082	0.106	2.93E-01
GP3	A2B	3.13E-01	1.352	1.339	9.31E-02	2.808	1.672	6.50E-02
GP4	FA2	**3.16E-04**	0.034	0.009	8.86E-01	-0.002	0.017	2.41E-02
GP5	M5	2.77E-01	-1.309	1.204	5.35E-01	-0.524	0.846	2.38E-01
GP6	**FA2B**	**6.09E-22**	0.312	0.032	**1.96E-05**	0.248	0.058	**<2.22E-16**
GP7	A2[3]G1	**2.26E-01**	-0.277	0.228	6.56E-01	-0.102	0.229	2.58E-01
GP8	**A2BG1FA2[6]G1**	**3.37E-22**	-0.281	0.029	**1.59E-05**	-0.202	0.047	**<2.22E-16**
GP9	**FA2[3]G1**	**1.32E-15**	-0.289	0.036	1.02E-03	-0.244	0.074	**1.13E-14**
GP10	**FA2[6]BG1**	**1.00E-06**	0.198	0.041	**1.72E-04**	0.314	0.084	**1.70E-09**
GP11	**FA2[3]BG1**	**2.10E-05**	1.432	0.337	1.69E-02	1.142	0.478	**4.41E-06**
GP12	A2G2	7.24E-01	0.045	0.126	3.65E-01	0.184	0.203	3.60E-01
GP13	A2BG2	4.03E-01	-0.889	1.063	8.51E-02	1.699	0.987	4.53E-01
GP14	FA2G2	**5.10E-04**	-0.065	0.019	7.08E-01	0.012	0.033	4.57E-02
GP15	**FA2BG2**	3.81E-02	0.306	0.148	3.68E-03	0.778	0.268	**3.82E-04**
GP16	FA2[6]G1S1 FA2[3]G1S1	6.47E-02	-0.200	0.108	7.65E-02	-0.325	0.183	1.08E-02
GP17	A2G2S1	6.71E-02	0.473	0.258	4.51E-01	0.046	0.061	7.67E-02
GP18	A2BG2S1 FA2G2S1	1.60E-01	-0.038	0.027	5.53E-01	0.025	0.042	6.36E-01
GP19	FA2BG2S1	1.98E-01	-0.157	0.122	3.17E-01	-0.173	0.173	1.10E-01
GP20	FA2FG2S1	5.00E-03	-2.223	0.792	5.27E-01	-0.191	0.301	2.04E-02
GP21	A2G2S2	7.69E-03	-1.052	0.395	6.73E-01	0.018	0.041	1.53E-01
GP22	A2BG2S2	6.63E-02	2.003	1.091	7.98E-01	0.189	0.738	1.62E-01
GP23	**FA2G2S2**	1.23E-03	-0.389	0.121	3.51E-02	-0.341	0.162	**2.06E-04**
GP24	FA2BG2S2	1.83E-01	0.153	0.115	6.05E-01	-0.067	0.130	6.28E-01

Glycan peaks and derived traits that were significantly associated with type 2 diabetes in the meta-analysis are in bold font. Structure abbreviations are as follows: F, α-1,6-linked core fucose; A, number of antenna's; B, bisecting GlcNac β1-4 linked to β1-3 mannose; M, number of mannose residues; Gx, number of β1-4 linked galactoses; [3]G1, galactose on the antenna of the α1-3 linked mannose; [6]G1, galactose on the antenna of the α1-6 linked mannose; Sx, number of sialic acids linked to galactose. Red: positive association between glycan and clinical trait; blue: negative association.

	Discovery population			Replication population			Meta-analysis
Derived traits	**p-value**	**β**	**S.E.**	**p-value**	**β**	**S.E.**	**p-value**
FGS/(FG+FGS)	5.78E-04	0.064	0.019	3.68E-01	0.024	0.027	3.30E-03
FBGS/(FBG+FBGS)	5.80E-03	-0.023	0.008	2.33E-03	-0.042	0.014	**3.98E-05**
FGS/(F+FG+FGS)	6.14E-01	-0.009	0.017	7.09E-01	0.009	0.025	9.60E-01
FBGS/(FB+FBG+FBGS)	**4.81E-07**	-0.054	0.011	1.13E-03	-0.052	0.016	**8.37E-09**
FG1S1/(FG1+FG1S1)	**2.00E-06**	0.172	0.036	3.65E-01	0.043	0.047	**1.60E-04**
FG2S1/(FG2+FG2S1+FG2S2)	**1.30E-05**	0.086	0.020	3.65E-01	0.031	0.034	**3.96E-04**
FG2S2/(FG2+FG2S1+FG2S2)	6.29E-01	-0.013	0.027	2.80E-02	-0.075	0.034	4.83E-02
FBG2S1/(FBG2+FBG2S1+FBG2S2)	**1.45E-04**	-0.055	0.015	2.38E-02	-0.054	0.024	**2.69E-05**
FBG2S2/(FBG2+FBG2S1+FBG2S2)	5.61E-02	0.025	0.013	2.51E-01	-0.022	0.019	6.98E-01
FtotalS1/FtotalS2	5.31E-01	-0.041	0.065	4.53E-02	0.175	0.087	2.72E-01
FS1/FS2	4.04E-03	0.076	0.027	**7.79E-04**	0.145	0.043	**9.77E-06**
FBS1/FBS2	**2.18E-04**	-1.212	0.328	6.55E-01	-0.245	0.548	5.71E-03
FBStotal/FStotal	1.40E-02	1.586	0.646	9.64E-01	0.040	0.902	9.97E-02
FBS1/FS1	3.41E-01	0.908	0.954	6.80E-01	-0.583	1.413	7.54E-01
FBS1/(FS1+FBS1)	3.34E-01	1.341	1.387	7.06E-01	-0.852	2.258	7.26E-01
FBS2/FS2	**1.63E-08**	0.877	0.155	2.46E-03	0.650	0.215	**2.08E-09**
FBS2/(FS2+FBS2)	**6.68E-09**	4.886	0.843	5.68E-03	4.188	1.514	**3.80E-09**
G0n	**1.91E-09**	0.046	0.008	3.35E-01	0.012	0.012	**3.04E-06**
G1n	**1.79E-19**	-0.149	0.017	1.49E-03	-0.079	0.025	**<2.22E-16**
G2n	1.21E-02	-0.030	0.012	3.69E-01	0.017	0.019	3.32E-01
Fn total	8.89E-01	-0.006	0.040	8.23E-01	-0.011	0.047	7.94E-01
FG0n total/G0n	2.23E-01	0.042	0.034	4.58E-01	-0.030	0.041	8.10E-01
FG1n total/G1n	9.72E-01	-0.003	0.079	5.91E-01	0.037	0.069	7.02E-01
FG2n total/G2n	7.37E-02	-0.037	0.021	8.22E-01	-0.006	0.027	1.79E-01
Fn	**2.64E-14**	-0.109	0.014	**1.42E-05**	-0.105	0.024	**2.22E-16**
FG0n/G0n	**7.29E-09**	-0.066	0.011	**2.13E-05**	-0.080	0.019	**2.50E-12**
FG1n/G1n	**6.77E-16**	-0.112	0.014	**4.66E-07**	-0.127	0.025	**<2.22E-16**
FG2n/G2n	**8.60E-09**	-0.095	0.017	2.00E-01	-0.026	0.020	**2.08E-06**
FBn	**1.35E-17**	0.141	0.016	**2.37E-08**	0.179	0.032	**<2.22E-16**
FBG0n/G0n	**6.98E-13**	0.096	0.013	**2.60E-07**	0.130	0.025	**<2.22E-16**
FBG1n/G1n	**1.12E-16**	0.119	0.014	**5.50E-09**	0.162	0.028	**<2.22E-16**
FBG2n/G2n	**5.03E-12**	0.181	0.026	5.21E-02	0.065	0.033	**2.01E-09**
FBn/Fn	**3.96E-17**	0.088	0.010	**3.81E-06**	0.117	0.025	**<2.22E-16**
FBn/Fn total	**3.71E-17**	0.133	0.016	**5.66E-08**	0.162	0.030	**<2.22E-16**

Supplementary Table S5. Associations of IgG glycans and derived traits adjusted for age, sex, BMI, smoking, HDL-cholesterol, non-HDL-cholesterol, smoking and serum creatinine.

Direct glycan peaks		Discovery population			Replication population			Meta-analysis
Glycan peak	**Glycan structure**	**p-value**	**β**	**S.E.**	**p-value**	**β**	**S.E.**	**p-value**
GP1	FA1	4.27E-02	-3.110	1.534	6.34E-01	0.268	0.563	3.59E-01
GP2	A2	7.87E-01	0.033	0.121	3.61E-01	0.095	0.104	3.80E-01
GP3	A2B	7.77E-01	-0.473	1.667	8.23E-02	2.985	1.718	3.55E-01
GP4	FA2	1.30E-01	0.017	0.012	8.71E-01	-0.003	0.017	4.03E-01
GP5	M5	8.52E-01	0.283	1.517	7.77E-01	-0.241	0.852	9.20E-01
GP6	**FA2B**	**2.45E-08**	0.228	0.041	**3.89E-05**	0.240	0.058	**1.84E-11**
GP7	A2[3]G1	3.89E-01	-0.246	0.285	7.24E-01	-0.079	0.224	4.12E-01
GP8	**A2BG1 FA2[6]G1**	**1.59E-09**	-0.215	0.036	**2.10E-05**	-0.201	0.047	**1.10E-12**
GP9	**FA2[3]G1**	**4.30E-05**	-0.189	0.046	3.16E-03	-0.222	0.075	**1.08E-06**
GP10	**FA2[6]BG1**	6.56E-03	0.142	0.052	**4.93E-04**	0.298	0.085	**9.96E-06**
GP11	**FA2[3]BG1**	3.13E-03	1.283	0.434	2.63E-02	1.101	0.496	**3.28E-04**
GP12	A2G2	8.23E-01	-0.035	0.158	4.44E-01	0.153	0.200	6.53E-01
GP13	A2BG2	3.59E-01	-1.222	1.333	6.31E-02	1.828	0.983	3.92E-01
GP14	FA2G2	6.86E-02	-0.042	0.023	8.82E-01	0.005	0.032	2.98E-01
GP15	FA2BG2	1.72E-01	0.256	0.187	1.02E-02	0.695	0.270	4.32E-03
GP16	FA2[6]G1S1 FA2[3]G1S1	8.96E-01	-0.018	0.137	1.37E-01	-0.273	0.184	2.18E-01
GP17	A2G2S1	3.30E-01	0.312	0.321	3.24E-01	0.061	0.061	1.68E-01
GP18	A2BG2S1 FA2G2S1	6.69E-01	-0.015	0.035	7.26E-01	0.014	0.041	9.99E-01
GP19	FA2BG2S1	7.04E-01	0.060	0.158	3.24E-01	-0.171	0.173	6.02E-01
GP20	FA2FG2S1	1.79E-01	-1.340	0.998	6.70E-01	-0.128	0.300	2.37E-01
GP21	A2G2S2	7.19E-02	-0.923	0.513	5.09E-01	0.028	0.042	5.28E-01
GP22	A2BG2S2	1.17E-01	2.202	1.404	7.34E-01	0.250	0.736	2.09E-01
GP23	FA2G2S2	5.21E-01	-0.102	0.159	5.26E-02	-0.315	0.163	5.67E-02
GP24	FA2BG2S2	1.16E-02	0.382	0.151	6.78E-01	-0.055	0.132	2.01E-01

	Discovery population			Replication population			Meta-analysis
Derived traits	**p-value**	**β**	**S.E.**	**p-value**	**β**	**S.E.**	**p-value**
FGS/(FG+FGS)	3.38E-03	0.071	0.024	3.80E-01	0.024	0.027	1.11E-02
FBGS/(FBG+FBGS)	6.30E-01	-0.005	0.011	5.45E-03	-0.038	0.014	1.41E-02
FGS/(F+FG+FGS)	6.06E-01	0.011	0.022	7.34E-01	0.009	0.025	5.55E-01
FBGS/(FB+FBG+FBGS)	6.07E-02	-0.026	0.014	1.89E-03	-0.050	0.016	**3.28E-04**
FG1S1/(FG1+FG1S1)	**3.49E-04**	0.165	0.046	2.89E-01	0.050	0.047	2.01E-03
FG2S1/(FG2+FG2S1+FG2S2)	7.10E-03	0.067	0.025	4.38E-01	0.027	0.035	2.10E-02
FG2S2/(FG2+FG2S1+FG2S2)	4.31E-01	0.028	0.035	4.35E-02	-0.068	0.034	2.88E-01
FBG2S1/(FBG2+FBG2S1+FBG2S2)	2.59E-02	-0.041	0.018	3.07E-02	-0.053	0.024	2.05E-03
FBG2S2/(FBG2+FBG2S1+FBG2S2)	9.96E-03	0.043	0.017	3.91E-01	-0.017	0.019	3.31E-01
FtotalS1/FtotalS2	1.15E-01	-0.129	0.082	1.27E-01	0.140	0.092	8.57E-01
FS1/FS2	5.91E-01	0.018	0.034	4.70E-03	0.126	0.045	1.15E-02
FBS1/FBS2	1.38E-03	-1.345	0.420	5.43E-01	-0.335	0.551	1.25E-02
FBStotal/FStotal	4.00E-02	1.696	0.826	9.83E-01	0.019	0.895	1.87E-01
FBS1/FS1	3.70E-01	1.093	1.219	6.43E-01	-0.654	1.412	8.33E-01
FBS1/(FS1+FBS1)	3.73E-01	1.571	1.763	6.91E-01	-0.893	2.245	7.97E-01
FBS2/FS2	**7.42E-04**	0.680	0.201	5.89E-03	0.593	0.215	**1.96E-05**
FBS2/(FS2+FBS2)	**6.27E-04**	3.723	1.089	8.62E-03	4.019	1.530	**2.67E-05**
G0n	1.76E-03	0.029	0.009	3.23E-01	0.012	0.012	6.00E-03
G1n	**1.00E-06**	-0.097	0.020	2.75E-03	-0.075	0.025	**7.40E-08**
G2n	2.05E-01	-0.019	0.015	5.01E-01	0.012	0.018	7.77E-01
Fn total	8.60E-01	0.009	0.050	7.14E-01	-0.017	0.046	8.64E-01
FG0n total/G0n	5.23E-01	0.027	0.043	3.75E-01	-0.035	0.040	7.79E-01
FG1n total/G1n	8.24E-01	0.022	0.098	6.74E-01	0.028	0.067	6.41E-01
FG2n total/G2n	6.78E-01	-0.011	0.026	7.30E-01	-0.009	0.027	5.96E-01
Fn	**6.00E-06**	-0.082	0.018	**2.37E-05**	-0.104	0.025	**8.90E-10**
FG0n/G0n	**4.06E-04**	-0.051	0.014	**2.76E-05**	-0.080	0.019	**4.16E-08**
FG1n/G1n	**2.00E-06**	-0.084	0.018	**1.92E-06**	-0.122	0.026	**2.36E-11**
FG2n/G2n	4.54E-03	-0.058	0.021	2.19E-01	-0.025	0.020	5.94E-03
FBn	**2.10E-07**	0.109	0.021	**9.07E-08**	0.174	0.033	**1.13E-13**
FBG0n/G0n	**1.00E-05**	0.075	0.017	**5.62E-07**	0.130	0.026	**2.65E-11**
FBG1n/G1n	**9.91E-07**	0.089	0.018	**4.08E-08**	0.155	0.028	**2.04E-13**
FBG2n/G2n	**8.10E-05**	0.129	0.033	8.35E-02	0.057	0.033	**1.24E-04**
FBn/Fn	**3.79E-07**	0.067	0.013	**1.54E-05**	0.111	0.026	**5.25E-11**
FBn/Fn total	**3.42E-07**	0.103	0.020	**1.80E-07**	0.159	0.030	**3.63E-13**

Glycan peaks and derived traits that were significantly associated with type 2 diabetes in the meta-analysis are in bold font (p-value <8.62E-4). Structure abbreviations are as follows: F, α-1,6-linked core fucose; A, number of antenna's; B, bisecting GlcNac β1-4 linked to β1-3 mannose; M, number of mannose residues; Gx, number of β1-4 linked galactoses; [3]G1, galactose on the antenna of the α1-3 linked mannose; [6]G1, galactose on the antenna of the α1-6 linked mannose; Sx, number of sialic acids linked to galactose. Red: positive association between glycan and clinical trait; blue: negative association. S.E., standard error.

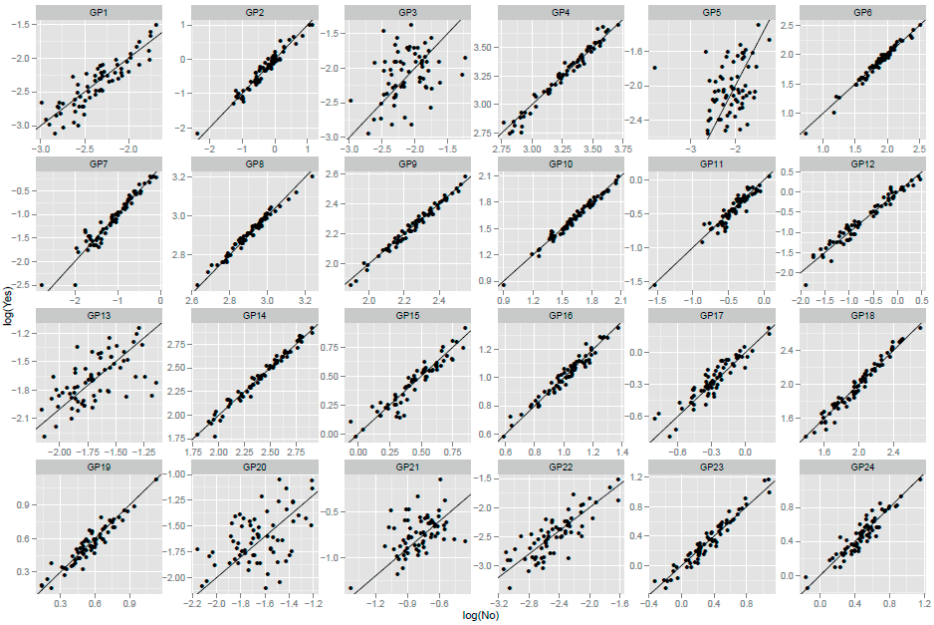

Supplementary figure S1. Correlation between measurements of replicated samples in the Discovery cohort (69 samples out of 2688) per glycan peak.

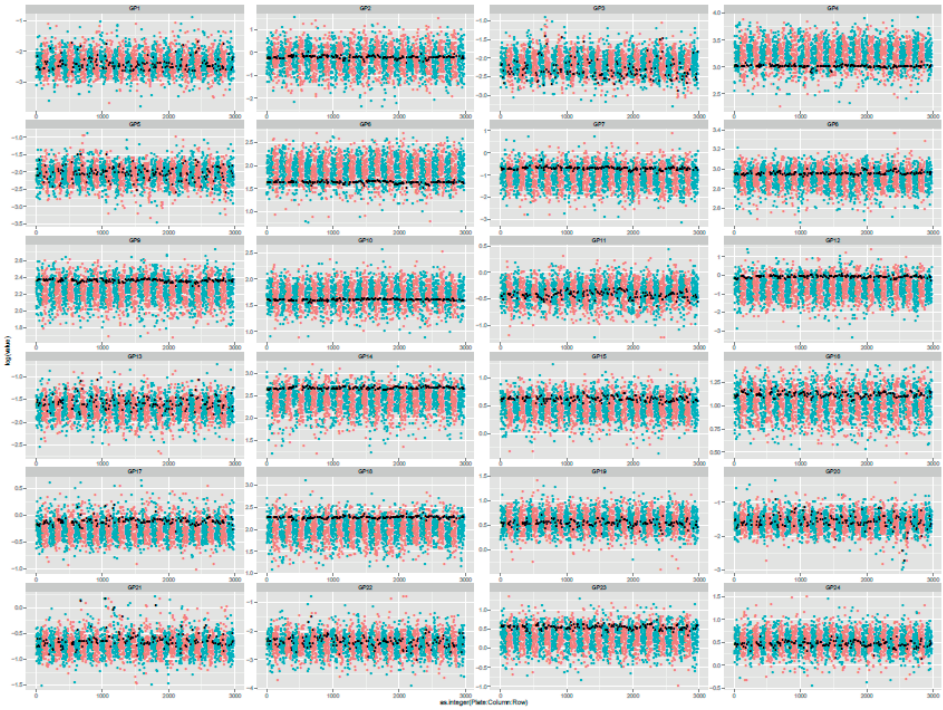

Supplementary figure S2. Variation in measurements of standard samples in the Discovery cohort (n=153, ca. 5 samples per plate) per glycan peak.

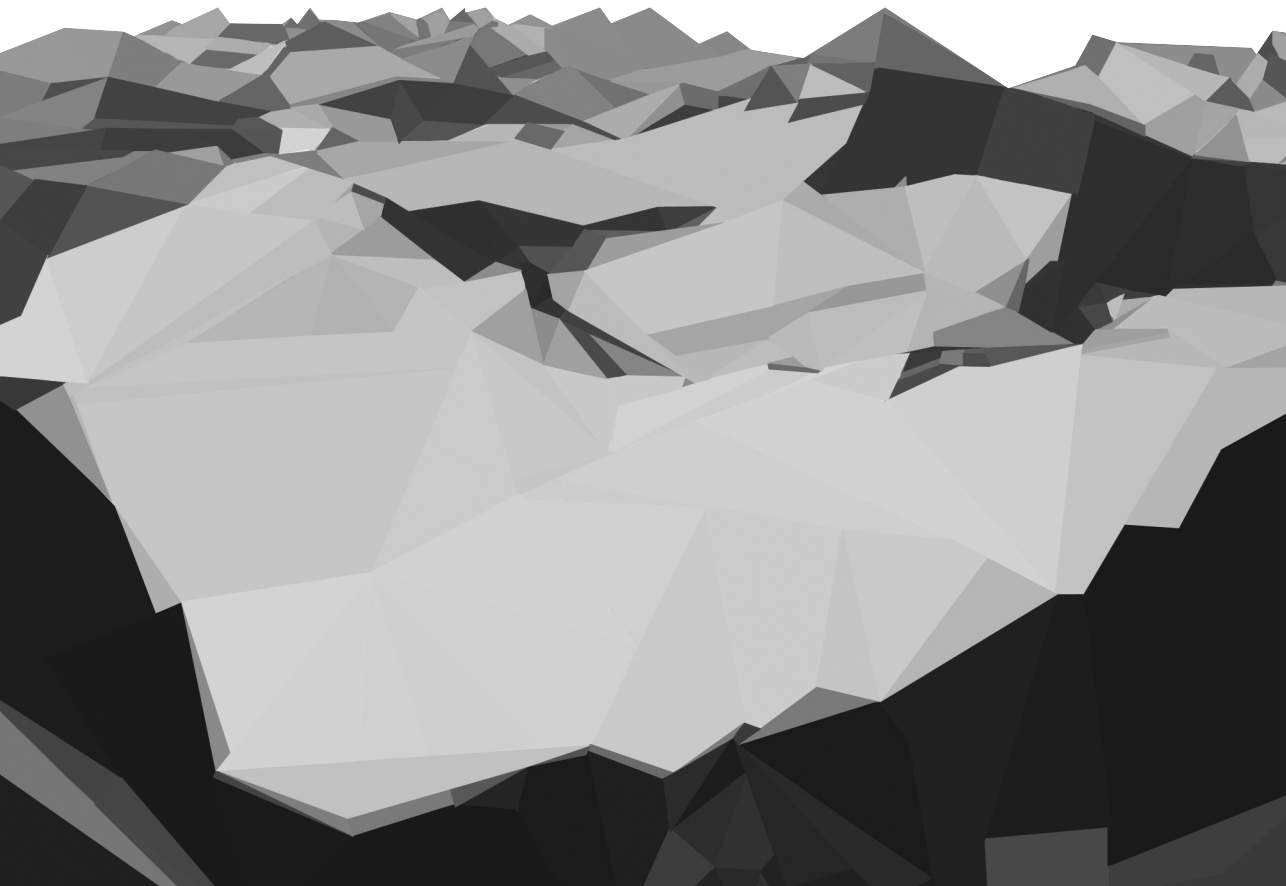

CHAPTER 5

Iodixanol ultracentrifugation as a suitable method for isolating HDL to test its anti-inflammatory function

Manuscript in preparation

Abstract

The anti-inflammatory function of HDL may contribute to its protective role in cardiovascular disease. However, the method used to isolate HDL from plasma may affect the result of in vitro readouts of HDL anti-inflammatory function. We compared three isolation methods of HDL on its anti-inflammatory function, using tumor necrosis factor α (TNFα)-induced expression of vascular cell adhesion molecule-1 (VCAM-1) by human coronary artery endothelial cells as a readout. HDL was isolated by sequential salt density flotation, removal of apoB-containing lipoproteins by precipitation with polyethylene glycol (PEG), and by iodixanol density gradient ultracentrifugation. HDL isolated with all three methods reduced the TNFα-induced VCAM-1 expression to a similar extent. DGUC with iodixanol is a non-ionic, non-toxic, and faster method for isolating HDL than sequential salt density flotation and isolates HDL presumably free from plasma proteins, in contrast to HDL isolation by precipitating apolipoprotein-B containing particles with PEG. We conclude that isolation of HDL with iodixanol density gradient ultracentrifugation is suitable for subsequent testing of HDL anti-inflammatory function.

Introduction

High-density lipoprotein-cholesterol (HDL-C) levels in plasma are inversely linked with the risk of cardiovascular disease (CVD) [1]. However, accumulating evidence points at a relationship between cardiovascular risk and impaired HDL function, rather than its cholesterol concentration [2,3]. The anti-inflammatory function of HDL describes the ability to downregulate signals of endothelial inflammation and monocyte activation and to reduce the migration of monocytes through the endothelium [4-6]. This anti-inflammatory function has been reported as disturbed in type 2 diabetes, acute myocardial infarction, and end-stage renal disease [7-10]. To assess HDL anti-inflammatory function with ex vivo readouts, HDL is isolated from plasma [11]. However, the influence of isolation methods on these readouts is largely unknown [12].

Sequential salt density flotation by ultracentrifugation is the most used HDL isolation method but exposes HDL to high centrifugal forces and high salt concentrations, thereby altering the composition of HDL [13-15] and potentially also its function [16,17]. Additionally, sequential flotation techniques are laborious and time-consuming, making them less suitable for investigating HDL function in large cohorts. A frequently used faster method for HDL isolation removes non-HDL lipoproteins, containing apolipoprotein(apo)-B, from plasma with polyethylene glycol (PEG) [18-21]. However, this method affects the composition and size distribution of HDL particles [22]. Density gradient ultracentrifugation (DGUC) in iodixanol, a non-ionic, non-toxic medium, is an alternative relatively fast method of HDL isolation [23,24]. For both these methods, it is unknown whether they affect readouts of HDL anti-inflammatory function.

In this study, we compared the effect of HDL isolation with PEG-precipitation, iodixanol DGUC, or conventional sequential salt density flotation by ultracentrifugation on HDL anti-inflammatory function, using inhibition of tumor necrosis factor α (TNFα)-induced VCAM-1 expression by endothelial cells as readout.

Methods

Plasma samples

Fasting blood samples were collected in EDTA tubes from healthy volunteers, who did not smoke or use any medication. Blood was immediately centrifuged, and plasma was stored at -80°C. After isolation, HDL was stored at 4°C until use for maximally 7 days unless stated otherwise. All volunteers provided written informed consent.

Materials

Optiprep™ (60% w/v iodixanol) and PEG-6000 were obtained from Sigma-Aldrich, Gillingham, UK. Human coronary artery endothelial cells (HCAECs, Cat CC -2585) were purchased from Lonza (Basel, Switzerland) and cultured in EBM-2-basal medium supplemented with EGM-2-MV SingleQuots and fetal calf serum (FCS). Inhibitor of nuclear factor kappa-B kinase 2-inhibitor (IKK2i) (SC514) was obtained from Calbiochem (Merck, Darmstadt, Germany). Mouse anti-human VCAM-1 conjugated to phycoerythrin fluorochrome (CD106PE) was obtained from eBioscience (San Diego, USA). TNFα was purchased from Bio-Techne (Abingdon, Great Britain).

For ultracentrifugation, Quickseal polyallomer centrifugation tubes, a Beckman NVTi65.2 rotor, and an Optima XL-100K ultracentrifuge were used (Beckman Coulter, Palo Alto, USA). The Canto-II (Becton Dickinson, Franklin Lakes, USA) was used for flow cytometry.

Lipids and apolipoproteins were measured with commercially available kits (DiaSys Diagnostic Systems GmbH, Holzheim, Germany) on an automated Selectra-E analyzer (Vital Scientific, Spankeren, The Netherlands).

Isolation of HDL

Method 1: sequential salt density flotation

HDL was isolated with sequential salt density flotation as described previously [25]. In the first step, 2.1 mL of a KBr solution (density 1.063g/mL) was underlayered with 3 mL of plasma brought to a density of 1.063 g/mL by dissolving KBr, and centrifuged for 20 hours at 220,000g and 4°C in a NVTi65.2 rotor. The floating lipid layer, containing VLDL, IDL, and LDL, was discarded. Next, the density of the remaining HDL-containing solution was adjusted to 1.23 g/mL by adding KBr. This HDL-solution was layered underneath the same volume of a 1.21 g/mL KBr-solution and centrifuged for 44 h at 220,000g and 4°C. The HDL-containing floating layer was collected into a fresh tube, adjusted to a density of 1.23 g/mL, layered under a 1.21 g/mL KBr solution, and recentrifuged (44 hours, 220,000g, 4°C). Thereafter, the HDL-containing floating layer was collected and dialyzed overnight against PBS. This preparation is denoted as HDL_{seq}.

Method 2: HDL isolation by PEG precipitation

ApoB-containing lipoproteins were removed by mixing 0.6 mL plasma with 0.3 mL PEG-solution (36% PEG-6000 in 10mM HEPES, pH 8.0), followed by 30 minutes incubation on ice and centrifugation (30min, 2000g), as described previously [19]. The HDL-containing supernatant was collected and is denoted as $HDL_{PEG.}$

Method 3: single-step iodixanol density gradient ultracentrifugation

HDL was isolated from plasma with a single ultracentrifugation step, using a self-generating iodixanol gradient as previously described [23], with some modifications. Optiprep™ (60%

iodixanol w/v) was mixed with 1.5 mL plasma to obtain a final concentration of 12% iodixanol (w/v) and was layered underneath Optiprep™ mixed with saline to a concentration of 9% iodixanol. The tubes were centrifuged for 2.5 hours (246,000g, 4°C) and then fractionated from the bottom (aspiration speed 1.25mL/min, 20 fractions, 0.25mL/fraction). The HDL-containing fractions (fractions 1-7) were pooled and will hereafter be referred to as $HDL_{IxDGUC1}$.

Method 4: two-step iodixanol density gradient ultracentrifugation

In the first step, HDL was separated from the apoB-containing lipoproteins: 1.5mL plasma was mixed with Optiprep™ to a final iodixanol concentration of 14%, overlayered with 9% iodixanol (w/v) in saline, and centrifuged for 2 hours (246.000g and 20°C). To separate HDL from plasma proteins, the tubes were fractionated from the bottom (aspiration speed 1.18mL/min, 44 fractions, 0.1mL/fraction) and the first 16 fractions, containing the HDL, were pooled. These fractions were mixed with the Optiprep™ solution to a final iodixanol concentration of 38% (w/v), overlayered with a 38% (w/v) iodixanol solution in saline, and centrifuged for 2 hours at 246.000g and 20°C. Again, the tubes were fractionated from the bottom. Fractions 34-42 were pooled and are denoted from hereon as $HDL_{IxDGUC2}$.

TNFα-induced VCAM1 expression by HCAEC

HCAECs were grown to confluence in gelatine-coated culture flasks with medium containing 10% FCS in a humidified chamber (37°C, 5% CO_2). For experiments, HCAECs (passage 7-9) were seeded in 1% FCS-containing medium (0.2 million cells per well; 12-well gelatine-coated plates) and incubated overnight. Cells were pre-incubated for 4 hours with isolated HDL or the following experimental controls: 1) phosphate buffered saline (PBS; pH 7.4); 2) isolation material solution without HDL; or 3) 100 µM IKK2i. Thereafter, TNFα was added to the culture medium and the cells were incubated for an additional 17 hours. Subsequently, cells were prepared for the measurement of VCAM-1 expression. All conditions were tested in triplicate unless stated otherwise.

Measurement of VCAM-1 expression by flowcytometry

Adherent cells were washed with PBS, collected by scraping, and centrifuged (3 min, 3000rpm). Cell pellets were suspended in staining buffer (1% BSA in PBS) and incubated with CD106PE antibodies (1:20, 20min, in the dark at room temperature). Thereafter, cells were washed once with staining buffer and analysed by flow cytometry ($1x10^4$ events per sample). Viable cells were gated and cell populations assigned using the Infinicyt software.

Incubation of HDL in glucose

$HDL_{IxDGUC2}$ was glycated *in vitro* by incubation with 800mM glucose for 7 days at 37°C, followed by overnight dialysis against PBS. As controls, we used freshly isolated $HDL_{IxDGUC2}$

and $HDL_{IxDGUC2}$ stored for 7 days at 37°C in PBS without glucose, both also dialyzed overnight against PBS.

Statistical analysis

Unless stated otherwise, the mean VCAM-1 expression of the TNF-α stimulated PBS control was used as reference value and set at 100%. Outliers were identified with the Rout method (Q set at 1%) and the data was tested for normality with the D'Agostino and Pearson omnibus K2 test. Differences between the conditions were analyzed with a one-way ANOVA and corrected for multiple comparisons with Tukey's test. All analyses were performed in Graphpad Prism, version 6 [26].

We constructed a univariate general linear model (SPSS, IBM statistics, version 22) with the difference in VCAM-1 inhibition between $HDL_{IxDGUC2}$ and the iodixanol control as the dependent variable, to test whether $HDL_{IxDGUC2}$ inhibited TNFα-induced VCAM-1 expression in a dose-dependent manner compared to the isolation material control. The three HDL concentrations (0.71uM, 1.5uM, and 3.0uM) were entered as fixed factor and the TNFα-induced VCAM-1 expression in the presence of the corresponding iodixanol isolation material control as covariate.

Results

First, we tested the effect of $HDL_{IxDGUC1}$ and HDL_{PEG} on TNFα-induced VCAM-1 expression. $HDL_{IxDGUC1}$ and HDL_{PEG} reduced the VCAM-response by 21-34% (figure 1).

Next, we tested HDL isolated by the two-step iodixanol DGUC method, which theoretically also removes unbound plasma proteins. Figure 2 shows the distribution of cholesterol, ApoA-I, and ApoB across the fractions for the two steps. ApoB-values in the pooled HDL were below the detection limit of the assay (0.135g/L). $HDL_{IxDGUC2}$ suppressed the TNFα-induced VCAM-1 expression in the range of 0.7-3 μM apoA-I (Figure 3). A dose-response effect in TNF-α induced VCAM-1 inhibition was apparent for HDL compared to the PBS control, but not compared to the isolation material control (p=0.72).

Then, we directly compared the effects of $HDL_{IxDGUC2}$, HDL_{PEG}, and HDL_{seq} on TNF-α-induced VCAM-1 expression (Figure 4A). Irrespective of the isolation method, HDL decreased the response to a similar extent (13-25%). At concentrations present in the HDL preparation, iodixanol slightly decreased TNF-α-induced VCAM-1 expression, while PEG did not. In Figure 4B, the effect of the HDL preparations relative to their respective controls is shown. HDL_{PEG} showed the strongest inhibition of TNFα-induced VCAM-1 expression (28%). $HDL_{IxDGUC2}$ and HDL_{seq} were similarly effective (14 to 18% inhibition).

Finally, we examined whether the anti-inflammatory function of $HDL_{IxDGUC2}$ was reduced by *in vitro* glycation. Figure 4B shows that incubation of $HDL_{IxDGUC2}$ in excess glucose dimin-

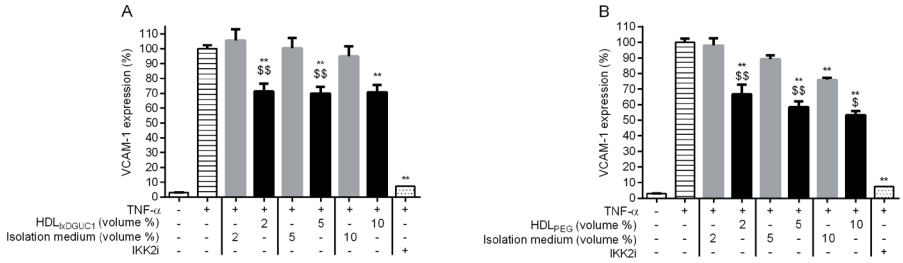

Figure 1. Effect of HDL isolated using IxDGUC1 or PEG on TNF-α induced VCAM-1 expression on HCAEC.

VCAM-1 expression (mean ± SEM) is shown in the absence or in the presence of TNFα (0.5ng/ml)and HDL$_{IxDGUC1}$ (A) or HDL$_{PEG}$ (B). IKK2i was used as control to block TNF-α induced effects on VCAM-1 expression through NFκB. HDL was isolated from plasma from 2 healthy individuals in 2 separate experiments (all conditions in duplo). Mean ApoA-I concentration of four HDL preparations was 0.54uM in 2% HDL$_{IxDGUC1}$ and 0.66uM in 2% HDL$_{PEG}$. **, p-value <0.01 compared to PBS control (without HDL or isolation medium). P-values compared to the corresponding isolation medium added in the same volume percentage: $ p<0.05; $$ p<0.01.

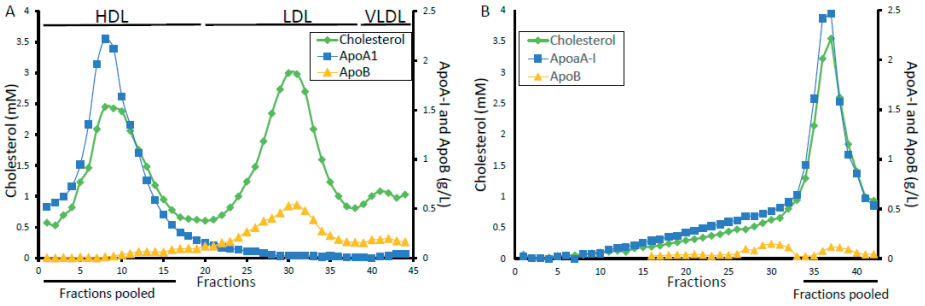

Figure 2. HDL separation by two-step iodixanol density gradient centrifugation.

Cholesterol, ApoA-I and ApoB concentrations in the fractions with decreasing density are shown (A). The ApoA-I-containing fractions 1-16 were pooled for the second centrifugation step (B). Fractions 34-42 were pooled and represent HDL$_{IxDGUC2}$. In figure B, all apoB-measurements were below the detection limit (0.15g/L) of the assay.

ished its ability to reduce the TNFα-induced VCAM-1 expression. Notably, a similar effect was observed with HDL that had been stored without glucose for the same period of time at 37^{0}C.

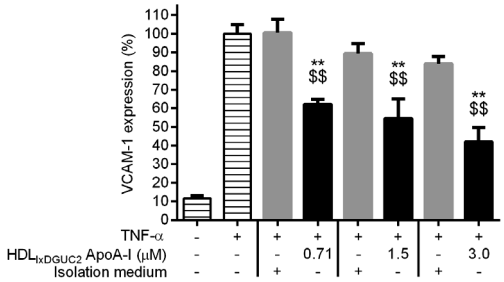

Figure 3. Dose-response effect of HDLIxDGUC2 on TNFα induced VCAM-1 expression.

VCAM-1 expression (mean ± SEM) is shown primed by TNF-α (2ng/ml). The TNFα-induced VCAM-1 expression in the presence of PBS was set at 100%. Results are the average of 3 independent experiments. $HDL_{IxDGUC2}$ was added in apoA-I concentrations of 0.71, 1.5, and 3.0 μM. As control, the iodixanol isolation solution was added corresponding to the volume of the $HDL_{IxDGUC2}$. Statistical significance compared to PBS control: ** p<0.01. Statistical significance compared to corresponding isolation material control: $$ p<0.01.

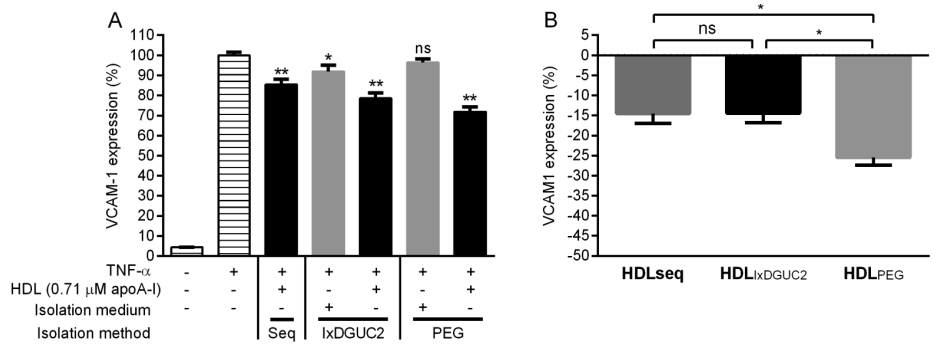

Figure 4. Comparison of the effect of HDLSeq, HDLIxDGUC2, and HDLPEG on TNF-α stimulated VCAM-1 expression by HCAEC.

Results are the mean of 3 independent experiments with pooled HDL isolated from plasma of 3 healthy volunteers. The concentration of HDL added was based on the ApoA-I concentration (0.71μM). A) VCAM-1 expression (mean ± SEM) is shown in the absence or in the presence of TNF-α (10ng/ml) and PBS, iodixanol (3.9 volume % isolation medium), and PEG (2 volume % isolation medium) as controls for HDL_{Seq}, $HDL_{IxDGUC2}$ and HDL_{PEG}, respectively. P-values compared to TNF-α stimulated PBS control: * p<0.05; ** p<0.0001. B) Inhibition of TNF-α stimulated VCAM-1 expression (mean ± SEM) in the presence of HDL_{seq}, $HDL_{IxDGUC2}$, and HDL_{PEG} relative to their respective controls; * p<0.05.

Discussion

Here we show that HDL isolated by iodixanol density gradient ultracentrifugation (DGUC) showed similar anti-inflammatory function as HDL isolated with PEG-precipitation or

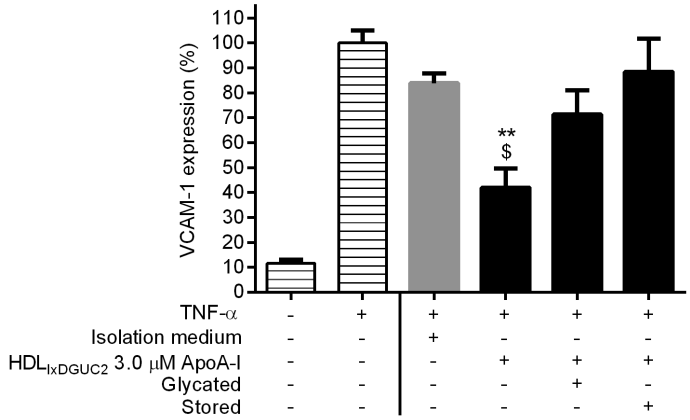

Figure 5. Effect of glycation of HDLIxDGUC2 on its anti-inflammatory function.

VCAM-1 expression (mean ± SEM) is shown primed by TNF-α (2ng/ml). The TNFα-induced VCAM-1 expression in the presence of PBS was set at 100%. Results are the average of 3 independent experiments. $HDL_{IxDGUC2}$ was added in a concentration of 3.0 μM apoA-I. Statistical significance compared to PBS control: ** p<0.01. Statistical significance compared to corresponding isolation material control: $ p<0.05.

sequential salt density flotation, using TNFα induced VCAM-1 expression on HCAEC as a readout. The inhibitory effect of $HDL_{IxDGUC2}$ on the TNFα-induced VCAM-1 expression was abolished by *in vitro* glycation or storage at 37°C for 7 days. Compared to sequential salt density flotation, the two-step iodixanol DGUC is a relatively fast and mild method for isolation of HDL free from both apoB-containing lipoproteins and unbound plasma proteins, and suitable for testing HDL's anti-inflammatory function as we showed here.

Sequential salt density flotation is the conventional method for HDL isolation. The high ionic strengths, prolonged centrifugation and dialysis time may lead to oxidative damage and denaturation of HDL and HDL-bound proteins [15,27]. Advantages of the iodixanol DGUC over the salt-based sequential flotation method are that iodixanol is non-toxic and non-ionic, and isolation requires shorter centrifugation times (4 versus 50 hours, respectively)[14]. It might therefore cause less changes in HDL composition [15]. In addition, $HDL_{IxDGUC2}$ inhibited TNFα-induced VCAM-1 expression at much lower apoA-I concentrations in our study than routinely used in studies testing HDL isolated with other methods [28-30]. Although increasing concentrations of $HDL_{IxDGUC2}$ resulted in stronger VCAM-1 inhibition compared to the PBS control, no dose-response effect was seen compared to the iodixanol control. Possible explanations are the limited amount of measurements, an inhibiting effect of iodixanol on TNFα induced VCAM-1 expression, or the relatively small range of HDL concentrations. Currently, we are testing if the iodixanol DGUC method removes unbound plasma proteins from the HDL during the second centrifugation step [23,31].

Previous studies have shown that *in vitro* treatment of HDL with excess glucose abolishes its anti-inflammatory function [32,33], an effect that appeared to be preserved in HDL

isolated by the two-step iodixanol DGUC. Since a similar loss of anti-inflammatory response was also seen upon incubation at 37°C for 7 days without excess glucose, it is uncertain whether this is due to the glucose incubation or to storage itself. We incubated HDL with a supra-physiological glucose concentration. In the near future, we will investigate whether physiological concentrations of glucose also result in loss of HDL anti-inflammatory function.

An even faster and less stringent method for HDL isolation is PEG-precipitation. This method preserves pre-β-HDL, but fails to remove plasma proteins including albumin, transferrin and haptoglobin [34,35]. PEG has been reported to modify HDL composition, but common readouts of HDL anti-oxidative function or cholesterol efflux were not affected [22]. Most of the PEG has been shown to remain behind in HDL isolated with PEG precipitation [22]. Although high concentrations of PEG (1.2% v/v PEG in cell culture medium) decreased VCAM-1 significantly by 25% (figure 1), PEG did not affect VCAM-1 expression at the lower concentrations used in our further experiments (0.2% v/v PEG) (figure 4A). TNFα-induced VCAM-1 expression was more strongly inhibited by HDL_{PEG} than by the other HDL preparations, which could be due to the HDL itself but might also be caused by the PEG and plasma proteins remaining behind in the HDL preparation.

Strengths and limitations

We directly compared anti-inflammatory function of HDL that was isolated with three different methods. HDL function research is a growing field and knowledge on how the methodology affects the outcome is crucial for proper interpretation of the role of HDL in disease. Certain limitations apply to our work. We used HDL isolated from plasma obtained from a limited number of healthy volunteers. In addition, only one read-out for HDL anti-inflammatory function was tested and therefore we cannot comment on the effects of these isolation methods on other readouts or on tests for other HDL functions.

Conclusion

Our data show that the two-step iodixanol DGUC method it is a relatively fast method for HDL isolation, resulting in HDL free from apoB-containing lipoproteins and presumably also of unbound plasma proteins. In addition, less adverse effects on HDL composition are expected than with sequential salt density flotation or PEG precipitation. Although more research is necessary to confirm our findings and expand them to other read-outs of HDL anti-inflammatory function, we believe iodixanol DGUC is a suitable method for HDL isolation when testing HDL anti-inflammatory function.

References

1. Gordon DJ, Probstfield JL, Garrison RJ, et al. High-density lipoprotein cholesterol and cardiovascular disease. Four prospective American studies. Circulation 1989;79:8-15.
2. Rader DJ, Tall AR. The not-so-simple HDL story: Is it time to revise the HDL cholesterol hypothesis? Nat Med 2012;18:1344-6.
3. Srivastava RAK. Dysfunctional HDL in diabetes mellitus and its role in the pathogenesis of cardiovascular disease. Mol Cell Biochem 2017;.
4. Cockerill GW, Rye KA, Gamble JR, Vadas MA, Barter PJ. High-density lipoproteins inhibit cytokine-induced expression of endothelial cell adhesion molecules. Arterioscler Thromb Vasc Biol 1995;15:1987-94.
5. Murphy AJ, Woollard KJ, Hoang A, et al. High-density lipoprotein reduces the human monocyte inflammatory response. Arterioscler Thromb Vasc Biol 2008;28:2071-7.
6. Navab M, Imes SS, Hama SY, et al. Monocyte transmigration induced by modification of low density lipoprotein in cocultures of human aortic wall cells is due to induction of monocyte chemotactic protein 1 synthesis and is abolished by high density lipoprotein. J Clin Invest 1991;88:2039-46.
7. Annema W, Willemsen HM, de Boer JF, et al. HDL function is impaired in acute myocardial infarction independent of plasma HDL cholesterol levels. J Clin Lipidol 2016;10:1318-28.
8. Morgantini C, Natali A, Boldrini B, et al. Anti-inflammatory and antioxidant properties of HDLs are impaired in type 2 diabetes. Diabetes 2011;60:2617-23.
9. Kaseda R, Jabs K, Hunley TE, et al. Dysfunctional high-density lipoproteins in children with chronic kidney disease. Metabolism 2015;64:263-73.
10. Yamamoto S, Yancey PG, Ikizler TA, et al. Dysfunctional high-density lipoprotein in patients on chronic hemodialysis. J Am Coll Cardiol 2012;60:2372-9.
11. Rosenson RS, Brewer HB,Jr, Chapman MJ, et al. HDL measures, particle heterogeneity, proposed nomenclature, and relation to atherosclerotic cardiovascular events. Clin Chem 2011;57:392-410.
12. Assessing the functional properties of high-density lipoproteins: An emerging concept in cardiovascular research. United Kingdom: 2013. Triolo M., Annema W., Dullaart R.P.F., Tietge U.J.F. (Accessed 3, 7).
13. Kunitake ST, Kane JP. Factors affecting the integrity of high density lipoproteins in the ultracentrifuge. J Lipid Res 1982;23:936-40.
14. Munroe WH, Phillips ML, Schumaker VN. Excessive centrifugal fields damage high density lipoprotein. J Lipid Res 2015;56:1172-81.
15. Stahlman M, Davidsson P, Kanmert I, et al. Proteomics and lipids of lipoproteins isolated at low salt concentrations in D2O/sucrose or in KBr. J Lipid Res 2008;49:481-90.
16. Camont L, Lhomme M, Rached F, et al. Small, dense high-density lipoprotein-3 particles are enriched in negatively charged phospholipids: relevance to cellular cholesterol efflux, antioxidative, antithrombotic, anti-inflammatory, and antiapoptotic functionalities. Arterioscler Thromb Vasc Biol 2013;33:2715-23.
17. Heinecke JW. The protein cargo of HDL: implications for vascular wall biology and therapeutics. J Clin Lipidol 2010;4:371-5.
18. Demacker PN, Hessels M, Toenhake-Dijkstra H, Baadenhuijsen H. Precipitation methods for high-density lipoprotein cholesterol measurement compared, and final evaluation under routine operating conditions of a method with a low sample-to-reagent ratio. Clin Chem 1997;43:663-8.
19. Kappelle PJ, de Boer JF, Perton FG, et al. Increased LCAT activity and hyperglycaemia decrease the antioxidative functionality of HDL. Eur J Clin Invest 2012;42:487-95.

20. Asztalos BF, de la Llera-Moya M, Dallal GE, Horvath KV, Schaefer EJ, Rothblat GH. Differential effects of HDL subpopulations on cellular ABCA1- and SR-BI-mediated cholesterol efflux. J Lipid Res 2005;46:2246-53.
21. Triolo M, Annema W, de Boer JF, Tietge UJ, Dullaart RP. Simvastatin and bezafibrate increase cholesterol efflux in men with type 2 diabetes. Eur J Clin Invest 2014;44:240-8.
22. Davidson WS, Heink A, Sexmith H, et al. The effects of apolipoprotein B depletion on HDL subspecies composition and function. J Lipid Res 2016;57:674-86.
23. Graham JM, Higgins JA, Gillott T, et al. A novel method for the rapid separation of plasma lipoproteins using self-generating gradients of iodixanol. Atherosclerosis 1996;124:125-35.
24. Harman NL, Griffin BA, Davies IG. Separation of the principal HDL subclasses by iodixanol ultracentrifugation. J Lipid Res 2013;54:2273-81.
25. Ashby DT, Rye KA, Clay MA, Vadas MA, Gamble JR, Barter PJ. Factors influencing the ability of HDL to inhibit expression of vascular cell adhesion molecule-1 in endothelial cells. Arterioscler Thromb Vasc Biol 1998;18:1450-5.
26. GraphPad Software, La Jolla California USA. Anonymous . (, at www.graphpad.com).
27. Timasheff SN. The control of protein stability and association by weak interactions with water: how do solvents affect these processes? Annu Rev Biophys Biomol Struct 1993;22:67-97.
28. Park SH, Park JH, Kang JS, Kang YH. Involvement of transcription factors in plasma HDL protection against TNF-alpha-induced vascular cell adhesion molecule-1 expression. Int J Biochem Cell Biol 2003;35:168-82.
29. Patel S, Drew BG, Nakhla S, et al. Reconstituted high-density lipoprotein increases plasma high-density lipoprotein anti-inflammatory properties and cholesterol efflux capacity in patients with type 2 diabetes. J Am Coll Cardiol 2009;53:962-71.
30. Nicholls SJ, Lundman P, Harmer JA, et al. Consumption of saturated fat impairs the anti-inflammatory properties of high-density lipoproteins and endothelial function. J Am Coll Cardiol 2006;48:715-20.
31. Yee MS, Pavitt DV, Tan T, et al. Lipoprotein separation in a novel iodixanol density gradient, for composition, density, and phenotype analysis. J Lipid Res 2008;49:1364-71.
32. Hedrick CC, Thorpe SR, Fu MX, et al. Glycation impairs high-density lipoprotein function. Diabetologia 2000;43:312-20.
33. Hoang A, Murphy AJ, Coughlan MT, et al. Advanced glycation of apolipoprotein A-I impairs its anti-atherogenic properties. Diabetologia 2007;50:1770-9.
34. Robinson MW, Scott DG, Bacon PA, Walton KW, Coppock JS, Scott DL. What proteins are present in polyethylene glycol precipitates from rheumatic sera? Ann Rheum Dis 1989;48:496-501.
35. Hyun J. Specific proteins precipitated by polyethylene glycol during assays for circulating C1q precipitable immune complexes. Am J Clin Pathol 1983;80:777-8.

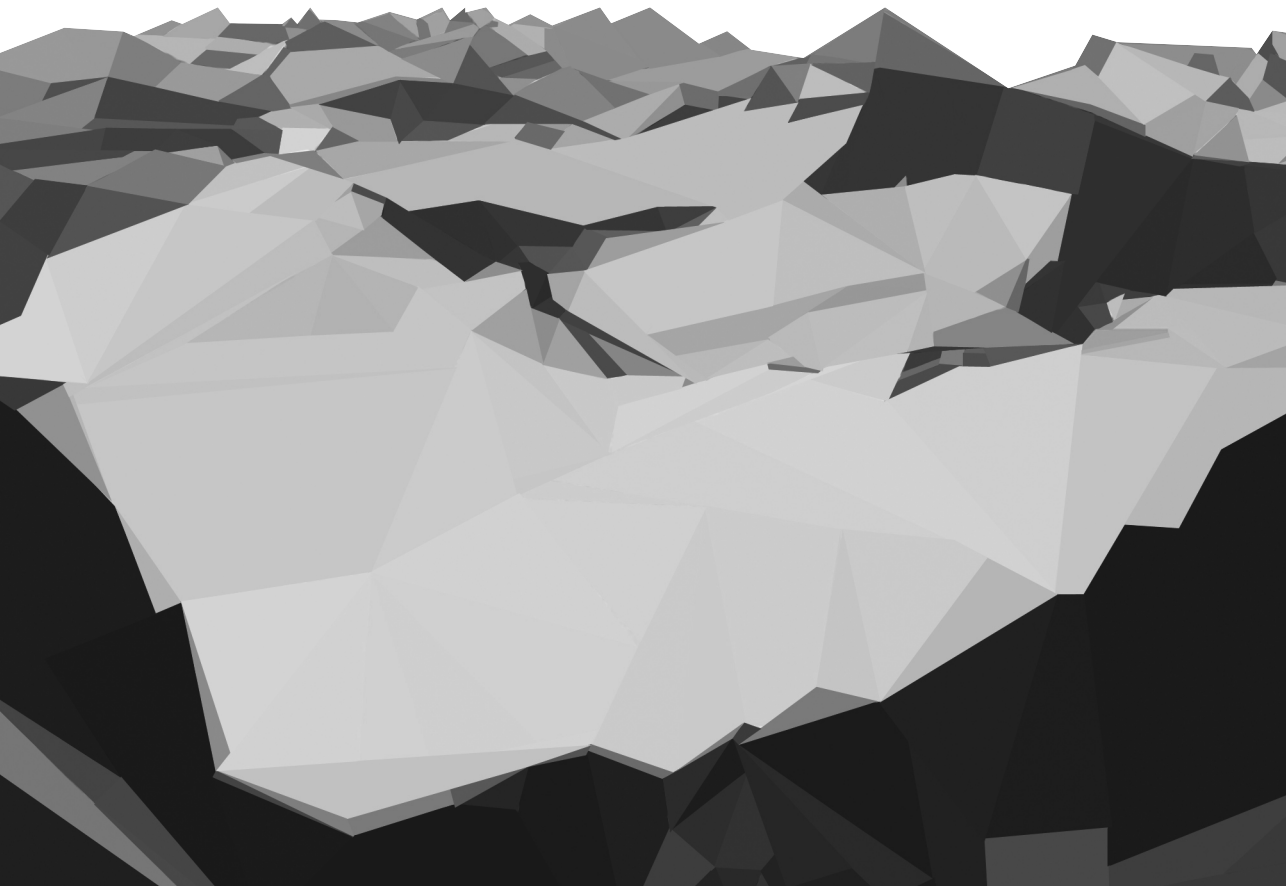

CHAPTER 6

The anti-inflammatory function of HDL in type 2 diabetes: a systematic review

Roosmarijn FH Lemmers, Mandy van Hoek, Aloysius G Lieverse, Adrie JM Verhoeven, Eric JG Sijbrands, Monique T Mulder

Journal of Clinical Lipidology 2017 May - Jun;11(3):712-724.e5.

Abstract

Background: Inflammation is a pathophysiological factor in diabetes and its cardiovascular complications. HDL suppresses inflammation in healthy individuals. The relationship of HDL with diabetes and cardiovascular disease may be explained by HDL function rather than by HDL cholesterol level. In diabetes, HDL seems to become dysfunctional.

Objective: We performed a systematic review to answer the following research questions: Is the anti-inflammatory function of HDL diminished in individuals with diabetes and if so, what causes this?

Methods: We systematically searched Medline and Embase and included original research articles on the anti-inflammatory effects of HDL or HDL-based interventions in diabetes or diabetes models. We assessed the risk of bias of all included studies.

Results: Fourteen studies were included. These showed great heterogeneity in methodology, study populations, and diabetes models. Overall, HDL from subjects with type 2 diabetes displayed a reduced ability to suppress inflammatory processes and inflammation markers. However, the mechanisms and the *in vivo* effects remain largely unknown. No studies reported on HDL from individuals with other types of diabetes. In most studies, the risk of bias was high or could not be assessed.

Conclusions: HDL isolated from individuals with type 2 diabetes showed a decreased ability to suppress inflammation. However, the direction of causality and the underlying mechanisms are unknown and should be investigated. For development of treatments directed at restoring HDL anti-inflammatory function in diabetes, a standardized method for assessing HDL anti-inflammatory function needs to be developed and *in vivo* biomarkers must be identified.

Introduction

Diabetes is an increasing worldwide healthcare problem and a leading cause of kidney failure, blindness and amputations [1]. Moreover, cardiovascular disease (CVD) is the most common cause of death in diabetes [2]. Diabetes and its vascular complications are largely driven by inflammation [3,4], which can be suppressed by HDL in healthy individuals[5]. HDL has several functional effects. In diabetes, HDL shows a reduced capacity for protecting the vascular system [6]. The molecular basis of this dysfunction, including the role of HDL's anti-inflammatory capacity is unknown. Most of our knowledge on HDL function originates from *in vitro* and *ex vivo* studies. Approaches and methods differ between research groups, complicating the interpretation of data on HDL function. Therefore, clinical implications remain unclear.

HDL is best-known for the inverse association of the HDL cholesterol content with CVD [7] and diabetes [8]. However, recent studies suggest that these relationships are not causal, since therapies aimed at increasing HDL-cholesterol have not been able to decrease CVD risk [9], nor did genetically decreased HDL-cholesterol increase the risk of CVD or diabetes [10,11]. Since the HDL particle consists of many constituents besides cholesterol [12], other, currently unknown factors may explain how HDL influences CVD risk. Of the many functions of HDL, cholesterol retrieval from the vascular wall (cholesterol efflux) has been mostly studied. HDL also inhibits oxidation and apoptosis, boosts endothelial nitric oxide production [13-15], and inhibits activation of immune cells and migration through the endothelium [16-18]. The latter characteristic is described as the anti-inflammatory function of HDL.

The anti-inflammatory function of HDL is most frequently measured as its effect on adhesion of monocytes to, and migration through, the endothelial cell layer induced by oxidized LDL, and as the expression of adhesion molecules on endothelial cells or monocytes. These are all considered early steps in vascular inflammation [19]. Potential determinants of HDL's anti-inflammatory function are the particle size and composition. Plasma HDL is a heterogeneous population of particles varying in size, number and lipid and protein composition [20]. The size ranges from small dense HDL3 to large buoyant HDL2, and in diabetes there appears to be a preponderance of HDL3 particles [21]. Moreover, lipid oxidation and protein glycation with subsequent formation of advanced glycation end products (AGEs) are well known pathogenic processes in diabetes as well [4], which may affect HDL function. Statins and fibrates, which are commonly used in T2D, have been reported to improve HDL function [22,23], but whether they improve the anti-inflammatory function of HDL in T2D is uncertain. Recent, experimental interventions aimed at improving HDL function are performed with reconstituted HDL (rHDL) and apoA-1 mimetic peptides [24].

We performed a systematic review describing the anti-inflammatory function of HDL in diabetes. Our research questions are: Is the anti-inflammatory capacity of HDL diminished in individuals with diabetes? If so, what are the underlying mechanisms? We restricted

our review to the direct effects of HDL on inflammation and therefore do not describe indirect effects through cholesterol efflux or oxidation or the relationship between HDL-cholesterol of HDL and inflammation. We systematically searched Medline and Embase databases and reviewed all original research articles investigating the effects of HDL or HDL-based interventions on vascular inflammation or activation of circulating immune cells in diabetes.

Materials and methods

Review protocol

The review protocol was drafted prior to the search process. The inclusion criteria were the following: 1) original research article; 2) addressing the anti-inflammatory function of HDL, defined as the effect of HDL or its main constituent, apolipoprotein AI (apoA-I), on inflammation markers or immune cells; 3) studying diabetes, defined as diabetes diagnosed by a physician, an established mouse model of diabetes, or an *ex vivo* diabetes model; and 4) published in English or Dutch. Studies were excluded if less than 50% of the study population had diabetes or if the full article could not be retrieved.

Literature search

We searched Medline (PubMed, 1966 – 2.2.2016) and Embase databases (OVID, 1974 – 2.2.2016) for eligible articles with the following search terms: diabetes; high density lipoprotein; apolipoprotein A1; apolipoprotein A2; apolipoprotein A; anti-inflammat*; inflammat*; pro-inflammat*; immunomodulat*; inflammatory index; propert*; function*; functional*; dysfunction*; quality. The search terms were broad to include all possibly eligible publications. Appendix 1 shows the complete search strategies. We checked for duplicate publications by juxtaposing author names and titles. Additionally, we hand-searched the reference lists of all included articles and all review articles describing HDL anti-inflammatory function in diabetes. The search was supervised by a senior librarian.

Study selection

Two independent researchers assessed eligibility by screening all titles and abstracts; in case of disagreement, a third researcher was consulted and consensus was reached. Subsequently, the full-text of the remaining articles was assessed by one researcher; when in doubt, a second researcher was consulted and consensus was reached. When the full-text of an article could not be retrieved from the internet, a copy was requested from the authors.

Data extraction and items

We developed a data extraction form that was pilot-tested on two included studies and refined accordingly. Two researchers independently extracted data from the included studies and discussed the findings. In case of disagreement, the findings were discussed with a third researcher until consensus was reached.

Information was extracted on the following items which were deemed necessary to evaluate study results: 1) study aim and design; 2) study population (source population, in- and exclusion criteria, sample size, number of persons with diabetes); 3) outcome measurement (method of measuring HDL anti-inflammatory function, HDL isolation method, and cell type); 4) if applicable, type of intervention; 5) results, both regarding HDL anti-inflammatory function and other outcome measurements; and 6) conclusions.

Risk of bias assessment

Two researchers independently assessed the risk of bias across several domains. This assessment only applies to parts of the studies concerning HDL anti-inflammatory function in diabetes. All intervention studies were reviewed with the Cochrane Collaboration's tool for assessing risk of bias [25]; random sequence generation, allocation concealment and incomplete data were considered key domains. For observational studies, we used a quality assessment form based on the Critical Appraisal Skills Programme checklists for case-control and cohort studies [26]. The following items were evaluated for observational studies: selection bias; bias in outcome measurement; classification bias; applicability of results to individuals with diabetes; and appropriateness of the analyses. Selection of cases and controls and analysis of results were considered key domains. The summary assessment was based on the key domains. We did not exclude studies based on their risk of bias.

Results

Study selection

Our systematic search resulted in 1179 unique articles. Out of the 122 articles selected after screening the titles and abstracts, 6 fulfilled our inclusion criteria and 39 relevant reviews were identified. Of 1 review no full-text could be retrieved; no papers were excluded based on language. From the reference lists of these 45 articles, 7 additional original research articles were identified and included. This resulted in 13 original research articles describing 14 studies that were applicable to our research question. Figure 1 shows the flow diagram.

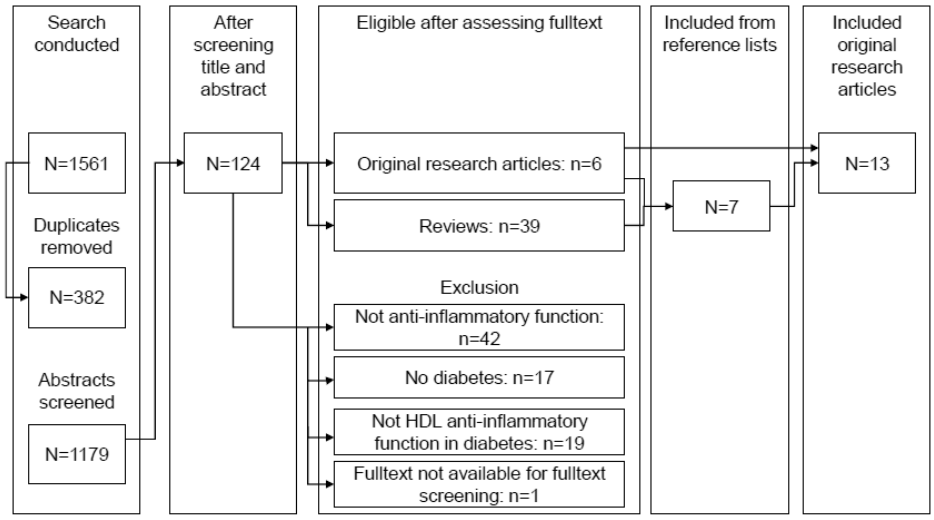

Figure 1. Flow diagram of literature selection.

Study description

Out of 14 included studies, 5 were randomized controlled trials in humans, 5 were observational, and 4 were placebo-controlled intervention studies in animals. Nine studies tested HDL isolated from persons with type 2 diabetes (T2D) for its anti-inflammatory effects *ex vivo* [27-34]. The other studies used mouse models [35-37] or *in vitro* glycated HDL, apoA-I, or reconstituted HDL (rHDL) [38,39]. The anti-inflammatory capacity of HDL was not tested in relation to vascular disease, nor was its function in persons with type 1 diabetes (T1D).

A variety of readouts were used to express the effects of HDL on inflammation. Most frequently used were adhesion molecule expression by endothelial cells or monocytes [28,32,33,38] and the HDL inflammatory index (HII) [30,31,34]; the latter assesses the effect of HDL on trans-endothelial migration of monocytes induced by oxidized LDL. Across all studies, three different endothelial cell types and three different kinds of monocytes were used to assess the effect of HDL. The HDL isolation methods differed from density gradient ultracentrifugation and fast protein liquid chromatography to apolipoprotein-B (apoB)-depletion with polyethylene glycol. Because of this heterogeneity in methodology, we deemed meta-analyzing the results not meaningful. A description per study is given in table 1 and a summary of the risk of bias assessment in table 2. The risk of bias assessment is specified in supplementary tables S1 and S2. In many studies, insufficient information was supplied to determine the risk of bias regarding the anti-inflammatory function of HDL in diabetes (unclear risk of bias).

HDL anti-inflammatory function: diabetes versus healthy controls.

Three studies compared the anti-inflammatory properties of HDL between persons with T2D and healthy controls. The largest study, a case-control study by Morgantini et al. [30], showed an HII above 1.0 for HDL from persons with T2D (pro-inflammatory HDL) and an HII below 1.0 for healthy subjects (anti-inflammatory HDL). Pro-inflammatory HDL in persons with T2D was also described by Watson et al. (mean HII>1.55) [31] and by Bloedon et al. (mean HII 1.18) [34] in cohorts containing 76% and 70% of persons with diabetes, respectively. Correspondingly, Liu et al. [29] showed that incubation of lipopolysaccharide (LPS)-stimulated macrophages with HDL from persons with T2D resulted in a 50% higher TNF-α concentration and an 83% higher IL-1β concentration than incubation with healthy HDL. Also, HDL3 of persons with newly diagnosed diabetes was pro-inflammatory in the study by Tong et al. [28]: compared to healthy HDL3, T2D-HDL3 increased monocyte adherence to human umbilical vein endothelial cells (HUVEC) and increased expression of intercellular adhesion molecule-1 (ICAM-1) and vascular cell adhesion molecule-1 (VCAM-1) by HUVEC [28]. The risk of bias in these studies was either unclear or high.

Determinants of the anti-inflammatory function of HDL in diabetes

Glycation

The influence of *in vitro* glycation on the anti-inflammatory function of HDL was investigated in 4 studies [29,32,38,39], of which one also investigated *in vivo* glycation [32]. *In vitro* glycated HDL or apoA-I was obtained by incubating isolated HDL or apoA-I from healthy subjects with high concentrations of glucose, ribose, or methylglyoxal. Table 3 shows the glycation protocol per study.

Liu et al. [29] found that *in vitro* glycation of HDL reduced its ability to suppress TNF-α and IL-1β production by LPS-stimulated macrophages. *In vitro* glycated HDL no longer reduced monocyte adhesion to human aortic endothelial cells induced by oxidized LDL, as shown by Hedrick et al. [39]. The effect of glycating apoA-I was comparable to that of glycating HDL in the studies by Hoang et al. [38] and Liu et al. [29]: after *in vitro* glycation, apoA-I no longer diminished PMA-stimulated CD11b expression on monocytes [38], and delipidated HDL no longer suppressed cytokine production by macrophages [29]. In the study by Nobécourt et al. [32], rHDL containing glycated apoA-I did not decrease *in vitro* ICAM-1 and VCAM-1 expression, while rHDL containing unmodified apoA-I did. In rabbits, carotid-artery inflammation decreased after infusion with unmodified apoA-I or rHDL, but less after infusion with glycated apoA-I or rHDL and not at all after infusion with apoA-I obtained from persons with T2D [32].

In these studies, HDL glycation was monitored by advanced glycation end products (AGE) levels of the HDL. Three studies reported 1.5-10 fold higher AGE levels in T2D-HDL than in healthy HDL [29,32,38]. However, AGE levels of *in vitro* glycated HDL were even 5-150 fold higher than of T2D-HDL (Table 3).

Table 1. Details of the included studies.

Source	Aim	Design	Inclusion criteria
Triolo 2014 [27]	HDL function in T2D and effect of lipid-lowering therapy	randomized, placebo-controlled cross-over	T2D, nonsmoking, male, >18y old. No insulin, lipid-lowering drugs, thiazolidinediones or antihypertensives. No CVD, hypertension, or disease of thyroid or liver. No cholesterol >9.0mmol/L, TG>4.5mmol/L., nor albuminuria >20mg/L.
Tong 2013 [28]	AI effect of HDL in T2D vs healthy controls	case-control	Cases: T2D, 40-75y old, no T2D treatment before inclusion, no vascular disease, no statins. Controls: unknown
Liu 2012 [29]	AI effect of HDL in T2D and after glycation	case-control and observational	Cases: diabetes, no insulin, HbA1c>7.0%, no CVD. Controls: normal glucose tolerance, no family history of diabetes.
Morgantini 2011 [30]	HDL function in T2D vs healthy controls, and effect of L-4F treatment in vitro	case-control	Cases: T2D. No inflammatory disease, recent CVD event, cancer, kidney or liver disease, nor use of AI / antioxidant drugs. Controls: healthy, age-and sex-matched.
Watson 2011 - IV study [31]	Safety and tolerability of L-4F in CHD or equivalent	Randomized, double-blind, placebo-controlled intervention	Stable CHD or equivalent, 18-75y old, stable statin dose, HbA1c <9.0%.
Watson 2011 -SC study [31]	Safety and tolerability of L-4F in CHD or equivalent	Randomized, double-blind, placebo-controlled intervention	Stable CHD or equivalent, 18-75y old, stable statin dose, HbA1c <9.0%.
Morgantini 2010 [35]	Effect of D-4F on atherosclerosis in mice with diabetes	Case-control study with placebo-controlled intervention in cases	apoE-/- mice cases: streptozotocin-induced diabetes
Nobecourt 2010 [32]	Effect of glycation on AI properties of apoA-I	1. *in vivo*: randomized placebo-controlled intervention. 2. *In vitro*: observational	*In vivo*: Chow-fed NZW male rabbits. HDL isolate from T2D subjects with end-stage renal disease or healthy humans.
Patel 2009 [33]	Effect of rHDL infusion on HDL function in T2D	Randomized, placebo-controlled, double-blind, cross-over intervention	T2D. No major illness incl. CHD, no PPAR agonists, metformin, lipid-modifying therapy, or anticoagulants

Study subjects - #	Readout of HDL anti-inflammatory function	HDL isolation	Intervention	Treatment duration	Notes
14 (100% DM)	*Ex vivo:* thrombin-induced MCP1-mRNA expression by HUVEC	PEG-precipitation to deplete plasma from apoB	simvastatin and / or bezafibrate (orally)	4 x 8 weeks	Experimental controls differed from patient HDL samples (did not include isolation material (PEG)) No correction for amount of HDL.
30 (50% DM)	*Ex vivo:* ICAM-1 and VCAM-1 expression (HUVEC) and monocyte adhesion (THP-1 cells)	DGUC; 1.13-1.21g/ml.	n.a	n.a.	Only HDL3
12 (50% DM)	*Ex vivo* and *in vitro*: LPS-stimulated IL1-β and TNF-α production by macrophages (THP-1 cells).	DGUC; 1,063-1,21g/ml	n.a	n.a.	Crucial experiment only compares effect of HDL between cases and controls, does not compare effect of HDL with LPS alone. Other experiments were not done with patient material.
124 (75% DM)	Ex vivo and in vitro: HII (HAEC)	FPLC	n.a	n.a.	
72 (60% DM)	*Ex vivo:* HII (HAEC)	FPLC	L-4F (IV)	7 days	High intra-assay variability (21%). No power calculation. No diabetes subgroup analysis. Industry-sponsored.
108 (76% DM)	*Ex vivo:* HII (HAEC)	FPLC	L-4F (SC)	28 days	High intra-assay variability (21%). No power calculation. No diabetes subgroup analysis. Industry-sponsored
20 mice (50% DM)	*In vivo:* Macrophage immunostaining in and atherosclerotic plaque size at aortic root	n.a.	D-4F (orally)	8 weeks	
In vivo: 27 rabbits. HDL from 6 T2D patients	1. *in vivo*: neutrophil infiltration, VCAM-1 + ICAM-1 expression in carotid artery 2. *in vitro*: TNF-α induced VCAM-1 and ICAM-1 expression (HCAEC)	Sequential UC; 1.063-1.21g/ml	lipid-free apoA-I or rHDL (IV)	1 dose	Patient apoA-I not used in *in vitro* experiments. Glycation levels much higher *in vitro* than *in vivo*.
13 (100% DM)	1. *ex vivo:* TNF-α stimulated VCAM1 + ICAM1 expression (HCAEC) 2. *in vivo:* CD11b expression on patient PBMCs	sequential UC; 1.063-1.21g/ml	rHDL (IV)	1 dose	

Table 1. Details of the included studies. (*continued*)

Source	Aim	Design	Inclusion criteria
Bloedon 2008 [34]	1. D-4F safety, tolerability, PK and PD in CHD or risk equivalent. 2. D-4F effect on HDL function.	Randomized, placebo-controlled, double-blind, intervention	Stable CHD or risk equivalent, 21-75y old, >4w statin use, HbA1c <10%. No CHF, NYHA III/IV AP, or uncontrolled hypertension. No niacin >500mg, fibrate, increased CK, or albumin <2.5mg/dl.
Peterson 2008 [36]	L-4F effect on inflammatory markers in mice with diabetes	Placebo-controlled intervention	Cases: ob/ob mice, 9w old, established diabetes. Controls: age- and sex-matched lean mice
van Linthout 2008 [37]	Effect of human apoA-I gene transfer on diabetic cardiomyopathy in rats	Case-control and placebo-controlled intervention	Streptozotocin-induced diabetes in Sprague-Dawley rats, blood glucose ≥300mg/dL
Hoang 2007 [38]	Effect of glycation on of HDL/apoA-I function	1. HDL function: observational 2. Glycation status: case-control	AI effects: pooled plasma from healthy donors. Glycation status: DM with nephropathy vs healthy volunteers.
Hedrick 2000 [39]	Effect of glycation on HDL function	Observational	Healthy human donors

AI: anti-inflammatory, AP: angina pectoris, apoB: apolipoprotein B, apoE: apolipoprotein E, CHF: congestive heart failure, CVD: cardiovascular disease, DGUC: density gradient ultracentrifugation, DM: diabetes mellitus, FPLC: fast protein liquid chromatography, HAEC: human aortic endothelial cells, HCAEC: human coronary artery endothelial cells, HII: HDL inflammatory index, ICAM-1: intercellular adhesion molecule 1, LPS: lipopolysaccharide, MCP-1: monocyte chemoattractant protein-1, n.a.: not applicable, NYHA: New York Heart Association, NZW: New-Zealand White, PBMC: peripheral blood mononuclear cell, PD: pharmacodynamics, PEG: polyethylene glycol, PK: pharmacokinetics, PPAR: peroxisome proliferator-activated receptor, rHDL: reconstituted HDL, T2D: type 2 diabetes, TG: triglycerides, UC: ultracentrifugation, VCAM-1: vascular cell adhesion molecule 1.

	Study subjects - #	Readout of HDL anti-inflammatory function	HDL isolation	Intervention	Treatment duration	Notes
	50 (70% DM)	Ex vivo and in vitro: HII (HAEC)	FPLC	D-4F (orally)	1 dose	No diabetes subgroup analysis
	36 (55% DM)	*In vivo:* plasma IL-6, IL-1β, and adiponectin levels	n.a.	L-4F (intra-peritoneally)	6 weeks	
	18 (67% DM)	*In vivo:* mRNA levels of VCAM1, ICAM1 and TNF-α in cardiomyocytes	n.a.	human apoA-I gene transfer	6 weeks	
	Glycation status: 15 (66.7% DM)	*Ex vivo:* CD11b expression (THP-1 monocytes)	Sequential UC (density range not specified)	n.a	n.a.	Functional experiments not done with patient HDL.
	5 (no DM)	*In vitro:* LDL-stimulated monocyte adhesion (HAEC, monocytes from healthy subjects)	DGUC (density range not specified)	n.a	n.a.	Functional experiments not done with patient HDL.

Table 2a. Risk of bias summary for the included observational studies.

	Tong 2013 [28]	Liu 2012 [29]	Morgantini 2011 [30]	Nobecourt 2010 - in vitro arm [32]	van Linthout 2008 [37]	Hoang 2007 [38]	Hedrick 2000 [39]
Selection cases	?	?	?	n.a.	-	n.a.	n.a.
Selection controls	+	+	?	?	-	+	?
Outcome measurement	-	-	-	-	-	-	-
Classification bias	-	?	?	-	-	+	-
Clinical applicability	?	?	-	+	+	+	+
Analysis of results	-	-	-	-	-	-	+
Overall risk of bias regarding our study question	+	+	?	?	-	+	+

- = low risk of bias, + = high risk of bias, ? = insufficient information to evaluate risk of bias. I.v.: intravenous, s.c.: subcutaneous, n.a. = not applicable. Key domains are underlined.

Table 2b. Risk of bias summary for the included intervention studies.

	Triolo 2014 [27]	Watson 2011 – i.v. study [31]	Watson 2011 – s.c. study [31]	Morgantini 2010 [35]	Nobecourt 2010 [32]	Patel 2009 [33]	Bloedon 2008 [34]	Peterson 2008 [36]	van Linthout 2008 [37]
Random sequence generation	?	?	?	?	?	?	?	+	+
Allocation concealment	?	?	?	?	?	?	?	+	+
Blinding of participants and personnel	-	-	-	-	-	-	-	-	-
Blinding of outcome measurement	-	-	-	-	-	-	-	-	-
Imcomplete outcome data	-	-	-	?	-	-	-	?	?
Selective reporting	?	-	?	?	?	?	?	?	?
Other sources of bias	-	-	-		-	-	+	-	-
Overall risk of bias regarding our study question	?	?	?	?	?	?	?	+	+

- = low risk of bias, + = high risk of bias, ? = insufficient information to evaluate risk of bias. I.v.: intravenous, s.c.: subcutaneous, n.a. = not applicable. Key domains are underlined.

Table 3. Details on in vitro glycation studies

	Glycation method	Anti-oxidant added?	Effect on HDL anti-inflammatory function	in vitro glycation: relative to healthy HDL	in vivo glycation: relative to healthy HDL
Liu 2012 [29]	7 days incubation. 5, 10, 25, or 50mmol/L glucose	yes	TNF-α and IL1-β secretion ↑ (20-50%)	Glycation of lysines in apoA-I: 28x ↑	Glycation of lysines in apoA-I: 4x ↑
Hoang 2007 [38]	18 hours incubation. 500mmol/L ribose, dialysis, 5 day storage.	no	PMA-induced CD11b on monocytes ↑	CML: 50-100x ↑	CML: 10x ↑
Nobécourt 2010 [32]	24 hours incubation with 1.5 (lipid-free apoA-I) or 3.0mM (rHDL) methylglyoxal, dialysis.	no	Endothelial VCAM-1 and ICAM-1 expression ↑	CML: 1,8x ↑ CEL: 17,8x ↑ MG-H2: 186x ↑ Arginine, lysine, and tryptophan: 15-40% modified	CML: 1.7x ↑ CEL: 4,5x ↑ MG-H2: 1,3x ↑ Arginine, lysine and tryptophan: no modification
Hedrick 2000 [39]	1 week incubation. 25mmol/L glucose.	no	Monocyte adhesion ↑	CML: 1.6x ↑ Fructoselysine: 3x ↑	n.a.

CEL: Nε-carboxyethyllysine, CML: Nε-carboxymethyllysine, ICAM-1: intercellular adhesion molecule-1, VCAM-1: vascular cell adhesion molecule-1, MG-H2: (2S)-2-amino-5-(2-amino-5-methyl-4-oxo-4,5-dihydro-imidazol-1-yl)-pentanoic acid, n.a.: not applicable, PMA: phorbol 12-myristate 13-acetate

Plasma levels of HbA1c reflect long-term *in vivo* glycation burden [40]. Two studies reported on the association between HDL anti-inflammatory function and HbA1c. HbA1c levels correlated with monocyte chemotactic protein-1 (MCP-1) mRNA levels in thrombin-stimulated macrophages [27], but no correlation was found with the HII [30]. The risk of bias in these studies was either unclear or high.

Other determinants of HDL anti-inflammatory function in diabetes

The concentration of HDL constituents was related to its anti-inflammatory function in one study: the apoA-I and phospholipid concentrations in the HDL particle correlated negatively with endothelial cell expression of VCAM-1 and ICAM-1 in the presence of HDL [33].

Several systemic factors were considered as modulators of HDL anti-inflammatory function. Plasma levels of serum amyloid A, a marker of systemic inflammation, correlated with the HII [30]. Baseline BMI, waist circumference, total cholesterol, and apoB but not apoA-I correlated with individual changes in thrombin-induced MCP-1 mRNA levels in HUVECs after lipid-lowering treatment [27]. Risk of bias in these studies was unclear.

Interventions and anti-inflammatory function of HDL

Four studies investigated whether interventions with apoA-I mimetics, rHDL, statins, or fibrates could improve the anti-inflammatory function of HDL in T2D [27,31,33,34], partly based on results obtained with animal models of diabetes [35-37]. The risk of bias was either unclear or high in these studies.

Patel et al. [33] studied the short-term effects of infusing persons with T2D with rHDL, reconstituted from apoA-I and phospholipids. rHDL decreased plasma levels of soluble VCAM-1 but not soluble ICAM-1 or C-reactive protein (CRP). It also significantly reduced the expression of the adhesion molecule CD11b on circulating monocytes and adhesion of neutrophils to a fibrinogen matrix. Moreover, 4 and 72 hours after rHDL infusion, isolated HDL decreased TNF-α induced VCAM-1 expression in human coronary artery endothelial cells more than after placebo infusion. This reduced VCAM-1 expression correlated with an increase in plasma HDL after the rHDL infusion [33]. In rats with streptozotocin-induced diabetes, raising apoA-I levels through gene transfer of human apoA-I decreased cardiac expression of ICAM-1, VCAM-1 and TNF-α to levels similar to those in non-diabetic rats [37]. Simultaneously, apoA-I gene transfer decreased cardiac oxidative stress and apoptosis.

Two intervention studies used the apo-AI mimetic peptides D-4F or L-4F, which are based on the α-helical amphipathic repeats in apoA-I that bind phospholipids [24]. In the study by Bloedon et al. [34], D-4F treatment changed the HII from a pro- to an anti-inflammatory value 8 hours after a single oral dose, while placebo treatment did not. *In vitro* treatment of plasma from T2D individuals with D-4F also reduced the HII. Watson et al. [31] reported that L-4F treatment of persons with CVD, of whom the majority had diabetes, did not

improve the HII nor did it suppress plasma levels of CRP. *In vitro* treatment of plasma from T2D individuals with L-4F did reduce the HII [30,31].

In diabetic mice, D-4F treatment decreased the macrophage content of atherosclerotic plaques as well as the lesion size [35]. L-4F treatment of diabetic mice decreased plasma levels of IL-1β and IL-6 and increased adiponectin, coinciding with improved insulin sensitivity and decreased oxidative stress [36].

Regarding lipid-lowering therapy, Triolo et al. [27] found that treatment with simvastatin, bezafibrate, or both failed to improve the anti-inflammatory function of HDL in individuals with T2D, as measured *ex vivo* by thrombin-induced MCP1 mRNA expression in HUVECs.

Discussion

The results from this systematic review indicate a diminished anti-inflammatory function of HDL in T2D subjects compared to healthy controls. The direction of causality and the underlying mechanisms remain to be elucidated. Whether this dysfunction can be extended to T1D or whether a relationship exists with vascular disease in diabetes has not been investigated. Restoring the anti-inflammatory effects of HDL through rHDL infusion or apoA-I mimetic peptides shows potential, but the evidence is limited and the effect on clinical end-points in diabetes has not been studied.

Three studies concluded that the anti-inflammatory capacity of HDL in persons with T2D was decreased compared to healthy subjects. A simplified overview of the current evidence is given in figure 2. Considering that different outcome assessments were used, and that no contradictory results have been published, this conclusion is robust. However, the controls were slightly - although not statistically significant - younger than the cases in two of the studies [29,30], possibly leading to an over-estimation of the difference. Moreover, publication bias cannot be excluded. A decreased anti-inflammatory function of HDL seems to be a common feature of diseases with a pro-inflammatory state, which has also been reported for cardiovascular and chronic kidney disease [5]. Morgantini et al. excluded subjects with kidney disease or other major diseases [30], showing that at least part of the dysfunction is specific for T2D. It is unclear whether T2D causes dysfunctional HDL or vice versa. HDL could become dysfunctional due to mechanisms such as inflammation or glycation in diabetes, or dysfunctional HDL could cause T2D through dysfunction of the β-cell. Some evidence exists for the latter process [41]. However, to the best of our knowledge, whether HDL influences the β-cell through an effect on inflammation is unknown.

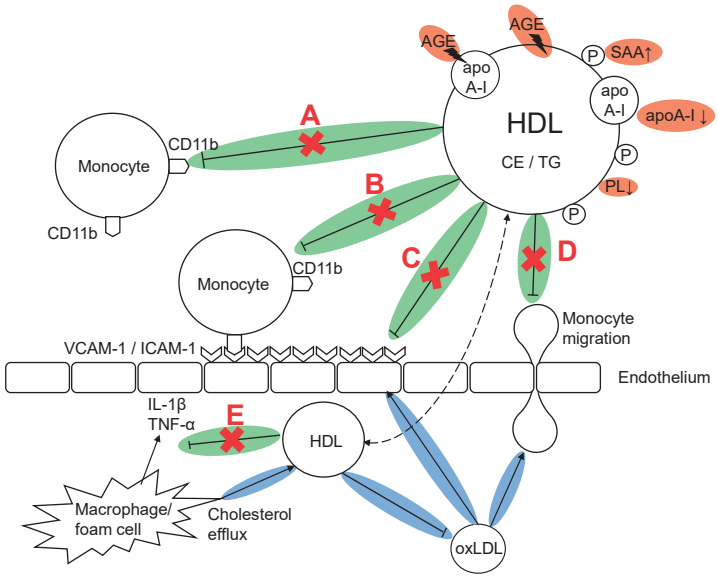

Figure 2. Schematic overview of HDLs loss of anti-inflammatory capacity in T2D.

In green: inflammatory processes that HDL normally inhibits, but does not or less so in T2D. A) expression of the adhesion molecule CD11b expression on monocytes; B) adhesion of monocytes to endothelial cells; C) expression of the adhesion molecules VCAM-1 and ICAM-1 on endothelial cells; D) monocyte migration through the endothelium; and E) cytokine release by macrophages. In orange: potential determinants of the loss of HDL anti-inflammatory capacity in T2D, as described in this review. In blue: mechanisms through which HDL may inhibit inflammation indirectly, but which are outside the scope of this review. Depicted are the effect of HDL on 1) cholesterol removal from foam cells, making them less pro-inflammatory, and 2) LDL oxidation in the subendothelial space, which is a pro-inflammatory trigger. All readouts reported in this review were investigated in plasma, therefore the anti-inflammatory effects of HDL in the subendothelial space are not exactly known. AGE: advanced glycation end products, apoA-I: apolipoprotein A-I, CE: cholesterol esters, HDL: high density lipoprotein, ICAM: intercellular adhesion molecule-1, IL-1β: interleukin-1β, oxLDL: oxidated LDL, P: protein, PL: phospholipids, SAA: serum amyloid A, TG: triacyl glycerols, TNF-α: tumor necrosis factor-α, VCAM-1: vascular cell adhesion molecule-1.

To better understand why the anti-inflammatory capacity of HDL is decreased in diabetes, its determinants need to be elucidated. Determinants that have been studied in diabetes were non-enzymatic glycation, HDL composition, and systemic factors. HDL constitutes a very heterogeneous population of particles. In healthy persons, small-dense HDL particles (HDL3) are thought to express HDLs anti-atherogenic properties to a higher extent than large HDL2 particles [42]. However, large-scale clinical studies frequently suggest that large HDL is anti-atherogenic and small HDL is pro-atherogenic [43]. Due to the strong associations between the number of large HDL particles, HDL-cholesterol, the total number of HDL particles and the total number of LDL particles, it is difficult to assign an anti-atherogenic function to a specific HDL subpopulation [43]. Small and large HDL had a similar effect on

oxidation of LDL, as a proxy of HDLs anti-inflammatory function, in healthy persons [44]. Thus, which HDL particles are responsible for its anti-inflammatory capacity and how they relate to the loss of function in T2D remains to be clarified.

Non-enzymatic glycation is a major pathophysiological process in diabetes complications [4]. There is evidence that *in vitro* glycation reduces HDL anti-inflammatory capacity [29,32,38,39]. Several pathophysiological mechanisms may explain this finding. AGE formation leads to changes in the conformation and surface charge of HDL apolipoproteins [45] and diminishes the activity of HDL-bound enzymes like lecithin-cholesterol acyltransferase [45] and para-oxonase-1 (PON-1) [39,46,47]. Furthermore, AGEs binding to the AGE-receptor generate pro-inflammatory signals [48]. However, AGE levels in HDL after *in vitro* glycation were 5-150 fold higher than after *in vivo* glycation in T2D subjects [29,32,38], and no correlation was seen between the HII and HbA1c levels. Therefore, *in vitro* findings may not directly translate to the *in vivo* situation. Whether *in vivo* glycation of HDL has a direct effect on its anti-inflammatory effects in T2D cannot be concluded from the current literature. Of note, in the study by Nobécourt et al. [32], HDL was isolated from subjects with T2D who also suffered from end-stage renal disease, which by itself renders HDL dysfunctional [49-51]. Therefore, the contribution of glycation to the loss of HDLs anti-inflammatory function in this study is unclear.

Patel et al. [33] studied HDL composition as a determinant and found that apoA-I and phospholipid concentration correlated positively with HDLs anti-inflammatory capacity in T2D. Insights into the underlying molecular mechanisms are, however, limited. In healthy subjects, HDL anti-inflammatory function correlated negatively with HDL content of cholesteryl-esters, triglycerides, and sphingolipids, notably sphingomyelin and ceramides [44,52]. In addition, sphingosine-1-phospate (S1P) has important signaling functions in vascular and immune cell function, especially when bound to HDL [53,54]. HDL-bound S1P increased HDLs ability to protect endothelial cells in T2D [28,55] but was decreased by glycation [55,56]. Other potential determinants are the proteins bound to HDL. For example, HDL-bound PON-1, an anti-oxidative protein, shows diminished activity in T2D [57], and the total proteome is changed in CVD [58]. Finally, the amount of oxidized phospholipids (oxPL) bound to HDL correlated negatively to HDLs anti-oxidative function in T2D [30]. Since all these factors are associated with the anti-inflammatory function of HDL in healthy persons or with other functions of HDL in T2D, changes in the lipidome, proteome or oxPL content of HDL might also influence its anti-inflammatory function in diabetes.

Systemic inflammation [30] and body composition [27] correlated with the anti-inflammatory function of HDL in diabetes. Inflammation has been shown to change HDL from anti- to pro-inflammatory in subjects undergoing cardiac surgery [59]. Body fat in healthy young men correlated negatively to HDLs anti-oxidative function [60], which in turn is related to the anti-inflammatory function [61]. The impact of these systemic factors on HDLs anti-inflammatory function in diabetes need to be further elucidated.

Insights into the mechanisms involved in HDLs anti-inflammatory dysfunction may lead to new possibilities for intervention. The effects of intervention were investigated for rHDL, apoA-I mimetics, and lipid-lowering medication. Remarkably, the basic question as to whether loss of HDL anti-inflammatory capacity can be altered by glucose regulation in diabetes has, to the best of our knowledge, not been reported. In men with metabolic syndrome, however, weight loss through diet and exercise was shown to change HDL from pro- to anti-inflammatory even though HDL-cholesterol levels decreased [62].

HDL-based interventions reduced inflammation in animal models of diabetes, and improved the anti-inflammatory function of HDL from humans with T2D, although the evidence in humans is less robust than in animal models of diabetes. rHDL infusions increased the anti-inflammatory effects of HDL mainly through increasing the amount of HDL in plasma [33]. In addition, it improved cholesterol efflux [33], reduced fasting plasma glucose and increased insulin levels [63]. In a human cohort of whom less than 25% had diabetes, rHDL infusion improved atherosclerotic plaque composition and *in vitro* cholesterol efflux [64,65]. However, the therapy is expensive, rHDL has to be administered intravenously, and the optimal composition for treatment of diabetes and its complications remains to be defined [66].

Little evidence is available for the efficacy of apoA-I mimetic peptides in humans with diabetes. The studies by Bloedon [34] and Watson [31] only showed an at most small beneficial effect of apoA-I mimetic peptides in subjects of whom the majority had diabetes. After these studies had been published, it became evident that the dosage of mimetic peptide rather than the plasma levels determines its efficacy [67-69]. Recent evidence in mice shows that oral administration of transgenic tomatoes expressing the apoA-I mimetic L-6F reduces systemic inflammation by reducing inflammatory oxPL in the intestine [70]. As intestinal inflammation and gut microbiota may play a role in the development of diabetes [71], this supports the potential of apoA-I mimetics in individuals with diabetes.

Taken together, HDL-based therapies show potential in diabetes for decreasing inflammation, but studies investigating hard clinical end-points and chronic effects are scarce. Studies aiming at HDL metabolism thus far have not shown a reduction of clinical end-points [72]. Of note, these studies investigated apoA-I formulations or targeted HDL-cholesterol, thereby disregarding other components of HDL. Since the biological effects of HDL are broad, a more thorough understanding is needed for the development of HDL-based interventions that could result in a reduction of clinical end-points [72].

Neither statin nor fibrate treatment improved the anti-inflammatory function of HDL in diabetes, although it did improve cholesterol efflux [27]. This study included only men and may have been underpowered for changes in anti-inflammatory function. In contrast, simvastatin treatment did improve the HII in persons with high CVD risk, especially in the small subgroup of persons with diabetes [73]. Statins down-regulate ATP-binding cas-

sette transporter-1 expression, which not only regulates cholesterol efflux but also HDLs anti-inflammatory function [67]. More research is needed to investigate the effect of lipid-lowering therapy on HDL function and the therapeutic consequences in diabetes.

This paper critically reviewed the evidence on the anti-inflammatory effects of HDL in diabetes. The major strengths are the systematic approach and the quality assessment by multiple independent researchers. A limitation is that study selection was difficult since the anti-inflammatory function of HDL is inconsistently defined. Since no uniform assay for measuring HDLs anti-inflammatory function exists, consensus on what the best assay is remains to be sought. Moreover, it is unknown whether the *in vivo* anti-inflammatory function of HDL is an independent trait, or secondary to for example its anti-oxidative function. In this review, we have focused only on studies investigating the direct effects of HDL on inflammation markers and processes.

Several limitations regarding the included studies need to be considered. First, most studies were cross-sectional and therefore not suitable for assessing causality or reverse causality of HDL dysfunction in diabetes. Second, there was huge heterogeneity in study methodology and outcome measures, making meta-analyzing the results not meaningful. Third, only a few studies have directly investigated patient-derived HDL. Where possible, we have compared and discussed the *in vitro* and *ex vivo* outcomes. Finally, nearly all included studies contained either insufficient information to determine the risk of bias, or had a high risk of bias.

To summarize, this systematic review strongly supports the conclusion that the ability of HDL to suppress inflammatory signals is diminished in T2D. However, the exact underlying mechanisms, direction of causality, and consequences *in vivo* cannot be determined from the current literature. Potential determinants modulating HDL function include *in vivo* glycation of HDL, HDL size, HDL lipidome, and HDL proteome. ApoA-I mimetic peptides and rHDL are potential treatment options for restoring HDL function in diabetes, but large trials investigating clinically relevant outcomes in diabetes are lacking. Consensus about the best method to measure HDL anti-inflammatory capacity needs to be reached. Subsequently, future research may reveal the *in vivo* implications of *in vitro* and *ex vivo* results, and lead to identification of *in vivo* biomarkers for the effects of HDL on inflammation in individuals with diabetes. Additional prospective studies are required for determining causality. These results might clarify how HDL anti-inflammatory function is lost in diabetes and establish its determinants and relation to vascular complications. This improved knowledge on HDL biology could enable development of treatments directed at restoring HDL function, which might eventually decrease the burden of disease.

References

[1] WHO Media Centre. Diabetes Fact Sheet N°312. 2015;2015.

[2] International Diabetes Federation - Complications of diabetes. ;2016.

[3] Donath MY, Shoelson SE. Type 2 diabetes as an inflammatory disease. Nat Rev Immunol. 2011;11:98-107.

[4] Forbes JM, Cooper ME. Mechanisms of diabetic complications. Physiol Rev. 2013;93:137-188.

[5] Saemann MD, Poglitsch M, Kopecky C, Haidinger M, Horl WH, Weichhart T. The versatility of HDL: a crucial anti-inflammatory regulator. Eur J Clin Invest. 2010;40:1131-1143.

[6] Kontush A., John CM. Why is HDL functionally deficient in type 2 diabetes? Curr Diabetes Rep. 2008;8:51-59.

[7] Gordon DJ, Probstfield JL, Garrison RJ, Neaton JD, Castelli WP, Knoke JD, Jacobs DR,Jr, Bangdiwala S, Tyroler HA. High-density lipoprotein cholesterol and cardiovascular disease. Four prospective American studies. Circulation. 1989;79:8-15.

[8] Wilson PW, Meigs JB, Sullivan L, Fox CS, Nathan DM, D'Agostino RB S. Prediction of incident diabetes mellitus in middle-aged adults: the Framingham Offspring Study. Arch Intern Med. 2007;167:1068-1074.

[9] Keene D, Price C, Shun-Shin MJ, Francis DP. Effect on cardiovascular risk of high density lipoprotein targeted drug treatments niacin, fibrates, and CETP inhibitors: meta-analysis of randomised controlled trials including 117,411 patients. BMJ. 2014;349:g4379.

[10] Haase CL, Tybjaerg-Hansen A, Qayyum AA, Schou J, Nordestgaard BG, Frikke-Schmidt R. LCAT, HDL cholesterol and ischemic cardiovascular disease: a Mendelian randomization study of HDL cholesterol in 54,500 individuals. J Clin Endocrinol Metab. 2012;97:E248-56.

[11] Haase CL, Tybjaerg-Hansen A, Nordestgaard BG, Frikke-Schmidt R. HDL Cholesterol and Risk of Type 2 Diabetes: A Mendelian Randomization Study. Diabetes. 2015;64:3328-3333.

[12] Heinecke JW. The protein cargo of HDL: implications for vascular wall biology and therapeutics. J Clin Lipidol. 2010;4:371-375.

[13] Kontush A, Chantepie S, Chapman MJ. Small, dense HDL particles exert potent protection of atherogenic LDL against oxidative stress. Arterioscler Thromb Vasc Biol. 2003;23:1881-1888.

[14] Riwanto M, Rohrer L, Roschitzki B, Besler C, Mocharla P, Mueller M, Perisa D, Heinrich K, Altwegg L, von Eckardstein A, Luscher TF, Landmesser U. Altered activation of endothelial anti- and pro-apoptotic pathways by high-density lipoprotein from patients with coronary artery disease: role of high-density lipoprotein-proteome remodeling. Circulation. 2013;127:891-904.

[15] Gordon S.M., Hofmann S., Askew D.S., Davidson W.S. High density lipoprotein: It's not just about lipid transport anymore. Trends Endocrinol Metab. 2011;22:9-15.

[16] Cockerill GW, Rye KA, Gamble JR, Vadas MA, Barter PJ. High-density lipoproteins inhibit cytokine-induced expression of endothelial cell adhesion molecules. Arterioscler Thromb Vasc Biol. 1995;15:1987-1994.

[17] Murphy AJ, Woollard KJ, Hoang A, Mukhamedova N, Stirzaker RA, McCormick SP, Remaley AT, Sviridov D, Chin-Dusting J. High-density lipoprotein reduces the human monocyte inflammatory response. Arterioscler Thromb Vasc Biol. 2008;28:2071-2077.

[18] Navab M, Imes SS, Hama SY, Hough GP, Ross LA, Bork RW, Valente AJ, Berliner JA, Drinkwater DC, Laks H. Monocyte transmigration induced by modification of low density lipoprotein in cocultures of human aortic wall cells is due to induction of monocyte chemotactic protein 1 synthesis and is abolished by high density lipoprotein. J Clin Invest. 1991;88:2039-2046.

[19] Weber C, Noels H. Atherosclerosis: current pathogenesis and therapeutic options. Nat Med. 2011;17:1410-1422.
[20] Rosenson RS. The High-Density Lipoprotein Puzzle: Why Classic Epidemiology, Genetic Epidemiology, and Clinical Trials Conflict? Arterioscler Thromb Vasc Biol. 2016;36:777-782.
[21] Garvey WT, Kwon S, Zheng D, Shaughnessy S, Wallace P, Hutto A, Pugh K, Jenkins AJ, Klein RL, Liao Y. Effects of insulin resistance and type 2 diabetes on lipoprotein subclass particle size and concentration determined by nuclear magnetic resonance. Diabetes. 2003;52:453-462.
[22] Ansell BJ, Fonarow GC, Navab M, Fogelman AM. Modifying the anti-inflammatory effects of high-density lipoprotein. Curr Atheroscler Rep. 2007;9:57-63.
[23] Autran D, Attia N, Dedecjus M, Durlach V, Girard-Globa A. Postprandial reverse cholesterol transport in type 2 diabetic patients: effect of a lipid lowering treatment. Atherosclerosis. 2000;153:453-460.
[24] White CR, Garber DW, Anantharamaiah GM. Anti-inflammatory and cholesterol-reducing properties of apolipoprotein mimetics: a review. J Lipid Res. 2014;55:2007-2021.
[25] Higgins JPT, Green S. Cochrane Handbook for Systematic Reviews of Interventions. 2011;2015.
[26] Critical Appraisal Skills Programme (CASP). 2014;2014.
[27] Triolo M, Annema W, de Boer JF, Tietge UJ, Dullaart RP. Simvastatin and bezafibrate increase cholesterol efflux in men with type 2 diabetes. Eur J Clin Invest. 2014;44:240-248.
[28] Tong X, Peng H, Liu D, Ji L, Niu C, Ren J, Pan B, Hu J, Zheng L, Huang Y. High-density lipoprotein of patients with type 2 diabetes mellitus upregulates cyclooxgenase-2 expression and prostacyclin I-2 release in endothelial cells: relationship with HDL-associated sphingosine-1-phosphate. Cardiovasc Diabetol. 2013;12:27-2840-12-27.
[29] Liu D, Ji L, Zhang D, Tong X, Pan B, Liu P, Zhang Y, Huang Y, Su J, Willard B, Zheng L. Nonenzymatic glycation of high-density lipoprotein impairs its anti-inflammatory effects in innate immunity. Diabetes Metab Res Rev. 2012;28:186-195.
[30] Morgantini C, Natali A, Boldrini B, Imaizumi S, Navab M, Fogelman AM, Ferrannini E, Reddy ST. Anti-inflammatory and antioxidant properties of HDLs are impaired in type 2 diabetes. Diabetes. 2011;60:2617-2623.
[31] Watson CE, Weissbach N, Kjems L, Ayalasomayajula S, Zhang Y, Chang I, Navab M, Hama S, Hough G, Reddy ST, Soffer D, Rader DJ, Fogelman AM, Schecter A. Treatment of patients with cardiovascular disease with L-4F, an apo-A1 mimetic, did not improve select biomarkers of HDL function. J Lipid Res. 2011;52:361-373.
[32] Nobecourt E, Tabet F, Lambert G, Puranik R, Bao S, Yan L, Davies MJ, Brown BE, Jenkins AJ, Dusting GJ, Bonnet DJ, Curtiss LK, Barter PJ, Rye KA. Nonenzymatic glycation impairs the antiinflammatory properties of apolipoprotein A-I. Arterioscler Thromb Vasc Biol. 2010;30:766-772.
[33] Patel S, Drew BG, Nakhla S, Duffy SJ, Murphy AJ, Barter PJ, Rye KA, Chin-Dusting J, Hoang A, Sviridov D, Celermajer DS, Kingwell BA. Reconstituted high-density lipoprotein increases plasma high-density lipoprotein anti-inflammatory properties and cholesterol efflux capacity in patients with type 2 diabetes. J Am Coll Cardiol. 2009;53:962-971.
[34] Bloedon LT, Dunbar R, Duffy D, Pinell-Salles P, Norris R, DeGroot BJ, Movva R, Navab M, Fogelman AM, Rader DJ. Safety, pharmacokinetics, and pharmacodynamics of oral apoA-I mimetic peptide D-4F in high-risk cardiovascular patients. J Lipid Res. 2008;49:1344-1352.
[35] Morgantini C, Imaizumi S, Grijalva V, Navab M, Fogelman AM, Reddy ST. Apolipoprotein A-I mimetic peptides prevent atherosclerosis development and reduce plaque inflammation in a murine model of diabetes. Diabetes. 2010;59:3223-3228.

[36] Peterson SJ, Drummond G, Kim DH, Li M, Kruger AL, Ikehara S, Abraham NG. L-4F treatment reduces adiposity, increases adiponectin levels, and improves insulin sensitivity in obese mice. J Lipid Res. 2008;49:1658-1669.

[37] Van Linthout S, Spillmann F, Riad A, Trimpert C, Lievens J, Meloni M, Escher F, Filenberg E, Demir O, Li J, Shakibaei M, Schimke I, Staudt A, Felix SB, Schultheiss HP, De Geest B, Tschope C. Human apolipoprotein A-I gene transfer reduces the development of experimental diabetic cardiomyopathy. Circulation. 2008;117:1563-1573.

[38] Hoang A, Murphy AJ, Coughlan MT, Thomas MC, Forbes JM, O'Brien R, Cooper ME, Chin-Dusting JP, Sviridov D. Advanced glycation of apolipoprotein A-I impairs its anti-atherogenic properties. Diabetologia. 2007;50:1770-1779.

[39] Hedrick CC, Thorpe SR, Fu MX, Harper CM, Yoo J, Kim SM, Wong H, Peters AL. Glycation impairs high-density lipoprotein function. Diabetologia. 2000;43:312-320.

[40] Nathan DM, Turgeon H, Regan S. Relationship between glycated haemoglobin levels and mean glucose levels over time. Diabetologia. 2007;50:2239-2244.

[41] Kruit JK, Brunham LR, Verchere CB, Hayden MR. HDL and LDL cholesterol significantly influence beta-cell function in type 2 diabetes mellitus. Curr Opin Lipidol. 2010;21:178-185.

[42] Kontush A, Chapman MJ. Antiatherogenic small, dense HDL--guardian angel of the arterial wall? Nat Clin Pract Cardiovasc Med. 2006;3:144-153.

[43] Kontush A. HDL particle number and size as predictors of cardiovascular disease. Front Pharmacol. 2015;6:218.

[44] Camont L, Lhomme M, Rached F, Le Goff W, Negre-Salvayre A, Salvayre R, Calzada C, Lagarde M, Chapman MJ, Kontush A. Small, dense high-density lipoprotein-3 particles are enriched in negatively charged phospholipids: relevance to cellular cholesterol efflux, antioxidative, antithrombotic, anti-inflammatory, and antiapoptotic functionalities. Arterioscler Thromb Vasc Biol. 2013;33:2715-2723.

[45] Nobecourt E, Davies MJ, Brown BE, Curtiss LK, Bonnet DJ, Charlton F, Januszewski AS, Jenkins AJ, Barter PJ, Rye KA. The impact of glycation on apolipoprotein A-I structure and its ability to activate lecithin:cholesterol acyltransferase. Diabetologia. 2007;50:643-653.

[46] Mastorikou M, Mackness B, Liu Y, Mackness M. Glycation of paraoxonase-1 inhibits its activity and impairs the ability of high-density lipoprotein to metabolize membrane lipid hydroperoxides. Diabet Med. 2008;25:1049-1055.

[47] Ferretti G, Bacchetti T, Marchionni C, Caldarelli L, Curatola G. Effect of glycation of high density lipoproteins on their physicochemical properties and on paraoxonase activity. Acta Diabetol. 2001;38:163-169.

[48] Ott C, Jacobs K, Haucke E, Navarrete Santos A, Grune T, Simm A. Role of advanced glycation end products in cellular signaling. Redox Biol. 2014;2:411-429.

[49] Kaseda R, Jabs K, Hunley TE, Jones D, Bian A, Allen RM, Vickers KC, Yancey PG, Linton MF, Fazio S, Kon V. Dysfunctional high-density lipoproteins in children with chronic kidney disease. Metabolism. 2015;64:263-273.

[50] Tolle M, Huang T, Schuchardt M, Jankowski V, Prufer N, Jankowski J, Tietge UJ, Zidek W, van der Giet M. High-density lipoprotein loses its anti-inflammatory capacity by accumulation of pro-inflammatory-serum amyloid A. Cardiovasc Res. 2012;94:154-162.

[51] Yamamoto S, Yancey PG, Ikizler TA, Jerome WG, Kaseda R, Cox B, Bian A, Shintani A, Fogo AB, Linton MF, Fazio S, Kon V. Dysfunctional high-density lipoprotein in patients on chronic hemodialysis. J Am Coll Cardiol. 2012;60:2372-2379.

[52] Patel S, Puranik R, Nakhla S, Lundman P, Stocker R, Wang XS, Lambert G, Rye KA, Barter PJ, Nicholls SJ, Celermajer DS. Acute hypertriglyceridaemia in humans increases the triglyceride content and decreases the anti-inflammatory capacity of high density lipoproteins. Atherosclerosis. 2009;204:424-428.

[53] Poti F, Simoni M, Nofer JR. Atheroprotective role of high-density lipoprotein (HDL)-associated sphingosine-1-phosphate (S1P). Cardiovasc Res. 2014;103:395-404.

[54] Maceyka M, Harikumar KB, Milstien S, Spiegel S. Sphingosine-1-phosphate signaling and its role in disease. Trends Cell Biol. 2012;22:50-60.

[55] Tong X, Lv P, Mathew AV, Liu D, Niu C, Wang Y, Ji L, Li J, Fu Z, Pan B, Pennathur S, Zheng L, Huang Y. The compensatory enrichment of sphingosine -1- phosphate harbored on glycated high-density lipoprotein restores endothelial protective function in type 2 diabetes mellitus. Cardiovasc Diabetol. 2014;13:82-2840-13-82.

[56] Brinck JW, Thomas A, Lauer E, Jornayvaz FR, Brulhart-Meynet MC, Prost JC, Pataky Z, Lofgren P, Hoffstedt J, Eriksson M, Pramfalk C, Morel S, Kwak BR, van Eck M, James RW, Frias MA. Diabetes Mellitus Is Associated With Reduced High-Density Lipoprotein Sphingosine-1-Phosphate Content and Impaired High-Density Lipoprotein Cardiac Cell Protection. Arterioscler Thromb Vasc Biol. 2016;36:817-824.

[57] Nobecourt E, Jacqueminet S, Hansel B, Chantepie S, Grimaldi A, Chapman MJ, Kontush A. Defective antioxidative activity of small dense HDL3 particles in type 2 diabetes: relationship to elevated oxidative stress and hyperglycaemia. Diabetologia. 2005;48:529-538.

[58] Vaisar T, Pennathur S, Green PS, Gharib SA, Hoofnagle AN, Cheung MC, Byun J, Vuletic S, Kassim S, Singh P, Chea H, Knopp RH, Brunzell J, Geary R, Chait A, Zhao XQ, Elkon K, Marcovina S, Ridker P, Oram JF, Heinecke JW. Shotgun proteomics implicates protease inhibition and complement activation in the antiinflammatory properties of HDL. J Clin Invest. 2007;117:746-756.

[59] Van Lenten BJ, Hama SY, de Beer FC, Stafforini DM, McIntyre TM, Prescott SM, La Du BN, Fogelman AM, Navab M. Anti-inflammatory HDL becomes pro-inflammatory during the acute phase response. Loss of protective effect of HDL against LDL oxidation in aortic wall cell cocultures. J Clin Invest. 1995;96:2758-2767.

[60] Roberts CK, Katiraie M, Croymans DM, Yang OO, Kelesidis T. Untrained young men have dysfunctional HDL compared with strength-trained men irrespective of body weight status. J Appl Physiol (1985). 2013;115:1043-1049.

[61] Kelesidis T, Currier JS, Huynh D, Meriwether D, Charles-Schoeman C, Reddy ST, Fogelman AM, Navab M, Yang OO. A biochemical fluorometric method for assessing the oxidative properties of HDL. J Lipid Res. 2011;52:2341-2351.

[62] Roberts CK, Ng C, Hama S, Eliseo AJ, Barnard RJ. Effect of a short-term diet and exercise intervention on inflammatory/anti-inflammatory properties of HDL in overweight/obese men with cardiovascular risk factors. J Appl Physiol (1985). 2006;101:1727-1732.

[63] Drew BG, Duffy SJ, Formosa MF, Natoli AK, Henstridge DC, Penfold SA, Thomas WG, Mukhamedova N, de Courten B, Forbes JM, Yap FY, Kaye DM, van Hall G, Febbraio MA, Kemp BE, Sviridov D, Steinberg GR, Kingwell BA. High-density lipoprotein modulates glucose metabolism in patients with type 2 diabetes mellitus. Circulation. 2009;119:2103-2111.

[64] Shaw JA, Bobik A, Murphy A, Kanellakis P, Blombery P, Mukhamedova N, Woollard K, Lyon S, Sviridov D, Dart AM. Infusion of reconstituted high-density lipoprotein leads to acute changes in human atherosclerotic plaque. Circ Res. 2008;103:1084-1091.

[65] Tardif JC, Gregoire J, L'Allier PL, Ibrahim R, Lesperance J, Heinonen TM, Kouz S, Berry C, Basser R, Lavoie MA, Guertin MC, Rodes-Cabau J, Effect of rHDL on Atherosclerosis-Safety and Efficacy

(ERASE) Investigators. Effects of reconstituted high-density lipoprotein infusions on coronary atherosclerosis: a randomized controlled trial. JAMA. 2007;297:1675-1682.

[66] Kontush A, Chapman MJ. High-Density Lipoproteins, Structure, Metabolism, Function and Therapeutics. 1st ed. Hoboken: Wiley; 2011.

[67] Getz GS, Reardon CA. Apolipoprotein A-I and A-I mimetic peptides: a role in atherosclerosis. J Inflamm Res. 2011;4:83-92.

[68] Reddy ST, Navab M, Anantharamaiah GM, Fogelman AM. Apolipoprotein A-I mimetics. Curr Opin Lipidol. 2014;25:304-308.

[69] Navab M, Reddy ST, Van Lenten BJ, Buga GM, Hough G, Wagner AC, Fogelman AM. High-density lipoprotein and 4F peptide reduce systemic inflammation by modulating intestinal oxidized lipid metabolism: novel hypotheses and review of literature. Arterioscler Thromb Vasc Biol. 2012;32:2553-2560.

[70] Chattopadhyay A, Navab M, Hough G, Grijalva V, Mukherjee P, Fogelman HR, Hwang LH, Faull KF, Lusis AJ, Reddy ST, Fogelman AM. Tg6F ameliorates the increase in oxidized phospholipids in the jejunum of mice fed unsaturated LysoPC or WD. J Lipid Res. 2016;57:832-847.

[71] Delzenne NM, Cani PD, Everard A, Neyrinck AM, Bindels LB. Gut microorganisms as promising targets for the management of type 2 diabetes. Diabetologia. 2015;58:2206-2217.

[72] Kingwell BA, Chapman MJ, Kontush A, Miller NE. HDL-targeted therapies: progress, failures and future. Nat Rev Drug Discov. 2014;13:445-464.

[73] Ansell BJ, Navab M, Hama S, Kamranpour N, Fonarow G, Hough G, Rahmani S, Mottahedeh R, Dave R, Reddy ST, Fogelman AM. Inflammatory/antiinflammatory properties of high-density lipoprotein distinguish patients from control subjects better than high-density lipoprotein cholesterol levels and are favorably affected by simvastatin treatment. Circulation. 2003;108:2751-2756.

Appendix 1. Search strategy

PubMed

((((((diabet*[tiab] OR "Diabetes Mellitus"[Mesh])))) AND (((((((((“Lipoproteins, HDL"[Mesh]) OR HDL*[tiab]) OR high density lipoprotein[tiab]) OR apolipoprotein A1[tiab]) OR apolipoprotein A2[tiab]) OR “Apolipoproteins A"[Mesh]) OR apolipoprotein A[tiab]))))) AND ((((((anti-inflammat*[tiab]) OR inflammat*[tiab]) OR pro-inflammat*[tiab]) OR immunomodulat*[tiab]) OR Inflammatory index[tiab])))) AND ((propert*[tiab]) OR ((((((function[tiab]) OR functions[tiab]) OR functional*[tiab]) OR dysfunction*[tiab]) OR quality[tiab])))))

Embase

1	exp diabetes mellitus/
2	“diabet*”.ti,sh,ab.
3	1 or 2
4	exp high density lipoprotein/
5	exp apolipoprotein A/ or exp apolipoprotein A2/ or exp apolipoprotein A1/
6	“HDL*”.ti,sh,ab.
7	high density lipoprotein.ti,sh,ab.
8	apolipoprotein A.ti,sh,ab.
9	apolipoprotein A1.ti,sh,ab.
10	apolipoprotein A2.ti,sh,ab.
11	4 or 5 or 6 or 7 or 8 or 9 or 10
12	“anti-inflammat*”.ti,sh,ab.
13	“antiinflammat*”.ti,sh,ab.
14	“inflammat*”.ti,sh,ab.
15	“pro-inflammat*”.ti,sh,ab.
16	“proinflammat*”.ti,sh,ab.
17	“immunomodulat*”.ti,sh,ab.
18	12 or 13 or 14 or 15 or 16 or 17
19	“propert*”.ti,sh,ab.
20	“function*”.ti,sh,ab.
21	“dysfunction*”.ti,sh,ab.
22	quality.ti,sh,ab.
23	19 or 20 or 21 or 22
24	3 and 11 and 18 and 23

Supplementary table S1. Risk of bias assessment for the included observational studies.

	Selection cases	Selection controls	Outcome measurement	Classification bias	Analysis of results	Overall risk of bias regarding our study question
Tong 2013 [19]	?: Source population and selection method unknown, relatively irrelevant. -: selection criteria clear. -: No power calculation but statistical significance was reached.	+: Selection method, definition and source population unknown.	-: Outcome measurement standardized.	-: Objective: HbA1c and glucose measured in all subjects	-: Appropriate analysis.	High: source population and selection of controls unclear
Liu 2012 [20]	?: Source population unknown, relatively irrelevant. -: No power calculation but statistical significance was reached.	+: Selection and source population unknown. +: Younger than T2D patients	-: Relevant outcome measurement	?: no objective measurement of diabetes (HbA1c or glucose) described in controls. Unlikely that they have diabetes.	-: Appropriate analysis.	High: high risk of selection bias in controls.
Morgantini 2011 [21]	?: Case selection not entirely clear. -: Source population and inclusion criteria well described. - Large population	-: Selection and source population clear. ?: Very healthy controls, slightly younger than cases.	-: Method clear and standardized. -: Relevant outcome measurement.	?: no objective measurement of diabetes (HbA1c or glucose) in controls, Unlikely that they have diabetes.	-: Appropriate analysis.	Unclear: possible selection bias, slightly younger controls than cases.
Nobecourt 2010 - in vitro arm [23]	n/a: (glycated *in vitro*)	?: Source population and selection unclear.	-: Method clear and standardized. -: Relevant outcome measurement.	-: Standardized and objective: glycation levels in apoA-1 and rHDL.	-: Appropriate analysis.	Unclear: possible selection bias.
van Linthout 2008 [28]	-: clear description	-: clear description	-: Method clear and standardized. - Relevant outcome measurement.	-: Standardized and objective: glucose measured	-: Appropriate analysis.	Low: good basal study
Hoang 2007 [29]	Function experiments: n.a.: (glycated *in vitro*). *in vivo* glycation measurement: +: source population unknown +: selection criteria unclear.	+: selection and source population unclear.	-: Method clear and standardized. -: Relevant outcome measurement.	+: no HbA1c or glucose described in cases nor controls	-: Appropriate analysis.	High: unclear selection of cases and controls.
Hedrick 2000 [30]	n/a: (glycated in vitro)	?: Selection and source population unclear	-: Method clear and standardized. -: Relevant outcome measurement. ?: effect oxidation not excluded	-: glycation levels and oxidation products measured in all HDL preparations.	+: Compared to fresh HDL instead of HDL treated similarly to glycated HDL	High: poor comparisons in analysis and selection of healthy subjects unclear.

CML: Nε-carboxymethyllysine, LPS: lipopolysaccharide, n.a.: not applicable, rHDL: reconstituted HDL,T2D: type 2 diabetes

Supplementary Table S2. Details on the risk of bias assessment of intervention studies.

	Random sequence generation	Allocation concealment	Blinding of participants and personnel	Blinding of outcome measurement	Imcomplete outcome data	Selective reporting	Other sources of bias	Overall risk of bias regarding our study question
Triolo 2014 [18]	?: randomized cross-over design, method of sequence generation unknown.	?: method of concealment not described	-: double-blind study. -: Method not described, but unlikely to influence outcome, (objective: MCP-1 mRNA)	-: not described, but unlikely to influence outcome (objective)	-: no missing outcome data.	?: primary outcome results well reported; no study protocol found.	-: carry-over unlikely. No washout but placebo period in between single treatments and double treatment was last.	Unclear: randomization process unknown
Watson 2011 – i.v. study [22]	?: method of sequence generation unknown. Baseline differences in race and sex in smaller groups.	?: method of concealment not described	-: double-blind study. -: Method not described. Unlikely to influence outcome (objective: HII)	-: not described, but unlikely to influence outcome (objective)	-: 2 of 72 patients withdrew consent, no discontinuation due to AE and no deaths. Unlikely to have a clinically relevant impact on outcome.	-: study protocol reported; outcome measurements reported as pre-specified	-	Unclear: randomization process unknown
Watson 2011 – s.c. study [22]	?: method of sequence generation unknown. Small baseline difference in race.	?: method of concealment not described	-: double-blind study. -: Method not described, but unlikely to influence outcome (objective: HII)	-: not described, but unlikely to influence outcome (objective)	-: 3 of 108 patients withdrew consent, 1 discontinued due to SAE (unrelated). All in L4F group. Unlikely to relate to change in HII.	?: study protocol reported but outcome measurements not specified in detail	-	Unclear: randomization process unknown

Supplementary Table S2. Details on the risk of bias assessment of intervention studies. (*continued*)

	Random sequence generation	Allocation concealment	Blinding of participants and personnel	Blinding of outcome measurement	Imcomplete outcome data	Selective reporting	Other sources of bias	Overall risk of bias regarding our study question
Morgantini 2010 [26]	?: method of sequence generation unknown.	?: method of concealment not described.	-: no blinding, but unlikely to influence outcome (objective: macrophage immunostaining and aortic root plaque size)	-: blinded outcome measurement	?: missing data from 6 mice, reason not given. Macrophage content analyzed for only 20 mice, unclear how they were chosen.	?: primary outcome results well reported; no study protocol found	-	Unclear: randomization process and reason for missing data unknown
Nobecourt 2010 [23]	?: Method of sequence generation unknown. Baseline differences not described.	?: method of concealment not described.	-: no blinding, but unlikely to influence outcome (objective: adhesion molecule expression)	-: outcome measurement blinded or objective	-: no missing outcome data	?: primary outcome results well reported; no study protocol found	-	Unclear: randomization process unknown
Patel 2009 [24]	?: Method of sequence generation unknown. No interaction between intervention order and outcome.	?: method of concealment not described	-: double-blind study, method not described, but unlikely to influence outcome (objective: adhesion molecule expression)	-: not described, but unlikely to influence outcome (objective)	-: no missing outcome data	?: primary outcome results well reported; no study protocol found	-: carry-over unlikely (wash-out period of 4 weeks), no period effect.	Unclear: randomization process unknown
Bloedon 2008 [25]	?: method of sequence generation unknown.	?: method of concealment not described	-: double-blind study, method not described, but unlikely to influence outcome (HII)	-: blinded outcome measurement in different lab than study lab	-: no missing outcome data	?: primary outcome results well reported; no study protocol found	+: baseline imbalance in HII	Unclear: randomization process unknown and baseline imbalance in HII

Supplementary Table S2. Details on the risk of bias assessment of intervention studies. (*continued*)

	Random sequence generation	Allocation concealment	Blinding of participants and personnel	Blinding of outcome measurement	Imcomplete outcome data	Selective reporting	Other sources of bias	Overall risk of bias regarding our study question
Peterson 2008 [27]	+: no randomization	+: no randomization	-: no blinding described, but unlikely to influence outcome (objective: cytokine concentrations)	-: not described, but unlikely to influence outcome (objective)	?: number of included mice unknown,	?: primary outcome results well reported; no study protocol found	-	High: no randomization
van Linthout 2008 [28]	+: no randomization	+: no randomization	-: no blinding described, but unlikely to influence outcome (objective: cytokine mRNA)	-: not described, but unlikely to influence outcome (objective)	?: number of included rats unknown	?: primary outcome results well reported; no study protocol found	-	High: no randomization

MCP-1: monocyte chemoattractant protein-1, PEG: polyethylene glycol, HII: HDL inflammatory index, AE: adverse event, SAE: serious adverse event, apoA-1: apolipoprotein A-1. Underlined domains: key domains.

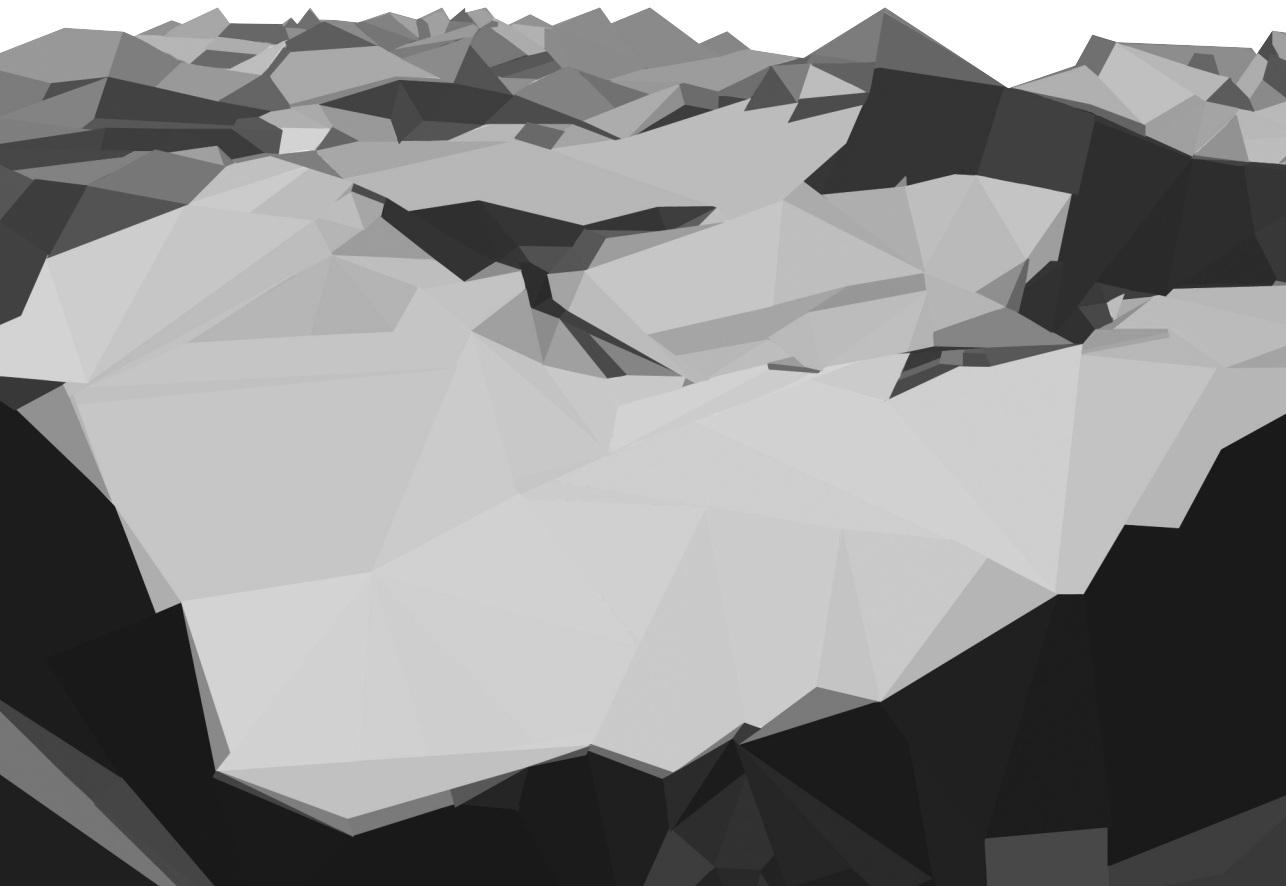

CHAPTER 7

Summary

Summary

N-glycosylation

In **part II** of this thesis, I studied patterns of protein *N*-glycosylation in type 2 diabetes. In **chapter 2,** I presented the DiaGene study, a multi-centre, prospective, extensively phenotyped type 2 diabetes cohort study with concurrent inclusion of diabetes-free individuals at baseline as controls in the city of Eindhoven, The Netherlands. Cases and controls were as groups well-matched for age, which precludes that differences between cases and controls are driven by age. I found considerable complication rates among the patients. Even though the cardiovascular risk factors LDL-cholesterol and blood pressure were more stringently treated at the outpatient clinics of the hospitals, the complication rates were higher than in primary care. A selection of type 2 diabetes susceptibility variants was tested in our study and had higher allele frequencies in cases than in controls as expected, with the exception of the variant in the *KCNJ11* gene. This multi-centre, prospective, type 2 diabetes cohort is well-suited for studying glycomics and other omics layers in the future. Moreover, the prospective information on diabetes complications in this population will enable investigating causal determinants of diabetes complications in future projects.

In this thesis, I examined whether and how *N*-glycan patterns in subjects with type 2 diabetes differed from those in healthy subjects. In **chapter 3**, I showed that several features of the total plasma *N*-glycome were strongly associated with the presence of type 2 diabetes. In type 2 diabetes, changes in sialic acid linkage were found, with less triantennary structures with α2,3-linked sialylation and more diantennary structures with α2,6-linked sialylation. In addition, bisection of fucosylated and sialylated structures was higher in cases than in controls. When studying protein-specific *N*-glycosylation of IgG in **chapter 4**, I found less sialylation of bisecting fucosylated structures, more bisecting in fucosylated structures, and less galactosylation in individuals with type 2 diabetes. Furthermore, with IgG *N*-glycans it was possible to predict the presence of type 2 diabetes relatively well in a cross-sectional exploration, capturing information of several combined clinical parameters. For both IgG and total plasma *N*-glycans, glycosylation patterns in type 2 diabetes showed pro-inflammatory characteristics that have been described in other inflammatory diseases as well, but also previously unreported changes. Both the inflammatory and non-inflammatory *N*-glycan patterns can be involved in the pathophysiology of type 2 diabetes and its complications. Figure 1 summarizes the *N*-glycan features associated with type 2 diabetes in our study after correction for multiple clinical type 2 diabetes risk factors.

Figure 1. N-glycan structures associated with type 2 diabetes.

	Increased in type 2 diabetes		Decreased in type 2 diabetes	
IgG *N*-glycome	Bisecting of fucosylated sialylated glycans	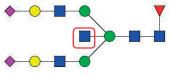	Galactosylation	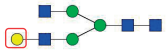
			Sialylation of fucosylated bisecting structures	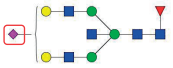
Plasma *N*-glycome	Sialylation per galactose of fucosylated A2		Fucosylation of A2	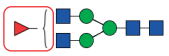
	α2,6-linked sialylation per galactose in A2	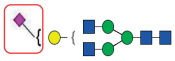	α2,3-linked sialylation of fucosylated A3	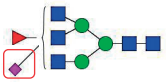
			Bisection of fucosylated sialylated A2	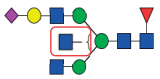

A2, diantennary; A3, triantennary; purple diamond, sialic acid; yellow circle, galactose; blue square, N-acetylglucosamine (GlcNAc); green circle, mannose; red triangle, fucose.

The anti-inflammatory function of HDL

In **part III** of this thesis, I studied the effects of the HDL particle on inflammatory signals in type 2 diabetes. In **chapter 5,** I showed that the method for isolating HDL, a crucial step in *ex vivo* studies of its functionality, can affect *in vitro* signals of endothelial inflammation. I found that HDL isolated with iodixanol density gradient ultracentrifugation (DGUC) is able to inhibit TNF-α induced VCAM-1 expression on human coronary artery endothelial cells. Iodixanol DGUC is a good alternative for salt-based sequential DGUC for studying TNF-α induced VCAM-1 expression as a readout of HDL anti-inflammatory function. Moreover, this method is faster, less expensive, and less likely to alter HDL composition, which makes it more feasible to study HDL anti-inflammatory function in larger populations. Of note, since iodixanol itself might also decrease VCAM-1 expression, the isolation material without HDL should always be used as an experimental control.

The anti-inflammatory effects of HDL are likely diminished or lost in type 2 diabetes, as was shown in the systematic review in **chapter 6**. Figure 2 shows an overview of the diminished anti-inflammatory effects of HDL in type 2 diabetes, as currently known from literature, and potential mechanisms for this dysfunction. However, studies investigating HDL anti-inflammatory function in type 2 diabetes are scarce, small, and not all of high quality. The exact underlying mechanisms, directions of associations, and consequences for the human *in vivo* situation are not convincingly present in the current literature. Furthermore, whether the effects of HDL on inflammation are related to diabetes complications has not been studied extensively.

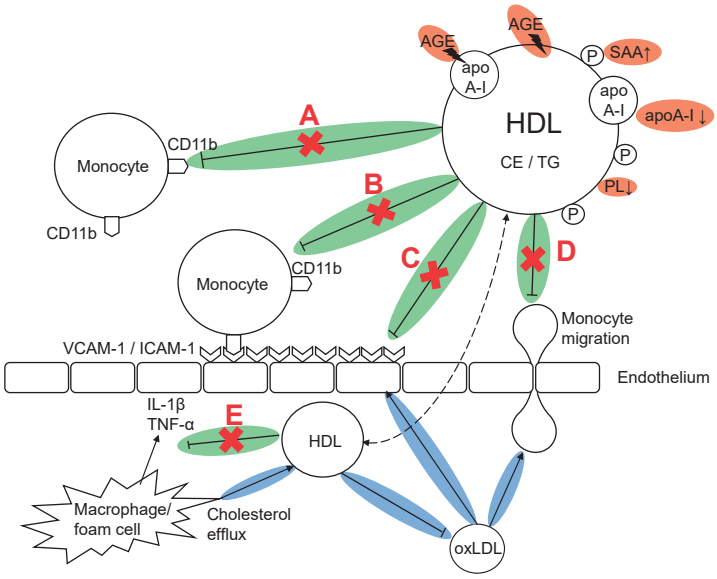

Figure 2. Schematic overview of HDL's loss of anti-inflammatory capacity in T2D.

In green: inflammatory processes that HDL normally inhibits, but does not or less so in T2D. A) expression of the adhesion molecule CD11b expression on monocytes; B) adhesion of monocytes to endothelial cells; C) expression of the adhesion molecules VCAM-1 and ICAM-1 on endothelial cells; D) monocyte migration through the endothelium; and E) cytokine release by macrophages. In orange: potential determinants of the loss of HDL anti-inflammatory capacity in T2D, as described in this review. In blue: mechanisms through which HDL may inhibit inflammation indirectly, but which are outside the scope of this review. Depicted are the effect of HDL on 1) cholesterol removal from foam cells, making them less pro-inflammatory, and 2) LDL oxidation in the subendothelial space, which is a pro-inflammatory trigger. All readouts reported in this review were investigated in plasma, therefore the anti-inflammatory effects of HDL in the subendothelial space are not exactly known. AGE: advanced glycation end products, apoA-I: apolipoprotein A-I, CE: cholesterol esters, HDL: high density lipoprotein, ICAM: intercellular adhesion molecule-1, IL-1β: interleukin-1β, oxLDL: oxidated LDL, P: protein, PL: phospholipids, SAA: serum amyloid A, TG: triacyl glycerols, TNF-α: tumor necrosis factor-α, VCAM-1: vascular cell adhesion molecule-1.

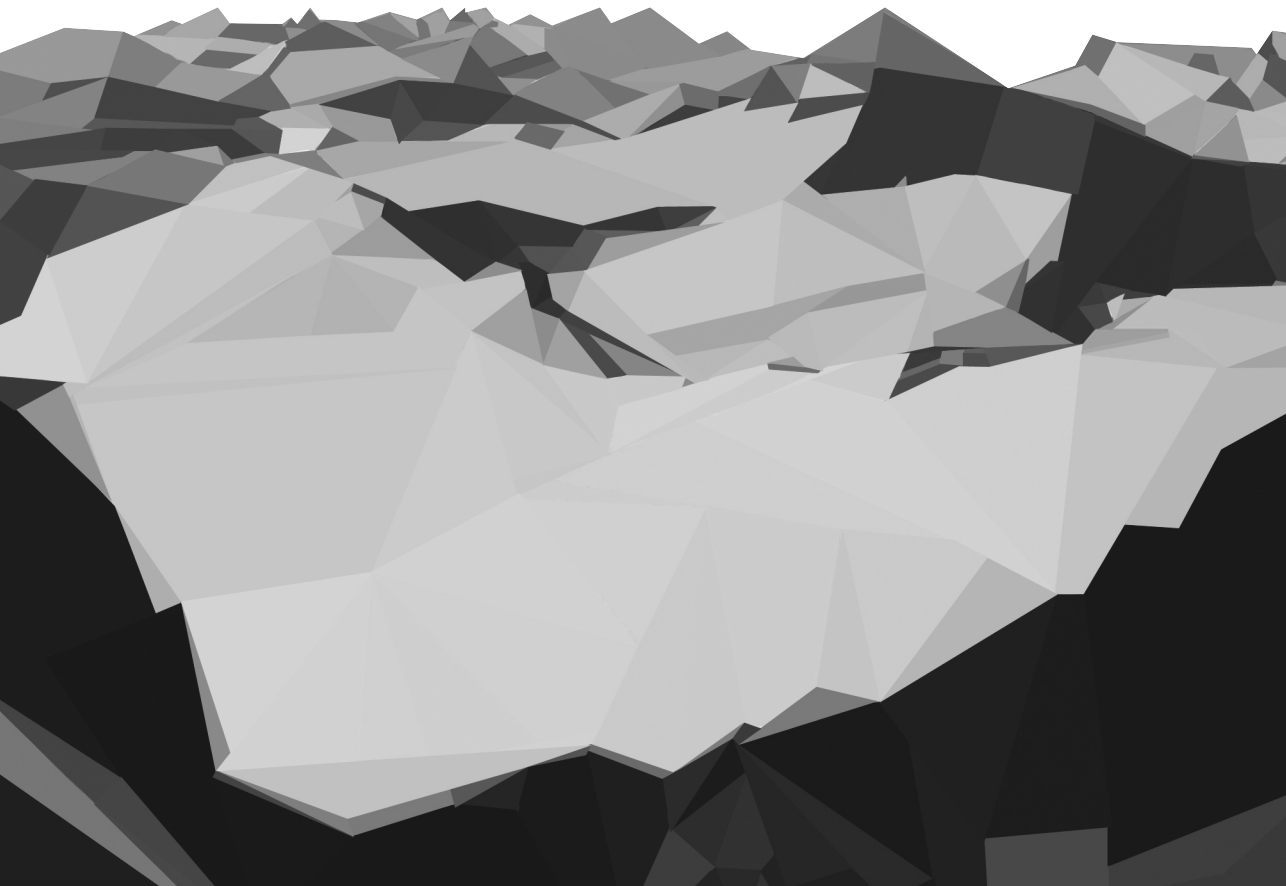

CHAPTER 8

General Discussion

General discussion

Type 2 diabetes is a chronic disease with huge morbidity and excess mortality. Currently, approximately one million people suffer from this disease in the Netherlands [1]. The pathophysiology of type 2 diabetes and its complications is still incompletely understood. Furthermore, even with our best treatment efforts, we can only reduce the risk of vascular complications by approximately 50% [2-4]. In order to improve prediction, prevention, and treatment we need to increase knowledge on the pathophysiology. In this thesis, I explored two promising pathways linking metabolic and inflammatory disturbances in type 2 diabetes. I investigated whether protein *N*-glycosylation and the anti-inflammatory function of HDL are altered in type 2 diabetes and if so, how they might relate to type 2 diabetes pathophysiology. These pathophysiological insights could aid in finding new therapeutic targets and contribute to personalized medicine. My findings are mostly explorative in nature and offer a basis for further studies of these processes in type 2 diabetes and its complications. Here, I will discuss my main findings with their strengths and limitations, hypothesize on how they might be related to the pathophysiology of type 2 diabetes, and propose directions for future research including hypotheses on how our findings could be related to vascular complications and how they could aid in improving personalized medicine.

N-glycosylation - General

N-glycans are sugar chains attached to proteins as posttranslational modifications. Typically, 2-5 glycans are bound to a protein in the endoplasmic reticulum and extensively modified in the Golgi system. Their synthesis is intricately regulated by hundreds of enzymes and influenced by genetic, epigenetic, and environmental factors, leading to a large variability in glycans [5]. This large variability in glycans, their complexity, their stability in a steady state within one individual but ability to quickly respond to changes in the body, e.g. within 24 hours after surgery [6], makes it possible for *N*-glycans to capture information on pathophysiological processes. Figure 1 shows the most important structural features of *N*-glycans as discussed in this thesis.

N-glycosylation - Pathophysiological insights

I found strong associations between *N*-glycans and type 2 diabetes for both the total plasma *N*-glycome and the protein-specific *N*-glycosylation of IgG. This shows that not only glycoprotein plasma levels but also the enzymatic regulation of *N*-glycosylation is altered in type 2 diabetes. Strengths are that I investigated *N*-glycans with very detailed and state-of-the art techniques, especially for studying sialylation, and that this study is among the first studies of the *N*-glycome in type 2 diabetes. Moreover, our population is currently the largest type 2 diabetes cohort in which the *N*-glycome has been measured.

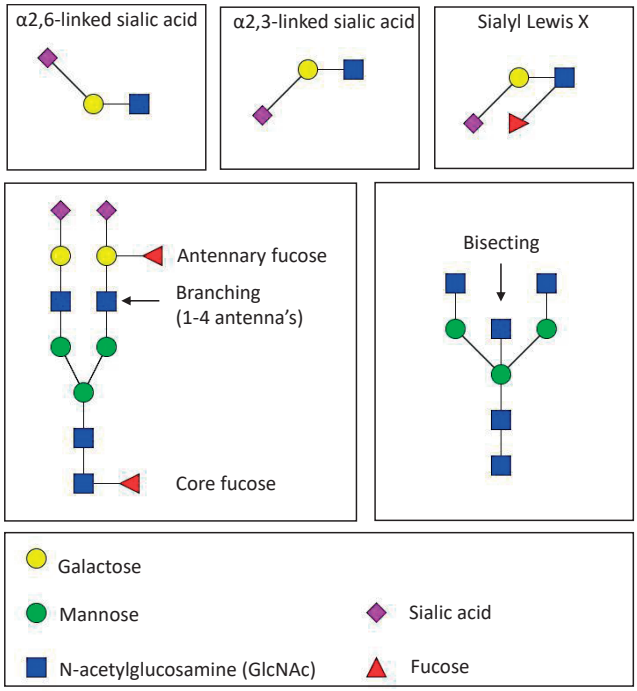

Figure 1. Glycan structures discussed in this thesis.

I studied *N*-glycans in prevalent type 2 diabetes and therefore cannot comment on causality. Most likely, the relationship between *N*-glycans and type 2 diabetes reflects a multitude of disturbances and their interactions. However, Keser et al. recently showed *N*-glycan patterns in individuals at risk for type 2 diabetes that are similar to our findings in type 2 diabetes, showing that already before onset of the disease some of these *N*-glycan patterns are different from those in healthy people [7]. A limitation is that unfortunately parameters of systemic inflammation, such as C-reactive protein, were not available. In addition, I studied *N*-glycans in individuals under treatment for their diabetes. If and how diabetes treatment affects *N*-glycosylation is unknown. Our study lacked power to study the effect of medication in cases alone, therefore we are currently extending our sample size through collaborations. Notwithstanding these limitations, our findings are robust and generate hypotheses for future studies. *N*-glycosylation had not been extensively studied in diabetes before, but a few studies have suggested that factors that regulate or are regulated by *N*-glycosylation modulate pathways relevant in the pathophysiology of type 2 diabetes. These factors (presented in table 1) include glycosyltransferase activity, glycan receptors, the unfolded protein response, and the complement system, and will be discussed below.

Table 1. Potential mechanisms linking N-glycans with type 2 diabetes as discussed in this thesis

N-glycan feature	Potential pathways
Plasma N-glycan features in type 2 diabetes compared to healthy controls	
Increased α2,6-linked sialic acid	Activation of siglec-2 on the pancreatic β-cell Activation of siglec-2 on the B-cell, thereby decreasing B-cell activation Limiting adipogenesis and / or inflammation
Decreased α2,3- and increased α2,6-linked sialic acid	Modulation of siglec-3 and glucagon mRNA production in the α-cell
Increased *N*-glycan branching	On glucagon receptor: decreased sensitivity for glucagon Modulator between diet, obesity and disease
Altered *N*-glycosylation in general	Modulatory role between endoplasmic reticulum stress and insulin action
Decreased IgG galactosylation	Activation of the complement system through the lectin pathway (related to inflammation of adipose tissue and endothelium and to insulin resistance)
Decreased IgG sialylation	Regulation of the T-helper response

In my studies, the strongest associations between *N*-glycans and type 2 diabetes were found for sialylation features, particularly the balance between α2,3- and α2,6-linked sialic acid. Sialylation is also increased in individuals at risk for type 2 diabetes, as reported by Keser et al. [7]. Although this study did not differentiate the type of sialic acid linkage, I would expect this to be due to increased α2,6-linked sialic acid, considering our own findings. Alpha2,6-sialic acid is known to interact with sialic-acid-binding immunoglobulin like lectin (siglec)-2 (CD22). Siglecs are sialic acid receptors previously thought to be present on immune cells only [8], but siglec-2 (CD22) was recently discovered on the pancreatic β-cell as well by Dharmadakari et al. [9], as discussed in chapter 3. Its role on the β-cell is not clear yet, but in immunity siglec-2 downregulates B-cell activation through binding to the B-cell receptor on the same cell, thereby making it unavailable for activation, as well as through binding Toll-like-receptors [10]. A potential modulating role of the increased α2,6-linked sialic acid which I found in type 2 diabetes in β-cell activation and inflammation should be subject to future research.

In this same study, siglec-3, recognizing both α2,3- and α2,6-linked sialic acids [11], was found on pancreatic α-cells. Dharmadakari, et al., found increased siglec-3 expression in pancreatic tissue of individuals with type 2 diabetes compared to pancreas tissue of healthy controls, in addition to increased glucagon mRNA levels [9]. In future research, it should be assessed how higher α2,6-linked but lower α2,3-linked sialic acid in type 2 diabetes than in healthy subjects relate to α-cell function and glucagon levels.

The genetic locus *ST6GAL1* is associated with type 2 diabetes in South East Asians [12]. *ST6GAL1* codes for the enzyme beta-galactoside α2,6-sialyltransferase-1 (ST6Gal1), which is responsible for attaching α2,6-linked sialic acid to glycoproteins. The intracellular expression of the enzyme ST6Gal1 is tissue specific, but ST6Gal1 is also present in the blood

where it controls extracellular α2,6-sialylation. Circulating ST6Gal1 increases glycoprotein α2,6-sialylation after glycoprotein secretion from the cell. Its plasma levels rise during inflammation [13]. It was recently reported that circulating ST6Gal1 controls the sialylation of IgG [14], although circulating ST6Gal1 levels were not associated with IgG sialylation in a human aging study [15]. Our findings of increased α2,6-linked sialylation of the plasma *N*-glycome are in line with increased ST6Gal1 activity, but how the decreased IgG sialylation in type 2 diabetes relates to ST6Gal1 activity is unclear. Besides plasmatic ST6Gal1 activity, B-cell specific regulation of intracellular ST6Gal1 should be considered. As discussed in chapter 3, an inflammation-limiting role of plasmatic ST6Gal1 has been proposed in a human aging study [15]. In addition, it down-regulates adipogenesis in visceral adipose tissue of mice through α2,6-sialylation of integrin-β1, which inhibited preadipocyte differentiation [16]. In this mouse study, ST6Gal1 activity was glycoprotein specific and did not affect sialylation of all glycoproteins in the adipose tissue [16]. Altogether, these effects of ST6Gal1 lead to the hypothesis that the increased α2,6-linked sialylation that we found in type 2 diabetes could be protective through limiting adipogenesis, inflammation, or both. However, to understand this better, glycoprotein specific effects of tissue-specific as well as circulating ST6Gal1 activity should be assessed in future studies. The *ST6GAL1* SNP rs16861329 was not associated with type 2 diabetes in Caucasians in the discovery meta-analysis of the DIAGRAM consortium [17]. We will need to study whether *ST6GAL1* is associated with type 2 diabetes in our study. If this is the case, a potential causal relationship between α2,6-linked sialylation and type 2 diabetes can be studied with a Mendelian randomization approach.

More *N*-glycan branching was present in individuals with or in those at risk for type 2 diabetes than in healthy subjects, both in my study and in the study by Keser et al. [7] *N*-glycan branching of the glucagon receptor and of glucose transporter 2 (GLUT-2) can modulate glucose metabolism [18-20]. Johswitch et al. showed that knockout of *N*-acetylglucosaminyltransferase (GnT)-V, the glycosyltransferase adding a 4th antenna to an *N*-glycan, decreased *N*-glycan branching in mice, which reduced the sensitivity of the glucagon receptor to glucagon. Glucagon normally increases glucose levels, and the reduced glucagon receptor sensitivity through GnT-V knockout resulted in high glucagon levels but also low insulin levels and hypoglycemia [18]. A potential although speculative hypothesis is that the increased *N*-glycan branching in type 2 diabetes is reflective of increased GnT-V expression and related to increased branching of the glucagon receptor, resulting in hyperglycemia through increased glucagon signaling. Ohtsubo, et al., observed that decreased branching led to hyperglycemia in mice. They found that decreased expression of the glycosyltransferase GnT-IVa, a glycosyltransferase that also increases glycan branching, reduced glycan branching of GLUT-2 on β-cells in both mice and humans, resulting in GLUT-2 internalization. This increased GLUT-2 internalization impaired the glucose-sensing abilities of the β-cell, which decreased insulin secretion and caused hyperglycemia [19,20].

Intriguingly, in wild-type mice, a high-fat diet decreased GnT-IVa activity [19]. However, in humans, increased and not decreased *N*-glycan branching of plasma glycoproteins was associated with type 2 diabetes both in our study (chapter 3) and in that of Keser, et al. [7]. Possibly, only specific glycoproteins with low plasma levels show decreased branching in type 2 diabetes, or the altered GnT-IVa activity in the pancreas is tissue-specific and not reflected in the total plasma *N*-glycome. In my study, the association between increased *N*-glycan branching and type 2 diabetes lost most of its strength after adjustment for the models that included BMI, indicating that this association might be modulated by obesity. *N*-glycan branching might also act as a modulator between diet and disease, as was shown by Ohtsubo, et al., in mice [19]. Therefore, further studies are required on *N*-glycan branching in type 2 diabetes to investigate the relationship with diet, obesity, and their interactions, as well as tissue-specific alterations.

The unfolded protein response (UPR) also comprises a potential link between *N*-glycans and type 2 diabetes. The UPR ensures proper functioning of the endoplasmic reticulum (ER) after high-stress situations [21] and is activated by erratic protein folding through erratic *N*-glycosylation [22]. However, whether ER stress affects *N*-glycosylation is unclear. In type 2 diabetes, high free fatty acid levels, oxidation, inflammation, non-enzymatic glycation, and insulin resistance all aggravate ER stress [23]. With sustained ER stress, the UPR switches from cell survival to apoptosis mode, insulin receptor signaling is disrupted, insulin sensitivity decreased, and β-cell survival reduced [21,22]. Sustained ER stress is also associated with advanced atherosclerosis [23-25]. The *N*-glycosylation pattern in type 2 diabetes seems to contain more subtle changes that are unlikely to be severe enough for direct activation of the UPR through incorrect protein folding and sustained ER stress. More plausible is a modulatory role for *N*-glycans between ER stress, insulin action, and atherosclerosis, or between nutrient excess and disturbed glucose metabolism through sustained ER stress. This is speculative but calls for further investigation.

In type 2 diabetes, I found lower IgG galactosylation and sialylation, which both make IgG pro-inflammatory [26]. It is tempting to speculate that the lower galactosylation of IgG in type 2 diabetes compared to healthy subjects is pro-inflammatory through activation of the complement system. Activation of the complement system is related to insulin resistance, endothelial inflammation, and adipose tissue metabolism and inflammation [27]. However, the complement system can be activated through different pathways and the lectin pathway, which is activated by incompletely galactosylated IgG [26,28], has actually been suggested to have anti-atherosclerotic effects [27]. Future studies should assess the specific effects of incompletely galactosylated IgG on the complement system and its different activating pathways in type 2 diabetes.

The pro-inflammatory effects of decreased IgG sialylation are possibly mediated by regulation of the T-helper type 2 response but the exact pathway is not entirely clear [29]. As discussed in chapter 4, IgG *N*-glycan patterns in type 2 diabetes are not only different from

patterns in healthy subjects, but also from those in subjects with other diseases including chronic kidney disease and hypertension. For instance, in my study, decreased sialylation in type 2 diabetes was mainly due to decreased sialylation of fucosylated bisecting structures, while in chronic kidney disease decreased sialylation was seen in fucosylated non-bisecting structures [30]. These differences in *N*-glycosylation patterns compared to subjects with other diseases than type 2 diabetes are subtler than the differences compared to healthy subjects, and their functional and clinical relevance remain to be elucidated.

The inflammatory potential of IgG is also dependent on the IgG subclass [31]. Recently, differential N-glycosylation of IgG1, IgG2, and IgG4 was studied in relation to parameters of inflammatory and metabolic health [32]. This study showed that decreased IgG sialylation and galactosylation were associated with poor metabolic health. The associations were stronger for IgG1 and IgG4 than for IgG2 and it was suggested that IgG1 and IgG4 have a more prominent role in inflammation than IgG2 [32]. The role of IgG in the low-grade inflammation in type 2 diabetes is largely unknown. Decreased total IgG levels have been reported in type 2 diabetes [33] but also increased levels of IgG directed against gut bacteria [34]. Information on *N*-glycosylation of the different IgG subclasses including IgG3 in relation to their different effector functions could contribute to our understanding of the role of IgG and its *N*-glycosylation in type 2 diabetes.

To test these hypotheses on how altered *N*-glycosylation is related to type 2 diabetes pathophysiology, multiple strategies can be combined. First of all, we need to understand the direction of the associations between *N*-glycan patterns and type 2 diabetes. Whether these associations are causal should be studied with prospective follow-up studies for incident type 2 diabetes and with Mendelian randomization. Second, we need to know how the plasma *N*-glycome patterns in type 2 diabetes are related to plasma levels of specific glycoproteins. This can be studied by investigating the plasma proteome in relation to the plasma *N*-glycome. Third, coupling *N*-glycome and proteomics data to other omics layers, including the metabolome, genome, and epigenome will increase insight in their interactions and pathophysiological pathways. For studying these interactions, a systems biology approach should be used, which analyzes biological processes as a whole instead of as separate components [35]. Fourth, the functional effects of *N*-glycosylation patterns of glycoproteins of interest should be investigated in type 2 diabetes, including those of IgG. Eventually, the aim is to identify specific glycoproteins with altered *N*-glycosylation affecting their function to increase insight in type 2 diabetes pathophysiology and identify new therapeutic targets.

HDL anti-inflammatory function - General

For over 50 years, it has been known that a low HDL-cholesterol (HDL-c) concentration is associated with increased cardiovascular risk [36]. However, the causality of this relationship has been questioned in the last years, since genetically low HDL-c does not increase car-

diovascular disease risk [37] and therapies increasing HDL-c do not decrease the incidence of cardiovascular disease [38,39]. Low HDL-c is associated with inflammatory and metabolic disturbances such as smoking, obesity, and type 2 diabetes [40]. It has been proposed that low HDL-cholesterol is a marker of other processes that increase cardiovascular risk [36,40]. HDL function is a more likely characteristic of HDL through which it exerts protective effects [41]. How good HDL functions in protecting the body against cardiovascular disease, is thought to be based on its protein and lipid components [42,43]. So far, over 100 different proteins and over 200 lipid species have been identified as HDL constituents [43-46] and the proteome composition is associated with cardiovascular disease [47,48]. Since HDL is a small particle, it cannot carry all these different lipids and proteins simultaneously, which means that what we call HDL actually comprises an extremely heterogeneous group of particles [45]. This compositional heterogeneity together with the continuous remodeling of circulating HDL have contributed to the idea of a modulatory role of HDL in metabolism, inflammation, and vascular disease.

HDL anti-inflammatory function - Pathophysiological insights

The role of HDL in modulating inflammation is of high interest since it directly relates metabolic disturbances in type 2 diabetes to a pro-inflammatory state. However, HDL represents a heterogeneous group of particles with a complex biology, which is currently incompletely understood. I aimed to clarify the anti-inflammatory function of HDL in type 2 diabetes. However, before studying HDL anti-inflammatory function in a more translational or clinical setting, we first need to have a robust methodology of testing it, especially when investigating the HDL structure-function relationship. The main strength of the work in my thesis is that I have critically assessed the methodology of HDL anti-inflammatory function experiments as well as the available literature on the anti-inflammatory function of HDL in type 2 diabetes. I have thus created an overview of the current knowledge of this topic and identified gaps in this field. Of note, since writing this systematic review, 2 more studies showed a loss of anti-inflammatory function in type 2 diabetes [49,50]; none were published that did not see a loss of anti-inflammatory function. The most important limitation of my work on HDL anti-inflammatory function in type 2 diabetes is that of yet I have not been able to study how these altered anti-inflammatory effects of HDL are related to other HDL functions such as inhibiting LDL oxidation and removing cholesterol from plaques. Although more indirectly, these HDL functions have also been related to inflammation.

HDL function is thought to be modulated by its lipidome and proteome [42,43]. The HDL lipidome and proteome were altered in type 2 diabetes [51,52] and coronary artery disease [47]. Regarding the structure-function relationship, describing the effect of HDL components on its function, the apoA-I and phospholipid content increased the *ex vivo* anti-inflammatory function of HDL in type 2 diabetes [53] while serum amyloid A (SAA) bound to HDL decreased

the anti-inflammatory function [50]. This structure-function relationship of HDL is of high interest since reconstituted HDL (rHDL) is a therapeutic strategy under development for cardiovascular disease. rHDL consists primarily of apoA-I and phospholipids, but can also be enriched by specific proteins and especially lipids, which can greatly enhance its effect [54]. Knowing which HDL components are key to specific functional properties could therefore have direct therapeutic consequences.

The effects of unhealthy diets and lack of exercise on HDL function could clarify HDL dysfunction in type 2 diabetes. A healthy diet and physical activity are strategies that not only improve glucose regulation but potentially also increase HDL-cholesterol and eventually decrease inflammation. Moreover, a number of studies have shown that these lifestyle interventions can improve HDL anti-oxidative properties and increase cholesterol efflux, possibly by changing HDL composition [40,55-58]. Another aspect of interest is the enzymatic glycosylation of the HDL proteome and lipidome. Krishnan et al. recently showed that HDL glycoprotein levels as well as their specific *O*- and *N*-glycans in healthy individuals differed from those of individuals with metabolic syndrome or type 2 diabetes undergoing hemodialysis [59]. For example, in HDL of subjects with metabolic syndrome compared to healthy subjects, apoC-III without or with one sialic acid was increased while apoC-III with two sialic acids was decreased, which has also been shown by Savinova, et al. [60]. On the contrary, HDL of hemodialysis patients was in general enriched in apoC-III with two sialic acids, although a specific disialylated glycan was lower in hemodialysis patients than in healthy subjects [59]. Furthermore, isolated HDL with pro-inflammatory effects on monocytes had higher levels of apoCIII, disialylated glycans on α1-antitrypsin, and of glycans without sialic acid on α2-HS-glycoprotein, while levels of apoCIII with 1 sialic acid were lower than in HDL with anti-inflammatory effects. Thus, glycosylation patterns on HDL glycoproteins were indicative of the inflammatory effects of HDL on monocytes [59]. In the context of my findings on altered *N*-glycosylation in type 2 diabetes, it should be investigated whether glycosylation of HDL apolipoproteins is associated with loss of HDL anti-inflammatory function in type 2 diabetes. Measurement of the enzymatic glycosylation of HDL glycoproteins could further increase our understanding of the effects of HDL on inflammation. Moreover, their potential as biomarker for the anti-inflammatory function of HDL should be assessed.

To improve the functional studies with HDL, consensus on the best methodology for *ex vivo* experiments should become available. Currently, both HDL isolation and readouts of anti-inflammatory function are laborious and have a large variability, therefore they are not well-suited for analyses of large cohorts. As discussed in chapter 5, density gradient ultracentrifugation with iodixanol could overcome the problem of laborious and detrimental isolation of HDL, which would make studying HDL anti-inflammatory function in large cohorts more feasible. Of note, the suitability of iodixanol isolation for other readouts of

the anti-inflammatory function of HDL and for other functions has not been studied and should be clarified before using iodixanol DGUC in other experimental set-ups.

More studies investigating HDL isolated from patients with type 2 diabetes are necessary, preferably in prospective settings or with a Mendelian randomization approach, using HDL-bound proteins that are related to its functional effects. Furthermore, these studies should aim to identify which components of HDL influence its effects on inflammation, whether HDL composition is altered in type 2 diabetes, and how this altered composition relates to loss of anti-inflammatory function. Ideally, HDL composition in relation to its function should be investigated in a more dynamic setting as well, for instance by studying potential alterations in HDL function in the postprandial state instead of in the fasting state only.

Future research into complications of type 2 diabetes

N-glycosylation

The identified associations of *N*-glycans and type 2 diabetes might also be involved in the pathophysiology of complications of type 2 diabetes. We have not been able to study this yet but are currently including more subjects in our studies through collaborations for this goal. Only a few reports are available about *N*-glycosylation and complications of type 2 diabetes. In the study by Testa, et al., altered (desialylated) plasma glycan levels in type 2 diabetes were more pronounced in individuals with diabetes complications than in those without [61], although these differences were not statistically significant. Of course, the sample size was relatively small, and these findings require further investigation preferably with a method that also measures sialylation. *N*-glycosylation patterns have also been related to diabetic retinopathy [62] and to kidney function [30], although most subjects in this latter study did not have diabetes. In addition to an influence on inflammation, other mechanisms of interest in the link between *N*-glycans and diabetes complications are sialylation of LDL and fibrinogen. Lowly sialylated LDL has been found to increase LDL uptake in atherosclerotic plaques [63,64] and has been associated with coronary artery disease [65]. Sialylation of fibrinogen influences clot formation by affecting its solubility and polymerization [66,67]. Regarding IgG glycosylation, a mechanism of interest in complications of diabetes is activation of the complement system, which leads to increased deposition of membrane attack compositions in target tissues and has been associated with micro- and macrovascular complications of type 2 diabetes [68]. Preferably, relationships between *N*-glycan patterns and complications of type 2 diabetes should be tested in large, prospective studies. New insights in the pathophysiology of complications of diabetes are highly needed to improve prediction and treatment [69].

HDL anti-inflammatory function

Similarly, whether the effects of HDL on inflammation are related to vascular complications of type 2 diabetes should be clarified. Recently, it was shown that the loss of anti-inflammatory function of HDL was related to coronary artery disease [49] and diabetic nephropathy [50]. Up to date, HDL function has mostly been studied cross-sectional, and the relationship of HDL anti-inflammatory function to incident cardiovascular disease or other diabetes complications is unknown. However, one study found that cholesterol efflux, describing the ability of HDL to take up cholesterol from peripheral tissues, was inversely correlated with incident cardiovascular disease in a general population and was a better predictor of cardiovascular disease than HDL-c [70]. In this thesis, I focused on the direct effects of HDL on inflammatory parameters, but ultimately the different functions of HDL appear to be interrelated, at least to some extent [43]. Comprehensive study methods are necessary to determine the exact role of HDL in vascular inflammation and diabetes complications.

Future research into personalized medicine

N-glycosylation

Personalizing disease classification based on disease phenotypes and personalizing treatment options in type 2 diabetes represent a challenge, since the disease encompasses a large spectrum of metabolic disturbances and many pathways interact [71]. Currently, prediction models for type 2 diabetes and its complications, such as the UKPDS or the Framingham score, are able to identify persons at high risk, but usually overestimate individual risk [72-74]. Although at the moment measuring *N*-glycans is complex and therefore not likely to be implemented in present-day diabetes prediction, this could change with future technical developments. The added value of *N*-glycans in personalized medicine lies in their ability to capture interactions between genetics, epigenetics, and environmental factors [75,76]. The high area under the curve of IgG *N*-glycans for predicting type 2 diabetes, see chapter 4, provides circumstantial evidence for this capturing of the combination of susceptibility and exposures and could improve personalized medicine in type 2 diabetes [77]. The glycan signatures might identify which processes are disturbed in which patients, paving the way for individualized decision making in treatment options, and a better identification of individuals at risk for type 2 diabetes or its complications.

N-glycans have been more extensively studied as biomarkers for cancer than for other diseases. Fascinatingly, not only are there indications that specific plasma *N*-glycan patterns are present in several cancers, but also that measuring *N*-glycosylation of known cancer biomarkers improves their ability to differentiate cancer from benign disorders. Examples of such glycoprotein biomarkers in cancer are α-fetoprotein for hepatocellular cancer and prostate-specific antigen (PSA) for prostate cancer [78]. Biomarkers for risk prediction in type 2 diabetes currently do not improve risk prediction for type 2 diabetes [79], but similar

to cancer biomarkers, it should be studied whether coupling *N*-glycan measurements to plasma levels of these biomarkers improves their discriminative capacity.

First, to investigate the predictive potential of *N*-glycans, the relationship between incident type 2 diabetes and total plasma and IgG *N*-glycans needs to be determined. A parallel approach could be to investigate how the extremes in the *N*-glycan patterns that I found in type 2 diabetes relate to disease phenotype, as these extreme phenotypes could identify differential components within the disease [71]. Second, whether *N*-glycans can improve current risk prediction models for complications of type 2 diabetes should be studied. And third, *N*-glycan patterns need to be assessed in response to glucose- or lipid-lowering treatment to explore tailoring of treatment decisions.

HDL anti-inflammatory function

HDL function is difficult to capture in one measurement and will not easily be integrated in clinical diagnostics. The most promising surrogate for HDL function in personalized medicine lies in compositional elements of HDL, thus HDL-bound proteins, lipids, and possibly also their glycans. As discussed above, HDL composition is related to its functional effects [42,43]. A better understanding on how HDL composition is related to both HDL anti-inflammatory function and clinical outcomes is necessary and needs to be studied in large, prospective studies. Bio-active components of HDL that are related to its function and to clinical outcomes offer a new chance for risk prediction.

Conclusion and perspectives

In this thesis, I examined *N*-glycosylation and the anti-inflammatory function of HDL in type 2 diabetes. Although most findings in this thesis are explorative and cannot immediately be translated to patient care, they do indicate that *N*-glycosylation and HDL anti-inflammatory function are altered in type 2 diabetes. Both processes relate metabolic disturbances in type 2 diabetes to a pro-inflammatory state, which most probably has a major pathophysiological role in type 2 diabetes and its complications. Furthermore, both *N*-glycans and HDL are complex and highly variable structures and are able to quickly adapt to changes in the physiological environment. This complexity and diversity also gives these structures more potential to actively contribute to the extremely complex pathophysiology of type 2 diabetes and its complications. More knowledge on these processes, especially when investigated in their totality with for instance systems biology approaches, can increase our understanding of type 2 diabetes and might aid in early detection of disease susceptibility and in identifying specific disease phenotypes. Moreover, it can improve personalized medicine strategies and be translated or integrated into better tailored therapeutic strategies. My findings on *N*-glycosylation and HDL anti-inflammatory function are promising and warrant further investigation in this common and dire disease.

Table 2. Overview of what this thesis has added to our knowledge.

What was known?
N-glycans • *N*-glycan patterns of plasma proteins and IgG are associated with type 2 diabetes risk factors, including BMI, lipids, smoking, ageing, and inflammation • Monogalactosylated, core-fucosylated diantennary *N*-glycans are lower in individuals with type 2 diabetes than in healthy controls • *N*-glycan sialylation, galactosylation and branching are increased in individuals at risk for type 2 diabetes
HDL • Multiple functions of HDL are decreased or lost in type 2 diabetes • HDL can diminish inflammation in healthy individuals, but does not seem to be able to do so in individuals with type 2 diabetes
What does this thesis add?
N-glycans • Sialylation and bisection of plasma glycoproteins are higher in type 2 diabetes than in healthy individuals • In type 2 diabetes, α2,6-linked sialylation is higher and α2,3-linked sialylation lower than in healthy subjects • IgG sialylation and galactosylation are lower and bisection is higher in type 2 diabetes than in healthy individuals, resulting in more pro-inflammatory IgG
HDL • Iodixanol density gradient ultracentrifugation, a cheaper and quicker method than the conventional sequential density gradient ultracentrifugation method, can be used to isolate HDL for testing HDL anti-inflammatory function • From analyzing all available literature, we can conclude that HDL anti-inflammatory function can be decreased in type 2 diabetes, but larger and prospective studies of high quality are necessary to confirm this.

References

1. Diabetesfonds. Anonymous . (Accessed 7/13, 2017, at https://www.diabetesfonds.nl/over-diabetes/soorten-diabetes/verschil-tussen-diabetes-type-1-en-2).
2. Gaede P, Vedel P, Larsen N, Jensen GV, Parving HH, Pedersen O. Multifactorial intervention and cardiovascular disease in patients with type 2 diabetes. N Engl J Med 2003;348:383-93.
3. Holman RR, Paul SK, Bethel MA, Matthews DR, Neil HA. 10-Year Follow-Up of Intensive Glucose Control in Type 2 Diabetes. N Engl J Med 2008;359:1577-89.
4. Zoungas S, Arima H, Gerstein HC, et al. Effects of intensive glucose control on microvascular outcomes in patients with type 2 diabetes: a meta-analysis of individual participant data from randomised controlled trials. Lancet Diabetes Endocrinol 2017;5:431-7.
5. Lauc G, Rudan I, Campbell H, Rudd PM. Complex genetic regulation of protein glycosylation. Mol Biosyst 2010;6:329-35.
6. Novokmet M, Lukic E, Vuckovic F, et al. Changes in IgG and total plasma protein glycomes in acute systemic inflammation. Sci Rep 2014;4:4347.
7. Keser T, Gornik I, Vuckovic F, et al. Increased plasma N-glycome complexity is associated with higher risk of type 2 diabetes. Diabetologia 2017;.
8. Crocker PR, Paulson JC, Varki A. Siglecs and their roles in the immune system. Nat Rev Immunol 2007;7:255-66.
9. Dharmadhikari G, Stolz K, Hauke M, et al. Siglec-7 restores beta-cell function and survival and reduces inflammation in pancreatic islets from patients with diabetes. Sci Rep 2017;7:45319.
10. Jellusova J, Nitschke L. Regulation of B cell functions by the sialic acid-binding receptors siglec-G and CD22. Front Immunol 2012;2:96.
11. Brinkman-Van der Linden EC, Varki A. New aspects of siglec binding specificities, including the significance of fucosylation and of the sialyl-Tn epitope. Sialic acid-binding immunoglobulin superfamily lectins. J Biol Chem 2000;275:8625-32.
12. Kooner JS, Saleheen D, Sim X, et al. Genome-wide association study in individuals of South Asian ancestry identifies six new type 2 diabetes susceptibility loci. Nat Genet 2011;43:984-9.
13. Bhide GP, Colley KJ. Sialylation of N-glycans: mechanism, cellular compartmentalization and function. Histochem Cell Biol 2017;147:149-74.
14. Jones MB, Oswald DM, Joshi S, Whiteheart SW, Orlando R, Cobb BA. B-cell-independent sialylation of IgG. Proc Natl Acad Sci U S A 2016;113:7207-12.
15. Catera M, Borelli V, Malagolini N, et al. Identification of novel plasma glycosylation-associated markers of aging. Oncotarget 2016;7:7455-68.
16. Kaburagi T, Kizuka Y, Kitazume S, Taniguchi N. The Inhibitory Role of alpha2,6-Sialylation in Adipogenesis. J Biol Chem 2017;292:2278-86.
17. Morris AP, Voight BF, Teslovich TM, et al. Large-scale association analysis provides insights into the genetic architecture and pathophysiology of type 2 diabetes. Nat Genet 2012;44:981-90.
18. Johswich A, Longuet C, Pawling J, et al. N-glycan remodeling on glucagon receptor is an effector of nutrient sensing by the hexosamine biosynthesis pathway. J Biol Chem 2014;289:15927-41.
19. Ohtsubo K, Takamatsu S, Minowa MT, Yoshida A, Takeuchi M, Marth JD. Dietary and genetic control of glucose transporter 2 glycosylation promotes insulin secretion in suppressing diabetes. Cell 2005;123:1307-21.
20. Ohtsubo K, Chen MZ, Olefsky JM, Marth JD. Pathway to diabetes through attenuation of pancreatic beta cell glycosylation and glucose transport. Nat Med 2011;17:1067-75.

21. Hummasti S, Hotamisligil GS. Endoplasmic reticulum stress and inflammation in obesity and diabetes. Circ Res 2010;107:579-91.
22. Freeze HH, Esko JD, Parodi AJ. Chapter 36. Glycans in Glycoprotein Quality Control. In: Varki A, Cummings RD, Esko JD, et al, eds. Essentials of Glycobiology. 2nd ed. Cold Spring Harbor (NY): Cold Spring Harbor Laboratory Press, 2009.
23. Dong Y, Fernandes C, Liu Y, et al. Role of endoplasmic reticulum stress signalling in diabetic endothelial dysfunction and atherosclerosis. Diab Vasc Dis Res 2017;14:14-23.
24. Myoishi M, Hao H, Minamino T, et al. Increased endoplasmic reticulum stress in atherosclerotic plaques associated with acute coronary syndrome. Circulation 2007;116:1226-33.
25. Thorp E, Li G, Seimon TA, Kuriakose G, Ron D, Tabas I. Reduced apoptosis and plaque necrosis in advanced atherosclerotic lesions of Apoe-/- and Ldlr-/- mice lacking CHOP. Cell Metab 2009;9:474-81.
26. Gornik O, Pavic T, Lauc G. Alternative glycosylation modulates function of IgG and other proteins - implications on evolution and disease. Biochim Biophys Acta 2012;1820:1318-26.
27. Hertle E, Stehouwer CD, van Greevenbroek MM. The complement system in human cardiometabolic disease. Mol Immunol 2014;61:135-48.
28. Malhotra R, Wormald MR, Rudd PM, Fischer PB, Dwek RA, Sim RB. Glycosylation changes of IgG associated with rheumatoid arthritis can activate complement via the mannose-binding protein. Nat Med 1995;1:237-43.
29. Anthony RM, Kobayashi T, Wermeling F, Ravetch JV. Intravenous gammaglobulin suppresses inflammation through a novel T(H)2 pathway. Nature 2011;475:110-3.
30. Barrios C, Zierer J, Gudelj I, et al. Glycosylation Profile of IgG in Moderate Kidney Dysfunction. J Am Soc Nephrol 2016;27:933-41.
31. Vidarsson G, Dekkers G, Rispens T. IgG subclasses and allotypes: from structure to effector functions. Front Immunol 2014;5:520.
32. Plomp R, Ruhaak LR, Uh HW, et al. Subclass-specific IgG glycosylation is associated with markers of inflammation and metabolic health. Sci Rep 2017;7:12325,017-12495-0.
33. Guo X, Meng G, Liu F, et al. Serum levels of immunoglobulins in an adult population and their relationship with type 2 diabetes. Diabetes Res Clin Pract 2016;115:76-82.
34. Mohammed N, Tang L, Jahangiri A, de Villiers W, Eckhardt E. Elevated IgG levels against specific bacterial antigens in obese patients with diabetes and in mice with diet-induced obesity and glucose intolerance. Metabolism 2012;61:1211-4.
35. Zierer J, Menni C, Kastenmuller G, Spector TD. Integration of 'omics' data in aging research: from biomarkers to systems biology. Aging Cell 2015;14:933-44.
36. Toth PP, Barter PJ, Rosenson RS, et al. High-density lipoproteins: a consensus statement from the National Lipid Association. J Clin Lipidol 2013;7:484-525.
37. Haase CL, Tybjaerg-Hansen A, Qayyum AA, Schou J, Nordestgaard BG, Frikke-Schmidt R. LCAT, HDL cholesterol and ischemic cardiovascular disease: a Mendelian randomization study of HDL cholesterol in 54,500 individuals. J Clin Endocrinol Metab 2012;97:E248-56.
38. Briel M, Ferreira-Gonzalez I, You JJ, et al. Association between change in high density lipoprotein cholesterol and cardiovascular disease morbidity and mortality: systematic review and meta-regression analysis. BMJ 2009;338:b92.
39. Keene D, Price C, Shun-Shin MJ, Francis DP. Effect on cardiovascular risk of high density lipoprotein targeted drug treatments niacin, fibrates, and CETP inhibitors: meta-analysis of randomised controlled trials including 117,411 patients. BMJ 2014;349:g4379.

40. Marz W, Kleber ME, Scharnagl H, et al. HDL cholesterol: reappraisal of its clinical relevance. Clin Res Cardiol 2017;.
41. Gordon S.M., Hofmann S., Askew D.S., Davidson W.S. High density lipoprotein: It's not just about lipid transport anymore. Trends Endocrinol Metab 2011;22:9-15.
42. Heinecke JW. The protein cargo of HDL: implications for vascular wall biology and therapeutics. J Clin Lipidol 2010;4:371-5.
43. Camont L, Lhomme M, Rached F, et al. Small, dense high-density lipoprotein-3 particles are enriched in negatively charged phospholipids: relevance to cellular cholesterol efflux, antioxidative, antithrombotic, anti-inflammatory, and antiapoptotic functionalities. Arterioscler Thromb Vasc Biol 2013;33:2715-23.
44. Davidson WS, Silva RA, Chantepie S, Lagor WR, Chapman MJ, Kontush A. Proteomic analysis of defined HDL subpopulations reveals particle-specific protein clusters: relevance to antioxidative function. Arterioscler Thromb Vasc Biol 2009;29:870-6.
45. Gordon SM, Remaley AT. High density lipoproteins are modulators of protease activity: Implications in inflammation, complement activation, and atherothrombosis. Atherosclerosis 2017;259:104-13.
46. Rezaee F, Casetta B, Levels JH, Speijer D, Meijers JC. Proteomic analysis of high-density lipoprotein. Proteomics 2006;6:721-30.
47. Vaisar T, Pennathur S, Green PS, et al. Shotgun proteomics implicates protease inhibition and complement activation in the antiinflammatory properties of HDL. J Clin Invest 2007;117:746-56.
48. Vaisar T, Mayer P, Nilsson E, Zhao XQ, Knopp R, Prazen BJ. HDL in humans with cardiovascular disease exhibits a proteomic signature. Clin Chim Acta 2010;411:972-9.
49. Sun JT, Liu Y, Lu L, et al. Diabetes-Invoked High-Density Lipoprotein and Its Association With Coronary Artery Disease in Patients With Type 2 Diabetes Mellitus. Am J Cardiol 2016;.
50. Mao JY, Sun JT, Yang K, et al. Serum amyloid A enrichment impairs the anti-inflammatory ability of HDL from diabetic nephropathy patients. J Diabetes Complications 2017;31:1538-43.
51. Gomez Rosso L, Lhomme M, Merono T, et al. Poor glycemic control in type 2 diabetes enhances functional and compositional alterations of small, dense HDL3c. Biochim Biophys Acta 2017;1862:188-95.
52. Stahlman M, Fagerberg B, Adiels M, et al. Dyslipidemia, but not hyperglycemia and insulin resistance, is associated with marked alterations in the HDL lipidome in type 2 diabetic subjects in the DIWA cohort: impact on small HDL particles. Biochim Biophys Acta 2013;1831:1609-17.
53. Patel S, Drew BG, Nakhla S, et al. Reconstituted high-density lipoprotein increases plasma high-density lipoprotein anti-inflammatory properties and cholesterol efflux capacity in patients with type 2 diabetes. J Am Coll Cardiol 2009;53:962-71.
54. Darabi M, Guillas-Baudouin I, Le Goff W, Chapman MJ, Kontush A. Therapeutic applications of reconstituted HDL: When structure meets function. Pharmacol Ther 2016;157:28-42.
55. Roberts CK, Ng C, Hama S, Eliseo AJ, Barnard RJ. Effect of a short-term diet and exercise intervention on inflammatory/anti-inflammatory properties of HDL in overweight/obese men with cardiovascular risk factors. J Appl Physiol (1985) 2006;101:1727-32.
56. Patel S, Puranik R, Nakhla S, et al. Acute hypertriglyceridaemia in humans increases the triglyceride content and decreases the anti-inflammatory capacity of high density lipoproteins. Atherosclerosis 2009;204:424-8.
57. Hansel B, Bonnefont-Rousselot D, Orsoni A, et al. Lifestyle intervention enhances high-density lipoprotein function among patients with metabolic syndrome only at normal low-density lipoprotein cholesterol plasma levels. J Clin Lipidol 2016;10:1172-81.

58. Millar CL, Duclos Q, Blesso CN. Effects of Dietary Flavonoids on Reverse Cholesterol Transport, HDL Metabolism, and HDL Function. Adv Nutr 2017;8:226-39.
59. Krishnan S, Shimoda M, Sacchi R, et al. HDL Glycoprotein Composition and Site-Specific Glycosylation Differentiates Between Clinical Groups and Affects IL-6 Secretion in Lipopolysaccharide-Stimulated Monocytes. Sci Rep 2017;7:43728.
60. Savinova OV, Fillaus K, Jing L, Harris WS, Shearer GC. Reduced apolipoprotein glycosylation in patients with the metabolic syndrome. PLoS One 2014;9:e104833.
61. Testa R, Vanhooren V, Bonfigli AR, et al. N-glycomic changes in serum proteins in type 2 diabetes mellitus correlate with complications and with metabolic syndrome parameters. PLoS One 2015;10:e0119983.
62. Inafuku S, Noda K, Amano M, et al. Alteration of N-Glycan Profiles in Diabetic Retinopathy. Invest Ophthalmol Vis Sci 2015;56:5316-22.
63. Tertov VV, Sobenin IA, Gabbasov ZA, Popov EG, Orekhov AN. Lipoprotein aggregation as an essential condition of intracellular lipid accumulation caused by modified low density lipoproteins. Biochem Biophys Res Commun 1989;163:489-94.
64. Camejo G, Lopez A, Lopez F, Quinones J. Interaction of low density lipoproteins with arterial proteoglycans. The role of charge and sialic acid content. Atherosclerosis 1985;55:93-105.
65. Ruelland A, Gallou G, Legras B, Paillard F, Cloarec L. LDL sialic acid content in patients with coronary artery disease. Clin Chim Acta 1993;221:127-33.
66. Dang CV, Shin CK, Bell WR, Nagaswami C, Weisel JW. Fibrinogen sialic acid residues are low affinity calcium-binding sites that influence fibrin assembly. J Biol Chem 1989;264:15104-8.
67. Okude M, Yamanaka A, Morimoto Y, Akihama S. Sialic acid in fibrinogen: effects of sialic acid on fibrinogen-fibrin conversion by thrombin and properties of asialofibrin clot. Biol Pharm Bull 1993;16:448-52.
68. Ghosh P, Sahoo R, Vaidya A, Chorev M, Halperin JA. Role of complement and complement regulatory proteins in the complications of diabetes. Endocr Rev 2015;36:272-88.
69. Kahn SE, Cooper ME, Del Prato S. Pathophysiology and treatment of type 2 diabetes: perspectives on the past, present, and future. Lancet 2014;383:1068-83.
70. Rohatgi A, Khera A, Berry JD, et al. HDL cholesterol efflux capacity and incident cardiovascular events. N Engl J Med 2014;371:2383-93.
71. McCarthy MI. Painting a new picture of personalised medicine for diabetes. Diabetologia 2017;60:793-9.
72. Abbasi A, Peelen LM, Corpeleijn E, et al. Prediction models for risk of developing type 2 diabetes: systematic literature search and independent external validation study. BMJ 2012;345:e5900.
73. Simmons RK, Coleman RL, Price HC, et al. Performance of the UK Prospective Diabetes Study Risk Engine and the Framingham Risk Equations in Estimating Cardiovascular Disease in the EPIC- Norfolk Cohort. Diabetes Care 2009;32:708-13.
74. Herder C, Kowall B, Tabak AG, Rathmann W. The potential of novel biomarkers to improve risk prediction of type 2 diabetes. Diabetologia 2014;57:16-29.
75. Zoldos V, Novokmet M, Beceheli I, Lauc G. Genomics and epigenomics of the human glycome. Glycoconj J 2013;30:41-50.
76. Lauc G. Precision medicine that transcends genomics: Glycans as integrators of genes and environment. Biochim Biophys Acta 2016;1860:1571-3.
77. Franks PW, McCarthy MI. Exposing the exposures responsible for type 2 diabetes and obesity. Science 2016;354:69-73.

78. Almeida A, Kolarich D. The promise of protein glycosylation for personalised medicine. Biochim Biophys Acta 2016;1860:1583-95.
79. Nowak C, Sundstrom J, Gustafsson S, et al. Protein Biomarkers for Insulin Resistance and Type 2 Diabetes Risk in Two Large Community Cohorts. Diabetes 2016;65:276-84.

Nederlandse Samenvatting

N-glycosylatie

In deel 2 van dit proefschrift heb ik patronen van eiwit *N*-glycosylatie in type 2 diabetes bestudeerd. In **hoofdstuk 2** presenteer ik de DiaGene studie. In deze studie hadden de mensen met type 2 diabetes en de gezonde controles een verglijkbare leeftijd, wat voorkomt dat verschillen tussen de twee groepen niet toegeschreven kunnen worden aan een verschil in leeftijd. Een aanzienlijk deel van de mensen met type 2 diabetes had complicaties van hun ziekte. Ondanks een striktere behandeling van de cardiovasculaire risicofactoren LDL-cholesterol en hoge bloeddruk hadden mensen die in de tweede lijn door de specialist werden behandeld meer complicaties dan mensen die in de eerste lijn door de huisarts werden behandeld. Afgezien van de variant in het *KCNJ11* gen zag ik dat genetische risicovarianten voor type 2 diabetes vaker voorkwamen in mensen met type 2 diabetes dan in de gezonde controles. Dit benadrukt dat dit multicenter type 2 diabetes cohort goed geschikt is voor omics onderzoeken. Bovendien maakt de prospectieve data voor diabetescomplicaties het mogelijk om causale determinanten van diabetescomplicaties te bestuderen in de toekomst.

In **hoofdstuk 3** heb ik laten zien dat verschillende kenmerken van het totale plasma *N*-glycoom sterk geassocieerd zijn met de aanwezigheid van type 2 diabetes. Met name de verbinding van siaalzuur met de onderliggende glycaanstructuur was anders in type 2 diabetes, waarbij er minder structuren met α2,3-gelinkt en meer structuren met α2,6-gelinkt siaalzuur werden gezien. Daarnaast was er meer bisectie van gefucosyleerde gesialyleerde structuren in type 2 diabetes. Wat betreft eiwit-specifieke *N*-glycosylering van IgG, beschreven in **hoofdstuk 4**, was er minder sialylatie van bisecterende, gefucosyleerde structuren, meer bisectie van gefucosyleerde structuren en minder galactosylatie in type 2 diabetes. Bovendien konden de *N*-glycanen van IgG de aanwezigheid van type 2 diabetes in onze populatie relatief goed voorspellen, waarbij ze informatie van verschillende klinische parameters leken te combineren. Voor zowel IgG en plasma *N*-glycanen reflecteerden de glycosylatiepatronen in type 2 diabetes deels een pro-inflammatoire situatie, zoals ook al beschreven in andere inflammatoire ziektes, en deels veranderingen die specifiek zouden kunnen zijn voor diabetes. Natuurlijk kunnen zowel de inflammatoire als de niet-inflammatoire veranderingen in glycosylatie betrokken zijn bij de pathofysiologie van type 2 diabetes en haar complicaties. Figuur 1 laat de *N*-glycanen zien die geassocieerd zijn met type 2 diabetes in onze populatie.

Figuur 1. N-glycanen die anders zijn in type 2 diabetes dan in gezonde personen.

	Verhoogd in type 2 diabetes		Verlaagd in type 2 diabetes	
IgG *N*-glycoom	Bisectie van gefucosyleerde gesialyleerde glycanen	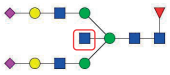	Galactosylatie	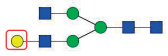
			Sialylatie van gefucosyleerde bisecterende structuren	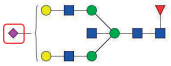
Plasma *N*-glycoom	Sialylatie per galactose van gefucosyleerde diantennaire structuren		Fucosylatie van diantennaire structuren	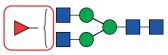
	α2,6-gelinkt siaalzuur per galactose in diantennaire structuren	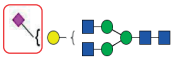	α2,3-gelinkt siaalzuur aan gefucosyleerde triantennaire structuren	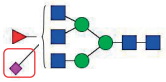
			Bisectie van gefucosyleerde gesialyleerde diantennaire structuren	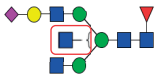

Paarse diamant, siaalzuur; gele cirkel, galactose; blauw vierkant, N-acetylglucosamine; groene cirkel, mannose; rode driehoek, fucose.

De anti-inflammatoire functie van HDL

In **deel 3** van dit proefschrift heb ik de effecten van HDL op signalen van inflammatie bestudeerd in type 2 diabetes. In **hoofdstuk 5** laat ik zien dat de methode waarmee HDL geïsoleerd wordt, een cruciale stap in *ex vivo* studies van HDL functie, het effect van HDL op signalen van endotheel-inflammatie kan beïnvloeden. HDL geïsoleerd met iodixanol dichtheidsgradient ultracentrifugatie (DGUC) kan TNF-α geïnduceerde VCAM-1 expressie inhiberen op humane coronairarterie cellen. DGUC met iodixanol is een goed alternatief voor DGUC met een zoutgradiënt bij het bestuderen van de TNF-α geïnduceerde VCAM-1 expressie als een maat voor de anti-inflammatoire functie van HDL. Bovendien is deze methode sneller, minder duur, en beïnvloedt zij de samenstelling van HDL minder, wat het bestuderen van HDL in grotere populaties beter mogelijk maakt. Van belang is wel dat iodixanol zonder HDL als experimentele controle wordt mee genomen aangezien iodixanol mogelijk ook zelf VCAM-1 expressie enigszins kan verlagen.

De anti-inflammatoire effecten van HDL zijn waarschijnlijk verminderd of verloren in type 2 diabetes, zoals ik laat zien in de systematische review in hoofdstuk 6. Figuur 2 laat een overzicht zien van de afgenomen anti-inflammatoire effecten van HDL in type 2 diabetes inclusief mogelijke mechanismen, voor zover op dit moment bekend in de literatuur. Helaas zijn studies die de anti-inflammatoire effecten van HDL onderzoeken in type 2 diabetes schaars, klein, en niet allemaal van hoge kwaliteit. De precieze onderliggende mechanismen, de richting van de associatie, en consequenties voor de *in vivo* situatie in

mensen konden niet bepaald worden uit de bestaande literatuur. Bovendien is de relatie van de anti-inflammatoire functie van HDL met diabetescomplicaties nauwelijks bestudeerd.

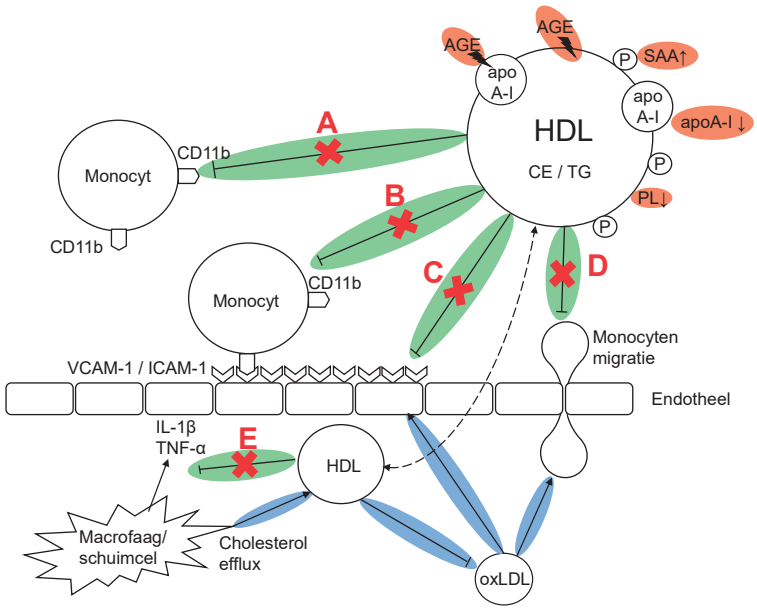

Figuur 2. Schematisch overzicht van de verminderde anti-inflammatoire functie van HDL in type 2 diabetes.

Groen: inflammatoire processen die HDL normaal remt, maar niet of minder in type 2 diabetes. A) expressie van het adhesiemolecuul CD11b op monocyten; B) adhesie van monocyten aan endotheelcellen; C) expressie van de adhesie moleculen VCAM-1 en ICAM-1 op endotheelcellen; D) monocytenmigratie door het endotheel; en E) cytokine afgifte door macrofagen. Oranje: mogelijke determinanten van verminderde anti-inflammatoire capaciteit van HDL in type 2 diabetes. Blauw: mechanismen via welke HDL inflammatie mogelijk indirect remt, maar die buiten de strekking van mijn onderzoek vallen. Afgebeeld zijn het effect van HDL op 1) cholesterolverwijdering uit schuimcellen, waardoor ze minder pro-inflammatoir worden, en 2) LDL oxidatie in de subendotheliale ruimte, wat een pro-inflammatoire trigger is. Alle maten voor de anti-inflammatoire functie van HDL zijn onderzocht in plasma, dus de precieze effecten van HDL in de subendotheliale ruimte zijn niet bekend. AGE: advanced glycation end product, apoA-I: apolipoproteine A-I, CE: cholesterolesters, HDL: high density lipoprotein, ICAM: intercellular adhesion molecule-1, IL-1β: interleukin-1β, oxLDL: geoxideerd LDL, P: proteïne, PL: fosfolipiden, SAA: serum amyloid A, TG: triacyl glycerols, TNF-α: tumor necrosis factor-α, VCAM-1: vascular cell adhesion molecule-1.

Dankwoord

Het tot stand komen van dit proefschrift ging met pieken en dalen, waarbij ik regelmatig wat hulp, steun of gezelligheid kon gebruiken. Daarom wil ik graag iedereen bedanken die mij in deze periode heeft bijgestaan.

Te beginnen bij prof.dr. E.J.G. Sijbrands. Beste Eric, dank je wel voor het vertrouwen dat je altijd in me had, een enorme stimulans om elke keer de draad opnieuw op te pakken. En natuurlijk dank voor de gezelligheid tijdens de dinsdagmiddag overleggen en de DiaGene bijeenkomsten (met etentjes natuurlijk).

Ook dank aan mijn co-promotoren, dr. M. van Hoek en dr. A.G. Lieverse. Mandy, jouw optimisme en pragmatiek hebben ertoe geleid dat het publiceren van artikelen soepel verliep. Je bent een grote inspiratie en steun in dit traject geweest, en ik hoop dat we de komende jaren zo samen kunnen blijven werken. Louis, ik sta elke keer weer versteld van de hoeveelheid ideeën voor nieuwe onderzoeken die jij hebt. Jouw enthousiasme en vertrouwen werkten aanstekelijk, vooral in combinatie met een kopje thee, een sinaasappel en de goed gevulde snoeppot. Hopelijk kunnen we de komende jaren nog meer van jouw ideeën tot uitvoer gaan brengen!

Aan mijn leescommissie, prof.dr. C.M. van Duijn, prof.dr. O.H. Franco Duran en prof. dr. H.R.Haak, hartelijk dank voor de tijd en moeite die jullie hebben genomen om mijn proefschrift te beoordelen. Nog een speciaal woord van dank voor Harm: bij jou ben ik ooit mijn wetenschappelijke carrière begonnen als semi-arts en ook deze onderzoeksplek was op jouw aanbevelen. Ik ben dan ook erg blij dat jij dit proefschrift wilde beoordelen

De overige commissieleden, prof.dr. H Pijl, prof.dr. C.D.A. Stehouwer, prof.dr. B.H.R. Wolfenbuttel, hartelijk dank dat jullie plaats willen nemen in mijn commissie.

De artikelen waar dit proefschrift uit bestaat zouden niet mogelijk zijn geweest zonder alle mede-auteurs. Dank voor al het werk aan de verschillende stukken! Een aantal mensen wil ik daarbij in het bijzonder bedanken. T.T.W. van Herpt, Thijs, het begon allemaal bij de DiaGene. Dank dat ik deze gevulde biobank van jou over mocht nemen. De goede gesprekken, fietstochtjes, en koppen koffe met jou hielpen altijd om te relativeren en vooruit te kijken. Dr. V. Dotz, Victoria, thank you for teaching me about glycans and R, I have always enjoyed working with you and am very proud of our paper. Prof.dr. M. Wuhrer, Manfred, dank voor de mogelijkheid om zoveel over glycans te leren in samenwerking met jouw lab. C.M. Groot-van Ruijven, Corrien, dank voor jouw inzet en werk bij het opzetten van het HDL onderzoek. Ik heb veel van je kunnen leren, al vrees ik wel dat mijn talenten in het stickers plakken groter bleken dan in het pipetteren. L.C. van der Zee-van Vark, Leonie, ook jij dank voor al jouw werk in het HDL onderzoek, samen kwamen we er elke keer weer uit en gelukkig is gedeelde smart dan ook weer halve smart. Dr. W.A. Dik, Wim, zonder jou hadden we het HDL onderzoek niet op kunnen zetten. Dank je wel voor jouw enthousiasme hierin. Dr. M.T. Mulder, Monique, dank voor jouw geduld, creativiteit en

doorzettingsvermogen, deze hebben ervoor gezorgd dat we het HDL onderzoek nog niet hebben opgegeven. Dr. A.J.M. Verhoeven, Adrie, jij bedankt voor jouw kennis en strikte morele kompas, die ervoor gezorgd hebben dat het HDL onderzoek steeds beter werd en wordt.

Naast wetenschappelijke steun was ook de andere steun van collega's belangrijk. Het begon allemaal al die jaren geleden in Eindhoven in het onderzoekshok en plaatsing in het escalatieteam. Thomas, Steffie, Dorien, Hester, Joyce, Anne, Hao Ran, zonder jullie gezelligheid, goede gesprekken en slechte muziek was het schrijven van dit proefschrift veel lastiger geweest. Het was altijd fijn om al die leuke, minder leuke, of ronduit bizarre gebeurtenissen samen te kunnen bespreken en verwerken. Anne, bedankt dat ik extra monsters af mocht nemen in jouw studie, het artikel staat nog steeds op de planning! Collega's van het escalatieteam, dank voor de gezelligheid tijdens de diensten, de samenwerking bij de acute patiënten en het aanhoren van alle onderzoeksverhalen. Hanny, dank je wel voor jouw hulp bij alle administratieve kanten van het onderzoek, fijn dat jij altijd oog had voor de details hierbij en alles zo goed regelde. Hanneke, jij bedankt voor je altijd luisterende oor en het snel regelen van alle administratieve zaken. Collega assistenten, internisten en MDL-artsen uit het MMC, hartelijk dank voor de gezelligheid, borrels en skireisjes en jullie interesse in mijn onderzoek. Mede door jullie heb ik een mooie tijd gehad in het MMC.

Ook de tijd in Rotterdam was lang zo leuk niet geweest zonder alle collega's van het lab en de gezamenlijke lunches, koffie- en theepauzes en borrels. Ik wil jullie met name ook bedanken voor de waardevolle gesprekken en het begrip als ik het moeilijk had. Het was een hele fijne familie om bij te horen! Reyhana, Kirsten, Sandra, Mardin, dank voor jullie steun in het verwerken van de tegenslagen in het onderzoek maar ook in het vieren van de resultaten. Sunny, dank voor het overnemen van de DiaGene, ik heb alle vertrouwen dat jij de biobank netjes beheert en dat er een hoop nieuw mooi onderzoek uit voort zal komen. Edith Padberg, hartelijk dank voor het strak regelen van alles wat geregeld moest worden, een grote steun in het leven van de arts-onderzoeker.

Inmiddels heeft de reis voortgeleid naar Breda. Alle collega's in het Amphia bedankt voor de gezelligheid, collegialiteit en de zeer leerzame opleidingsplek. De Brabantse gezelligheid binnen ons team zorgt ervoor dat ik altijd met plezier naar mijn werk ga.

Jolien en Inge, mijn paranymfen, wat fijn dat jullie mij deze dag willen ondersteunen! Jullie kennen mij door en door en ik weet dat jullie er altijd zijn als ik jullie nodig heb. Jolien, het voetballen en borrelen bij DBSV bleek een solide basis voor onze vriendschap. Ik geniet altijd enorm van onze vakanties samen met veel buitenlucht en beweging, maar met name ook heel veel praten en genieten (en oké ook af en toe eten en drinken). Dank ook dat je mij hebt geënthousiasmeerd voor vrijwel al mijn huidige hobby's, en ook voor

het aandragen van voldoende voedsel tijdens het uitoefenen hiervan. Inge, één van de eerste personen die ik heb leren kennen in Maastricht en vaste partner in crime tijdens onze studententijd (samen met Karen natuurlijk). Nooit uitgepraat, maar altijd een luisterend oor. Het leren praten en luisteren tegelijk was een zeer leerzame les van jullie twee. Dank voor jouw eeuwige enthousiasme, energie, en het regelen van altijd weer nieuwe uitjes.

Vrienden waren er altijd weer om even te ontspannen en te praten, allemaal ontzettend bedankt voor alle gezelligheid en steun! Een paar mensen wil ik in het bijzonder bedanken. Anniek, mijn oudste (langst bestaande?) vriendinnetje. Tijdens onze kleutertijd begonnen met samen spelen en dit doen we gelukkig nog steeds. Tevens ontwerper van de omslag van mijn boekje, ik ben er heel blij mee! Jij en Jonathan (Roomies!) vormden vorig jaar een echt thuis voor mij. Deze bijzondere tijd vergeet ik nooit meer. Evelien, Fee, altijd fijn om even samen te ontspannen en bij te kletsen. Het is hoog tijd om weer eens een dansje te plegen! Karen, van jou is er echt maar één. Nooit om een woord verlegen, maar tussen alle onzin kraam je ook veel zinnige inzichten uit. Altijd in voor een borreltje, sporten, of brak een filmpje op de bank kijken, maar ook altijd bereikbaar als het leven even niet zo leuk is. Ollie, na een geslaagde eerste training infuus prikken volgde een goede vriendschap met het vieren van alle kleine en grote mijlpalen. We hebben menig proefschriftverdriet samen kunnen verdrinken in een flesje wijn, en het afronden van dit proefschrift en daarna van het jouwe vieren we zeker als jij terug bent uit Australië.

Ooms en tantes, neven en nichten, ik ben altijd weer blij om deel uit te maken van onze ietwat gekke maar gezellige familie. Ik ben blij dat we de band vast hebben kunnen houden, ook al zien we elkaar niet altijd even vaak. Janna en Micha, we zijn vrij verschillend maar hebben door het samen opgroeien ook een hoop overeenkomsten. Ik weet dat ik altijd op jullie kan terugvallen en geniet van de momenten samen. Janna, bedankt voor alle gesprekken waarin jouw praktische denken mijn overgeanalyseer een halt toeroept, en natuurlijk voor het lenen van jullie kinderen als ik afleiding nodig heb, van wie ik altijd enorm geniet. Pappa en mamma, dank je wel dat jullie mijn nieuwsgierigheid hebben gestimuleerd en het me altijd mogelijk maakten om nieuwe dingen uit te proberen. Pappa, jouw wetenschappelijke ambities zijn enigszins gestrand toen je begreep dat je daar een computer bij moest gebruiken, maar je bleef altijd trouw geïnteresseerd in de mijne. Ik ben blij dat je me zo goed kent en altijd een goed advies hebt als ik dat nodig heb. Mamma, je hebt helaas weinig mee gekregen van mijn onderzoek, maar ik herinner me jouw vertrouwen in mij van vroeger. Ik mis je en wilde dat je erbij kon zijn vandaag.

Jasper, jij kwam pas in mijn leven tijdens het afronden van dit proefschrift, maar ik hoop dat je er nooit meer uit verdwijnt. Jij brengt mij tot rust en maakt mijn leven leuker en makkelijker. Ik hou van je en weet zeker dat we samen nog een hoop bergen zullen bedwingen.

Curriculum vitae

Roosmarijn Lemmers werd geboren op 15 juli 1988 te Zeist. Ze groeide op in Langbroek en Doorn, en voltooide in 2005 cum laude het gymnasium aan het Revius Lyceum te Doorn. Datzelfde jaar begon ze aan de studie geneeskunde in Maastricht. Tijdens haar bachelor was ze actief bij studentenvoetbalvereniging DBSV Red Socks, waar ze in 2007-2008 ook bestuurslid was, en studentenvereniging KoKo. Tussen haar bachelor en master nam ze een jaar vrij om onder andere Noors te leren en stage te lopen bij revalidatieziekenhuis Sunnaas Sykehus te Noorwegen. In 2012 voltooide Roosmarijn haar master geneeskunde in Maastricht en begon zij met haar eerste baan als arts-assistent interne geneeskunde in het Máxima Medisch Centrum te Veldhoven. Vanuit hier kon zij begin 2013 starten met haar promotieonderzoek in samenwerking met de afdeling interne geneeskunde in het Erasmus MC, wat uiteindelijk heeft geresulteerd in dit proefschrift. Sinds september 2017 werkt Roosmarijn als arts-assistent interne geneeskunde in het Amphia ziekenhuis te Breda, waar zij 1 januari 2018 is begonnen aan de opleiding tot internist. In haar vrije tijd houdt zij zich bezig met eten, koken, sporten en plezier maken samen met familie en vrienden.

PhD Portfolio

Naam	Roosmarijn Lemmers
Department	Internal Medicine
Research school	Cardiovascular Research School Erasmus University Rotterdam (COEUR)
Promotor	Prof.dr. E.J.G. Sijbrands
PhD-period	2013-2018

PhD training	**Year**	**ECTS**
General academic skills		
Good Clinical Practice	2013	1
Biomedical English Writing and Communication	2015	2
Research skills		
COEUR		
- Lecture: HDL's Protein Cargo: Friend or Foe in Cardioprotection	2013	0.1
- Molecular biology in atherosclerosis and cardiovascular research	2014	1.5
Erasmus Summer Programme		
- Case-Control studies	2013	0.7
- Markers and Prognostic Research	2013	0.7
- Joint Models for Longitudinal and Survival Data	2016	0.7
Molmed Courses		
- Basic Course on 'R'	2016	1.8
- SNP course	2016	2
Dutch Heart Foundation		
- Vascular Biology	2013	2
- Thrombosis and Haemostasis	2014	2
Symposia and conferences		
Workshop 'The interplay of glucose and lipid metabolism', TUe	2013	0.45
Dutch Cardiovascular Conference, Ermelo*	2014	0.6
Wetenschapsavond Máxima Medisch Centrum, Veldhoven*	2014	0.15
IAS HDL workshop, Rome*	2014	0.9
EASD scientific meeting, Vienna*	2014	1.5
NVDO Jonge Onderzoekers Bijeenkomst, Soesterberg**	2015	0.6
Wetenschapsdagen Interne Geneeskunde, Antwerpen	2016	0.3
EASD scientific meeting, Munich*	2016	1.2
Internal Medicine research symposia, Rotterdam**	2016	0.6
Wetenschapsdagen Interne Geneeskunde, Antwerpen**	2017	0.6
** Poster presentation, ** oral presentation*		
Presentations and teaching		
Presentations at the Internal Medicine Departments of EMC and MMC		2.1
Poster and oral presentations at symposia		1.6
Teaching and student supervision		5.7
Total		30.8